THE

LONDON, EDINBURGH, AND DUBLIN

PHILOSOPHICAL MAGAZINE

AND

JOURNAL OF SCIENCE.

[SEVENTH SERIES.]

MARCH 1936.

XLIII. *The Catalytic Combustion of Methane.*—Part I.

By W. DAVIES, *B.Sc., Ph.D.**

LANGMUIR † has shown that the catalytic combustion of carbon monoxide on platinum depends on the adsorption of oxygen and that reaction takes place only when carbon monoxide molecules in the gas phase collide with oxygen atoms adsorbed on the platinum surface. Under these conditions every collision between a carbon monoxide molecule and an adsorbed oxygen atom is effective, but if the carbon monoxide reaches the platinum and becomes adsorbed it is thereby rendered inactive towards oxygen, whether the latter is in the free gas state or adsorbed in adjacent spaces on the surface. The catalytic combustion of hydrogen on platinum takes place in a similar manner under normal conditions, but Langmuir has suggested that an alternative reaction between adsorbed hydrogen and oxygen may become possible in this case after the structure of the platinum surface has been modified by the special kind of heat treatment to which it is subjected in the course of the normal reaction.

By a method of investigation, based on observations of the rates of heating of metallic wires suspended freely

* Communicated by Prof. W. T. David, Sc.D., M.Inst.C.E.

† Trans. Far. Soc. xvii. p. 607 (1921–1922).

in combustible gaseous mixtures, the writer * has obtained results in experiments with hydrogen and carbon monoxide which appear to be in accord with Langmuir's hypothesis; but similar experiments with methane, which form the subject of this paper, suggest that reaction does not take place between methane in the gas phase and oxygen adsorbed on the surface of platinum. Catalytic action appears to be controlled in this instance by a different mechanism, which probably involves the adsorption of both reactants. It is therefore influenced by several factors which do not affect the hydrogen and carbon monoxide reactions.

The temperature at which catalytic combustion is initiated on an electrically heated platinum wire in methane and air, or methane and oxygen, varies within very wide limits according to the relative proportions in which methane and oxygen are present in the atmosphere surrounding the wire. In experiments with very small concentrations of methane in air no reaction takes place on the wire until its temperature approaches 1000° C., but as the temperature rises above this point the rate of heating of the wire by combustion increases rapidly up to the melting-point of platinum. With very large quantities of methane in air, on the other hand, combustion is initiated at temperatures below 400° C. In this case, however, the catalytic activity of the wire decreases rapidly with further rise of temperature and combustion is completely suppressed before the wire reaches its melting-point.

It has been shown previously that the catalytic combustion of hydrogen is initiated on a platinum wire at about 200° C.†. In this paper it is shown that when small quantities of hydrogen and methane are present together in air the hydrogen reaction is still initiated at about 200° C., whilst the methane remains inert until the temperature of the wire is raised to about 900° C. The wire thus acts as a preferential catalyst for the combustion of hydrogen in these mixtures over the temperature range 200°–900° C. It is found, however, that this range diminishes rapidly when the ratio of methane to oxygen in the mixture is increased. At temperatures

* Phil. Mag. xvii. p. 233 (1934); xix. p. 309 (1935).
† *Ibid.* p. 1.

above 1200° C. the conditions become more favourable to the methane reaction and less favourable to the hydrogen reaction, and the rate of combustion of methane eventually becomes greater than that of hydrogen as the temperature of the wire approaches the melting-point of platinum.

Results of Experiments.

(1) *Platinum Wire in Methane and Air.*

(a) *Excess Air.*

A new platinum wire is inactive towards methane in these mixtures until it has been heated by the current for a short period to a temperature of about 1400° C., in contact with methane and air. After combustion has once been established in this way the wire becomes active at a much lower temperature, and it remains in this state as long as it is not exposed to a gas or vapour which can produce a toxic effect by adsorption.

The results shown in fig. 1 were obtained with a wire of ·001 inch diameter and 6·4 inches long, when suspended freely in a horizontal position within a closed vessel having a capacity of 1 cubic foot. The temperatures attained by the wire when supplied with different inputs of electrical energy were observed when the vessel was filled with air and with mixtures of methane and air in various proportions at a pressure of 1 atmosphere. The curve A shows the temperatures in air and the curves B–F show the corresponding temperatures in mixtures of from 1 per cent. to 5 per cent. of methane and air. Catalytic combustion is initiated at the points where these curves suddenly bend upwards and rise above the air curve, and until the wire has been heated by the current to the temperatures indicated at these points there is no evidence that an exothermic reaction of any kind is taking place on its surface. The minimum temperatures required to initiate combustion on the wire in these mixtures vary from about 760° C. to about 970° C., according to the proportion of methane to air; but combustion is not established over the whole of the wire at these temperatures, its appearance immediately after the commencement of combustion indicates that only a small fraction of its surface is catalytically active

at first, but as the temperature rises the proportion of active surface increases rapidly, and the wire glows uniformly over the whole of its length at temperatures above 1300° C.

Fig. 1.

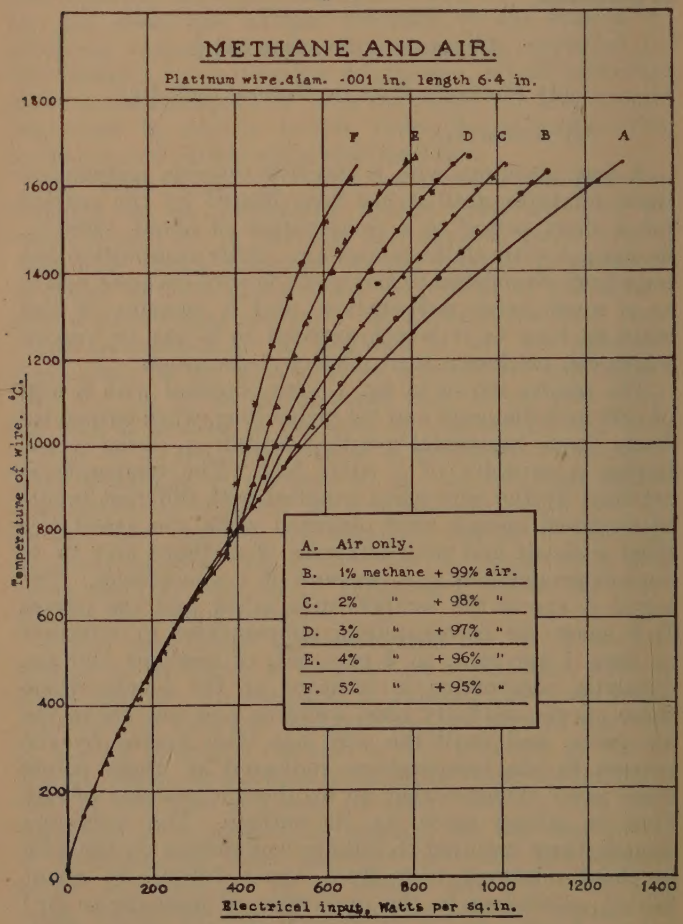

The input of electrical energy is plotted horizontally in fig. 1 and is expressed in watts per square inch of the nominal surface area of the wire. The horizontal inter-

cepts between the curve A and each of the curves B–F therefore indicate the rates of heating of the wire by combustion at different temperatures, after making small corrections for the differences in the rates of cooling of the wire due to the variation in the thermal conductivity of the gaseous mixture with changes in methane

Fig. 2.

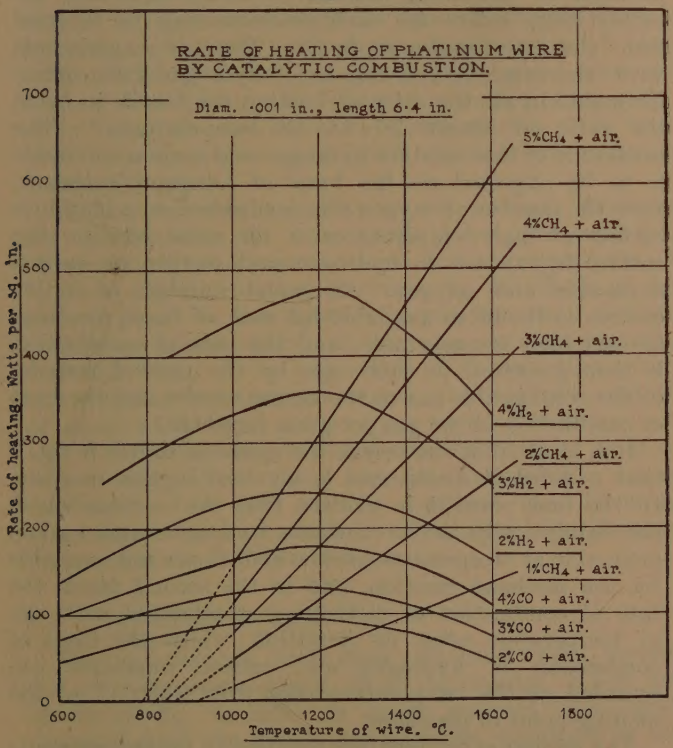

concentration. These corrections are determined experimentally by heating the wire electrically in mixtures of methane and nitrogen instead of air; combustion is then suppressed, and the input of electrical energy just balances the heat loss.

The rates of heating of the wire by catalytic combustion in the experiments shown in fig. 1, obtained in the

manner described above, are plotted against wire temperatures in fig. 2, together with the results obtained in previous experiments with similar concentrations of hydrogen and air and carbon monoxide and air. After due allowance has been made for the effect of the external factors which govern the rate of transfer of the reacting gases to the active centres the relative proportions of the total surface of the wire which are catalytically active for each reaction may be inferred from the rates shown in fig. 2. Thus, in experiments with the same concentrations of hydrogen and carbon monoxide in air the rates of heating are found to be in the ratio of about 2·7 at all temperatures *. The constancy of this ratio for hydrogen and carbon monoxide is to be expected on the basis of Langmuir's theory, since the number of oxygen atoms adsorbed on a platinum surface at high temperatures is the same whether the surface is exposed to hydrogen and oxygen or carbon monoxide and oxygen. An equal number of active centres is therefore available for each of these reactions at very high temperatures, and the rate of combustion is then governed in each case by the rate of transfer of the combustible gas to the active centres and the heat of combustion of the gas per gram molecule.

It is clear from the results for methane shown in fig. 2 that a different mechanism is involved in this reaction. In the first place it is evident that the centres which are catalytically active towards hydrogen and carbon monoxide at temperatures below 800° C. are not available for the methane reaction, and in the second place the rate of combustion of methane is accelerated with rise of temperature after its initiation, whilst the rates of combustion of hydrogen and carbon monoxide are retarded as the temperature rises from 1200° C. to the melting-point of platinum.

The minimum temperature required to initiate catalytic combustion on the wire in the experiments shown in fig. 1 decreases from about 970° C. to about 760° C. as the methane concentration increases from 1 per cent. to 5 per cent. Experiments with stronger mixtures show that the initiation temperature is lowered progressively as the ratio of methane to air increases. Thus, with 9·5 per cent. of methane and air combustion is initiated at about

* Phil. Mag. xvii. p. 241 (1934).

660° C., but the wire in this instance is immediately afterwards raised to the melting-point and fuses. This occurs, however, without igniting the gaseous mixture, and no explosion takes place. It is a well-known fact that explosive gaseous mixtures are not readily ignited by heated wires of small diameter. Shepherd and Wheeler * have shown that a platinum wire of the order of ·001 inch diameter can be fused by a fairly heavy current in mixtures of methane and air without causing ignition, and it has been shown by the writer † that no combustion in the gas phase takes place near the surface of a similar wire when it is heated electrically, or by catalytic combustion to a temperature of at least 1300° C. in the most explosive mixture of carbon monoxide and air.

The results obtained with excess methane mixtures are described in the next section, but the initiation temperatures for all the methane and air mixtures used in these experiments are shown in fig. 3. Each of the plotted points in this figure represents the mean of from four to ten observations with the same mixture but with different wires. It is important to observe that every new wire was first heated for a short time to a temperature of about 1400° C. in about 1 per cent. of methane and air, in order to bring it into a uniform state of activity before using it in these experiments. If this initial treatment of a new wire is omitted the initiation temperatures are variable and always considerably higher than those shown in fig. 3.

(b) *Excess Methane.*

The experiments with these mixtures were carried out as a separate series, since the results, which are shown in fig. 4, differ in many respects from those obtained with the excess air mixtures described in the previous section. The methane concentrations used in this series varied from 20 per cent. to 70 per cent.; therefore the thermal conductivities of the gaseous mixtures differed very considerably. For this reason, a system of base curves, *a–f*, are drawn in fig. 4, to show the temperatures attained by the wire when combustion is

* Safety in Mines Research Dept. Report No. 26 (1917).
† Phil. Mag. xix. p. 316 (1935).

suppressed in each mixture by substituting nitrogen for air. The temperatures recorded in the air mixtures are shown by the curves A–F, and the rates of heating by combustion are now represented directly by the horizontal intercepts between these curves and the corresponding nitrogen, or base curves.

Fig. 3.

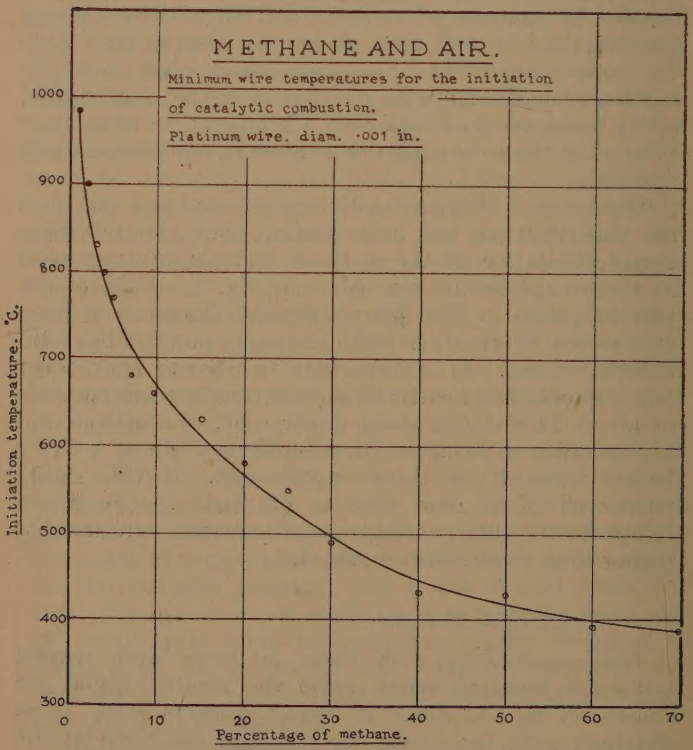

Reference has already been made to the fact that reaction starts at much lower temperatures in excess methane mixtures than in excess air mixtures, but it is to be noted that there is also a change in the mode of its initiation. As soon as the wire has been heated by the current to the required temperature combustion is now established suddenly over the whole of the

available catalytic surface, and the temperature of the wire therefore rises abruptly to higher values, as shown by the dotted lines in fig. 4, instead of gradually, as in

Fig. 4.

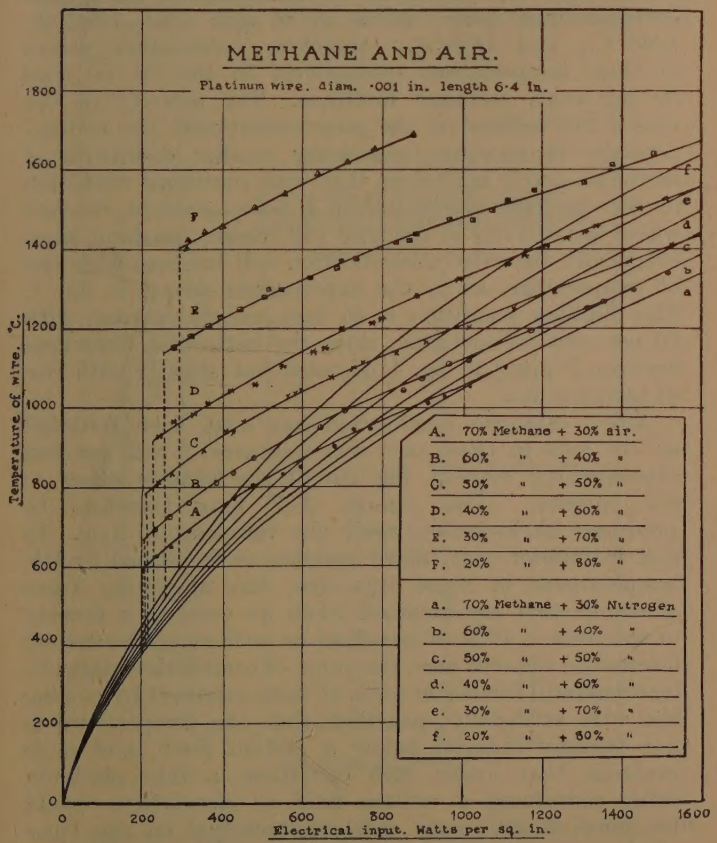

the experiments shown in fig. 1. The most remarkable contrast occurs, however, in the subsequent behaviour of the wire. When its temperature is raised after the initiation of combustion, by passing a heavier current through it, its catalytic activity diminishes rapidly

and the rate of combustion decreases, as shown by the convergence of the curves A–F, on to the base curves *a–f*, when the input of electrical energy is increased. In some of these mixtures combustion is completely suppressed when the wire reaches certain temperatures; thus the curves A, B, and C meet their corresponding base curves *a*, *b*, and *c* at 1080° C., 1260° C., and 1440° C.; therefore combustion ceases at these temperatures respectively in the 70, 60, and 50 per cent. methane mixtures. The activity of the wire is not reduced to the same extent with rise of temperature in mixtures containing smaller quantities of methane, and it is obvious that with continued reduction in the methane concentration a point must be reached where the activity of the wire will remain constant, since eventually the rate of combustion will increase with rise of temperature, as in the experiments shown in fig. 1. This limiting condition is, in fact, nearly reached with 20 per cent. of methane, since the horizontal intercepts between F and *f* in fig. 4 decrease but slightly with rise of temperature.

After catalytic combustion has once been initiated on the wire in these over-rich mixtures it will proceed subsequently without the aid of the heating effect of the current. The curves A–F may therefore be produced backwards to meet the temperature axis. In fact it follows that, since reaction is facilitated by low temperatures in these mixtures, the maximum rates of combustion are attained when no current is flowing in the wire. It is of practical as well as of theoretical interest to observe that the rates of combustion might be increased still further in some of these mixtures by cooling the wire artificially, provided that the temperature is not thereby reduced below a certain limit, and it is probable that under such conditions a thin platinum tube, containing a cooling fluid in circulation, would be more efficient as a catalyst, reckoned on the basis of the space-time yield of products, than a solid wire of the same external dimensions.

The maximum rates of heating of the wire by combustion in methane and air under the most favourable temperature conditions attainable with the present experimental method are plotted against the mixture composition in fig. 5. These rates of heating were estimated for the

excess air mixtures by extrapolating the curves in fig. 1 to 1750° C., and for the excess methane mixtures by producing the curves in fig. 4 back to the temperature axis. The rate of combustion appears to be directly proportional to the concentration of methane in the excess air mixtures, but it decreases more rapidly than would be the case if the linear relationship continued

Fig. 5.

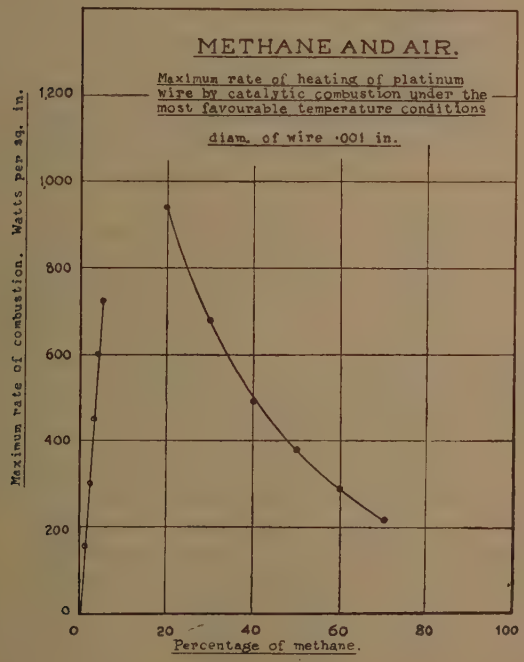

to hold on the over-rich side, from which it is to be inferred that a smaller proportion of the catalytic surface is active in the presence of an excess of methane. It is not possible to obtain experimental data in the neighbourhood of the complete combustion mixture, because the wire is immediately raised to the fusing-point when combustion is initiated; but it appears that the two portions of the curve in fig. 5 would meet and give a

maximum on the ordinate for the complete combustion mixture.

Another important phenomenon has been observed in the experiments with excess methane and air, but only a brief reference is made to it here since further experimental work is now being carried out to investigate it in greater detail. It is found that when the wire has been heated to a sufficiently high temperature to suppress combustion completely in very rich mixtures its catalytic activity is, for a time, completely destroyed. This is inferred from the fact that when the wire is cooled down subsequently its temperature follows the nitrogen curve instead of retracing the ascending curve. For example, when the wire is heated up in the first instance in 70 per cent. of methane and air its temperature rises along the curve A in fig. 4 until this curve meets the nitrogen curve *a*, at about 1080° C. Combustion is completely suppressed at this point, and if the wire is now cooled down, by reducing the current, its temperature falls along the curve *a* instead of along A. It is evident, therefore, that no combustion is taking place when the wire is cooling down through the range of temperatures in which it was previously catalytically active. This is an example of transient catalytic poisoning, since the wire can be readily restored to its original state of activity by withdrawing it from the methane mixture and heating it momentarily in air to a temperature of about 1500° C. The wire also appears to recover its activity very slowly to some extent in air at room-temperature. The temporary loss of activity which takes place under these circumstances is complete only if the wire is heated to a sufficiently high temperature in mixtures containing more than 60 per cent. of methane. If the methane concentration is less than 60 per cent., or if the temperature is not raised far enough to suppress combustion completely, the loss of activity is only partial, and recovery takes place more rapidly when the wire is cold.

(2) *Platinum Wire in Methane and Oxygen.*

It appears that nitrogen is not adsorbed by platinum to an appreciable extent at any temperature * ; therefore it is highly improbable that it can have any effect in the

* Langmuir, Trans. Far. Soc. xvii. p. 306 (1921–1922).

experiments described in the previous section beyond that of a diluent in the gas phase. The inhibition of the

Fig. 6.

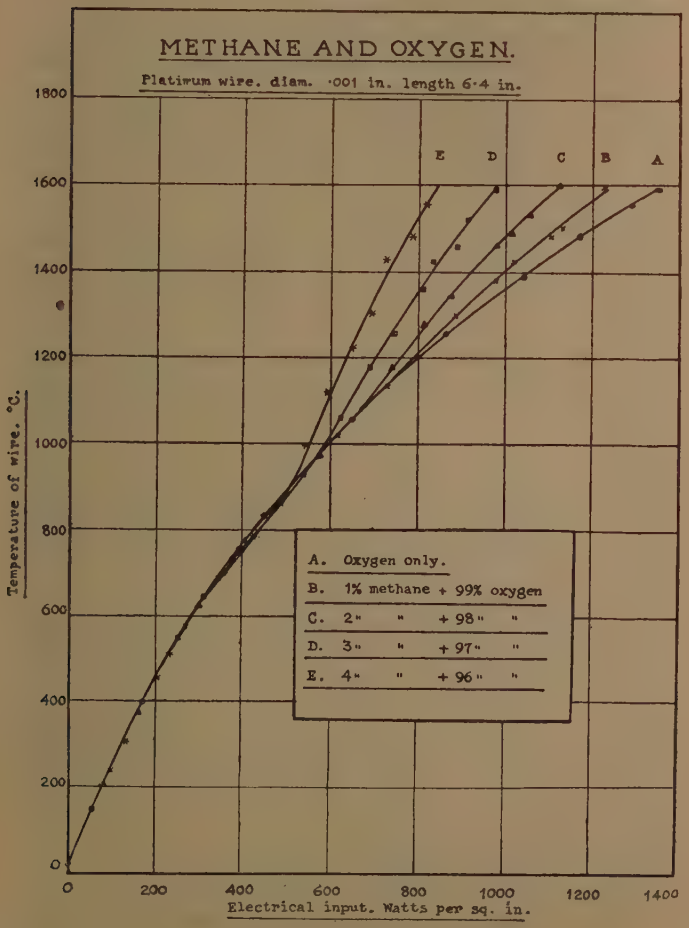

methane reaction at low temperatures in mixtures containing an excess of air is probably due to the existence of an impenetrable film of oxygen on the active centres which prevents the adsorption of methane. This view is

strongly supported by the fact that when oxygen is substituted for air the initiation of combustion is delayed until the wire has been heated by the current to temperatures which are considerably higher than those shown in fig. 3.

The results obtained with small quantities of methane in oxygen are shown in fig. 6. The curve A shows the temperatures attained by the wire in oxygen only. These are appreciably lower than the corresponding temperatures in air, on account of the fact that the thermal conductivity of oxygen is greater than that of nitrogen. The curves B–E show the temperatures recorded in mixtures of from 1 per cent. to 4 per cent. of methane and oxygen. Catalytic combustion is not initiated in these mixtures until the wire has been heated by the current to temperatures which are of the order of 200° C. above those required in the corresponding air mixtures, and the subsequent rates of combustion, as inferred from the horizontal intercepts between the curve A and each of the curves B–E in fig. 6, are considerably lower than the corresponding values at the same temperatures in the air mixtures shown in fig. 1. These results therefore lead to the conclusion that an appreciable proportion of the potentially active surface of the wire is rendered ineffective for the methane reaction when oxygen is substituted for air.

It should be pointed out that difficulties are encountered in the measurement of high wire temperatures by resistance thermometry in these mixtures, because the specific resistance of a thin platinum wire changes rapidly in oxygen at temperatures above 1400° C. The method adopted to secure reasonably accurate results under these conditions was to calibrate the wire before and after each experiment, and base the temperature measurements up to 1400° C. on the first calibration and those above this point on the second calibration.

(3) *Platinum Wire in Methane, Hydrogen, and Air.*

It has been stated previously that the catalytic combustion of hydrogen is initiated on a platinum wire at about 200° C., and that the subsequent rate of heating of the wire by combustion in hydrogen and air decreases as the temperature rises from 1200° C. to the melting-point of platinum. The temperature characteristics of

the hydrogen reaction therefore differ greatly from those of the methane reaction. The object of the experiments described in this section was to test the behaviour of the

Fig. 7.

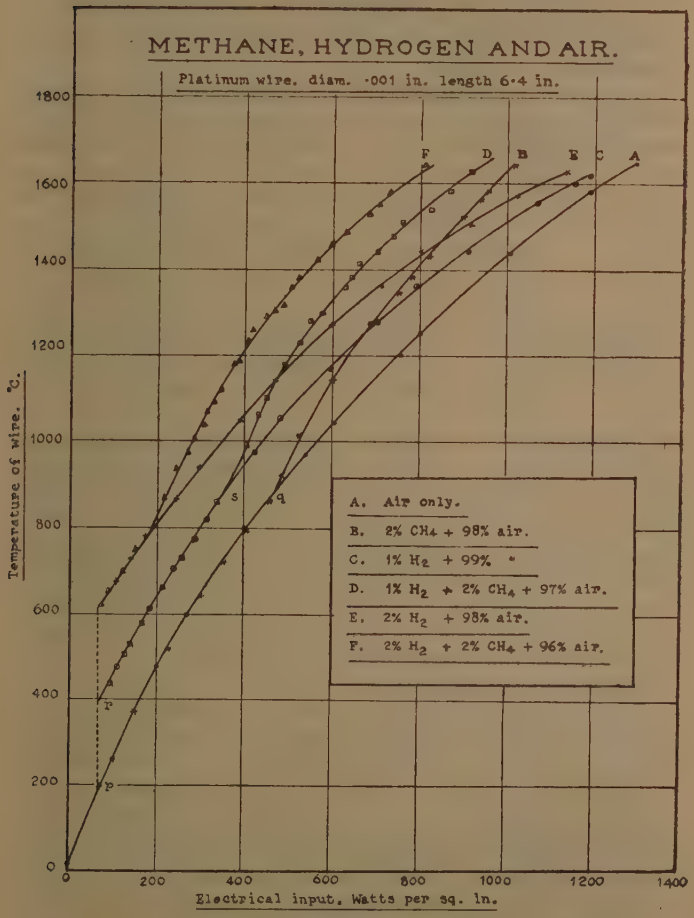

wire in the presence of both hydrogen and methane, in order to obtain a clearer insight into the mechanism of the methane reaction, assuming for this purpose that the hydrogen reaction is governed under all circumstances

by the conditions stated in Langmuir's theory. The results in fig. 7 show that when hydrogen and methane are present in small quantities only the two reactions proceed simultaneously without any appreciable change in their individual characteristics. The hydrogen reaction is still initiated at about 200° C., whilst the methane remains inert until the wire reaches a temperature of from 800° C. to 900° C.

Two series of experiments are represented in the results shown in fig. 7. The curves B, C, and D refer to the first series, which was carried out with 2 per cent. of methane and 1 per cent. of hydrogen in air, first separately and then together. With the methane the temperature of the wire follows the air curve A fairly closely up to the point q; combustion then begins, and the temperature rises subsequently along q–B. With the hydrogen the temperature follows the air curve only as far as p, since combustion is initiated in this case at about 200° C. The greater part of the catalytic surface becomes available for the hydrogen reaction at this point, and the temperature of the wire rises very rapidly to r, after which it follows the curve r–s–C. When the hydrogen and methane are present together the temperature rises along p–r–s–D, *i. e.*, it follows the hydrogen curve again up to s and then rises above this curve to D. It appears therefore that between 200° C. and 860° C. the wire only promotes the combustion of hydrogen, since the combustion of methane evidently does not begin until the wire reaches the latter temperature. From this point the two reactions proceed simultaneously as the temperature rises to the melting-point of platinum.

The curves B, E, and F show the results obtained in the second series of experiments, which was carried out with 2 per cent. of methane and 2 per cent. of hydrogen, in the same sequence as before. There appears to be a definite tendency for the methane reaction to begin at a lower temperature in both cases when the mixture contains hydrogen than when methane only is present, and this fact is of significance in view of the suggestion which has been put forward that the oxygen film obstructs the methane reaction at low temperatures, since the adsorbed oxygen is now removed not only by evaporation but also by reaction with hydrogen to form water vapour which does not remain on the surface. The methane thus

gains access to the platinum at a lower temperature than would otherwise be the case.

Further evidence, which goes to show that there is no appreciable mutual interference between the hydrogen and methane reactions when they proceed simultaneously, is derived from an analysis of the rates of combustion, as shown in the following table :—

Combustible gas in air.	Rate of heating by combustion (watts per square inch).	
	1200° C.	1600° C.
1 per cent H_2 (*a*)	125	85
2 per cent. CH_4 (*b*).....	120	260
1 per cent. H_2+2 per cent. CH_4	260	350
(*a*)+(*b*)	245	345
2 per cent. H_2 (*c*)	240	170
2 per cent. H_2+2 per cent. CH_4	380	440
(*b*)+(*c*)	360	430

Within the limits of experimental error the rate of heating of the wire by combustion at any given temperature when both gases are present is equal to the sum of the rates obtained at the same temperature with each gas separately ; therefore it is highly probable that the two reactions are completely independent of one another under the stated conditions.

Discussion.

The availability of the active centres on the surface of a solid catalyst for any particular reaction depends on the nature of the gas or vapour which is adsorbed on them at any given instant. When the surface is exposed to an atmosphere containing several adsorbable gases adsorption may take place selectively according to the temperature of the surface and the relative proportions in which the gases are present. It follows therefore that when a metallic wire is placed in a gaseous mixture the possibility arises that a heterogeneous or surface reaction which can proceed rapidly under properly selected conditions may be retarded or stopped altogether either by varying the temperature of the wire,

by adding another gas to the system, or by merely altering the proportions of the gases in the original mixture.

Langmuir * has shown that the adsorbed gas layer on a solid is rarely if ever of more than unimolecular thickness and he has also shown that when oxygen is thus adsorbed by platinum it becomes extremely active towards hydrogen and carbon monoxide in the gas phase †. Any diminution in the extent of this oxygen film will therefore lead to a reduction in the rate of the catalytic combustion of these gases, and this can be brought about either by the replacement of the oxygen by some other gas, which will thus act as a catalytic poison, or by the evaporation of the oxygen from the surface.

In the experiments with small concentrations of methane and hydrogen in air, described in section 3, it is shown that the methane has no effect on the rate of combustion of hydrogen over the temperature range 200° C.–800° C. It is clear therefore that if the hydrogen reaction depends on the existence of an adsorbed oxygen film the presence of methane in small quantities does not affect this film at temperatures below 800° C., and it is also evident that methane in the gas phase does not react with oxygen adsorbed on platinum. The methane reaction is, in fact, inhibited until the temperature of the wire is raised to the point at which oxygen begins to evaporate rapidly from a platinum surface, and this seems to lead to the conclusion that the methane itself must reach the platinum before it will combine with oxygen by catalytic action. When the temperature of the wire is below 800° C. in the weak mixtures the access of methane to the active centres is obstructed by the oxygen film, and reaction therefore does not take place until this film begins to break up. The acceleration of the combustion of methane and the retardation of the combustion of hydrogen as the temperature of the wire rises above 1200° C. may be readily explained, according to this theory, on the perfectly justifiable assumption that the evaporation of oxygen takes place at a progressively increasing rate with rise of temperature.

According to Langmuir adsorption is a kinetic process which depends on a time lag between condensation and evaporation. Sometimes this time lag is so great that

* J. Am. Chem. Soc. xl. p. 1361 (1918).
† Trans. Far. Soc. xvii. p. 607 (1921–1922)

evaporation practically never occurs, but it may also become so small that the adsorbed molecules leave the surface before they are struck by other molecules from the gas phase. This conception of the mechanism of adsorption leads to the conclusion that an increase in the concentration of any molecular species in the gas phase will counteract the effect of the evaporation of this species from the surface in so far as it may be available for reaction in the heterogeneous phase and also in so far as it may remain as an obstacle to the adsorption of another gas. Thus, when oxygen is substituted for air, as in the experiments shown in fig. 6, the oxygen film becomes in effect more stable at high temperatures, and consequently a higher temperature is required to initiate the methane reaction than in the air mixtures. A similar explanation may also account for the decrease in the initiation temperatures in the methane air mixtures when the ratio of methane to air is increased, as shown in fig. 3.

Whilst the results obtained with the excess air and excess oxygen mixtures point to the conclusion that the methane itself must gain access to the platinum surface before reaction can take place, the experiments with excess methane mixtures, shown in fig. 4, indicate that combustion ceases under conditions which are obviously favourable to the adsorption of methane. The suppression of combustion in these mixtures occurs, however, when it may reasonably be supposed that most if not all of the oxygen has been removed from the surface of the wire, partly by evaporation and partly by combination with methane before combustion ceases. The active centres are now probably covered with methane only, and since no reaction takes place under these circumstances it appears that oxygen in the gas phase does not combine with the adsorbed methane. The results in general therefore lead to the conclusion that the heterogeneous combustion of methane on platinum involves the adsorption of both reactants.

My thanks are due to Professor W. T. David for his encouragement and for granting me every facility to carry out this work in his laboratory.

Engineering Department,
The University, Leeds.

XLIV. *Experiments on Supraconductive Tantalum.* By Dr. K. Mendelssohn *and* Miss J. R. Moore *.

Introduction.

THE determination of the magnetic threshold values in supraconductors, *i. e.*, the field strengths just sufficient to destroy supraconductivity, has proved to be of great value for the thermodynamical treatment [1], since it has been shown by experiment and theory that they indicate the difference in free energy between the supraconductive and the normal state. This relation has been verified for thallium [2], and calorimetric and magnetic experiments on tin, mercury, and lead [3] seem to indicate that it also holds for these substances, provided that they are sufficiently pure. The pure metals investigated so far are all distinguished by low melting-point, softness, and low characteristic temperature (Debye Θ). Until now no experiments of this kind have been carried out on the class of supraconductors with very different physical properties: high melting-point, hardness, and high Debye Θ as, Ta, Ti, etc.

Experiments on the magnetic threshold value, as well as on the change of induction, were therefore carried out on different samples of Ta. However, owing to the fact that the results obtained differed considerably from the behaviour of the other supraconductive elements our experiments so far can only be considered as a preliminary investigation.

Magnetic Threshold Values.

The magnetic disturbance of supraconductivity was determined in Ta-wire of 0·1 mm. diameter made by Siemens & Halske A. G., Berlin, and kindly given to us by Prof. F. Simon. The wire was mounted on a mica-plate and current and potential leads were connected by spot welding. The specimen was inserted in the experimental chamber of a helium liquefier [4]. The chamber was filled with helium gas and the temperature of the wire determined by the vapour pressure of the surrounding liquid helium. This arrangement proved satisfactory,

* Communicated by Prof. F. A. Lindemann, Ph.D., F.R.S.

as a change of the temperature in the liquefier of 0·01° was recorded in the specimen within less than 3 seconds.

The lower magnetic field strengths up to 1000 gauss were produced by solenoids, while for the higher fields an electro-magnet with iron core was employed. For this reason at higher field strength we determined the resistance as a function of temperature at different constant fields in order to avoid errors due to the hysteresis of the iron containing magnet. At field strengths below

Fig. 1.

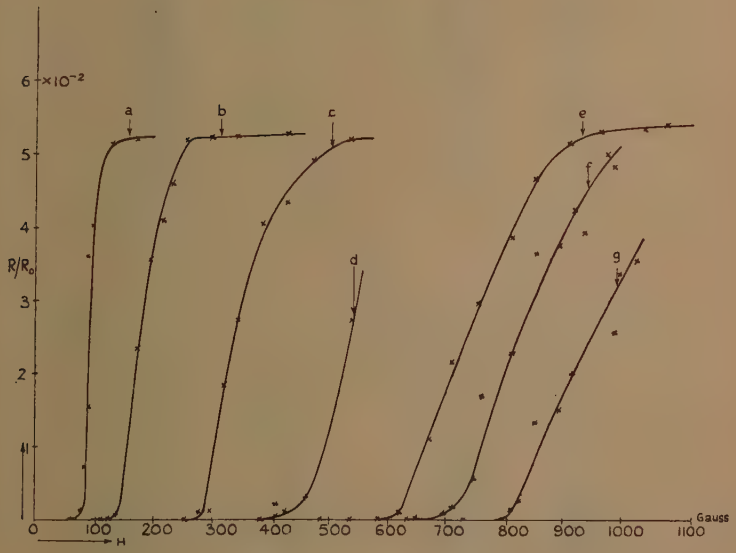

1000 gauss the resistance was determined as a function of the field strength at constant temperature.

Fig. 1 (Tables *a–g*), and fig. 2 (Tables 1–9), give the results at lower and higher field strength respectively. Fig. 3 gives the threshold curve indicating the field strengths at which half of the normal resistance was restored. Part of the threshold curve above 900 gauss seems to be displaced to lower temperatures. For these values a different piece of the wire was used, and it is possible that owing to inhomogeneity the threshold value is different in different parts of our wire.

The threshold curve of our Ta-wire differs in two essential points from the results obtained for all other pure metals. It is much steeper (1000–2000 gauss/

TABLE *a*.

4·325° K., $R_{\frac{1}{2}}$ at 90 gauss.

Field gauss.	$R/R_0 10^{-3}$.
103·5	40·3
87·0	35·9
70·2	7·05
64·2	1·15
49·7	0·0
68·5	1·15
77·0	15·07
94·9	40·15
128·5	51·3
171·0	52·0

TABLE *b*.

4·2° K., $R_{\frac{1}{2}}$ at 180 gauss.

Field gauss.	$R/R_0 10^{-3}$.
115·5	0·0
127·3	0·0
154·0	7·21
171·0	23·4
213·8	40·8
299·5	52·25
427·5	52·8
342·0	52·25
256·5	51·8
231·0	45·9
192·5	35·5
145·3	4·08
137·0	0·56

TABLE *c*.

4·03° K., $R_{\frac{1}{2}}$ at 338 gauss.

Field gauss.	$R/R_0 10^{-3}$.
256·5	0·0
342·0	27·2
427·5	43·3
535·0	52·0
543·0	52·0
385·2	40·6
471·0	49·2
299·5	1·15
278·0	1·15
319·0	18·3
256·5	00·0

TABLE *d*.

3·85° K., $R_{\frac{1}{2}}$ at 538 gauss.

Field gauss.	$R/R_0 10^{-3}$.
427·5	1·15
475·0	2·92
539·0	27·15
385·0	0·0
411·0	0·56
419·0	2·42

degree), and it is neither a parabola nor linear as $\left(\frac{dH}{dT}\right)$ passes a maximum at about 1700 gauss. A similar behaviour occurs in supraconductive alloys ($PbTl_2$), and could be explained by inhomogeneity of the specimen.

This assumption is supported by the fact that the transition temperature observed in this conductivity experi-

ment is higher than that which can be derived from experiments on the change of magnetic induction.

TABLE *e*.

3·68° K., $R_{\frac{1}{2}}$ at 742 gauss.

Field gauss.	$R/R_0 10^{-3}$.
1078	54·1
1037	53·7
965	53·1
908	51·6
852	46·4
812	38·6
756	29·7
711	21·5
670	10·95
487	0·0
538	0·0
608	0·84

TABLE *f*.

3·6° K., $R_{\frac{1}{2}}$ at 830 gauss.

Field gauss.	$R/R_0 10^{-3}$.
975	50·0
935	39·2
853	36·4
812	22·7
761	16·75
711	1·69
648	0·18
588	0·0
635	0·0
696	0·84
748	5·58
792	17·3
894	38·5
418	42·6
988	48·3

TABLE *g*.

3·51° K., $R_{\frac{1}{2}}$ at 960 gauss.

Field gauss.	$R/R_0 10^{-3}$.
1027	35·5
965	26·55
914	19·88
863	13·20
828	2·54
731	0·0
812	1·62
894	15·05
935	25·15
996	33·50

Magnetic Induction.

The change of induction was determined on three samples of tantalum.

Ta I were the spheres whose specific heat had been determined by Simon and Ruhemann [5]. They were made by Siemens & Halske A. G., and were given to us

by Prof. F. Simon. The purity of this sample is unknown.

Fig. 2.

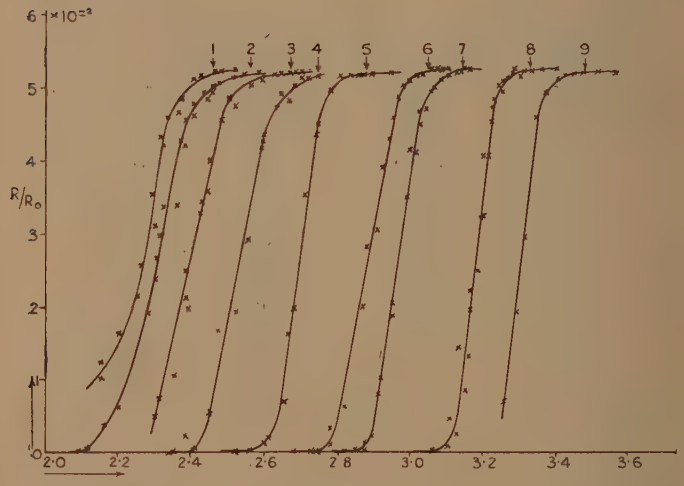

TABLE 1.

3110 gauss. $R_{\frac{1}{2}}$ at 2·245° K.

Temp. °K.	$R/R_0 10^{-3}$.	Temp. °PK.	$R/R_0 10^{-3}$.
2·15	10·2	2·15	12·3
2·20	16·2	2·25	21·4
2·26	25·4	2·30	30·9
2·29	35·05	2·32	41·8
2·31	42·9	2·365	46·2
2·33	45·7	2·40	50·3
2·37	48·2	2·43	51·4
2·405	50·75	2·48	52·0
2·415	51·4	2·52	52·3
2·46	52·0	2·56	52·4
2·52	52·4	2·615	52·4
		2·63	52·75
		2·68	52·75

Ta II was a rod of 2 mm. diameter and 65 mm. length, from Hopkin and Williams, the purity of which was given as 99 per cent.

TABLE 2.

3040 gauss. $R_{\frac{1}{2}}$ at 2·31° K.

Temp. °K.	$R/R_0 10^{-3}$.	Temp. °K.	$R/R_0 10^{-3}$.
		2·115	0·46
2·09	0·0	2·13	1·36
2·115	0·46	2·16	3·17
2·18	1·36	2·20	6·4
2·20	5·9	2·28	18·9
2·30	26·5	2·30	23·4
2·31	29·6	2·32	33·45
2·36	33·75	2·37	42·4
2·38	41·8	2·38	45·3
2·405	45·9	2·405	47·6
2·44	48·1	2·43	49·0
2·45	49·3	2·45	49·8
2·475	50·3	2·47	51·1
2·51	50·9	2·51	51·1
2·36	51·4	2·52	51·7
2·58	51·4	2·55	51·7
2·59	51·4	2·58	51·9
		2·62	51·9

TABLE 3.

2880 gauss. $R_{\frac{1}{2}}$ at 2·395° K.

Temp. °K.	$R/R_0 10^{-3}$.	Temp. °K.	$R/R_0 10^{-3}$.
2·30	4·70	2·31	7·1
2·38	24·6	2·38	21·0
2·425	34·2	2·42	32·7
2·45	43·25	2·45	39·8
2·50	47·9	2·48	45·1
2·55	50·2	2·52	47·25
2·59	50·7	2·56	50·0
2·63	51·4	2·59	50·8
2·65	51·4	2·625	51·3
2·30	4·73		
2·35	10·5		
2·39	19·6		
2·44	35·5		
2·50	48·4		
2·52	47·0		
2·58	51·0		
2·625	51·6		
2·57	51·2		
2·59	51·8		

Ta III was a rod of 1·9 mm. diameter and 35 mm. length from Harrington Bros. The purity of this specimen was given as 99·9 per cent.

TABLE 4.

2860 gauss. $R_{\frac{1}{2}}$ at 2·53° K.

Temp. °K.	$R/R_0 10^{-3}$.	Temp. °K.	$R/R_0 10^{-3}$.
2·38	2·4	2·37	0·0
2·595	43·1	2·41	0·46
2·675	47·9	2·45	4·7
2·71	50·8	2·52	19·0
2·805	51·3	2·55	28·9
2·86	51·3	2·59	42·4
2·47	16·5	2·63	46·9
2·545	30·1	2·68	49·9
2·59	41·3	2·70	51·1
2·64	48·75	2·74	51·1
2·715	51·6		

TABLE 5.

2160 gauss. $R_{\frac{1}{2}}$ at 2·69° K.

Temp. °K.	$R/R_0 10^{-3}$.	Temp. °K.	$R/R_0 10^{-3}$.
2·52	0·0	2·565	0·0
2·57	0·0	2·61	1·9
2·60	1·4	2·665	16·05
2·65	6·63	2·71	35·1
2·68	19·0	2·74	44·75
2·74	43·3	2·78	49·5
2·78	49·2	2·83	51·3
2·85	51·4	2·875	51·4
2·89	51·4		
2·94	51·4		

TABLE 6.

1680 gauss. $R_{\frac{1}{2}}$ at 2·88° K.

Temp. °K.	$R/R_0 10^{-3}$.	Temp. °K.	$R/R_0 10^{-3}$.
2·68	0·0	2·735	0·0
2·73	0·0	2·78	0·33
2·75	0·0	2·81	9·64
2·78	1·0	2·88	28·0
2·82	6·16	2·92	38·9
2·87	19·86	2·95	45·65
2·91	30·30	2·975	50·0
2·94	42·75	3·01	51·3
2·965	48·25	3·05	52·2
2·99	50·7	3·08	52·2
3·03	51·6		
3·06	52·2		
3·10	52·2		
3·15	52·4		

All three samples were first investigated by the method used by Keeley and Mendelssohn [3]. For this purpose

Table 7.

1570 gauss. $R_{\frac{1}{2}}$ at 2·96° K.

Temp. °K.	$R/R_0 10^{-3}$.	Temp. °K.	$R/R_0 10^{-3}$.
2·85	0·0	2·82	0·0
2·875	0·9	2·87	0·46
2·91	7·8	2·89	1·8
2·95	18·65	2·915	10·25
2·99	34·8	2·945	20·4
3·01	40·8	2·985	34·8
3·025	44·6	2·995	41·3
3·04	46·8	3·025	46·3
3·065	49·6	3·05	49·25
3·08	50·75	3·065	50·4
3·105	51·3	3·10	51·5
3·13	51·6	3·125	51·8
		3·135	52·0
		3·165	52·0

Table 8.

1120 gauss. $R_{\frac{1}{2}}$ at 3·175° K.

Temp. °K.	$R/R_0 10^{-3}$.	Temp. °K.	$R/R_0 10^{-3}$.
3·105	4·6	3·06	0·0
3·13	14·2	3·10	0·46
3·16	29·4	3·13	2·3
3·185	34·7	3·15	8·4
3·2	42·4	3·16	22·0
3·215	47·0	3·195	31·9
3·23	50·0	3·21	40·5
3·255	50·4	3·22	45·15
3·28	51·8	3·25	49·0
3·31	51·9	3·265	50·75
3·33	52·0	3·285	52·0
3·36	52·3	3·325	52·3
3·39	52·3	3·36	52·4
3·41	52·3	3·39	52·4

a rod of Ta I was made by grinding some spheres to cylindrical shape, and by welding them together.

At no temperature did Ta I and Ta II show any distinct field values at which the lines of force penetrated. The induction seemed, however, to decrease gradually. In

TABLE 9.

890 gauss. $R/R_{\frac{1}{2}}$ at 3·3° K.

Temp. °K.	$R/R_0 10^{-3}$.
3·255	6·9
3·29	19·0
3·31	29·2
3·345	45·5
3·37	49·0
3·40	50·9
3·425	51·2
3·45	51·5
3·51	51·7
3·56	51·7
3·62	51·7

Fig. 3.

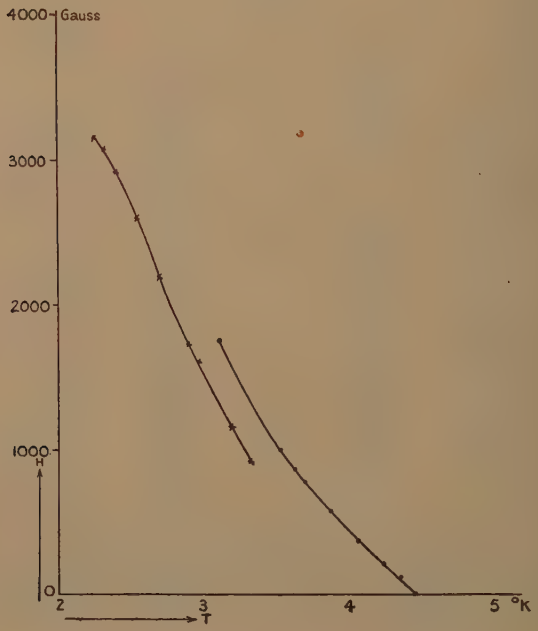

all cases a " freezing in " of the lines of force occurred, as has been observed in alloys. Ta III showed hardly any change of induction. Only at temperatures near 2° K. a very slight decrease in the permeability was noticeable.

This latter sample was tested again with a slightly different arrangement. Two coils with the same number of turns, but in opposite direction, were wound at some distance apart on a glass tube and the specimen was placed in one of them. The coils were put in series and connected to a ballistic galvanometer. When the coils were placed in a homogeneous external field, the ballistic throw of the galvanometer was zero so long as the specimen showed no change of permeability. The experiments with this method confirmed our first results, and again only below 2° K. a very small change of permeability occurred.

Finally, with this arrangement experiments were carried out on one of the spheres of Ta I. Owing to the shape of the specimen the results were somewhat complicated, and a blank experiment was therefore carried out by placing a tin sphere of the same size in the place of the tantalum sphere. The behaviour of supraconductive tin spheres has been investigated in detail by Mendelssohn and Babbitt [6]. From the field strengths at different temperatures at which magnetic flux first penetrated the specimen at the equator the penetration curve could be determined approximately (fig. 4). The experiments indicate, however, that there was no sharp field strength at which magnetic flux penetrated the supraconductive surface, but that the penetration of the magnetic field occurred more gradually. The " penetration curve " therefore merely indicates the field region in which the strongest change of induction occurs.

Conclusion.

The most striking feature of the results is the difference between the threshold and the " penetration " curve, which according to Gorter's treatment should coincide, and which actually coincide, apart from small deviations, for tin, as has been shown by Mendelssohn and Babbitt [6]. A behaviour similar to that of tantalum has been observed in supraconductive alloys [3]. Magnetic [7], and

calorimetric [8] measurements on alloys have led us to the conclusion that a " sponge " of high threshold value exists in the specimen which is responsible for the " freezing in " of magnetic flux and the difference in the threshold and the " penetration " curve. This assumption is strongly supported by recent experiments [9]. From the similarity of the results on tantalum therefore it appears possible that our specimens had the same structure as alloys. In alloys the formation of such a " sponge "

Fig. 4.

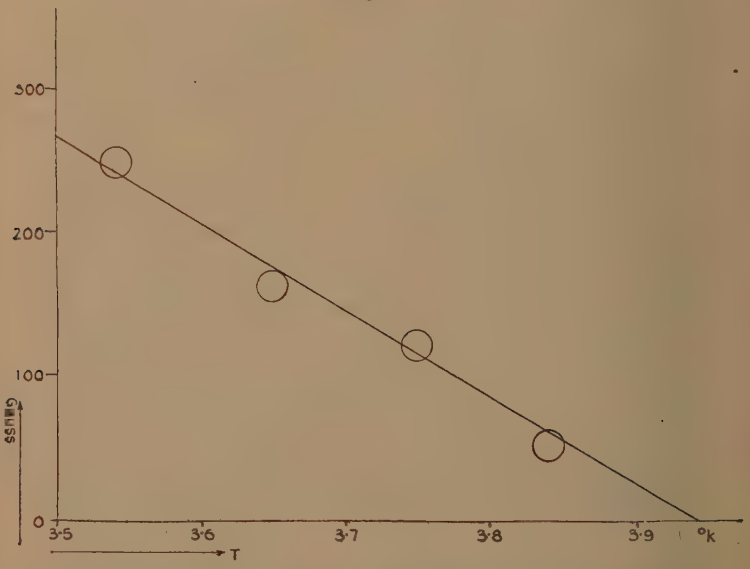

was suggested by their inhomogeneity, and it must be left to further more detailed investigation to find out whether this explanation also holds for tantalum.

As the purity of one of the samples was given as 99·9 per cent. the inhomogeneity may be due to disturbances of the lattice, which are not caused by impurities, but probably have to be ascribed to internal strain. The high threshold value may therefore be due not to a Ta-alloy, but even to pure Tantalum. We have pointed out in the case of alloys [7] [9], that the interpretation of the supraconductive state as a state of zero induction loses

its value for thermodynamical treatment as soon as regions are considered which are of the order of, or smaller than, the depth to which a magnetic field penetrates a supraconductor on its surface. The difference of free energy between the supraconductive and the normal metal at the same temperature will be much smaller for small isolated regions than for solid material, if we assume that a threshold field of the same strength destroys supraconductivity in both cases. If we postulate, however, that the difference in free energy between the two states shall be the same whether we consider small or wide supraconductive regions, we have to expect considerably higher magnetic threshold values for small regions. This would mean that supraconductivity should persist in higher field strengths in a very thin wire than in a thick wire of the same material at the same temperature.

A thermodynamical treatment of a partition into small supraconductive and normal regions has been recently attempted by Gorter [10] *. It has to be remembered, however, that such a spontaneous splitting up does not occur in pure supraconductive metals investigated so far. Only further experiments on pure Ta-specimens with undistorted lattice (if possible single crystals) can decide whether the splitting up in small supraconductive regions is spontaneous or caused by disturbances of the lattice.

An observation by Tarr and Wilhelm [11] on the magnetic behaviour of tantalum is in qualitative agreement with our experiments.

Summary.

(1) The magnetic threshold curve and the penetration curve of supraconductive tantalum were determined.

(2) The discrepancy between these curves has been discussed in respect to the thermodynamical behaviour of small supraconductive regions.

Our thanks are due to Professor F. A. Lindemann, F.R.S., for putting the facilities of the laboratory at our disposal, and for his interest in our work; to Dr. A. R. Meetham for his help during the experiments; and to

* *Added in proof.*—A more rigorous treatment has been carried out since by H. London, Proc. Roy. Soc. A, clii. p. 650 (1935).

Imperial Chemical Industries Ltd., who made this research possible for one of us.

References.

(1) C. J. Gorter and H. Casimir, *Physica*, i. p. 305 (1934).
(2) W. H. Keesom and J. A. Kok, *Comm. Phys. Lab.* Leiden, Nov. 230 *e* and 232 *a*.
(3) K. Mendelssohn and J. R. Moore, ' Nature,' cxxxiii. p. 413 (1934); T. C. Keeley and K. Mendelssohn, ' Nature,' cxxxiv. p. 773 (1934).
(4) F. Simon and E. Ahlberg, *Zeits. f. Phys.* lxxxi. p. 816 (1933).
(5) F. Simon and M. Ruhemann, *Zeits. f. Phys. Chem.* cxxix. p. 321 (1927).
(6) K. Mendelssohn and J. D. Babbitt, Proc. Roy. Soc. A, no. 873, cli. p. 316 (1935).
(7) K. Mendelssohn and J. R. Moore, ' Nature,' cxxxv. p. 826 (1935).
(8) K. Mendelssohn and J. R. Moore, Proc. Roy. Soc. A, no. 873, cli. p. 334 (1935).
(9) K. Mendelssohn, Proc. Roy. Soc. A, clii. p. 34 (1934).
(10) C. J. Gorter, *Physica*, ii. p. 449 (1935).
(11) F. G. A. Tarr and J. O. Wilhelm, Canad. Journ. Res. xii. p. 265 (1935).

XLV. *Asymptotic Solutions of Linear Differential Equations.* *By* Harold Jeffreys, *M.A., D.Sc., F.R.S.* *

AN asymptotic solution that I gave some years ago † and applied to certain tidal problems has received some attention in quantum physics. In my problems I was concerned only with the first term of the approximation, though means were provided for determining higher terms. In some recent developments the higher terms have been partially taken into account, and at the same time improvements in accuracy are being attempted. It seems desirable, therefore, to call attention afresh to a feature of the approximation that seems to have been overlooked.

The equation considered is taken in the form

$$\frac{d^2y}{dx^2} = (h^2\chi_0 + h\chi_1 + \chi_2)y, \quad . \quad . \quad . \quad . \quad (1)$$

where h is a large number and χ_0, χ_1 are functions of x,

* Communicated by the Author.
† Proc. Lond. Math. Soc. xxiii. pp. 428–436 (1923).

χ_0 not vanishing in the range considered. The attempted solution is in the form

$$y=\phi e^{h\omega}\left(1+\frac{f_1}{h}+\frac{f_2}{h^2}+\cdots\right), \quad . \quad . \quad . \quad (2)$$

whence by substituting and equating powers of h the terms may be found in turn. The solution is

$$\omega=\int \chi_0^{\frac{1}{2}}\,dx\,;\ \ \phi=\chi_0^{-\frac{1}{4}}\exp\int\frac{\chi_1}{2\omega}dx\,;\ \ 2\omega' f_1'=\chi_2-\frac{\phi''}{\phi}, \quad (3)$$

and if f_1 is omitted,

$$y\sim\chi_0^{-\frac{1}{4}}\exp\pm\int^x\left(h\chi_0^{\frac{1}{2}}+\frac{\chi_1}{2\chi_0^{\frac{1}{2}}}\right)dx. \quad . \quad . \quad (4)$$

The form that has been quoted, however*, is equivalent to

$$y\sim(h^2\chi_0+h\chi_1+\chi_2)^{-\frac{1}{4}}\exp\pm\int^x(h^2\chi_0+h\chi_1+\chi_2)\,dx. \quad (5)$$

At first sight this appears more accurate, since χ_2 is taken into account. But we see from (3) that χ_2 does not affect the solution until the term in h^{-1}, and if it is to be taken into account the rest of f_1, which will in general be of the same order of magnitude, should be included also.

A case is given in my paper (1.22) where the formula (4) is actually more accurate than (5).

Writing (3) in full, we have

$$f_1'=\frac{1}{8}\frac{\chi_0''}{\chi_0^{\frac{3}{2}}}-\frac{5}{32}\frac{\chi_0'^2}{\chi_0^{\frac{5}{2}}}-\frac{1}{4}\frac{\chi_1'}{\chi_0}+\frac{1}{4}\frac{\chi_1\chi_0'}{\chi_0^2}-\frac{1}{8}\frac{\chi_1^2}{\chi_0^{\frac{3}{2}}}+\frac{\chi_2}{2\chi_0}$$

$$=\frac{d}{dx}\left\{\frac{1}{8}\frac{\chi_0'}{\chi_0^{\frac{3}{2}}}-\frac{1}{4}\frac{\chi_1}{\chi_0}\right\}+\frac{1}{32}\frac{\chi_0'^2}{\chi_0^{\frac{5}{2}}}-\frac{1}{8}\frac{\chi_1^2}{\chi_0^{\frac{3}{2}}}+\frac{\chi_2}{2\chi_0},$$

whence

$$f_1=\frac{1}{8}\frac{\chi_0'}{\chi_0^{\frac{3}{2}}}-\frac{1}{4}\frac{\chi_1}{\chi_0}+\int^x\left(\frac{1}{32}\frac{\chi_0'^2}{\chi_0^{\frac{5}{2}}}-\frac{1}{8}\frac{\chi_1^2}{\chi_0^{\frac{3}{2}}}+\frac{\chi_2}{2\chi_0^{\frac{1}{2}}}\right)dx. \quad (6)$$

The lower limit may be chosen in any way that is convenient, for a constant addition to f_1 is equivalent to making an increase of order $1/h$ in the outside factor

* F. L. Arnot and G. O. Baines, Proc. Roy. Soc. A, cxlvi. p. 654 (1934).

of (4), or can be adjusted by a small change of the lower limit in the integral in (4).

The formula (6) should be the most accurate representation possible if h^{-2} is neglected, and any other formula not derivable from (3) will contain errors of order h^{-1} and will not in general be more accurate than (4).

Another way of deriving (6) is to assume

$$y=\exp\int \eta\, dx, \quad . \quad . \quad . \quad . \quad . \quad (7)$$

whence

$$\eta'+\eta^2=h^2\chi_0+h\chi_1+\chi_2. \quad . \quad . \quad . \quad . \quad (8)$$

Assuming

$$\eta=h\chi_0^{\frac{1}{2}}+\phi_0+\frac{\phi_1}{h} \quad . \quad . \quad . \quad . \quad . \quad (9)$$

and substituting in (8), we recover (6) on equating powers of h.

Near a zero of the coefficient in (1) the equation is that satisfied by the Airy integral, which is the relevant solution, and tables of this function as such would probably make continuation across such a point easier. All those yet published require transformation before they can be applied.

XLVI. *Application of Bessel Functions to the Solution of Problem of Motion of a Circular Disk in Viscous Liquid.* *By* Manohar Ray, *Calcutta* *.

Introduction.

It is known that the problem of the motion of a viscous liquid due to the slow rotation† of a body in the form of an ellipsoid of revolution about its axis can be solved with the help of the gravitational potential function of the ellipsoid, the fluid particles moving in circles perpendicular to the axis. The same method applies to translational motion ‡ of an ellipsoid. The case of the rotation of a circular disk is deduced from

* Communicated by the Author.

† M. Brillouin, 'Lecons sur la viscosité des liquides et des gaz,' T. 1 (Paris, 1907).

‡ H. Lamb, 'Hydrodynamics,' 6th ed. Art. 339.

that of the rotating ellipsoid of revolution by a limiting process in which the length of the axis of rotation is reduced to zero. In the present paper solutions of entirely new type in terms of Bessel functions are constructed applicable to the case of slow rotation of a circular disk in viscous liquid. The same method is applied to get solutions for the parallel and transverse motions of the disk, using every time integrals involving only Bessel functions. The couple and the resistance for rotation and translation, calculated from solutions obtained in this paper, are in agreement with the values calculated by the other method.

Part I.—Motion due to Rotation of Circular Disk.

1. *Solutions of the Equations of Motion.*

Let us make use of the cylindrical coordinates (r, ϕ, z), with the plane of the disk as the plane $z=0$, and the axis of rotation through the centre of the disk as the z-axis. As usual, we assume the radial and the axial components of velocity to be zero, and the azimuthal component v_ϕ and the pressure p to be independent of ϕ. The equations of motion, omitting the product terms, then reduce to the single equation,

$$\frac{\partial^2 v_\phi}{\partial r^2}+\frac{1}{r}\frac{\partial v_\phi}{\partial r}-\frac{v_\phi}{r^2}+\frac{\partial^2 v_\phi}{\partial z^2}=0. \quad . \quad . \quad . \quad (1)$$

The boundary conditions for the problem are,

$$\text{on} \quad z=0 \quad \text{and} \quad r \leqslant a, \quad v_\phi=r\widehat{\omega}, \quad . \quad . \quad . \quad . \quad (2)$$

$\widehat{\omega}$ being the angular velocity of the disk, and at infinity,

$$v_\phi=0. \quad . \quad . \quad . \quad . \quad . \quad . \quad . \quad . \quad (3)$$

We try to satisfy the above equation (1) by the assumption

$$v_\phi=e^{-\lambda z}\mathrm{R}, \quad . \quad . \quad . \quad . \quad . \quad . \quad (4)$$

where R is a function of r only, vanishing at infinity, so that the boundary condition (3) is automatically satisfied.

With the substitution (4), equation (1) becomes

$$\frac{d^2\mathrm{R}}{dr^2}+\frac{1}{r}\frac{d\mathrm{R}}{dr}+\left(\lambda^2-\frac{1}{r^2}\right)\mathrm{R}=0,$$

the solution of which is

$$\mathrm{R}=\mathrm{C}\mathrm{J}_1(\lambda r), \quad . \quad . \quad . \quad . \quad . \quad . \quad (5)$$

where C is some constant and J the symbol for Bessel function.

Thus, finally, we get

$$v_\phi = Ce^{-\lambda z}J_1(\lambda r). \quad . \quad . \quad . \quad . \quad . \quad (6)$$

This solution evidently satisfies the condition (3) for infinity (for region below the plane z is to be taken negative), but not the condition (2), that is, when we come on the disk itself. But we can construct the correct solution satisfying both the boundary conditions out of this.

2. *Construction of Integral Solutions.*

In order to satisfy the boundary condition (2) on the plane $z=0$, we construct a new solution in the form of infinite integral from the elementary solution (6).

Since

$$J_1(\lambda r) = \frac{\lambda r}{2}[J_0(\lambda r) + J_2(\lambda r)] \text{ *},$$

we assume for v_ϕ,

$$v_\phi = Ar\left[\int_0^\infty e^{-\lambda z}J_0(\lambda r)\sin a\lambda \frac{d\lambda}{\lambda} + \int_0^\infty e^{-\lambda z}J_2(\lambda r)\sin a\lambda \frac{d\lambda}{\lambda}\right]. \quad . \quad . \quad (7)$$

Now since

$$\int_0^\infty J_0(\lambda r)\sin a\lambda \frac{d\lambda}{\lambda} \quad \text{and} \quad \int_0^\infty J_2(\lambda r)\sin a\lambda \frac{d\lambda}{\lambda} \quad \text{both exist} \dagger,$$

$$\operatorname*{Lt}_{z\to 0}\int_0^\infty e^{-\lambda z}J_0(\lambda r)\sin a\lambda \frac{d\lambda}{\lambda} = \int_0^\infty J_0(\lambda r)\sin a\lambda \frac{d\lambda}{\lambda} \ddagger,$$

and

$$\operatorname*{Lt}_{z\to 0}\int_0^\infty e^{-\lambda z}J_2(\lambda r)\sin a\lambda \frac{d\lambda}{\lambda} = \int_0^\infty J_2(\lambda r)\sin a\lambda \frac{d\lambda}{\lambda},$$

due to uniform convergence of the integrals on the left in an interval including $z=0$.

Coming to (7) we have on $z=0$,

$$v_\phi = Ar\left[\int_0^\infty J_0(\lambda r)\sin a\lambda \frac{d\lambda}{\lambda} + \int_0^\infty J_2(\lambda r)\sin a\lambda \frac{d\lambda}{\lambda}\right].$$

* Watson, 'Theory of Bessel Functions,' 1922, p. 17, §2·12 (1).
† Watson, 'Theory of Bessel Functions,' 1922, p. 405, § 13·42.
‡ Bromwich, 'Theory of Infinite Series,' Art. 172.

The integrals have different values according as $r<$ or $>a$, and we give below the values* of the integrals and of few more used here or hereafter.

$$\left.\begin{aligned}
&\int_0^\infty J_0(\lambda r)\sin a\lambda\frac{d\lambda}{\lambda}=\begin{cases}\dfrac{\pi}{2} & \text{when } r\leqslant a\\ \sin^{-1}\dfrac{a}{r} & \text{when } r\geqslant a\end{cases},\\
&\int_0^\infty J_1(\lambda r)\sin a\lambda\frac{d\lambda}{\lambda}=\begin{cases}\dfrac{a}{a+\sqrt{a^2-r^2}} & \text{when } r\leqslant a\\ \dfrac{a}{r} & \text{when } r\geqslant a\end{cases},\\
&\int_0^\infty J_1(\lambda r)\cos a\lambda\frac{d\lambda}{\lambda}=\begin{cases}0 & \text{when } r\leqslant a\\ \dfrac{\sqrt{r^2-a^2}}{r} & \text{when } r\geqslant a\end{cases},\\
&\int_0^\infty J_2(\lambda r)\sin a\lambda\frac{d\lambda}{\lambda}=\begin{cases}0 & \text{when } r\leqslant a\\ \frac{1}{2}\sin\left(2\sin^{-1}\dfrac{a}{r}\right) & \text{when } r\geqslant a\end{cases},\\
&\int_0^\infty J_0(\lambda r)\sin a\lambda\,d\lambda=\begin{cases}\dfrac{1}{\sqrt{a^2-r^2}} & \text{when } r<a\\ 0 & \text{when } r>a\end{cases},\\
&\int_0^\infty J_1(\lambda r)\sin a\lambda\,d\lambda=\begin{cases}0 & \text{when } r<a\\ \dfrac{a}{r\sqrt{r^2-a^2}} & \text{when } r>a\end{cases},\\
&\int_0^\infty J_1(\lambda r)\cos a\lambda\,d\lambda=\begin{cases}\dfrac{\sqrt{a^2-r^2}-a}{r\sqrt{a^2-r^2}} & \text{when } r<a\\ \dfrac{1}{r} & \text{when } r>a\end{cases},\\
&\int_0^\infty J_2(\lambda r)\sin a\lambda\,d\lambda=-\begin{cases}\dfrac{(a-\sqrt{a^2-r^2})^2}{r^2\sqrt{a^2-r^2}} & \text{when } r<a\\ \dfrac{2a}{r^2} & \text{when } r>a\end{cases}.
\end{aligned}\right\}\quad(8)$$

* 'Theory of Bessel Functions,' 1922, p. 405, § 13·42

Substituting the values of the integrals from (8) we have on $z=0$,

$$v_\phi = \tfrac{1}{2}\mathrm{A}r\pi, \quad \text{for } r \leqslant a, \quad . \quad . \quad . \quad . \quad . \quad (9)$$

and

$$\mathrm{A}r\left[\sin^{-1}\frac{a}{r} + \frac{1}{2}\sin\left(2\sin^{-1}\frac{a}{r}\right)\right], \quad \text{for } r \geqslant a. \quad . \quad (10)$$

Comparing (2) and (9), we get

$$\mathrm{A} = \frac{2\widehat{\omega}}{\pi}. \quad . \quad . \quad . \quad . \quad . \quad . \quad . \quad (11)$$

Thus the solution (7) satisfies all the boundary conditions. It should be noted that this solution is valid only for $z \geqslant 0$. For the region $z < 0$, the same solution with the sign of z changed is to be taken. The continuity of the solution of $z=0$ is obvious. But we have to see that not only the velocity but also all the stress components on $z=0$, $z \geqslant a$ are continuous. We now prove that to provide for this condition we have to extend (7) further by the addition of another term. For continuity of stress it is evident that the shear $\mu \dfrac{\partial v_\phi}{\partial z}$ should be zero * on the plane $z=0$ for $r > a$.

Now from (7), we have on differentiation,

$$\frac{\partial v_\phi}{\partial z} = -\mathrm{A}r\left[\int_0^\infty e^{-\lambda z}\mathrm{J}_0(\lambda r)\sin a\lambda\, d\lambda + \int_0^\infty e^{-\lambda z}\mathrm{J}_2(\lambda r)\sin a\lambda\, d\lambda\right],$$

so that on $z=0$, $r > a$,

$$\frac{\partial v_\phi}{\partial z} = -\mathrm{A}r\,\frac{\sin\left(2\sin^{-1}\dfrac{a}{r}\right)}{\sqrt{r^2-a^2}},$$

substituting the values of the integrals from (8).

$$= -\frac{2\mathrm{A}a}{r}. \quad . \quad . \quad . \quad . \quad . \quad . \quad . \quad (12)$$

* The values of $\dfrac{\partial v_\phi}{\partial z}$ on $z=0$, $r>a$, calculated from those of v_ϕ for $z>0$ and $z<0$ are equal and opposite; hence for continuity of stress we make these values zero by adding another term.

Thus to the solution (7) we must add an additional term which will not violate the boundary condition (2), and whose z-derivative will annul (12). Let us take

$$v_\phi = Ar\left[\int_0^\infty e^{-\lambda z}J_0(\lambda r)\sin a\lambda\frac{d\lambda}{\lambda}+\int_0^\infty e^{-\lambda z}J_2(\lambda r)\sin a\lambda\frac{d\lambda}{\lambda}\right]$$
$$+B\int_0^\infty e^{-\lambda z}J_1(\lambda r)\cos a\lambda\frac{d\lambda}{\lambda}. \quad . \quad (13)$$

The value of the last integral in (13) is zero on the disk $z=0$, $r\leqslant a$, hence it does not affect the boundary condition (2).

Now the z-derivative of the last term is

$$-B\int_0^\infty e^{-\lambda z}J_1(\lambda r)\cos a\lambda\, d\lambda,$$

whose value on

$$z=0,\ r>a \quad \text{is} \quad -\frac{B}{r}. \quad . \quad . \quad . \quad . \quad (14)$$

Hence from (12), (13), and (14), we get

$$\text{on} \quad z=0,\ r>a, \qquad \frac{\partial v}{\partial z}=-\frac{2aA}{r}-\frac{B}{r}.$$

This should be zero by our assumption, which gives

$$B=-2aA. \quad . \quad . \quad . \quad . \quad . \quad . \quad . \quad (15)$$

Thus the complete solution is obtained in the form

$$v_\phi=\frac{2\widehat{\omega}r}{\pi}\int_0^\infty e^{-\lambda z}J_0(\lambda r)\sin a\lambda\frac{d\lambda}{\lambda}$$
$$+\frac{2\widehat{\omega}r}{\pi}\int_0^\infty e^{-\lambda z}J_2(\lambda r)\sin a\lambda\frac{d\lambda}{\lambda}-\frac{4a\widehat{\omega}}{\pi}\int_0^\infty e^{-\lambda z}J_1(\lambda r)\cos a\lambda\frac{d\lambda}{\lambda}.$$
$$. \quad . \quad . \quad (16)$$

This gives, for instance,

$$\text{on} \quad z=0,\ r\leqslant a, \qquad v_\phi=r\widehat{\omega},$$

$$\text{and on} \quad z=0,\ r\geqslant a, \quad v_\phi=\frac{2\widehat{\omega}r}{\pi}\left[\sin^{-1}\frac{a}{r}-\frac{a\sqrt{r^2-a^2}}{r^2}\right].$$

This agrees exactly with the result found in the paper cited in the introduction.

3. *Calculation of Moment of Rotation.*

Due to rotation the disk experiences a resisting couple from the viscous fluid which tends to oppose the rotation. This couple is given by the moment of the shear on it. For the shear we have

$$\tau = -\mu \frac{\partial v_\phi}{\partial z},$$

the moment of the shear in a circular ring of radius r and breadth dr is

$$d\mathrm{M} = r\,df\tau = -2\pi\mu\, r^2 \frac{\partial v_\phi}{\partial z}\,dr,$$

so that

$$\mathrm{M} = -2\pi\mu \int_0^a r^2 \frac{\partial v_\phi}{\partial z}\,dr \text{ on the disk } z=0.$$

That is,

$$\begin{aligned}\mathrm{M} = 4\widehat{\omega}\mu \Big[& \int_0^a r^3\,dr \Big\{ \int_0^\infty e^{-\lambda z} \mathrm{J}_0(\lambda r) \sin a\lambda\, d\lambda \\ & + \int_0^\infty e^{-\lambda z} \mathrm{J}_2(\lambda r) \sin a\lambda\, d\lambda \Big\} \\ & - 2a \int_0^a r^2\,dr \int_0^\infty e^{-\lambda z} \mathrm{J}_1(\lambda r) \cos a\lambda\, d\lambda \Big] \quad \text{on } z=0 \\ = 4\widehat{\omega}\mu \Big[& \int_0^a r^3\,dr \Big\{ \int_0^\infty \mathrm{J}_0(\lambda r) \sin a\lambda\, d\lambda \\ & + \int_0^\infty \mathrm{J}_2(\lambda r) \sin a\lambda\, d\lambda \Big\} \\ & - 2a \int_0^a r^2\,dr \int_0^\infty \mathrm{J}_1(\lambda r) \cos a\lambda\, d\lambda \Big],\end{aligned}$$

since these latter integrals exist,

$$\begin{aligned} = 4\widehat{\omega}\mu \Big[& \int_0^a r^3\,dr \Big\{ \frac{1}{\sqrt{a^2-r^2}} - \frac{(a-\sqrt{a^2-r^2})^2}{r^2\sqrt{a^2-r^2}} \Big\} \\ & - 2a \int_0^a r^2\,dr \Big\{ \frac{1}{r} - \frac{a}{r\sqrt{a^2-r^2}} \Big\} \Big]. \end{aligned}$$

Calculating these integrals we get at once,

$$\mathrm{M} = \frac{16}{3}\,\widehat{\omega}\mu a^3. \quad \ldots\ldots\ (17)$$

Doubling this result for the two sides of the disk, we get for the total moment of rotation,

$$M=\frac{32}{3}\hat{\omega}\mu a^3. \quad . \quad . \quad . \quad . \quad . \quad . \quad . \quad (18)$$

This value is the same as found in the other paper.

Part II.—Disk moving broadside-on.

1. *Solutions of the Equations of Motion.*

We regard in this case the disk to be fixed and the fluid to be streamng past it with uniform velocity U perpendicular to the disk. The direction of motion is taken as z-direction and the plane of the disk the z-plane with origin at the centre. In cylindrical coordinates (r, ϕ, z), assuming the azimuthal component of velocity to be zero, and all quantities to be independent of ϕ, the equations of motion, neglecting the quadratic terms, are

$$\left.\begin{aligned}\frac{\partial^2 v_r}{\partial r^2}+\frac{1}{r}\frac{\partial v_r}{\partial r}-\frac{v_r}{r^2}+\frac{\partial^2 v_r}{\partial z^2}&=\frac{1}{\mu}\frac{\partial p}{\partial r},\\ \frac{\partial^2 v_z}{\partial r^2}+\frac{1}{r}\frac{\partial v_z}{\partial r}+\frac{\partial^2 v_z}{\partial z^2}&=\frac{1}{\mu}\frac{\partial p}{\partial z}.\end{aligned}\right\} \quad . \quad . \quad . \quad (1)$$

To this is added the equation of continuity

$$\frac{\partial v_r}{\partial r}+\frac{v_r}{r}+\frac{\partial v_z}{\partial z}=0. \quad . \quad . \quad . \quad . \quad . \quad (2)$$

The boundary conditions are

on $z=0$, $\quad r\leqslant a$, $\quad v_z=v_r=0$, $\quad . \quad . \quad . \quad . \quad . \quad . \quad (3)$

and at infinity, $\quad v_z=U$, $\quad v_r=0$. $\quad . \quad . \quad . \quad . \quad . \quad (4)$

To solve equations (1) we take a stream function ψ in any meridian plane, given by

$$v_r=-\frac{1}{r}\frac{\partial \psi}{\partial z}, \quad v_z=\frac{1}{r}\frac{\partial \psi}{\partial r}, \quad . \quad . \quad . \quad . \quad (5)$$

which satisfies the equation (2) automatically.

Let us try the following assumptions

$$\psi=z^n e^{-\lambda z}R_1, \quad p=p_0+e^{-\lambda z}R_2, \quad . \quad . \quad . \quad (6)$$

where R_1 and R_2 are functions of r only, vanishing at infinity.

Making these substitutions in equations (1), we get

$$\frac{\lambda z^n}{r}\left(\frac{d^2R_1}{dr^2}-\frac{1}{r}\frac{dR_1}{dr}+\lambda^2 R_1\right)$$

$$-\frac{nz^{n-1}}{r}\left(\frac{d^2R_1}{dr^2}-\frac{1}{r}\frac{dR_1}{dr}+3\lambda^2 R_1\right)+\frac{3\lambda n(n-1)z^{n-2}}{r}R_1$$

$$-\frac{n(n-1)(n-2)z^{n-3}}{r}R_1=\frac{1}{\mu}\frac{dR_2}{dr},$$

and

$$\frac{z^n}{r}\left(\frac{d^3R_1}{dr^3}-\frac{1}{r}\frac{d^2R_1}{dr^2}+\frac{1}{r^2}\frac{dR_1}{dr}+\lambda^2\frac{dR_1}{dr}\right)$$

$$-\frac{2\lambda n z^n}{r}\frac{dR_1}{dr}+\frac{n(n-1)z^{n-2}}{r}\frac{dR_1}{dr}=-\frac{\lambda}{\mu}R_2.$$

These two equations are consistent only when $n=0$ or $n=1$. Taking $n=1$ we get as conditions of validity for all values of z,

$$\frac{d^2R_1}{dr^2}-\frac{1}{r}\frac{dR_1}{dr}+\lambda^2R_1=0,$$

$$\frac{d^2R_1}{dr^2}-\frac{1}{r}\frac{dR_1}{dr}+3\lambda^2R_1+\frac{r}{\mu}\frac{dR_2}{dr}=0,$$

$$\frac{d^3R_1}{dr^3}-\frac{1}{r}\frac{d^2R_1}{dr^2}+\frac{1}{r^2}\frac{dR_1}{dr}+\lambda^2\frac{dR_1}{dr}=0,$$

$$2\frac{dR_1}{dr}-\frac{r}{\mu}R_2=0.$$

These equations can all be satisfied by

$$R_1=Br J_1(\lambda r), \quad . \quad . \quad . \quad . \quad . \quad . \quad (7)$$

$$R_2=2B\mu\lambda J_0(\lambda r), \quad . \quad . \quad . \quad . \quad . \quad (8)$$

B being some constant and J the symbol for Bessel function.

These give

$$v_r=Be^{-\lambda z}(\lambda z-1)J_1(\lambda r), \quad . \quad . \quad . \quad . \quad . \quad (9)$$

$$v_z=Be^{-\lambda z}\lambda z J_0(\lambda r), \quad . \quad . \quad . \quad . \quad . \quad . \quad (10)$$

$$p=p_0+2B\mu\lambda e^{-\lambda z}J_0(\lambda r). \quad . \quad . \quad . \quad . \quad (11)$$

To facilitate the satisfaction of our boundary conditions we add to the above solutions (9), (10), and (11) some additional terms involving another constant A which are

solutions of (1) and (2) with p=constant. A complete system of elementary solutions may thus be written as

$$v_r = \mathrm{B}e^{-\lambda z}(\lambda z - 1)\mathrm{J}_1(\lambda r) + \mathrm{A}e^{-\lambda z}\mathrm{J}_1(\lambda r), \quad . \quad . \quad (12)$$

$$v_z = \mathrm{B}e^{-\lambda z}\lambda z\mathrm{J}_0(\lambda r) + \mathrm{A}e^{-\lambda z}\mathrm{J}_0(\lambda r), \quad . \quad . \quad . \quad . \quad (13)$$

and

$$p = p_0 + 2\mathrm{B}\mu\lambda e^{-\lambda z}\mathrm{J}_0(\lambda r), \quad . \quad . \quad . \quad . \quad (14)$$

the constant value of p obtained from the second system being involved in p_0.

2. *Construction of Integral Solutions.*

In order to satisfy the boundary conditions we construct new solutions in the forms of integrals from these elementary solutions (12), (13), and (14) thus,

$$v_z = \mathrm{B}z\int_0^\infty e^{-\lambda z}\mathrm{J}_0(\lambda r)\sin a\lambda\, d\lambda + \mathrm{A}\int_0^\infty e^{-\lambda z}\mathrm{J}_0(\lambda r)\sin a\lambda \frac{d\lambda}{\lambda} + \mathrm{U}, \quad . \quad (15)$$

$$v_r = \mathrm{B}z\int_0^\infty e^{-\lambda z}\mathrm{J}_1(\lambda r)\sin a\lambda\, d\lambda - \mathrm{B}\int_0^\infty e^{-z\lambda}\mathrm{J}_1(\lambda r)\sin a\lambda \frac{d\lambda}{\lambda} + \mathrm{A}\int_0^\infty e^{-\lambda z}\mathrm{J}_1(\lambda r)\sin a\lambda \frac{d\lambda}{\lambda}, \quad . \quad (16)$$

and

$$p = p_0 + 2\mu\mathrm{B}\int_0^\infty e^{-\lambda z}\mathrm{J}_0(\lambda r)\sin a\lambda\, d\lambda. \quad . \quad . \quad . \quad . \quad . \quad (17)$$

The addition of a constant term U to v_z does not disturb the equations (1) and (2), which, it should be remembered, are satisfied by both sets of terms involving A and B separately in (12), (13), and (14).

The above system evidently satisfies the boundary conditions at infinity.

Now, since the integrals

$$\int_0^\infty \mathrm{J}_0(\lambda r)\sin a\lambda\, d\lambda, \quad \int_0^\infty \mathrm{J}_0(\lambda r)\sin a\lambda \frac{d\lambda}{\lambda}, \quad \int_0^\infty \mathrm{J}_1(\lambda r)\sin a\lambda\, d\lambda$$

and

$$\int_0^\infty \mathrm{J}_1(\lambda r)\sin a\lambda \frac{d\lambda}{\lambda}$$

exist, we have

$$\operatorname*{Lt}_{z\to 0}\int_0^\infty e^{-\lambda z}J_0(\lambda r)\sin a\lambda\, d\lambda=\int_0^\infty J_0(\lambda r)\sin a\lambda\, d\lambda \text{ and so on.}$$

Substituting the values of the integrals from (8) in Part I., we have on $z=0$,

$$v_z=\frac{A\pi}{2}+U \qquad \text{for } r<a,$$

$$A\sin^{-1}\frac{a}{r}+U \qquad \text{for } r>a,$$

and

$$v=(A-B)\frac{a}{a+\sqrt{a^2-r^2}} \qquad \text{for } r<a$$

$$(A-B)\frac{a}{r} \qquad \text{for } r>a.$$

Thus the boundary condition (8) is satisfied if we take

$$\frac{A\pi}{2}+U=0, \quad . \quad . \quad . \quad . \quad . \quad . \quad (18)$$

and

$$A-B=0. \quad . \quad . \quad . \quad . \quad . \quad . \quad (19)$$

Hence the required solution is

$$v_z=U\left[1-\frac{2}{\pi}\int_0^\infty (1+\lambda z)e^{-\lambda z}J_0(\lambda r)\sin a\lambda\frac{d\lambda}{\lambda}\right], \quad (20)$$

$$v_r=-\frac{2Uz}{\pi}\int_0^\infty e^{-\lambda z}J_1(\lambda r)\sin a\lambda\, d\lambda, \quad . \quad . \quad . \quad . \quad (21)$$

and

$$p=p_0-\frac{4\mu U}{\pi}\int_0^\infty e^{-\lambda z}J_0(\lambda r)\sin a\lambda\, d\lambda. \quad . \quad . \quad . \quad . \quad (22)$$

These solutions, (20), (21), and (22), evidently satisfy the equations (1) and (2) and the boundary conditions (3) and (4), and are valid for the positive side of the z-plane. For the negative side of the z-plane we have to construct new solutions which will coincide with the above system on the plane $z=0$ in the region outside the disk, subject to the same boundary conditions.

This solution valid on the negative side of the z-plane is found, after some manipulation, to be $z \leqslant 0$.

$$v_z = U\left[1 - \frac{z}{\pi}\int_0^\infty e^{\lambda z}(1-\lambda z)J_0(\lambda r)\sin a\lambda \frac{d\lambda}{\lambda}\right], \quad (23)$$

$$v_r = -\frac{2Uz}{\pi}\int_0^\infty e^{\lambda z}J_1(\lambda r)\sin a\lambda\, d\lambda, \quad . \quad . \quad . \quad . \quad (24)$$

$$p = p_0 + \frac{4\mu U}{\pi}\int_0^\infty e^{\lambda z}J_0(\lambda r)\sin a\lambda\, d\lambda. \quad . \quad . \quad . \quad (25)$$

Note the plus sign before U in the expression for p in (25), as opposed to the negative sign in (22). The equations of motion will be satisfied for these values of v_r, v_z, and p. For $z=0$, $r>a$, p is continuous, as then the integral portion vanishes (by equation (8), Part I.).

3. *Calculation of the Resistance.*

We now consider the continuity of the stress-system on the plane $z=0$. On $z=$constant, the stress components are

$$p_{zz} = -p + 2\mu\frac{\partial v_z}{\partial z}, \quad p_{rz} = \mu\left(\frac{\partial v_z}{\partial r} + \frac{\partial v_r}{\partial z}\right),$$

$$p_{\phi z} = \mu\left(\frac{\partial v_\phi}{\partial z} + \frac{1}{r}\frac{\partial v_z}{\partial \phi}\right).$$

For $z>0$, we easily find from the first system (20), (21), (22),

$$p_{zz} = -p_0 + \frac{4\mu U}{\pi}\int_0^\infty e^{-\lambda z}J_0(\lambda r)\sin a\lambda\, d\lambda$$

$$+ \frac{4\mu U}{\pi}z\int_0^\infty e^{-\lambda z}\lambda J_0(\lambda r)\sin a\lambda\, d\lambda,$$

$$p_{zr} = \frac{4\mu U}{\pi}z\int_0^\infty e^{-\lambda z}\lambda J_1(\lambda r)\sin a\lambda\, d\lambda,$$

and

$$p_{z\phi} = 0.$$

Thus on $z=0$,

$$\left.\begin{aligned} p_{zz} &= -p_0 + \frac{4\mu U}{\pi}\cdot\frac{1}{\sqrt{a^2-r^2}}, \quad \text{for } r<a, \\ &-p_0 \quad . \quad . \quad . \quad . \quad . \quad \text{for } r>a, \end{aligned}\right\} \quad . \quad (26)$$

since $\int_0^\infty \lambda J_0(\lambda r) \sin a\lambda \, d\lambda$ exists and $p_{zr}=0$, since $\int_0^\infty \lambda J_1(\lambda r) \sin a\lambda d\lambda$ also exists.

It should be noticed that p_{zz} has infinite value on the edge $r=a$. This is due to the fact that the boundary condition taken at the edge does not correspond to real motion. Nevertheless the total resistance will be finite.

Calculating the stress-system from the solutions (23), (24), (25) for the negative side of the z-plane and proceeding to the limit $z=0$, we find

$$\left.\begin{aligned} p_{zz} &= -p_0 - \frac{4\mu U}{\pi} \frac{1}{\sqrt{a^2-r^2}}, \quad \text{for } r<a, \\ &\quad -p_0 \qquad\qquad\qquad\quad \text{for } r>a, \end{aligned}\right\} \quad . \quad (27)$$

and $p_{zr}=0$.

Thus the total stress perpendicular to the disk in the direction of motion is

$$P_{zz} = \frac{8\mu U}{\pi} \cdot \frac{1}{\sqrt{a^2-r^2}}.$$

The resistance experienced by the disk calculated in the usual way is

$$R = 2\pi \int_0^a r P_{zz} \, dr = 16\mu a U. \quad . \quad . \quad . \quad (28)$$

This result agrees with that found in the work cited in the introduction.

Part III.—Disk moving edgeways.

1. *Solutions of Equations of Motion.*

Our next part is to find out the resistance when the disk moves edgeways. We suppose the disk to be fixed and the fluid to be streaming past the disk with uniform velocity U parallel to the plane of the disk. Introducing cylindrical coordinates (r, ϕ, z) with the plane of the disk as the z-plane, we see that in the present case v_r, v_ϕ, v_z and p are not necessarily independent of ϕ, so that, neglecting product terms, the equations of motion are

$$\left.\begin{aligned}
&\frac{\partial^2 v_r}{\partial r^2}+\frac{1}{r}\frac{\partial v_r}{\partial r}-\frac{v_r}{r^2}+\frac{1}{r^2}\frac{\partial^2 v_r}{\partial \phi^2}-\frac{2}{r^2}\frac{\partial v_\phi}{\partial \phi}+\frac{\partial^2 v_r}{\partial z^2}=\frac{1}{\mu}\frac{\partial p}{\partial r},\\
&\frac{\partial^2 v_\phi}{\partial r^2}+\frac{1}{r}\frac{\partial v_\phi}{\partial r}-\frac{v_\phi}{r^2}+\frac{1}{r^2}\frac{\partial^2 v_\phi}{\partial \phi^2}+\frac{2}{r^2}\frac{\partial v_r}{\partial \phi}+\frac{\partial^2 v_\phi}{\partial z^2}=\frac{1}{\mu r}\frac{\partial p}{\partial \phi},\\
&\frac{\partial^2 v_z}{\partial r^2}+\frac{1}{r}\frac{\partial v_z}{\partial r}+\frac{1}{r^2}\frac{\partial^2 v_z}{\partial \phi^2}+\frac{\partial^2 v_z}{\partial z^2}=\frac{1}{\mu}\frac{\partial p}{\partial z},
\end{aligned}\right\} \quad (1)$$

and the equation of continuity is

$$\frac{\partial v_r}{\partial r}+\frac{v_r}{r}+\frac{1}{r}\frac{\partial v_\phi}{\partial \phi}+\frac{\partial v_z}{\partial z}=0. \quad . \quad . \quad . \quad (2)$$

The boundary conditions are

on $z=0$, $r \leqslant a$, $v_r=v_\phi=v_z=0$,

and at infinity,

$$v_r\cos\phi-v_\phi\sin\phi=U, \quad v_r\sin\phi+v_\phi\cos\phi=0, \quad v_z=0. \quad . \quad . \quad . \quad (3)$$

To solve the differential equations (1) and (2) we first take $p=$constant and substituting

$$v_r=e^{-\lambda z}\cos\phi R_1, \quad v_\phi=\pm e^{-\lambda z}\sin\phi R_1, \quad v_z=e^{-\lambda z}\cos\phi R_2,$$

where R_1, R_2 are functions of r only, we easily find that

$$\left.\begin{aligned}
v_r&=\{AJ_0(\lambda r)+BJ_2(\lambda r)\}e^{-\lambda z}\cos\phi,\\
v_\phi&=\{-AJ_0(\lambda r)+BJ_2(\lambda r)\}e^{-\lambda z}\sin\phi,\\
v_z&=(-A+B)e^{-\lambda z}\cos\phi J_1(\lambda r).
\end{aligned}\right\} \quad . \quad (4)$$

But I have found it difficult to guess a solution of (1) and (2) when p is not constant, for which case the following indirect course has been adapted. Making use of three dimensional rectangular coordinates (x, y, z), the corresponding equations of motion are

$$\left.\begin{aligned}
&\frac{\partial^2 u}{\partial x^2}+\frac{\partial^2 u}{\partial y^2}+\frac{\partial^2 u}{\partial z^2}=\frac{1}{\mu}\frac{\partial p}{\partial x},\\
&\frac{\partial^2 v}{\partial x^2}+\frac{\partial^2 v}{\partial y^2}+\frac{\partial^2 v}{\partial z^2}=\frac{1}{\mu}\frac{\partial p}{\partial y},\\
&\frac{\partial^2 w}{\partial x^2}+\frac{\partial^2 w}{\partial y^2}+\frac{\partial^2 w}{\partial z^2}=\frac{1}{\mu}\frac{\partial p}{\partial z},
\end{aligned}\right\} \quad . \quad . \quad . \quad (5)$$

and

$$\frac{\partial u}{\partial x}+\frac{\partial v}{\partial y}+\frac{\partial w}{\partial z}=0.$$

For the first case, taking p=constant and putting

$$u=e^{-\lambda z}u_1 \quad v=e^{-\lambda z}v_1, \quad w=e^{-\lambda z}w_1,$$

where u_1, v_1, w_1 are functions of x and y, the above equations reduce to

$$\left.\begin{aligned} &\frac{\partial^2 u_1}{\partial x^2}+\frac{\partial^2 u_1}{\partial y^2}+\lambda^2 u_1 =0,\\ &\frac{\partial^2 v_1}{\partial x^2}+\frac{\partial^2 v_1}{\partial y^2}+\lambda^2 v_1 =0,\\ &\frac{\partial^2 w_1}{\partial x^2}+\frac{\partial^2 w_1}{\partial y^2}+\lambda^2 w_1=0,\\ &\frac{\partial u_1}{\partial x}+\frac{\partial v_1}{\partial y}-\lambda w_1 =0. \end{aligned}\right\} \quad . \quad . \quad . \quad (6)$$

Passing now over to polar coordinates $(r,\ \phi)$ in the xy-plane, the first three equations of (6) are of the form

$$\frac{\partial^2 u_1}{\partial r^2}+\frac{1}{r}\frac{\partial u_1}{\partial r}+\frac{1}{r^2}\frac{\partial^2 u_1}{\partial \phi^2}+\lambda^2 u_1=0, \quad . \quad . \quad (7)$$

similar equations holding for v_1 and w_1 and the last equation, if v_r and v_ϕ be the components of u_1 and v_1 in the directions of r and ϕ, is

$$\frac{\partial v_r}{\partial r}+\frac{v_r}{r}+\frac{1}{r}\frac{\partial v_\phi}{\partial \phi}-\lambda w_1=0. \quad . \quad . \quad . \quad . \quad (8)$$

Putting $u_1=\mathrm{R}$, $v_1=0$, and $w_1=-\mathrm{R}_1\cos\phi$, so that $v_r=\mathrm{R}\cos\phi$, $v_\phi=-\mathrm{R}\sin\phi$, we at once see from (7) and (8) that

$$\mathrm{R}=\mathrm{J}_0(\lambda r) \quad \text{and} \quad \mathrm{R}_1=\mathrm{J}_1(\lambda r).$$

Similarly, putting

$$u_1=\mathrm{R}_2\cos 2\phi, \quad v_1=\mathrm{R}_2\sin 2\phi, \quad w_1=\mathrm{R}_3\cos\phi,$$

we see that

$$\mathrm{R}_2=\mathrm{J}_2(\lambda r) \quad \text{and} \quad \mathrm{R}_3=\mathrm{J}_1(\lambda r).$$

Thus when p=constant, we have

$$\left.\begin{aligned} u&=e^{-\lambda z}\{\mathrm{A}\mathrm{J}_0(\lambda r)+\mathrm{B}\mathrm{J}_2(\lambda r)\cos 2\phi\},\\ v&=\mathrm{B}e^{-\lambda z}\mathrm{J}_2(\lambda r)\sin 2\phi,\\ w&=e^{-\lambda z}(-\mathrm{A}+\mathrm{B})\mathrm{J}_1(\lambda r)\cos\phi. \end{aligned}\right\} \quad . \quad (9)$$

These solutions are the same as (4), which can be seen immediately if we remember that

$$v_r = u\cos\phi + v\sin\phi, \quad v_\phi = -u\sin\phi + v\cos\phi.$$

To solve the equations (5) when p is not constant, we put

$$u=(\lambda z-1)e^{-\lambda z}u_1', \quad v=(\lambda z-1)e^{-\lambda z}v_1',$$
$$w=\lambda z e^{-\lambda z}w_1' \quad p=\mu e^{-\lambda z}p_1',$$

where u_1', v_1', w_1', and p_1' are functions of x and y only.

Then the equations (5) give the following set of equations

$$\left.\begin{aligned} &\frac{\partial^2 u_1'}{\partial x^2}+\frac{\partial^2 u_1'}{\partial y^2}+\lambda^2 u_1'=0, \\ &\frac{\partial^2 v_1'}{\partial x^2}+\frac{\partial^2 v_1'}{\partial y^2}+\lambda^2 v_1'=0, \\ &\frac{\partial^2 w_1'}{\partial x^2}+\frac{\partial^2 w_1'}{\partial y^2}+\lambda^2 w_1'=0, \\ &\frac{\partial u_1'}{\partial x}+\frac{\partial v_1'}{\partial y}-\lambda w_1'=0, \end{aligned}\right\} \quad \left.\begin{aligned} &p_1'=2\lambda w_1', \\ &-2\lambda^2 u_1'=\frac{\partial p_1'}{\partial x}, \\ &-2\lambda^2 v_1'=\frac{\partial p_1'}{\partial y}, \\ &\frac{\partial^2 p_1'}{\partial x^2}+\frac{\partial^2 p_1'}{\partial y^2}+\lambda^2 p_1'=0. \end{aligned}\right\}$$

. . (10) . . (10*a*)

The equations (10) in u_1', v_1', w_1' are the same as (6), of which a set of solutions is (9). Hence for p not equal to constant, we can take the following solutions:

$$\left.\begin{aligned} u &= (\lambda z-1)e^{-\lambda z}u_1' = (\lambda z-1)e^{-\lambda z}\{\mathrm{C}J_0(\lambda r)+\mathrm{D}J_2(\lambda r)\cos 2\phi\}, \\ v &= (\lambda z-1)e^{-\lambda z}v_1' = \mathrm{D}(\lambda z-1)e^{-\lambda z}J_2(\lambda r)\sin 2\phi, \\ w &= \lambda z e^{-\lambda z}w_1' = \lambda z e^{-\lambda z}(-\mathrm{C}+\mathrm{D})J_1(\lambda r)\cos\phi, \\ p &= \mu e^{-\lambda z}p_1' = 2\mu\lambda e^{-\lambda z}(-\mathrm{C}+\mathrm{D})J_1(\lambda r)\cos\phi. \end{aligned}\right\}$$

. . . (11)

The value of p has been obtained from the set of equations (10*a*) involving p_1', all of which are satisfied by (11). If now we try to satisfy the equations (1) and (2) with v_r, v_ϕ, v_z, p obtained by putting

$$v_r = u\cos\phi + v\sin\phi, \quad v_\phi = -u\sin\phi + v\cos\phi, \quad v_z = w, \quad p = p,$$

and using the values of u, v, w, and p from the solutions (11), we find that those equations are satisfied only when

$$\mathrm{D}+\mathrm{C}=0. \quad . \quad . \quad . \quad . \quad . \quad . \quad (12)$$

A complete system of solutions is obtained by adding together the solutions (9) and (11).

2. *Construction of Integral Solutions.*

In order to satisfy the boundary conditions which in the rectangular system are

on $z=0$, $r \leqslant a$, $\quad u=v=w=0$, ... (13)

and at infinity, $\quad u=\mathrm{U}$, $v=w=0$, ... (14)

we construct integral solutions from the elementary solutions obtained from (9) and (11). These solutions can be written as, adding a constant to u,

$$\left.\begin{aligned}
u &= \mathrm{U}+(\mathrm{A}-\mathrm{C})\int_0^\infty e^{-\lambda z}\mathrm{J}_0(\lambda r)\sin a\lambda\,\frac{d\lambda}{\lambda} \\
&\quad +(\mathrm{B}-\mathrm{D})\cos 2\phi\int_0^\infty e^{-\lambda z}\mathrm{J}_2(\lambda r)\sin a\lambda\,\frac{d\lambda}{\lambda} \\
&\quad +Cz\int_0^\infty e^{-\lambda z}\mathrm{J}_0(\lambda r)\sin a\lambda\,d\lambda \\
&\quad +\mathrm{D}z\cos 2\phi\int_0^\infty e^{-\lambda z}\mathrm{J}_2(\lambda r)\sin a\lambda\,d\lambda, \\
v &= (\mathrm{B}-\mathrm{D})\sin 2\phi\int_0^\infty e^{-\lambda z}\mathrm{J}_2(\lambda r)\sin a\lambda\,\frac{d\lambda}{\lambda} \\
&\quad +\mathrm{D}z\sin 2\phi\int_0^\infty e^{-\lambda z}\mathrm{J}_2(\lambda r)\sin a\lambda\,d\lambda, \\
w &= (\mathrm{B}-\mathrm{A})\cos\phi\int_0^\infty e^{-\lambda z}\mathrm{J}_1(\lambda r)\sin a\lambda\,\frac{d\lambda}{\lambda} \\
&\quad +(\mathrm{D}-\mathrm{C})z\cos\phi\int_0^\infty e^{-\lambda z}\mathrm{J}_1(\lambda r)\sin a\lambda\,d\lambda, \\
p &= p_0+2\mu(\mathrm{D}-\mathrm{C})\cos\phi\int_0^\infty e^{-\lambda z}\mathrm{J}_1(\lambda r)\sin a\lambda\,d\lambda.
\end{aligned}\right\} \quad (15)$$

These solutions evidently satisfy the condition (14).

From (15) we have on $z=0$, $r \leqslant a$, on substituting the values of the integrals from (8) in Part I.,

$$u=\mathrm{U}+(\mathrm{A}-\mathrm{C})\frac{\pi}{2},$$

$$v=0,$$

$$w=0, \quad \text{if } \mathrm{A}-\mathrm{B}$$

Thus conditions (13) are satisfied if

$$A-C=-\frac{2U}{\pi}, \quad \ldots\ldots \quad (16)$$

and

$$A=B. \quad \ldots\ldots \quad (17)$$

3. *Calculation of Resistance.*

Now calculating the stress components

$$p_{zz}=-p+2\mu\frac{\partial w}{\partial z}, \; p_{zy}=\mu\left(\frac{\partial v}{\partial z}+\frac{\partial w}{\partial y}\right), \; p_{zx}=\mu\left(\frac{\partial u}{\partial z}+\frac{\partial w}{\partial x}\right),$$

from the solutions (15) and coming to the limit $z\to 0$, we see that

$$(p_{zz})_{z=0}=-p_0,$$

$$(p_{zy})_{z=0}=\mu(2D-B)\sin 2\phi\int_0^\infty J_2(\lambda r)\sin a\lambda\, d\lambda=0,$$

which vanishes on putting

$$2D=B, \quad \ldots\ldots \quad (18)$$

and

$$(p_{zx})_{z=0}=\mu\left[(2C-A)\int^\infty J_0(\lambda r)\sin a\lambda\, d\lambda + (2D-B)\int_0^\infty J_2(\lambda r)\sin a\lambda\, d\lambda\right]$$

$$=\mu(2C-A)\int_0^\infty J_0(\lambda r)\sin a\lambda\, d\lambda,$$

using (18).

The solutions for the negative side of the z-plane are obtained by simply reversing the sign of z in (15), and it is easily found that the solutions thus obtained satisfy the differential equations (5).

Calculating the resistance experienced by the disk, on the upper side, we have

$$R=2\pi\int_0^a (p_{zx})_{z=0} r\, dr$$

$$=2\pi\mu(2C-A)\int_0^a r\, dr\int_0^\infty J_0(\lambda r)\sin a\lambda\, d\lambda$$

$$=2\pi\mu a(2C-A).$$

Doubling the result for the two sides of the disk we get

$$R = 4\mu\pi(2C - A). \quad . \quad . \quad . \quad . \quad . \quad (19)$$

Thus the distributions of velocity and pressure are given by (15) with the constants determined by (12), (16), (17), and (18), which give also A and C, and further

$$2C - A = \frac{8U}{3\pi}.$$

Hence the total resistance experienced by the disk is

$$R = \frac{32}{3} a\mu U. \quad . \quad . \quad . \quad . \quad . \quad . \quad (20)$$

This result agrees quite well with that found by the other method.

In conclusion I wish to express my gratefulness to Prof. N. R. Sen for his kind help in this work.

United College of Science
and Technology, Calcutta.
17th July, 1935.

XLVII. *Light and Gravitation.*

By F. Tavani *.

LET O′ be the moving origin of a reference frame, describing a curve in a two-dimensional space, T and N unit vectors taken as axes of the moving frame on the tangent and the normal respectively to the curve described by $O'_1 - u_1 u_2$ the components of the velocity of O′ along the said axes, v the velocity of which u_1 and u_2 are the components at the times t_1 and t_2 correspondent to the same segment of the path and measured on the two axes of time †. Let O be the initial position of O′, $1/\rho$ the curvature of the path at the time mentioned, c the velocity of light as measured along one of the axes, P a luminous point, $\beta_1\,\beta_2$ the FitzGerald contraction along the axes T and N ‡, in whose directions the origin

* Communicated by the Author.

† F. Tavani, "The Meaning of Time in Lorentz Transformation," Phil. Mag., May 1935.

‡ F. Tavani, "Generalization of Lorentz Transformation," Phil. Mag., July, 1934.

moves, we have then for the expression of the velocity of P :

$$\frac{dP}{dt} = (c+\gamma_1 t_1)N+(c-\gamma_2 t_2)T, \quad . \quad . \quad (1)^*$$

where

$$\gamma_1=\beta_1(c+u_1)\frac{v}{\rho}, \quad \gamma_2=\beta_2(c+u_2)\frac{v}{\rho}.$$

We call these quantities, by analogy with the accelerated motion of a falling body, the acceleration of light along the axes T and N.

This analogy becomes still closer when we assume v to be so small that the quantities, v the arc and u_1 its tangent, tend towards a common limit †, so that γ_1 becomes $\beta_1\left(\frac{cv}{\rho}+\frac{v^2}{\rho}\right)N$ or $\frac{v^2}{\rho}$ for v very small. Thus the law of the motion of a luminous point along N, coincides within realizable circumstances with that of the fall of a heavy body, and this identity calls for a theory of gravitation such as to account for the similar behaviour of these two apparently so different cases.

The study of the phenomenon of gravitation can be divided into two parts :—(1) The origin and existence of the motion itself ; (2) the law of the motion. This second part is the object of this note. The first part, dealing with how does the motion come to exist, belongs to the construction of a synthetical view of the history of the motion of energy under all its forms, and to the question of whether there has ever been such an origin. Gravitation is only one form of motion in such general process, and when seen in this vast process it loses that aspect of a secret and mysterious agency with which it appears in a first study to our senses, as we shall see.

The general equation of the velocity of a point P * referred to a moving frame, whose origin O′ moves with a velocity v, becomes the equation (1), as already mentioned, when the velocity of P is the velocity of light. For a falling body referred to a moving frame, whose origin is a terrestrial point on the equator and the moving

* F. Tavani, "The Velocity of Light and the Generalized Lorentz Transformation," Phil. Mag., Nov. 1935, p. 839.

† Since $\lim \frac{u_1}{v} = \lim \frac{\text{tang } v}{v} = 1$.

axes T and N are respectively unit vectors on the tangent to the equator and the vertical passing through O′, its acceleration is $\frac{v^2}{\rho}$, ρ being the terrestrial radius of the equator. Both cases are particular cases of the general equation * above mentioned, and what is important is that the equation is established through a purely mathematical process, independently of any experimental fact and without introducing any notion of force or any characteristic property belonging to the substance of the falling body. If experiments concerning the falling of bodies were not known the said equation would guide us towards the experimental confirmation of the equation. What the equation supposes is only the reference of a point or a moving point to a moving frame, such as one of those frames with which nature supplies us, and not to any frame of fixed origin, arbitrarily chosen by us as it is supposed in the Theory of Relativity †. The reference reveals two characteristics of the motion, viz.: (1) A contraction or expansion in length denoted by $\beta_1, \beta_2, \beta_3$ ‡ in the linear direction of the motion of the origin, and (2) an acceleration along the axis N at the point of curvature $1/\rho$; and since these characteristics of the motion are independent of any intrinsic property of the moving bodies the suggestion arises whether they are due to factors different from those which individuate a body in its state of motion or rest.

Descartes assumes the position of a point O as being given, and through the reference to a frame of origin O quantities are supposed to be as they appear, while in reality the motion of the frame affects them in a way which remains hidden just because the motion of the origin remains hidden.

The intervention of a moving frame in the interpretation of phenomena begins with the experiment of Michelson and Morley. In that case the moving frame has as its origin a terrestrial point, and there is assumed that the earth describes with a constant velocity rectilinear segments of its orbit, within infinitesimal intervals of time, an approximate hypothesis, which is found to be sufficient

* Phil. Mag., Nov. 1935, *loc. cit.* p. 838, equation (4).

† A. S. Eddington, ' The Mathematical Theory of Relativity,' edition 1922, pp. 225 & 239, and pp. 41 & 42.

‡ Phil. Mag. 1934, *loc. cit.*

to solve the problem raised by that experiment. We could go further, and see that there are as many moving frames as there are planets or perceptual points within the planetary space. From the idea of a moving frame we passed to the conception of space-time, as the seat of phenomena, more suitable than the abstract geometrical space of Descartes, separated from time. Space without time, as that of Cartesian frame, is an abstraction, just as is time without space, viz., without motion *. It is motion that makes time visible in space ; but space-time, with a frame whose origin moves in a uniform and rectilinear motion, is also an abstraction, as we shall see. There are four coordinates, and analytically it is represented by a Lorentz transformation, which we shall call "of the simple type," to distinguish it from the "generalized Lorentz transformation" *, in which the origin, instead of moving in a space of one dimension, as it is assumed in the previous type, moves in a space of two, three, and higher geometrical dimensions along curved paths as are the orbits of planets and stars. The case of frames moving along such orbits is the real case which we find in nature, and to the generalized transformation of such case corresponds a space-time of six dimensions †. Frames in such a space give us a real representation of phenomena, and we shall see what becomes of gravitation when expressed through them. Meanwhile it is well to remember that fix Cartesian frames, as well as frames whose origin moves in straight lines, are unable to represent the phenomena as they are. None has ever seen what the world looks like when seen from these frames. We have already pointed out to what is due the success of a straight moving frame in Michelson-Morley experiment. Such frames do not exist in nature, and to devise methods in order to get our knowledge of the physical world free from them is like trying to eliminate imaginary intruders. On the other hand, moving frames along orbits described by heavenly bodies are not arbitrary frames, they are the frames with which nature supplies us, and we cannot avoid their interfering with our observations. We know our world from this earth, which is, so to speak, the observatory allotted to us by nature. The question for us is not to

* Within the realm of physics.

† Phil. Mag., July 1934, *loc. cit.* p. 190, and May 1935, p. 1056.

eliminate the use of frames, but to find a method of mathematical analysis founded on the use of frames supplied to us by nature—that is to say, of frames whose origin moves with a law which at first we assume to know with a certain approximation *.

With a frame whose origin moves in a space of three dimensions, in the Cartesian meaning, a space-time of

* The whole of the analytical geometry assumes a new aspect when to the simple coordinates x, y, z taken on to a Cartesian frame of fixed origin we replace X, Y, Z (Phil. Mag., July 1934, p. 190) of a frame whose origin moves with a given law. The change which so takes place in the analytical expressions of geometrical entities is followed by a corresponding change in the analytical dynamics, amongst the formulæ of which is of fundamental importance the expression of the velocity of a point P referred to a frame whose origin describes a curve (Phil. Mag., Nov. 1935). In the geometry of moving frames a point P is analytically expressed by the equation $\mathrm{P}=\mathrm{O}'+\beta_1(\mathrm{X}-u_1t_1)\mathrm{T}+\beta_2(\mathrm{Y}-u_2t_2)\mathrm{N}$ (Phil. Mag. *loc. cit.*) in the case that P does not participate in the motion of O′. If P possesses the motion of O′, so that it is fixed relatively to the said origin, then we have $\mathrm{P}=\mathrm{O}'+c_1\mathrm{T}+c_2\mathrm{N}$, where c_1 and c_2 are constant coordinates, and using for O′ its equation (4) p. 188 *loc. cit.*, we have $\mathrm{P}=\mathrm{O}+(\phi_1(t_1)\eta_1+\phi_2(t_2)\theta_1+c_1)\mathrm{T}+(\phi_1(t_1)\eta_2+\phi_2(t_2)\theta_2+c_2)\mathrm{N}$. From these equations we derive the expression of $\frac{d\mathrm{P}}{dt}$.

From the equation (4) Phil. Mag., Nov. 1935, expressing the value of $\frac{d\mathrm{P}}{dt}$, we can pass by means of a successive derivation to the expressions of $\frac{d^2\mathrm{P}}{dt^2}$, $\frac{d^3\mathrm{P}}{dt^3}$ $\cdots$ $\frac{d^n\mathrm{P}}{dt^n}$, and in each derivation we can always replace the quantities T′ and N′ by their values in function of N and T respectively by using the above formulæ of Frenet, giving T′ in function N and N′ in function of T. It is at this point that the theory of the moving frames leads to the conception of hyperspaces. For the expression of $\frac{d\mathrm{P}}{dt}$ two dimensions, those of T and N are sufficient. In order to pass from $\frac{d\mathrm{P}}{dt}$ to $\frac{d^2\mathrm{P}}{dt^2}$ we introduce a third dimension B, and from $\frac{d^2\mathrm{P}}{dt^2}$ to $\frac{d^3\mathrm{P}}{dt^3}$ a fourth dimension, that of unit vector c defined like TNB and perpendicular to the said vectors, the relation of perpendicularity being expressed *only analytically* *. The successive derivation of P and the correspondent introduction of a hypervector leads to the expression of $\frac{d^n\mathrm{P}}{dt^n}$ in a space of a space of $(n+1)$ dimensions, n being the index of the derivation. Thence it is easy to see that $\frac{v^2}{\rho}$ expresses the acceleration along N only in the case that the origin describes a plane curve, and this is a particular case of the more general one, in which the origin describes a path of a higher order.

* See Phil. Mag., April 1921, "Motion and Hyperspace," and *Atti della Reale Accademia delle Scienze d. Torino*, April 1924, note by the author.

six dimensions is attached, which, as far as our experience goes, coincides with our physical space, viz., with the seat of physical phenomena. In fact, with the moving origin a clock is also given, which marks the time of any event referred to the moving frame. The clock moves with the same motion of the origin, just as clocks on this earth move with the earth across the space, and for this reason are at rest relatively to the origin, while the hands move with a motion which is uniform relatively to the origin of the frame.

Since the clock moves with the origin O′, its motion takes place also along the three (or two) components of the velocity of O′, so that we have three (or two) values of time—t_1, t_2, t_3 *—each value in the direction of each component.

With the time of the clock we assume also the path of the origin to be given, the clock and the origin moving along the same path, as the clocks on this earth move with the same motion of the earth, therefore with t_1, t_2, t_3, also the unity vectors T, N, B, taken respectively on the tangent, normal and binormal to the path of O_1, are given. So if the curve of the path and the clock which is at rest relatively to the origin, with which it moves along the same path, are given, a frame of six axes—T, N, B, t_1, t_2, t_3 is determined. If we assume in our physical space a point, say on the earth or any planet, as the origin of a frame and a clock at rest relatively to it, the point thus taken will be the origin of a moving frame in a space of six dimensions, and such a space, as far as experience goes, coincides with the physical space.

In space-time of six dimensions thus defined T, N, B are functions of time, T function of t_1, N of t_2, B of t_3. Limiting ourselves to the frame (T N) the derivates of T and N are

$$\frac{d\mathrm{T}}{dt_1} = \frac{v}{\rho}\mathrm{N}, \quad \frac{d\mathrm{N}}{dt_2} = -\frac{v}{\rho}\mathrm{T}.$$

These equations stand on a purely mathematical ground, independent of any experience, free from any hypothesis about the presence of any force. It is through these

* See Phil. Mag., May 1935, p. 105. In order to determine the values t_1, t_2, t_3 it is sufficient to solve a problem of elementary mathematics, viz., to express the motion of a point describing a circumference while the centre of the latter moves along one of the geometrical axes with a velocity which is the velocity of O′ along the said axis.

equations that in the equation (1)—that is to say, the expression of $\frac{dP}{dt}$—appears the acceleration $\frac{v^2}{\rho}$, which is the value to which tends $\frac{u_1 v}{\rho}$, the nearer is v to the tangential component u_1. The acceleration is along the normal N, just as it happens in the phenomenon of gravitation.

Thus we arrive at the conclusion that "if an origin O′ describes with a velocity v a path ds of curvature $\frac{1}{\rho}$, the motion of a point P along the normal N possesses an acceleration $\frac{v^2}{\rho}$, independently of any hypothesis about the substance of P, whether P be a particle of light or of matter." If we ask, then, what is the phenomenon of gravitation: gravitation is simply the experimental confirmation of this conclusion.

If the origin O′ is fixed or describes a straight line, so that N is constant, the acceleration of the type $\frac{v^2}{\rho}$, which is the type verified by experience, would vanish. In fact in this case we would have $\frac{1}{\rho} = 0 \therefore \frac{v^2}{\rho} = 0$. Therefore for the existence of the acceleration $\frac{v^2}{\rho}$ it is necessary and sufficient that O′ should describe an orbit or curved path, a conclusion confirmed by our model of the universe.

After eliminating force as the cause of the acceleration along N let us see whether force may be the cause of the curvature of the path along T.

Such belief is expressed in the principle of inertia:—"A body starts from its position of rest through the action of a force, and does not change the speed *and direction*, but through the action of another force." Of this principle there is no evidence either *à priori* or *à posteriori* viz., experimentally

If an experiment is performed within the limits of a room our observation remains shut within such limits that we cannot perceive how facts really happen. A billiard ball, for instance, seems to describe a straight

line, but if we could refer the motion of the ball to the centre of the earth or of the sun we would see how far is the path from being a straight line. A similar remark applies for the constancy of the velocity. Nor is there an *à priori* evidence of the principle : indeed, there is no reason why our space should open straight paths to motion rather than curved paths, or that motion should spontaneously cover a straight rather than a curved path. It is obvious that in the geometrical space of fix origins and straight paths in order to explain gravitation and orbits we had to resort to factors outside of the motion, viz., to forces. In the geometrical Cartesian space, separated from time, T is constant and $T'=0$, while in the space-time of six dimensions, which coincides with our physical space, T is a function of time and $T'\neq 0$, so that this characteristic extends also to N and B. Therefore, while in the space of straight paths, viz., in the geometrical Cartesian space, which was assumed to represent our physical space, a spontaneous motion, viz., free from the continuous action of a force, is uniform and rectilinear, in a space of orbits a spontaneous motion is naturally accelerated and curvilinear, such as is observed in the fall of a body along N, the apparent vertical described by the body being in reality a curve formed by the successive positions of the body on the vector N during the rotary motion of the frame T N round the origin O′.

The above interpretation of the phenomenon of gravitation is based upon an interpretation of our physical space—that is to say, from the interpretation of our physical space as a space of orbits or a space-time of six dimensions we pass to the meaning of gravitation as the form of the natural motion, free from forces, in such a space. It is a new method of interpreting phenomena, different from the old one, according to which we pass from the meaning of phenomena supplied by a mere intuition to the nature of the space.

There are still, however, astronomical phenomena which seem to require, in order to explain their reciprocal positions, the work of some agency or condition which, although different from that mysterious attraction with which energy throughout its different stages up to that of matter seems to be endowed, they seem to express a certain action dependent on the distance. This may supply us with a new idea of force; this fact,

however, in linked with the history of energy from any of its moments, which we may assume as initial, down to the stage of matter, and such process becomes comparatively intelligible once the structure of our space is understood in the terms described in this note.

61 Burton Road,
London, S.W. 9.

XLVIII. *Probability in Wave Mechanics.*

By E. T. Hanson, *B.A.* *

Introduction.

IF it is possible to obtain the fundamental equations of wave mechanics from the principles of statistical mechanics the procedure should throw much light upon their interpretation.

Attempts to found the wave theory upon those principles have, however, met with very limited success.

Having by some means obtained a wave equation it has been found that the most satisfactory procedure is to associate the intensity of the wave with a probability of occurrence. The theory, thus established, is coherent, and the results have met with marked success. It is, however, necessary to establish the foundations more securely.

We must satisfy ourselves, from considerations of probability, as to how the association of intensity with a probability of occurrence can be justified, and it must also be shown that the wave equation itself is derivable from statistical probability theory.

It appears to be necessary to introduce into statistical theory a link, previously missing, which is essential for the direct derivation of the fundamental equations from the principles of statistical mechanics. The present paper introduces this link, which leads to an alternative interpretation of the ψ-function, and considers the significance of what is here called the probability of observed occurrence as distinct from the probability of occurrence. The probability of observed occurrence

* Communicated by the Author.

is fundamental, and the paper is largely concerned with its interpretation. In fact, the main problem is to determine the probability that some entity is observed in a given position at a given time in the light of Planck's hypothesis. The probability that a system is in an observable condition in a given configuration at a given time is defined, for Planck's hypothesis undoubtedly raises the question of observability.

This probability, which is of considerable importance, is shown to be a wave function. We have to find what is represented by the intensity of the wave.

Suppose that there is an equal probability that a property, belonging to a system, may be associated with any one of a cloud of points moving in a configuration space. Then the probability of occurrence of the property within a small region of the configuration space is proportional to the number of points within the region. If the moving points are very numerous they may be taken to form a continuous fluid.

If, then, some variable represents the relative probability of occurrence of a property, it may be visualized as the density of the property in a statistical fluid.

It may be inferred, from consideration of Planck's hypothesis, that the probability of a particle or electron being in a given position is not necessarily the same as the probability that it is observed in that position. The points constituting a cloud may move in strict accordance with dynamical laws, and this motion, which is unobserved, may be independent of Planck's constant h, while the observed motions depend upon h. The density of the cloud in the unobserved motion is a measure of the probability of occurrence.

It may be preferred to call this the probability of observed occurrence when $h=0$, assuming that observations are possible when such is the case.

The existence of h introduces marked changes into our classical conceptions, and the probability of observed occurrence may have no meaning without Planck's hypothesis.

The significant property which may be associated with every one of a cloud of points is the electric charge $-e$, for the charge is assumed to be constant and does not change in relativity mechanics in the way that the mass does.

The object of investigation is to associate the intensity of the wave with the relative probability of observed occurrence of electric charge.

Heisenberg, in his theory, proposed to omit at the outset all quantities that are not, and apparently cannot be, observed. He omits unobservables, and develops a discontinuous theory.

Schrödinger's idea is essentially different. Is it not possible to obtain the energy levels that are observed in atomic spectra by the application of a continuous mathematical analysis ?

Schrödinger formed a wave equation that gives the energy levels successfully. The equation, as will be shown, can be obtained from the principles of statistical mechanics.

What is the interpretation of the wave ? If the answer to the question is to be obtained from statistical principles the formulation of initial conditions is of vital importance, and some fundamental considerations are necessary.

It would appear, in the first place, that a comprehensive interpretation of Planck's hypothesis in its application to statistical theory has not yet been given.

This hypothesis suggests that observations are possible only when an integral number of quanta of action is possessed by the system under observation. This conclusion introduces a periodicity or wave-like element into the system, and one in which the phase of the individual wave is unobservable.

From where, however, are we to consider that the action should be measured ? In other words, what are we to take as the origin of action ?

We are not justified in asserting that the action is zero at any instant which we may choose as the initial instant at which the system is supposed to start.

We must enquire as to the amount of action which the system may possess when the motion at the chosen initial instant is that which would be postulated by the arbitrary initial conditions.

A statistical theory has to be formulated, keeping these basic ideas in view, and there is nothing in such considerations as these which prevents us from applying to the elementary points of a statistical assembly the classical Hamiltonian theory of dynamics.

In the second place, we have to enquire as to the proper form that the initial assemblies should take.

In statistical mechanics an assembly is specified by all the variables which are required to satisfy it. How should the corresponding specification be made for the probability assembly appropriate to a single electron? Suppose that there is an assembly of points, each of which may represent with equal probability the initial position of a particle or electron.

Suppose that this assembly is in steady motion, so that the component velocities of every point are functions of the coordinates and prescribed for all time *before* a force system is applied. If a given force system is applied to this assembly at a given time the points will thereafter move, or, we should rather say, continue to move in accordance with Hamiltonian principles.

There will be an infinite number of such assemblies, which may be taken singly or combined in groups so as to represent any required initial condition.

The motion of every assembly in the steady state will be called a prehistorical motion, because it is an initial motion which may be supposed to exist before we consider the history of the motion which takes place after the force system is applied.

One of the fundamental assumptions in statistical theory is that we may choose our initial positions in a configuration space at random. By the introduction of prehistorical motions we may also choose our prehistorical times at random. This is an important consideration which appears to be essential for the completion of the statistical postulates.

Statistical theory appears to give a comprehensible reason for the wave equation, and makes it possible to define precisely those variables that were previously left quite vague.

It would also appear that the imaginary i, as it occurs in wave mechanics, should be interpreted as the mathematical symbol for non-observability.

Initial Conditions and Prehistorical Motions.

If Planck's hypothesis is considered as suggesting that observations can be made only when some action function associated with the configuration of a system

possesses integral amounts of the fundamental constant of action h, how does this suggestion affect the initial conditions ? Since we cannot as yet say how the action function is to be defined, we must commence by considering any action function whatever.

Suppose that an integral of action, taken between any initial configuration P_1 at time t_1, and any future configuration P at time t, is denoted by A, where

$$A = \int_{t_1}^{t} B \, dt.$$

If A represents the action function above mentioned, and if we write

$$A = nh,$$

it would be inferred that an observation can be made when n has any integral value.

It is thus implied that an observation can always be made when $t = t_1$. Since this restricts the initial conditions it becomes necessary to revise the customary definition of these conditions. Considering a system which consists of a single particle, what is meant when we say that the initial conditions of motion of the particle are given ?

The initial conditions are usually defined by saying that the particle starts from a point P_1 at time t_1 in the direction P_1Q_1 with velocity u_1.

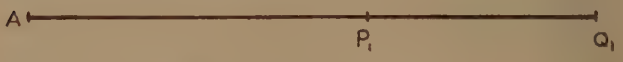

If the force system is given the subsequent motion of the particle is determinate. But there is another way of defining the initial conditions. We may suppose that the particle is travelling along the straight line AP_1Q_1 with constant velocity u_1, and that it arrives at P_1 at time t_1. At this time a force system is called into play. The subsequent motion of the particle is again determinate.

The motion along AP_1 before the force system is called into play may be called the prehistorical motion.

Let us now consider the prehistorical motion of an assembly, choosing one which may be defined as follows :— The prehistorical motion chosen is one in which a particle is travelling along the straight line AP_1Q_1 with constant

velocity, so that we are given only the path and the velocity.

Consistently with this definition we may assume that at any instant it is equally probable that the particle lies anywhere upon the straight line AP_1Q_1.

We have then to imagine that the straight line AP_1Q_1 is filled with a string of points equally spaced and very close together, and that the string of points is travelling along AP_1Q_1 with constant velocity. One set of initial conditions is represented by the velocity u_1. Suppose that a force system is called into play at any time t_1, then at a subsequent time t the string of points will be found to lie upon some curve, and we could proceed to examine the spacing of the points upon that curve. The string of points, before the force system is called into play, may be said to form an initial or prehistorical assembly.

The assemblies appropriate to a single particle are assemblies in three-dimensional space, and the prehistorical motions are assumed to be motions in parallel lines with uniform velocity.

It is clear that by choosing different directions and by varying the velocity all possible initial conditions may be obtained.

We shall commence with the most general type of initial assembly in steady motion in three-dimensional space, since the prehistorical motions postulated are special cases of this.

The general prehistorical motion of an assembly of points in space, corresponding to one set of initial conditions, is one in which the motion is always the same at a given location in the space, so that the conditions remain the same throughout all time.

It is our aim to find some property which is possessed by all such motions.

Treating the cloud of points as a continuous fluid, every element of which may be taken to represent the particle, it is permissible, at some initial prehistorical time t_0, to assume some arbitrary distribution of density of this fluid. It is natural that this should be a uniform distribution, and we commence by adopting this assumption.

We may say that, at time t_0, it is equally probable that the particle or electron may occupy any position within its domain. Let ρ be the density of the fluid

at the prehistorical time t at x, y, z, and let u, v, w be the component velocities of a point.

Following the usual procedure of statistical mechanics, it can be shown that

$$\frac{1}{\rho}\frac{\mathrm{D}\rho}{\mathrm{D}t}+\Delta=0, \quad \ldots\ldots \quad (1)$$

where $$\Delta=\frac{\partial u}{\partial x}+\frac{\partial v}{\partial y}+\frac{\partial w}{\partial z}.$$

Equation (1) is the expression of continuity, and $\mathrm{D}\rho/\mathrm{D}t$ represents the rate of increase of ρ as we follow a small group of points in its motion.

Since the motion is steady, Δ is a function of x, y, z only.

Equation (1) shows that, since ρ is assumed to be uniform initially, Δ must be constant. Further, since the total number of points in the cloud always remains the same, Δ must be zero.

It follows, then, that ρ must remain uniform throughout the prehistorical motion. Thus every prehistorical assembly satisfies the equation

$$\frac{\partial u}{\partial x}+\frac{\partial v}{\partial y}+\frac{\partial w}{\partial z}=0. \quad \ldots\ldots \quad (2)$$

Now the motion of a particle may coincide with the motion of any one of the points of the assembly, and we may therefore associate with every point a Hamiltonian Integral of Action.

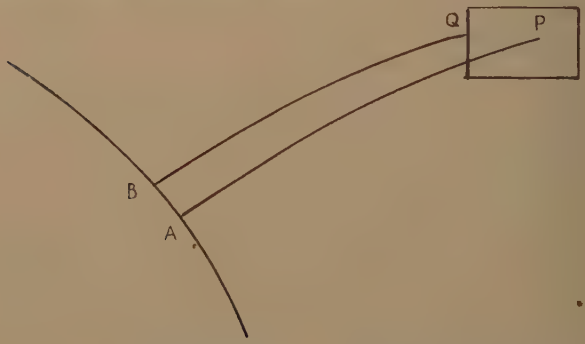

Let AP, BQ be any two neighbouring paths or stream-lines, and let AB lie upon a surface which may be taken as the origin of the Hamiltonian Integrals.

Let the Hamiltonian Integral be denoted by S_0, and let m be the mass of the particle. At a point P, therefore,

$$\frac{\partial S_0}{\partial x} = mu,$$

$$\frac{\partial S_0}{\partial y} = mv,$$

$$\frac{\partial S_0}{\partial z} = mw.$$

At a neighbouring point Q similar equations hold, and thus, if m is constant, equation (2) may be written in the form

$$\frac{\partial^2 S_0}{\partial x^2} + \frac{\partial^2 S_0}{\partial y^2} + \frac{\partial^2 S_0}{\partial z^2} = 0. \quad . \quad . \quad . \quad . \quad (3)$$

It should be noted that the first derivatives of S_0 are the components of a velocity whose resultant is along a stream-line, while the second derivatives refer in general to a change from a stream-line to the neighbouring one.

Equation (3) is the expression of a general property possessed by every prehistorical motion.

The conditions which all the prehistorical motions must satisfy may, for convenience, be set down as follows :—

(1) Each is a steady motion.

(2) In each the cloud of points is always uniformly distributed.

This is equivalent to saying that it is equally probable that the point which represents the system may be anywhere in the configuration space at any time.

(3) There is a further condition not yet considered.

If t_1 is the time at which the force system is brought into play all times previous to t_1 are called prehistorical times.

Now the prehistorical conditions are initial conditions, and it is the essence of statistical theory that some

probability should be allotted to all possible initial conditions.

Suppose that a point moving with the fluid is in the position P_1 at time t_1, and that when it is there the system possesses some property which depends upon the time that the point may be considered to have been in motion.

We have then to reckon the probability that the point is to be considered as having started from some point A in its prehistorical path.

Since this is obviously not infinitely probable we have also to reckon the probability that the point is to be considered as having started from any other point B in its prehistorical path.

This conclusion from statistical theory cannot be avoided, and whatever its physical significance its consequences must be examined.

Observability and the Quantum of Action.

According to Bohr's theory an atomic system may exist in a series of stationary states. With every state there may be associated some probability that the system is in that state.

The problem for investigation is the probability that the system is to be found in any one of its stationary states after an observation. To solve this problem we must take account of the configuration of the system at a given time in that state, and another problem arises which requires consideration before the first problem can be solved.

We have in fact to enquire as to the probability that an atomic system is in an observable condition in a given configuration when it is in a given state. If the system moves from one configuration at time t_0 to another configuration at time t while in the state under consideration, is it equally probable that the system is in an observable condition in both of these configurations ?

If it is not equally probable, we must find the law of probability.

Now Planck's theory of quanta of action may be interpreted for a particle or an electron in the following manner :—Suppose that the system is in an observable condition when the particle is at a point P_0 in the domain of the atom.

We may proceed upon the assumption that the system is in an observable condition when the particle is at a point P if the change in the action A involves an integral number of quanta of action h.

If the change in A does not involve an integral number of quanta Planck's hypothesis would lead to the conclusion that the system is not in an observable condition when the particle is at P.

This conclusion implies discontinuity. But we are not justified in asserting that this is the only interpretation, and that we can only proceed to develop the theory with the aid of a discontinuous mathematical process, for we have not yet seen how Planck's hypothesis is related to a statistical assembly.

We shall therefore interpret Planck's hypothesis in a way which makes a continuous process possible, and it is proposed to commence by asserting that the *probability* that the system is in an observable condition in any configuration is a continuous function of A.

If we admit this interpretation the following question must be asked :—What is the probability that the system is in an observable condition at the initial instant t_0, defined as the instant at which a force system is brought into play ? Here again we see a necessity for considering a prehistory of the motion.

The first consideration is to find the form of the probability function. For this purpose we shall denote prehistorical times by T, and subsequent times, from the instant at which the force system is brought into play, by t.

Suppose that the particle starts from Q_0 at the prehistorical time T_0 and arrives at P_0 at the time t_0, at which time the force system is called into play.

For one particular force system the particle will subsequently describe the path P_0P_1, arriving at P_1 at time t_1. For another force system the particle will subsequently describe the path P_0P_2, arriving at P_2 at time t_2. And so on.

Let A_1 be the value of A for the path $Q_0P_0P_1$, A_2 the value of A for the path $Q_0P_0P_2$, and so on.

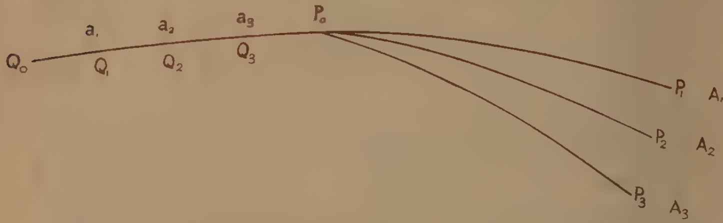

Now, in accordance with the postulates of statistical theory, we have to consider the probability that the particle must be reckoned as having started from any other point Q_1, Q_2, etc. to which prehistorical times are attached.

Let the probability that the particle must be reckoned to have started from Q_1 be θ_1, and let a_1 be that part of the action function due to travel from Q_0 to Q_1, the time of travel being T_1-T_0. Similar definitions are involved if the particle must be reckoned to have started from Q_2, and so on.

In this way the probability that the system is in an observable condition at any point, such as P_1, depends upon the initial conditions.

The function expressing the probability will be called the probability function. The probability function associated with any action function A will be denoted by P, and we shall write

$$P=f(A). \quad . \quad . \quad . \quad . \quad . \quad . \quad (4)$$

The probability that the system is in an observable condition if the particle is at P_1 at time t_1 may have any one of the values entered in the first line or row of the following scheme :—

$$\begin{array}{llll} \theta_1 f(A_1-a_1) & \theta_2 f(A_1-a_2) & \ldots\ldots & \theta_n f(A_1-a_n), \\ \theta_1 f(A_2-a_1) & \theta_2 f(A_2-a_2) & \ldots\ldots & \theta_n f(A_2-a_n), \\ \ldots\ldots & \ldots\ldots & \ldots\ldots & \ldots\ldots \\ \theta_1 f(A_n-a_1) & \theta_2 f(A_n-a_2) & \ldots\ldots & \theta_n f(A_n-a_n). \end{array}$$

The probability that it is in an observable condition if the particle is at P_2 at time t_2 may have any one of the

values entered in the second line of the above scheme, and so on.

The combined probability that the system is in an observable condition if the particle is at the point P_1 at time t_1, at the point P_2 at time t_2, and so on, may be put in a number of different ways.

One way is to take the product of all the terms forming a column in the above scheme. Each of these combinations or products forms an independent probability.

Another way is to take the product of all the terms forming a diagonal.

Now the two diagonals each contain all the variables. Every probability function is assumed to be single-valued, and therefore the combined probability is a unique function of the variables.

Thus the product of the terms forming one diagonal is the same function as the product of the terms forming the other diagonal. Hence

$$f(A_1-a_1)f(A_2-a_2)\ldots f(A_n-a_n)$$
$$=f(A_1-a_n)f(A_2-a_{n-1})\ldots f(A_n-a_1).$$

Thus

$$\log f(A_1-a_1)-\log f(A_1-a_n)+\log P_1$$
$$=\log f(A_n-a_1)-\log f(A_n-a_n)+\log P_n,$$

where P_1 and P_n are the remaining products. In this equation P_1 and P_n are independent of A_1, A_n, a_1, and a_n, and so we must put

$$P_1=P_n.$$

Also, since A_1, A_n, a_1, and a_n are all independent, each side of the remaining equation can only be a function of a_1 and a_n.

Treating a_1 and a_n as constants, and differentiating with respect to A_1 and A_n, we obtain

$$\frac{f'(A_1-a_1)}{f(A_1-a_1)}-\frac{f'(A_1-a_n)}{f(A_1-a_n)}=0=\frac{f'(A_n-a_1)}{f(A_n-a_1)}-\frac{f'(A_n-a_n)}{f(A_n-a_n)}.$$

It follows that

$$\frac{f'(A)}{f(A)}=\beta,$$

where β is a constant. We may therefore write

$$P=\theta_s e^{\beta A}, \quad \ldots\ldots\ldots \quad (5)$$

where θ_s is the probability that the particle is to be considered as starting from the point Q_s in its prehistorical motion. The same conclusion would be reached if it was assumed that P_1, P_2, P_3, ... all lay upon the same path described under one and the same force system.

Now, just as the initial distribution of density may be chosen quite arbitrarily, so θ_s may be chosen quite arbitrarily for every point. Hence θ_s may be taken as a constant in any one prehistorical motion.

If the system is in an observable condition when $A=0$, or, more correctly, if the probability that the system is in an observable condition when $A=0$ is unity, Planck's hypothesis is to be interpreted by saying that P is unity whenever A increases by an integral number of quanta of action h. Hence we must put

$$\beta=\pm\frac{2\pi i}{h}, \quad . \quad . \quad . \quad . \quad . \quad . \quad (6)$$

so that

$$P=ae^{\pm\frac{2\pi i}{h}A} \quad . \quad . \quad . \quad . \quad . \quad . \quad . \quad (7)$$

This expression appears at first sight to contain an ambiguity, and it will be noticed that in deriving it the probability functions are assumed to be unique. This assumption is, however, completely justified, for it will be seen that the two signs enter into the theory quite independently. In fact, one or other sign must be used throughout, and the two are combined only at the end.

In (7) a is the probability that a given set of initial conditions is associated with one of the prehistorical motions. Then P represents the probability that the system is in an observable condition for these initial data.

Let S be the Hamiltonian Integral of Action for the motion of mass m associated with a point, and write

$$A=S+B.$$

Then, if we retain the positive sign in the argument,

$$P=ae^{\frac{2\pi i}{h}(S+B)}.$$

If we write

$$\psi = \mathrm{P}e^{-\frac{2\pi i}{h}\mathrm{B}},$$

then

$$\psi = ae^{\frac{2\pi i}{h}\mathrm{S}}.$$

If, on the other hand, we retain the negative sign in the argument, and write

$$\overline{\mathrm{P}} = ae^{-\frac{2\pi i}{h}(\mathrm{S}+\mathrm{B})},$$

we obtain

$$\overline{\psi} = ae^{-\frac{2\pi i}{h}\mathrm{S}}.$$

Suppose in the end that it is our aim to determine the intensity. Then, whether we take P and P or ψ and $\overline{\psi}$, the intensity is the same, for

$$a^2 = \mathrm{P}\overline{\mathrm{P}} = \psi\overline{\psi}.$$

We shall therefore consider the properties of the functions ψ and $\overline{\psi}$, leaving till later consideration of the significance of the intensity.

We shall define ψ_0, to begin with, as the probability function for the prehistorical motion associated with the Hamiltonian Integral of Action S_0. The constant a may be dropped when we are considering any *one* prehistorical motion. Then

$$\psi_0 = e^{\frac{2\pi i}{h}\mathrm{S}_0} \quad . \quad . \quad . \quad . \quad . \quad . \quad . \quad (8)$$

The Probability Equation.

Let us now substitute (8) in (3).

By differentiation we have

$$\frac{\partial^2\psi_0}{\partial x^2} = \frac{2\pi i}{h}\frac{\partial^2 \mathrm{S}_0}{\partial x^2}\psi_0 - \frac{4\pi^2}{h^2}\left(\frac{\partial \mathrm{S}_0}{\partial x}\right)^2\psi_0.$$

Hence, by (3),

$$\nabla^2\psi_0 + \frac{4\pi^2}{h^2}\left\{\left(\frac{\partial \mathrm{S}_0}{\partial x}\right)^2 + \left(\frac{\partial \mathrm{S}_0}{\partial y}\right)^2 + \left(\frac{\partial \mathrm{S}_0}{\partial z}\right)^2\right\}\psi_0 = 0. \quad (9)$$

Equation (9) is a relation between ψ_0 and the kinetic energy of the particle in one of its prehistorical motions.

We have seen that the motions of the prehistorical assemblies may be defined as uniform motions, and it may be noted that, if we group together all uniform motions which possess the same kinetic energy, equation (9) will be common to the group.

Further, since the expression for the relativity mass is a constant for any group, equation (9) will be applicable to relativity theory. Taking any one group it is clear that, when the force system is applied, the total energy of every point is at once specified.

It is unnecessary to specify more precisely the partition of energy among the groups.

A range of total energies, corresponding to the applied force system, will be associated with each group, and we may pick out from every group points which possess any one given total energy. We have to find how to select from all the points those which possess permissible or observed energies. Statistical theory and Planck's hypothesis make such a selection possible. Now the probability function ψ_0 satisfies equation (9) at any time and at any place. Also, one of the representative points will be in the position P at time t, assuming that the force system has been in action for a time $t-t_0$.

We have to put the following question:—If the probability function ψ_0 satisfies equation (9), what equation is satisfied by the probability function ψ which is associated with the motion of the point which arrives at P at time t, having travelled from its initial position, which is its position when the force system is called into play, in time $t-t_0$?

We shall denote the Hamiltonian Integral of Action, corresponding to the motion of the point under the force system during the interval $t-t_0$, by S, and shall write

$$\psi = e^{\frac{2\pi i}{h}S},$$

in which the constant associated with the prehistorical motion has been made unity. Let us consider the equation

$$\psi\psi_1\psi_0 = 1, \quad \ldots\ldots\ldots \quad (10)$$

where

$$\psi_1 = e^{\frac{2\pi i}{h} S_1}.$$

Let us put

$$\psi\psi_0 = \psi_2,$$

so that

$$\frac{1}{\psi_1} = \psi_2 = e^{\frac{2\pi i}{h}(S_0+S)}$$

$$= e^{\frac{2\pi i}{h} S_2}, \quad \text{say.}$$

Then

$$\psi \nabla^2\psi_0 + \psi_0 \nabla^2\psi + 2\left\{ \frac{\partial\psi}{\partial x} \cdot \frac{\partial\psi_0}{\partial x} + \dots \right\} = \nabla^2\psi_2.$$

Now

$$\frac{\partial\psi}{\partial x} = \frac{2\pi i}{h} \frac{\partial S}{\partial x}\psi \quad \text{etc.},$$

and

$$\frac{\partial\psi_0}{\partial x} = \frac{2\pi i}{h} \frac{\partial S_0}{\partial x}\psi_0 \quad \text{etc.},$$

whence it follows that, if we make use of equation (9),

$$\frac{1}{\psi} \nabla^2\psi + \frac{4\pi^2}{h^2}\left\{ \left(\frac{\partial S}{\partial x}\right)^2 + \dots \right\}$$

$$= \frac{1}{\psi_2} \nabla^2\psi_2 + \frac{4\pi^2}{h^2}\left\{ \left(\frac{\partial S_2}{\partial x}\right)^2 + \dots \right\}.$$

Since

$$S_0 + S = S_2 = -S_1,$$

it is easily shown that

$$\frac{1}{\psi} \nabla^2\psi + \frac{4\pi^2}{h^2}\left\{ \left(\frac{\partial S}{\partial x}\right)^2 + \dots \right\} + \frac{1}{\psi_1} \nabla^2\psi_1$$

$$+ \frac{4\pi^2}{h^2}\left\{ \left(\frac{\partial S_1}{\partial x}\right)^2 + \dots \right\} = 0. \quad (11)$$

From the symmetry of (10) and (11) in ψ and ψ_1 we may conclude that either of these probability functions may be associated with the motion of a point.

Since, therefore, they must satisfy the same equation, we may write

$$\nabla^2\psi+\frac{4\pi^2}{h^2}\left\{\left(\frac{\partial S}{\partial x}\right)^2+\dots\right\}\psi=0, \quad . \quad . \quad (12)$$

and

$$\nabla^2\psi_1+\frac{4\pi^2}{h^2}\left\{\left(\frac{\partial S_1}{\partial x}\right)^2+\dots\right\}\psi_1=0. \quad . \quad . \quad (13)$$

It is now necessary to make use of the Hamiltonian equation, by introducing the time, in order to eliminate S from equation (12).

In non-relativity theory, if the forces can be derived from a potential V, the Hamiltonian equation is

$$-\frac{\partial S}{\partial t}=\frac{1}{2m}\left\{\left(\frac{\partial S}{\partial x}\right)^2+\dots\right\}+V.$$

Hence, inserting in (12),

$$\nabla^2\psi-\frac{8\pi^2 m}{h^2}\left\{\frac{\partial S}{\partial t}+V\right\}\psi=0.$$

But

$$\frac{\partial\psi}{\partial t}=\frac{2\pi i}{h}\frac{\partial S}{\partial t}\psi.$$

Hence

$$\nabla^2\psi+\frac{4\pi i m}{h}\frac{\partial\psi}{\partial t}-\frac{8\pi^2 m}{h^2}V\psi=0, \quad . \quad . \quad (14)$$

corresponding to

$$\psi=e^{\frac{2\pi i}{h}S}.$$

Likewise it can be shown that the conjugate $\bar{\psi}$ satisfies the equation

$$\nabla^2\bar{\psi}-\frac{4\pi i m}{h}\frac{\partial\bar{\psi}}{\partial t}-\frac{8\pi^2 m}{h^2}V\bar{\psi}=0, \quad . \quad . \quad . \quad (15)$$

corresponding to

$$\bar{\psi}=e^{-\frac{2\pi i}{h}S}.$$

It will be noted that equations (14) and (15) are linear and of the second order.

Now if we use the same process in order to eliminate S when relativity is taken into account we do not obtain an equation which is linear.

Since, in relativity theory, invariance demands that the equations should be linear, the process is not universally justified except in so far that it gives the general equations associated with the prehistorical motions.

We must therefore find a general method which is applicable to both non-relativity and relativity theories, and for this purpose we start with the general equations associated with the prehistorical motions.

Putting V=0 in equations (14) and (15), these general equations are

$$\nabla^2\psi_0+\frac{4\pi im}{h}\frac{\partial\psi_0}{\partial t}=0 \quad . \quad . \quad . \quad . \quad (16)$$

and

$$\nabla^2\bar{\psi}_0-\frac{4\pi im}{h}\frac{\partial\bar{\psi}_0}{\partial t}=0. \quad . \quad . \quad . \quad . \quad (17)$$

In relativity theory, if the forces have a potential V, the Hamiltonian equation is

$$\frac{1}{c^2}\left\{\left(\frac{\partial S}{\partial t}\right)+V\right\}^2=\left(\frac{\partial S}{\partial x}\right)^2+\left(\frac{\partial S}{\partial y}\right)^2+\left(\frac{\partial S}{\partial z}\right)^2+m_0^2c^2,$$

m_0 being the "rest" mass.

Inserting in (12), we obtain the equation

$$\nabla^2\psi+\frac{4\pi^2}{h^2}\left\{\frac{1}{c^2}\left(\frac{\partial S}{\partial t}+V\right)^2-m_0^2c^2\right\}\psi=0.$$

Now

$$\frac{\partial^2\psi}{\partial t^2}=\frac{2\pi i}{h}\frac{\partial^2 S}{\partial t^2}\psi-\frac{4\pi^2}{h^2}\left(\frac{\partial S}{\partial t}\right)^2\psi.$$

If the forces are absent we may put

$$V=0 \quad \text{and} \quad \partial^2S/\partial t^2=0.$$

Hence the general equation associated with the prehistorical motions in relativity theory is

$$\nabla^2\psi_0-\frac{1}{c^2}\frac{\partial^2\psi_0}{\partial t^2}-\frac{4\pi^2}{h^2}m_0^2c^2\psi_0=0. \quad . \quad . \quad (18)$$

The method to be considered is more general, for it depends upon the nature of the probability functions only, and not upon the form of the Hamiltonian equation, which is essentially different in relativity and non-relativity theories.

If ψ_0 is the probability function for the prehistorical motion and ψ the probability function for the motion under a specified force system, the two functions must be related by an equation

$$\psi_0 = \psi\psi_1,$$

where ψ_1 is a probability function. The particular form of ψ_1 can be obtained from consideration of the probability of occurrence.

Non-Relativity Theory.

The general equation associated with the prehistorical motions in non-relativity theory is equation (16), corresponding to

$$\psi_0 = e^{\frac{2\pi i}{h} S_0}.$$

Let us compare S_0, which is the integral taken along a path to the point P in the prehistorical motion during any interval $t - t_0$, with S, which is the integral taken along a path to the point P under the force system during the same interval $t - t_0$. Suppose that we write

$$S_0 = S + R,$$

where R is some action integral taken along the path described under the force system. Let us write

$$R = \int_{t_0}^{t} (a\,dx + b\,dy + c\,dz + g\,dt),$$

and let R be associated with the motion of a representative point moving in the path. The only restriction placed upon R is the obvious one that it vanishes when the force system is non-existent.

Now if δR is the change in R due to motion from P to a consecutive point Q in time δt, where the coordinates of Q relative to P are δx, δy, δz,

$$\delta R = a\,\delta x + b\,\delta y + c\,\delta z + g\,\delta t,$$

in which a, b, c, g have here to be evaluated at P. Hence

$$\frac{\partial R}{\partial x}=a, \quad \frac{\partial R}{\partial y}=b, \quad \frac{\partial R}{\partial z}=c, \quad \frac{\partial R}{\partial t}=g.$$

But we may write

$$\psi_0=e^{\frac{2\pi i}{h}(S+R)}$$

$$=\psi e^{\frac{2\pi i}{h}R}, \quad . \quad . \quad . \quad . \quad . \quad . \quad . \quad . \quad (19)$$

and, since ψ_0 satisfies equation (16), we shall be enabled to find how R enters into the corresponding equation satisfied by ψ.

It is readily found, in fact, that

$$\left(\frac{\partial}{\partial x}+\lambda a\right)^2\psi+\ldots+\ldots+2\lambda m\left(\frac{\partial}{\partial t}+\lambda g\right)\psi$$

$$+\lambda\left(\frac{\partial a}{\partial x}+\frac{\partial b}{\partial y}+\frac{\partial c}{\partial z}\right)\psi=0, \quad (20)$$

where

$$\lambda=\frac{2\pi i}{h}.$$

Now in the general problem, corresponding to all possible prehistorical motions, the probability that the system is in an observable condition and the probability of observed occurrence of the particle at the point P are closely associated. If the probability equations were the wave equations of some problem in classical optics their solutions would comprise a system of wave trains. The system is in an observable condition because the wave trains interfere. What is deduced and what is actually observed is a distribution of intensity.

Likewise in the statistical problem ψ and ψ are associated with the *probability* that the system is in an observable condition.

It will be shown that what is deduced is a probability of observed occurrence. It is supposed that a solution of equation (20) is given in the form

$$\psi=\rho e^{\frac{2\pi i}{h}\phi}=\rho e^{\lambda\Phi}, \quad . \quad . \quad . \quad . \quad . \quad . \quad (21)$$

and it is desired to interpret the meanings of ϕ and ρ.

Upon substitution of (21) in (20) we obtain

$$\rho\nabla^2\rho+\lambda\left\{\rho^2\left(\frac{\partial^2\phi}{\partial x^2}+\ldots\right)+\left(\frac{\partial\rho^2}{\partial x}\cdot\frac{\partial\phi}{\partial x}+a+\ldots\right)\right.$$
$$\left.+\rho^2\left(\frac{\partial a}{\partial x}+\ldots\right)\right\}+\lambda^2\rho^2\left\{\left(\frac{\partial\phi}{\partial x}+a\right)^2+\ldots\right\}$$
$$+\lambda m\left\{\frac{\partial\rho^2}{\partial t}+2\lambda\rho^2\left(\frac{\partial\phi}{\partial t}+g\right)\right\}=0. \quad . \quad . \quad (22)$$

Equation (22) is equivalent to

$$\rho\nabla^2\rho+\lambda\left[\frac{\partial}{\partial x}\left\{\rho^2\left(\frac{\partial\phi}{\partial x}+a\right)\right\}+\ldots+\ldots+m\frac{\partial\rho^2}{\partial t}\right]$$
$$+2\lambda^2\rho^2m\left[\frac{1}{2m}\left\{\left(\frac{\partial\phi}{\partial x}+a\right)^2+\ldots+\ldots\right\}+\frac{\partial\phi}{\partial t}+g\right]=0.$$

Writing $\frac{\partial\phi}{\partial x}=mu$ etc., it follows that, since $\lambda=\frac{2\pi i}{h}$,

$$\frac{\partial}{\partial x}\left\{\rho^2\left(u+\frac{a}{m}\right)\right\}+\ldots+\ldots+\frac{\partial\rho^2}{\partial t}=0 \quad . \quad (23)$$

and

$$-\frac{h^2}{8\pi^2m}\frac{\nabla^2\rho}{\rho}+\frac{1}{2m}\left\{\left(\frac{\partial\phi}{\partial x}+a\right)^2+\ldots\right\}+\frac{\partial\phi}{\partial t}+g=0.$$
$$. \quad . \quad . \quad (24)$$

Now, whatever value we may attribute to h, ϕ is an integral of action associated with the motion of a point. In particular, if $h=0$, ϕ will satisfy the Hamiltonian equation of what we may call classical dynamics, corresponding to a prescribed force system which depends upon the assumed constitution of the atom.

Suppose that the prescribed force system is derived from a scalar potential V. Then, from (24), it is clear that a, b, and c must vanish and g must be replaced by V.

In this case we must have

$$\frac{\partial}{\partial x}(\rho^2mu)+\ldots+\ldots+\frac{\partial}{\partial t}(\rho^2m)=0 \quad . \quad . \quad (25)$$

and

$$\frac{1}{2m}\left\{\left(\frac{\partial\phi}{\partial x}\right)^2+\ldots\right\}+\frac{\partial\phi}{\partial t}+V-\frac{h^2}{8\pi^2 m}\frac{\nabla^2\rho}{\rho}=0. \quad (26)$$

Now in one set of circumstances, essential to an observation, the probability that the system is in an observable condition is

$$\psi=\rho e^{+\frac{2\pi i}{h}\phi}.$$

In another set, independent of the first set but also essential to an observation, the probability that the system is in an observable condition is

$$\bar{\psi}=\rho e^{-\frac{2\pi i}{h}\phi}.$$

One must interpret the two signs in this way, since each is equally probable.

The probability of observed occurrence is the combined probability that the system is in an observable condition in both sets of circumstances.

Hence ρ^2, the intensity of the wave, is the relative probability of observed occurrence of some entity.

It is clear that this entity may be the electric charge, for in (25) m may be replaced by $-e$, since both m and $-e$ are constants in non-relativity theory. Thus ρ^2 may be looked upon as the relative density of a cloud of points moving with velocity components u, v, w which are derivable from equation (26).

The existence of the quantum potential in equation (26) introduces grave difficulties if the actual motion of the points were derivable from the same equation.

It is inconceivable that the actual motion should depend upon the probability that the system is in a certain configuration. Again, there is no apparent reason to suppose that the motion of a point does not obey classical laws.

Thus it would appear that the observed distribution of density is due to a hypothetical motion into which the quantum potential is introduced, while the unobserved distribution is due to a classical motion. Planck's hypothesis, in fact, modifies our conceptions as to how an assembly of points, obeying such classical motions, will behave under observation.

We shall examine the contrast between the probability of occurrence defined by putting $h=0$ and the probability of observed occurrence, defined by the existence of Planck's constant, in a particular case which is of great interest.

A Special Problem in Non-Relativity.

The initial procedure in the following analysis is analogous to that used by de Broglie in his theory, but he has applied his analysis to two cases only. One case is that in which there is no field, and in the other case the field is uniform; in both of those cases a continuous spreading of the wave takes place. But a more important case is that of a central field, and in this case there is no continuous spreading. The spreading is periodic.

Suppose that the initial conditions may be defined by any one of a set of prehistorical motions, which are represented by $S_1, S_2, \ldots S_n$. The probability that the system is in an observable condition in any one of these motions is

$$\psi_0 = a_1 e^{\frac{2\pi i}{h} S_1} + a_2 e^{\frac{2\pi i}{h} S_2} + \ldots,$$

where ψ_0 satisfies equation (16), viz.,

$$\nabla^2 \psi_0 + \frac{4\pi i m}{h} \frac{\partial \psi_0}{\partial t} = 0.$$

The constants a_1, a_2, etc. are the relative probabilities to be associated with each motion.

Consider an elementary solution,

$$\psi_{01} = A e^{\frac{2\pi i}{h}(\alpha x + \beta y + \gamma z - \kappa t + \lambda)},$$

in which A, α, β, γ, κ, λ are constants. Then

$$\nabla^2 \psi_{01} = -\frac{4\pi^2}{h^2}(\alpha^2 + \beta^2 + \gamma^2)\psi_{01}$$

and

$$\frac{4\pi i m}{h} \frac{\partial \psi_{01}}{\partial t} = \frac{8\pi^2 m}{h^2} \kappa \psi_{01}.$$

Thus

$$\alpha^2 + \beta^2 + \gamma^2 - 2m\kappa = 0.$$

Suppose that α and β are small. Then

$$\gamma=\sqrt{2m\kappa} \quad \text{approximately.}$$

Suppose also that

$$\kappa=n+\epsilon,$$

where ϵ is small. Then

$$\gamma=\sqrt{2mn}\left(1+\frac{\epsilon}{2n}\right) \quad \text{approximately.}$$

Let us denote $\sqrt{2mn}$ by M. Then

$$\alpha x+\beta y+\gamma z-\kappa t+\lambda=\alpha x+\beta y+\epsilon\left(\frac{\mathrm{M}}{2n}z-t\right)+\mathrm{M}z-nt+\lambda.$$

Hence

$$\psi_{01}=\mathrm{A}e^{\frac{2\pi i}{h}(\mathrm{M}z-nt)} \times\left[\cos\frac{2\pi}{h}\left\{\alpha x+\beta y+\epsilon\left(\frac{\mathrm{M}}{2n}z-t\right)+\lambda\right\} +i\sin\frac{2\pi}{h}\left\{\alpha x+\beta y+\epsilon\left(\frac{\mathrm{M}}{2n}z-t\right)-\lambda\right\}\right].$$

We shall suppose that $\lambda=0$ and that A is an even function of α, β, and ϵ. Hence if we write

$$\psi_{01}=\mathrm{B}e^{\frac{2\pi i}{h}(\mathrm{M}z-nt)},$$

$$\mathrm{B}=\mathrm{A}(\alpha\beta\epsilon)\left[\cos\frac{2\pi}{h}\left\{\alpha x+\beta y+\epsilon\left(\frac{\mathrm{M}}{2n}z-t\right)\right\} +i\sin\frac{2\pi}{h}\left\{\alpha x+\beta y+\epsilon\left(\frac{\mathrm{M}}{2n}z-t\right)\right\}\right].$$

Consider the triple integral

$$\int_{-\alpha_1}^{\alpha_1}\int_{-\beta_1}^{\beta_1}\int_{-\epsilon_1}^{\epsilon_1}\mathrm{B}\,d\alpha\,d\beta\,d\epsilon.$$

On account of the assumption made with regard to A it is not difficult to show that this integral is equal to

$$8\int_0^{\alpha_1}\int_0^{\beta_1}\int_0^{\epsilon_1}\mathrm{A}(\alpha\beta\epsilon)\cos\frac{2\pi}{h}\alpha x\cos\frac{2\pi}{h}\beta y \times\cos\frac{2\pi}{h}\epsilon\left(\frac{\mathrm{M}}{2n}z-t\right)d\alpha\,d\beta\,d\epsilon.$$

It is now further assumed that $A(\alpha\beta\epsilon)$ is a function which vanishes except when α, β, and ϵ are small.

Hence the upper limits of the triple integral may be replaced by ∞.

Thus, combining a suitable set of prehistorical motions, we may, by Fourier's theorem, write

$$\psi_0 = F_0' \left\{ x, y, \left(\frac{M}{2n} z - t\right) \right\} e^{\frac{2\pi i}{h}(Mz - nt)}, \quad . \quad (27)$$

and this is a solution of (16), F_0' being an even function of x, y, $\frac{M}{2n} z - t$.

It may be observed that by a change of axes, for which $\nabla^2\psi_0$ is invariant, we may write for z

$$l_1 x' + m_1 y' + n_1 z',$$

with corresponding expressions for x and y. We may now put

$$l_1 M = m u_0,$$

$$m_1 M = m v_0,$$

$$n_1 M = m w_0,$$

whence

$$n = \tfrac{1}{2} m (u_0^2 + v_0^2 + w_0^2).$$

Dropping the accents on the new variables x', y', z', we may write finally

$$\psi_0 = F_0(xyzt) e^{\frac{2\pi i}{h}(m u_0 x + m v_0 y + m w_0 z - nt)}, \quad . \quad . \quad (28)$$

in which F_0 is an even function of xyz when $t=0$.

The set of prehistorical motions is therefore such that (28) represents ψ_0 throughout all time. We may then assume that, at the instant $t=0$, a force system is brought into play.

It will be assumed that, after the force system has been brought into play, the equation to be satisfied is

$$\nabla^2\psi + \frac{4\pi i m}{h} \frac{\partial\psi}{\partial t} - \frac{8\pi^2 m}{h^2} V\psi = 0, \quad . \quad . \quad . \quad (29)$$

in which the forces have a potential V. The problem is to find $\psi(xyzt)$ when $\psi(xyz0)$ is known. In the present case $\psi = \psi_0$ when $t=0$.

The procedure is to introduce a transformation function T, and to write

$$\psi(xyzt) = \iiint f(x_0y_0z_0)\mathrm{T}(xyzx_0y_0z_0t)\,dx_0\,dy_0\,dz_0,$$

in which the limits of integration are $-\infty$ and $+\infty$.

The function T, considered as a function of x, y, z, and t, must satisfy (29), and ψ must reduce to $f(xyz)$ when $t=0$. Thus $f(xyz)=\psi_0$ when $t=0$.

We shall now write

$$\mathrm{T}=\mathrm{R}e^{\frac{2\pi i}{h}\mathrm{P}},$$

and, since this satisfies (29), we find that the following equations have to be satisfied :—

$$\frac{1}{2m}\left\{\left(\frac{\partial \mathrm{P}}{\partial x}\right)+\left(\frac{\partial \mathrm{P}}{\partial y}\right)^2+\left(\frac{\partial \mathrm{P}}{\partial z}\right)^2\right\}+\frac{\partial \mathrm{P}}{\partial t}+\mathrm{V}=\frac{h^2}{8\pi^2 m}\frac{\nabla^2\mathrm{R}}{\mathrm{R}}$$

and

$$\frac{\partial \mathrm{R}}{\partial x}\cdot\frac{\partial \mathrm{P}}{\partial x}+\frac{\partial \mathrm{R}}{\partial y}\cdot\frac{\partial \mathrm{P}}{\partial y}+\frac{\partial \mathrm{R}}{\partial z}\cdot\frac{\partial \mathrm{P}}{\partial z}+\tfrac{1}{2}\mathrm{R}\nabla^2\mathrm{P}+m\frac{\partial \mathrm{R}}{\partial t}=0.$$

The force system which will be considered is defined by

$$\mathrm{V}=\tfrac{1}{2}\kappa(x^2+y^2+z^2),$$

so that a particle is attracted to the origin by a force varying as the distance. The simple and sufficient assumption is made that R is a function of the time only.

Under these circumstances

$$\frac{1}{2m}\left\{\left(\frac{\partial \mathrm{P}}{\partial x}\right)^2+\left(\frac{\partial \mathrm{P}}{\partial y}\right)^2+\left(\frac{\partial \mathrm{P}}{\partial z}\right)^2\right\}+\frac{\partial \mathrm{P}}{\partial t}+\tfrac{1}{2}\kappa(x^2+y^2+z^2)=0 \quad . \quad (30)$$

and

$$\tfrac{1}{2}\mathrm{R}\nabla^2\mathrm{P}+m\frac{\partial \mathrm{R}}{\partial t}=0. \quad . \quad . \quad . \quad . \quad (31)$$

In order to find a complete integral of equation (30) we write

$$\mathrm{P}=\mathrm{F}\cot\alpha t+\mathrm{G}\tan\alpha t+\mathrm{H},$$

where F and G are functions of x, y, z, x_0, y_0, z_0 only, and H is a function of the time only. Let us write

$$\mathrm{F}=\beta\{(x-x_0)^2+(y-y_0)^2+(z-z_0)^2\},$$
$$\mathrm{G}=\gamma\{(x+x_0)^2+(y+y_0)^2+(z+z_0)^2\}.$$

Then

$$\frac{\partial \mathrm{P}}{\partial x}=2\beta(x-x_0)\cot\alpha t+2\gamma(x+x_0)\tan\alpha t,$$

$$\frac{\partial \mathrm{P}}{\partial t}=-\alpha\mathrm{F}\,\mathrm{cosec}^2\,\alpha t+\alpha\mathrm{G}\sec^2\alpha t+d\mathrm{H}/dt.$$

Hence, substituting in (30),

$$\frac{2}{m}\{\beta^2(x-x_0)^2\cot^2\alpha t+\gamma^2(x+x_0)^2\tan^2\alpha t+2\beta\gamma(x^2-x_0{}^2)\}+\ldots$$
$$+\{-\alpha\beta(x-x_0)^2(1+\cot^2\alpha t)+\alpha\gamma(x+x_0)^2(1+\tan^2\alpha t)\}+\ldots$$
$$+d\mathrm{H}/dt+\tfrac{1}{2}\kappa x^2+\ldots=0.$$

This equation is identically satisfied if

$$\left.\begin{aligned}&\gamma=-\beta=-\tfrac{1}{2}m\alpha,\\ &\kappa=4m\alpha^2,\\ \text{and}\quad &d\mathrm{H}/dt=0.\end{aligned}\right\}\quad\ldots\ldots\quad(32)$$

From the last it follows that H must be a constant, which may be taken as zero. We may now write

$$\mathrm{P}=\tfrac{1}{2}m\alpha\{(x-x_0)^2+(y-y_0)^2+(z-z_0)^2\}\cot\alpha t$$
$$-\tfrac{1}{2}m\alpha\{(x+x_0)^2+(y+y_0)^2+(z+z_0)^2\}\tan\alpha t.$$

From this equation we obtain

$$\nabla^2\mathrm{P}=3m\alpha(\cot\alpha t-\tan\alpha t).$$

Hence, substituting in (31),

$$\frac{1}{\mathrm{R}}\frac{d\mathrm{R}}{dt}=\tfrac{3}{2}\alpha(\tan\alpha t-\cot\alpha t),$$

and thus, upon integration,

$$\mathrm{R}=\mathrm{C}(\cos\alpha t\sin\alpha t)^{-\frac{3}{2}},$$

where C is a constant. We may, accordingly, write

$$T=C(\cos \alpha t \sin \alpha t)^{-\frac{1}{2}} e^{\frac{\pi i m}{h}\alpha\{\Sigma(x-x_0)^2 \cot \alpha t - \Sigma(x+x_0)^2 \tan \alpha t\}},$$

where the sign of summation Σ means that there are two similar terms containing y, z, y_0, z_0. In order to determine the constant C we shall write

$$t^{\frac{1}{2}}\xi = x_0 - x,$$
$$t^{\frac{1}{2}}\eta = y_0 - y,$$
$$t^{\frac{1}{2}}\zeta = z_0 - z.$$

Then

$$\psi(xyzt)=\int\int\int f\{t^{\frac{1}{2}}\xi+x,\ t^{\frac{1}{2}}\eta+y,\ t^{\frac{1}{2}}\zeta+z\}\, t^{\frac{3}{2}}\, d\xi\, d\eta\, d\zeta$$
$$\times C\,(\cos \alpha t \sin \alpha t)^{-\frac{3}{2}} e^{\frac{\pi i m}{h}\alpha\{(\xi^2+\eta^2+\zeta^2)t \cot \alpha t - \Sigma(x+x_0)^2 \tan \alpha t\}}.$$

As t approaches zero this expression becomes

$$\psi(xyz0)=f(xyz)C\alpha^{-\frac{3}{2}}\int\int\int e^{\frac{\pi i m}{h}(\xi^2+\eta^2+\zeta^2)}\, d\xi\, d\eta\, d\zeta,$$

the limits of integration being $-\infty$ and $+\infty$.

In order therefore that $\psi(xyz0)$ should be equal to $f(xyz)$ we must have

$$C\alpha^{-\frac{3}{2}}\left(\frac{h}{-im}\right)^{\frac{3}{2}}=1,$$

or

$$C=\left(\frac{-im\alpha}{h}\right)^{\frac{3}{2}}.$$

Now in (28) let us assume that when $t=0$

$$F_0(xyz)=e^{-\frac{x^2+y^2+z^2}{2\sigma^2}},$$

where σ is so small that F_0 is sensibly zero except when x, y, z are all small. Then we may write

$$f(x_0y_0z_0)=e^{\Sigma\left(-\frac{x_0^2}{2\sigma^2}+\frac{2\pi i}{h}mu_0x_0\right)}.$$

It follows that

$$\psi(xyzt)=\left(-\frac{im\alpha}{h}\right)^{\frac{3}{2}}(\cos \alpha t \sin \alpha t)^{-\frac{3}{2}}\int\int\int e^{K}\, dx_0\, dy_0\, dz_0,$$

where

$$\mathrm{K}=\Sigma\Big[-\frac{{x_0}^2}{2\sigma^2}+\frac{2\pi i}{h}mu_0x_0$$

$$+\frac{\pi im}{h}\alpha\{(x-x_0)^2\cot\alpha t-(x+x_0)^2\tan\alpha t\}\Big].$$

Hence

$$\mathrm{K}=\Sigma(\mathrm{A}x^2-\mathrm{B}{x_0}^2+\lambda_x x_0),$$

where

$$\mathrm{A}=\frac{\pi im}{h}\alpha\,(\cot\alpha t-\tan\alpha t),$$

$$\mathrm{B}=\frac{1}{2\sigma^2}-\frac{\pi im}{h}\alpha\,(\cot\alpha t-\tan\alpha t),$$

$$\lambda_x=\frac{2\pi i}{h}mu_0-\frac{2\pi im}{h}\alpha x\,(\cot\alpha t+\tan\alpha t).$$

Now

$$\int_{-\infty}^{+\infty}e^{-\mathrm{B}{x_0}^2+\lambda_x x_0}\,dx_0=\left(\frac{\pi}{\mathrm{B}}\right)^{\frac{1}{2}}e^{\frac{{\lambda_x}^2}{4\mathrm{B}}}.$$

Hence

$$\psi(xyzt)=\left(-\frac{im\alpha}{h}\right)^{\frac{3}{2}}(\cos\alpha t\sin\alpha t)^{-\frac{3}{2}}\left(\frac{\pi}{\mathrm{B}}\right)^{\frac{3}{2}}e^{\Sigma\left(\mathrm{A}x^2+\frac{{\lambda_x}^2}{4\mathrm{B}}\right)}.$$

Let us now write, for brevity,

$$\mathrm{M}=\frac{2m\alpha\pi}{h}.$$

Then

$$\mathrm{A}=i\mathrm{M}\cot 2\alpha t,$$

$$\mathrm{B}=\frac{1}{2\sigma^2}-i\mathrm{M}\cot 2\alpha t,$$

$$\lambda_x=i\mathrm{M}\left(\frac{u_0}{\alpha}-x\frac{2}{\sin 2\alpha t}\right).$$

Thus

$$\left(-\frac{im\alpha}{h}\right)^{\frac{3}{2}}(\tfrac{1}{2}\sin 2\alpha t)^{-\frac{3}{2}}\left(\frac{\pi}{\mathrm{B}}\right)^{\frac{3}{2}}$$

$$=\left\{\frac{-i\mathrm{M}}{\frac{1}{2\sigma^2}\sin 2\alpha t-i\mathrm{M}\cos 2\alpha t}\right\}^{\frac{3}{2}}.$$

Also

$$\frac{\lambda_x^2}{4B}=\frac{-M^2\left(\frac{1}{2\sigma^2}+iM\cot 2\alpha t\right)\left(\frac{u_0}{\alpha}-x\frac{2}{\sin 2\alpha t}\right)^2}{4\left(\frac{1}{4\sigma^4}+M^2\cot^2 2\alpha t\right)}.$$

Let us now write

$$\psi=\rho e^{\frac{2\pi i}{h}\phi},$$

$$\bar{\psi}=\rho e^{-\frac{2\pi i}{h}\phi}.$$

Also let

$$N=\frac{1}{4\sigma^4M^2}\sin^2 2\alpha t+\cos^2 2\alpha t.$$

Then

$$\rho^2=\left(\frac{1}{N}\right)^{\frac{3}{2}}e^{-\frac{1}{\sigma^2N}\Sigma\left(\frac{u_0}{2\alpha}\sin 2\alpha t-x\right)^2} \quad . \quad . \quad . \quad . \quad (33)$$

The right-hand side of (33) is the expression for the probability of observed occurrence.

Now

$$\frac{1}{4\sigma^4M^2}=\frac{1}{4\sigma^4}\frac{h^2}{4m^2\alpha^2\pi^2}$$

$$=\frac{h^2}{4\sigma^4m\kappa\pi^2} \quad \text{from (32).}$$

If κ and therefore α become zero we obtain the case in which there is no field. In this case (33) reduces to

$$\rho^2=\left(\frac{1}{N_0}\right)^{\frac{3}{2}}e^{-\frac{1}{\sigma^2N_0}\Sigma(u_0t-x)^2},$$

where

$$N_0=\frac{h^2t^2}{4\sigma^4m^2\pi^2}+1.$$

Hence the probability of occurrence defined by putting $h=0$ does not change for a point moving with the component velocities u_0, v_0, w_0.

When, however, κ is not zero the situation is very different.

It will be observed from (33) that for a point moving with component velocities

$$\frac{dx}{dt} = u_0 \cos 2\alpha t, \text{ etc.},$$

$$\rho^2 = \mathrm{N}^{-\frac{3}{2}}.$$

If $h=0$ an examination of the initial conditions indicates at once how the points of the assembly tend to crowd together when

$$2\alpha t = n\pi + \tfrac{1}{2}\pi,$$

so that at those times ρ^2 tends to become infinite.

If $4\sigma^4\mathrm{M}^2=1$, ρ^2 maintains the same value about a point moving with velocity components $u_0 \cos 2\alpha t$ etc.

If $4\sigma\,\mathrm{M}^2$ is very small, ρ^2 has a sensible value only at times in the neighbourhood of

$$t = \frac{n\pi}{2\alpha},$$

where $n=0, 1, 2, 3\ldots$

There is no continuous spreading, but the probability of observed occurrence is strictly periodic.

Let us now examine the function ϕ. It is not difficult to show that

$$\frac{\pi}{h}\phi = \frac{\mathrm{M}\cos 2\alpha t}{\mathrm{N}} \Sigma \left\{ \tfrac{1}{2}x^2 \left(\frac{1}{4\sigma^4\mathrm{M}^2} - 1 \right) \sin 2\alpha t + \frac{u_0}{2\alpha} x \right\}$$

$$+ \text{a function of } t.$$

Hence

$$\frac{\pi}{h}\frac{\partial\phi}{\partial x} = \frac{\mathrm{M}\cos 2\alpha t}{\mathrm{N}} \left\{ x \left(\frac{1}{4\sigma^4\mathrm{M}^2} - 1 \right) \sin 2\alpha t + \frac{u_0}{2\alpha} \right\}. \quad (34)$$

If $4\sigma^4\mathrm{M}^2=1$,

$$\frac{\partial\phi}{\partial x} = mu_0 \cos 2\alpha t.$$

But if $4\sigma^4\mathrm{M}^2$ is very small, the coefficient of x becomes important except in the neighbourhood of $t=n\pi/2\alpha$.

Relativity Theory.

In relativity we have to start with equation (18) as the general equation associated with the prehistorical motions.

Let us write, as in non-relativity theory,

$$\psi_0 = \psi e^{\frac{2\pi i}{h} \mathrm{R}},$$

in which

$$\mathrm{R} = \int_{t_0}^{t} (a\,dx + b\,dy + c\,dz + g\,dt).$$

The equation satisfied by ψ is then

$$\left(\frac{\partial}{\partial x} + \lambda a\right)^2 \psi + \ldots + \ldots - \frac{1}{c^2}\left(\frac{\partial}{\partial t} + \lambda g\right)^2 \psi + \lambda^2 m_0^2 c^2 \psi + \lambda\left(\frac{\partial a}{\partial x} + \frac{\partial b}{\partial y} + \frac{\partial c}{\partial z} - \frac{1}{c^2}\frac{\partial g}{\partial t}\right)\psi = 0, \quad (35)$$

where

$$\lambda = \frac{2\pi i}{h}.$$

Suppose now that a solution of (35) is given in the form

$$\psi = \rho e^{\lambda \phi},$$

then in the resulting equation, when $h=0$, ϕ must satisfy the Hamiltonian equation for the motion which results from the assumed constitution of the atom.

Substituting in (35), it follows that

$$\rho \Box^2 \rho + \lambda\left[\frac{\partial}{\partial x}\left\{\rho^2\left(\frac{\partial \phi}{\partial x} + a\right)\right\} + \ldots + \ldots - \frac{1}{c^2}\frac{\partial}{\partial t}\left\{\rho^2\left(\frac{\partial \phi}{\partial t} + g\right)\right\}\right] + \lambda^2 \rho^2\left[\left(\frac{\partial \phi}{\partial x} + a\right)^2 + \ldots + \ldots - \frac{1}{c^2}\left(\frac{\partial \phi}{\partial t} + g\right)^2 + m_0^2 c^2\right] = 0.$$

Let us assume that the forces are derived from a scalar potential V; then by putting $h=0$ it follows that a, b, c are all zero and $g=\mathrm{V}$.

Now $\partial\phi/\partial x = mu$, etc. Hence we must have

$$\frac{\partial}{\partial x}(\rho^2 mu) + \ldots + \ldots - \frac{1}{c^2}\frac{\partial}{\partial t}\left\{\rho^2\left(\frac{\partial\phi}{\partial t} + \mathrm{V}\right)\right\} = 0.$$

In this equation m is not a constant, and therefore ρ^2 is not the probability of observed occurrence.

If we put $h=0$, and consider the probability of occurrence, we obtain from the Hamiltonian equation

$$mc^2 = -\frac{\partial\phi}{\partial t} - \mathrm{V}.$$

In this case the equation of continuity is

$$\frac{\partial}{\partial x}(\rho^2 mc^2 u) + \ldots + \ldots + \frac{\partial}{\partial t}(\rho^2 mc^2) = 0. \quad . \quad (36)$$

If the entity associated with every point is the kinetic energy mc^2, equation (36) is an equation expressing continuity of kinetic energy.

It does not appear possible therefore to associate the intensity of the wave with the relative probability of observed occurrence of the electron at a given point at a given time. Hence a completely different method of approach is required.

We still retain the fundamental assumption that the intensity of the wave is the relative probability of observed occurrence of electric charge, so that the atom must now be filled with a distribution of charge and current density which is the observed equivalent of the electron in its motion. In non-relativity theory the velocity components and the density ρ^2 in the equivalent motion are determined by the single function ψ and its conjugate $\bar{\psi}$ if there are no vector potentials in the field.

In relativity theory, however, the velocity components do not under any circumstances satisfy the necessary conditions which make ρ^2 the density in the equivalent motion. Hence the single function ψ is insufficient to determine the equivalent motion. We must introduce four functions, which will then be sufficient to determine the density, the resultant velocity, and the direction of travel in the equivalent motion. It thus appears natural to expect a similarity between the fundamental equations of the quantum theory and Maxwell's equations

of the electromagnetic field, since we now require four variables to determine the equivalent charge and current densities.

Let us return to equation (18) and put

$$\frac{2\pi}{h} m_0 c = \mathrm{M}.$$

That equation then becomes

$$\nabla^2\psi_0 - \frac{1}{c^2}\frac{\partial^2\psi_0}{\partial t^2} - \mathrm{M}^2\psi_0 = 0. \quad . \quad . \quad . \quad (37)$$

Consider four variables, $\theta_1, \theta_2, \theta_3, \theta_4$, connected by the equations

$$\alpha\,\theta_3 + \beta\,\theta_4 + \gamma\,\theta_2 = 0,$$
$$\alpha'\theta_4 - \beta'\theta_3 + \gamma\,\theta_1 = 0,$$
$$\alpha\,\theta_1 + \beta'\theta_2 + \gamma'\theta_4 = 0,$$
$$\alpha'\theta_2 - \beta\,\theta_1 + \gamma'\theta_3 = 0,$$

in which $\alpha, \beta, \gamma, \alpha', \beta', \gamma'$ may be operators. If the operations are commutative each of the variables will satisfy the equation

$$(\alpha\alpha' + \beta\beta' - \gamma\gamma')\theta = 0.$$

Suppose that

$$\alpha = \frac{\partial}{\partial\alpha} - i\frac{\partial}{\partial y},$$

$$\alpha' = \frac{\partial}{\partial x} + i\frac{\partial}{\partial y},$$

$$\beta = \beta' = \frac{\partial}{\partial z},$$

$$\gamma = \frac{1}{c}\frac{\partial}{\partial t} + i\mathrm{M},$$

$$\gamma' = \frac{1}{c}\frac{\partial}{\partial t} - i\mathrm{M}.$$

Then it is found that $\theta_1, \theta_2, \theta_3, \theta_4$ each satisfies equation (37).

Now (37) is the general equation associated with the prehistorical motions. Hence $\theta_1\ \theta_2,\ \theta_3, \theta_4$ are probability functions associated with the prehistorical motions,

and the four equations can be shown to be invariant under a Lorentz transformation.

Let us now, for reasons already explained, put

$$\theta_s = \psi_s \, e^{\frac{2\pi i}{h}\int_{t_0}^{t}(a\,dx+b\,dy+c\,dz+g\,dt)}$$

$$(s=1, 2, 3, 4).$$

If, further, we write

$$\mathrm{L}_x = \frac{h}{2\pi i}\frac{\partial}{\partial x} + a,$$

$$\mathrm{L}_y = \frac{h}{2\pi i}\frac{\partial}{\partial y} + b,$$

$$\mathrm{L}_z = \frac{h}{2\pi i}\frac{\partial}{\partial z} + c,$$

$$\mathrm{L}_t = \frac{h}{2\pi i}\frac{\partial}{\partial t} + g,$$

we may put the equations satisfied by the ψ's in the following form :—

$$\left.\begin{aligned}
&(\mathrm{L}_x - i\mathrm{L}_y)\psi_3 + \mathrm{L}_z\psi_4 + \left(\frac{1}{c}\mathrm{L}_t + m_0 c\right)\psi_2 = 0,\\
&(\mathrm{L}_x + i\mathrm{L}_y)\psi_4 - \mathrm{L}_z\psi_3 + \left(\frac{1}{c}\mathrm{L}_t + m_0 c\right)\psi_1 = 0,\\
&(\mathrm{L}_x - i\mathrm{L}_y)\psi_1 + \mathrm{L}_z\psi_2 + \left(\frac{1}{c}\mathrm{L}_t - m_0 c\right)\psi_4 = 0,\\
&(\mathrm{L}_x + i\mathrm{L}_y)\psi_2 - \mathrm{L}_z\psi_1 + \left(\frac{1}{c}\mathrm{L}_t - m_0 c\right)\psi_3 = 0.
\end{aligned}\right\} \quad (38)$$

The conjugate equations are easy to write down.

Multiply the first equation of (38) throughout by $\bar{\psi}_2$ and the first of the conjugate equations throughout by ψ_2. Treat the other equations in a similar way and add all together. We then obtain

$$\frac{\partial}{\partial x}\{\psi_3\bar{\psi}_2 + \psi_2\bar{\psi}_3 + \psi_1\bar{\psi}_4 + \psi_4\bar{\psi}_1\}$$

$$+ \frac{\partial}{\partial y}\{-i\psi_3\bar{\psi}_2 + i\psi_2\bar{\psi}_3 - i\psi_1\bar{\psi}_4 + i\psi_4\bar{\psi}_1\}$$

$$+\frac{\partial}{\partial z}\{\psi_4\bar{\psi}_2+\psi_2\bar{\psi}_4-\psi_1\psi_3-\psi_3\bar{\psi}_1\}$$

$$+\frac{1}{c}\frac{\partial}{\partial t}\{\psi_1\bar{\psi}_1+\psi_2\bar{\psi}_2+\psi_3\bar{\psi}_3+\psi_4\bar{\psi}_4\}=0. \quad (39)$$

This equation corresponds to the equation of continuity of non-relativity theory.

Introducing the notation of electromagnetic theory, but remembering that the functions do not possess the same significance, we shall write

$$\psi_1=\mathrm{H}_x+i\mathrm{H}_y, \qquad \psi_2=\mathrm{H}_z+i\mathrm{H}_w,$$

$$\psi_3=-i\mathrm{E}_x+\mathrm{E}_y, \qquad \psi_4=-i\mathrm{E}_z+\mathrm{E}_w.$$

The variables E_w and H_w are additional to the variables required by Maxwell's theory of the free æther.

Substituting these expressions in (39), we get

$$\frac{\partial}{\partial x}\{\mathrm{E}_y\mathrm{H}_z-\mathrm{E}_z\mathrm{H}_y-\mathrm{E}_x\mathrm{H}_w+\mathrm{H}_x\mathrm{E}_w\}$$

$$+\frac{\partial}{\partial y}\{\mathrm{E}_z\mathrm{H}_x-\mathrm{E}_x\mathrm{H}_z-\mathrm{E}_y\mathrm{H}_w+\mathrm{H}_y\mathrm{E}_w\}$$

$$+\frac{\partial}{\partial z}\{\mathrm{E}_x\mathrm{H}_y-\mathrm{E}_y\mathrm{H}_x-\mathrm{E}_z\mathrm{H}_w+\mathrm{H}_z\mathrm{E}_w\}$$

$$+\frac{1}{2c}\frac{\partial}{\partial t}\{\mathrm{E}_x^2+\mathrm{E}_y^2+\mathrm{E}_z^2+\mathrm{H}_x^2+\mathrm{H}_y^2+\mathrm{H}_z^2+\mathrm{E}_w^2+\mathrm{H}_w^2\}=0.$$

. . . (40)

This equation is identical with the equation expressing Poynting's theorem when E_w and H_w are omitted and E, H are Maxwell's field intensities.

The expression within brackets in the last line of (40) is the intensity of the wave.

The expressions within brackets in the first three lines multiplied by $2c$ are the current components if the intensity of the wave represents the density of electric charge.

That this is the case is clear, for the relative probability of observed occurrence in any one of the events associated with ψ_1, ψ_2, ψ_3, ψ_4, and their conjugates is

$$\psi_1\bar{\psi}_1+\psi_2\bar{\psi}_2+\psi_3\bar{\psi}_3+\psi_4\bar{\psi}_4.$$

In order therefore to obtain an equivalent distribution of charge and current it is necessary to introduce four

probability functions, and, finally, by means of the equations of the electron theory the equivalent density of charge and of current components may be connected with the vector potentials and the scalar potential of the field.

These potentials are introduced as follows :—

If we write

$$\psi_s = \rho_s e^{\frac{2\pi i}{h}\phi} \qquad (s=1, 2\ \ 3, 4),$$

it is not difficult to show that, when $h=0$, ϕ satisfies the Hamiltonian equation

$$\left(\frac{\partial\phi}{\partial x}+a\right)^2+\left(\frac{\partial\phi}{\partial y}+b\right)^2+\left(\frac{\partial\phi}{\partial z}+c\right)^2 - \frac{1}{c^2}\left(\frac{\partial\phi}{\partial t}+g\right)^2 - m_0{}^2c^2=0,$$

which is the result of elimination of the ρ's from four linear equations.

If, then, A_x, A_y, A_z, and V are the components of the electromagnetic potentials, we must write

$$a=-\frac{e}{c}A_x,$$

$$b=-\frac{e}{c}A_y,$$

$$c=-\frac{e}{c}A_z,$$

$$g=eV.$$

The whole of the foregoing theory is based upon nothing more than a very natural interpretation of Planck's hypothesis in terms of probability, and by a strict adherence to the accepted laws of probability in statistical mechanics no assumptions are required. Moreover, little more is required of statistical theory than is necessary for the proper formulation of initial conditions.

The author is indebted to the Admiralty for permission to publish this paper.

Nov. 12th, 1935.

XLIX. *Magnetic Susceptibility of Single Crystals of Lead, Thallium, and Tin.*

By S. Ramachandra Rao, *M.A., Ph.D., F.Inst.P., and* K. C. Subramaniam, *B.Sc.(Hons.), Annamalai University, Annamalainagar, South India* *.

1. Introduction.

A THOROUGH and systematic investigation of the magnetic properties of metals was originally conducted by Honda [1] and Owen [2]. Their results enabled a clear elucidation of the magnetic behaviour of metals in general to be made. A metal can now be considered to be built up of a lattice of metallic ions, the remaining electrons of the individual atoms being considered free or partly bound in accordance with their energy values. In considering therefore the susceptibility of the metal (we are here dealing with non-ferromagnetic metals) we deal first with the susceptibility of the ions and second with the susceptibility of the extra-ionic electrons. The first component is constant for a given ion and is independent of the crystal direction. The second part is structure sensitive and is dependent on the several physical conditions associated with the metal under investigation.

These outer electrons of the atoms may be regarded as free in the metal. Their number may be assumed to be of the same order as the number of atoms. Pauli [3] considered these electrons to constitute an "electron gas," and elucidated that under such conditions they contribute a paramagnetic susceptibility $(\chi_A)_e$ for a gram atom of the metal given by

$$(\chi_A)_e \times 10^6 = 48{\cdot}17q/V_0[1-6{\cdot}113\times 10^{-9}(T/V_0)^2], \qquad (1)$$

where q is the number of electrons considered as free in the metal per atom, V_0 the width of the energy band occupied by the electrons in volts, and T the absolute temperature. Superposed over this we have the Landau diamagnetism [4] equal to one-third of the Pauli paramagnetism.

If the outer electrons are considered as bound there would be a diamagnetic contribution which would be dependent on the nature of binding of these electrons. This binding in metals may be homopolar (in which case

* Communicated by the Authors.

each valency electron is associated with two neighbouring atoms) or metallic (wherein the electrons are shared throughout the crystal). In the homopolar type of binding the susceptibility of the crystal is approximately equal to the sum of the susceptibility of the atoms ; on the other hand, in the metallic type the electrons would contribute a paramagnetic component and the susceptibility would be less than the calculated atomic value, or even paramagnetic, as in the case of white tin.

In view of these conclusions the diamagnetism of metallic crystals is of special interest, since the susceptibilities in different directions would give us definite pictures of the nature of binding of the outer electrons in different directions. In recent years some attention has been paid to this problem. McLennan and his associates [5] have determined the magnetic susceptibility of a number of metals, including zinc, cadmium, antimony, and tin. Focke [6] succeeded in preparing pure and perfect bismuth crystals, and studied their magnetic properties with great precision. Vogt [7] showed that solid mercury possesses a small magnetic anisotropy. These investigations confirm the fact that magnetic susceptibilities, like other physical properties such as electrical and heat conductivities, are structure sensitive.

In these experiments the magnetic susceptibilities of single crystals of lead, thallium, and tin have been investigated. To our knowledge thallium does not seem to have been studied before. It is of special interest, since on heating the crystal the close-packed hexagonal structure changes to the face-centred cubic type at temperatures above 235° C. The metal is remarkable also for the sudden drop (nearly 10 per cent.) in the diamagnetic susceptibility on melting at 300° C.

2. Experiments.

(a) *Preparation of Single Crystals.*

Single crystals were prepared by the method of slow cooling adopted by McLennan for zinc and cadmium. The metals were extra-pure from Kahlbaum. For the preparation of the crystals a tube, as shown in fig. 1, was used. ABC was of uniform section, with a diameter of nearly 5 mm. The end A was drawn sharply to almost a point, while at B there was a constriction. D was a

side-tube of fairly wide diameter attached to ABC. The tube was cleaned thoroughly, and sufficient quantity of the metal was placed in D. The end C was connected to a pump, and after reducing the pressure to a very low value the metal in D was melted with a Bunsen burner. After shaking carefully to remove all adsorbed gases the clean metal was allowed to flow in AB to a height of nearly 8 cm. After cooling the tube was sealed off at B.

The ordinary alarm-clock method was used to subject the metal to slow cooling. The temperature inside the furnace was kept about 20° C. above the melting-point of the metal studied. The rate of cooling was controlled by altering the diameter of the drum fixed on to the turning head of the clock. The consistency of the magnetic measurements showed that under such conditions perfect specimens of single crystals were obtained.

Fig. 1.

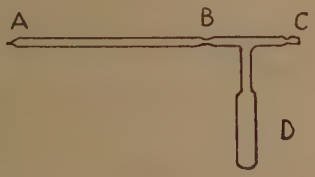

(b) *Compensating Device in the Guoy Method.*

The Guoy method was adopted for the measurements of the crystals. The Guoy force on the specimen was exactly balanced by an electrodynamic force, details of which are given below.

After several trials the following arrangement (fig. 2) was found to work consistently and satisfactorily. A steel wire of S.W.G. 36 and length about 25 cm. was stretched horizontally between the ends A and B, of which B was fixed while A could be adjusted by a screw (fig. 2 *a*). The wire could thus be kept at a suitable tension. A light aluminium strip of length 35 cm. and breadth 5 mm. was fixed rigidly across the middle of the wire, such that CF was 15 cm. A circular coil C_2, of diameter 10 cm., containing 100 turns of enamelled copper wire (S.W.G. 30), was wound and fixed in a horizontal plane with centre at E (8 cm. from D). Two fixed coils, C_1 and C_3. were

Fig. 2.

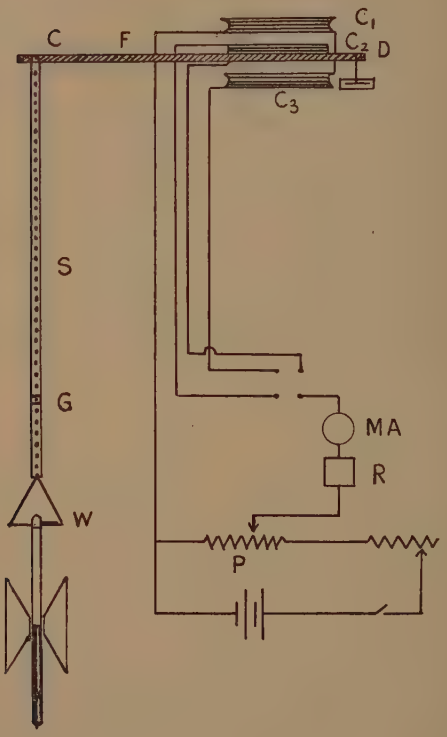

Fig. 2 *a*.

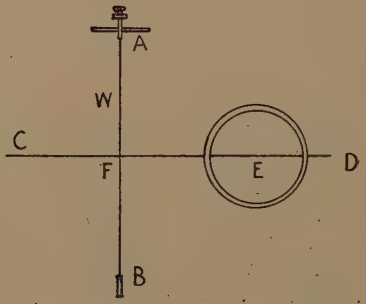

placed above and below C_2 and coaxially with it. Coils C_1 and C_3 contained 500 turns and were so connected in series permanently that the currents would flow through them in opposite directions.

The electrical connexions are also shown in fig. 2. The same current flows through the three coils, except that the current through C_2 could be reversed to vary the direction of the balancing force. It is well known that if a current i flows through the coils the force on the middle coil varies directly as i^2. The Guoy force on the specimen is thus directly proportional to the square of the current, which is measured accurately by a milli-ammeter. The rotating potentiometer P was used to vary the current.

(c) *The Suspension of the Crystal.*

A long aluminium strip was suspended vertically from the end C, the strip being made as light as possible by punching a large number of circular holes through it. A thin glass plate G was fixed on one such hole, and a horizontal line etched on the glass plate was observed through a microscope containing a fixed horizontal wire in the eyepiece scale.

To the end of the strip S was attached rigidly a light circular dial W of wood. The tube containing the crystal passed through a hole in the centre of the dial and was held in position by means of a metal clip. The dial was marked in degrees on its circumference, and the pointer attached to the clip read the position of the crystal with respect to the magnetic field. The position could be altered by rotating the end of the tube projecting above the clip without disturbing the apparatus.

(d) *Magnetic Field.*

A large Pye's electromagnet was used, the pole faces having a diameter of 3 cm. and being parallel to each other at a distance of $1\frac{1}{2}$ cm. Measurements were made at different field strengths for any given sample by varying the current through the electromagnet from 2 to 8 amperes. This current was measured with a Cambridge and Paul's ammeter reading correctly to 0·05 of an ampere.

(e) *Procedure.*

Water was taken as the standard substance. A glass tube of the same diameter and length as those used for the crystals was filled to half its length with water and sealed *in vacuo*. Measurements were made with the water surface exactly between the pole-pieces. It could be seen that compensation for the glass can be automatically secured by adjusting the length of the glass tube above the water surface to be equal to the length below.

To investigate a given specimen the crystal was suspended with its axis vertical and the metal surface symmetrically between the pole-faces. The arm CD was kept horizontal by adjusting suitable riders placed on it. The glass plate G was illuminated by a red lamp and the horizontal line was viewed through the microscope. On applying the magnetic field there was a deflexion of the etched line as seen in the microscope above or below, depending on whether the substance was dia- or paramagnetic. The line was now brought exactly to the original position by sending the compensating current through the coils. This current may be taken as a measure of the Guoy force on the specimen.

(f) *Heater.*

For investigating the susceptibility at higher temperatures a heater of suitable shape was constructed after several trials. Nickel silver wire was wound sparely, and tests conducted showed that the magnetic field was not appreciably affected by the winding. The heater was narrowed at the top and enclosed the crystal almost up to its upper surface. By adjusting the relative number of turns of the wire at different parts the heater had a uniform temperature inside. A mercury thermometer was inserted inside the heater and the inner temperature was read on it.

During the heating experiments the pole-faces were enclosed in tightly fitting cups made of copper sheets. These cups were wrapped around with padded cotton-sponge moistened with water. By drenching the covering repeatedly with water the pole-pieces were prevented from being heated during the measurements.

(g) *Calculation of the Specific Susceptibility.*

Let k_s be the volume susceptibility of the specimen, A_s the area of section, H the intensity of the magnetic field between the pole-faces, and i_s the compensating current. Then

$$\tfrac{1}{2}k_s A_s H^2 = C \cdot i_s^2, \quad . \quad . \quad . \quad . \quad . \quad . \quad (2)$$

where C is a constant depending on the apparatus. Similarly for water

$$\tfrac{1}{2}k_w A_w H^2 = C \cdot i_w^2 \quad . \quad . \quad . \quad . \quad . \quad (3)$$

when the determination of i_w is made at the same field strength. Hence

$$k_s = \frac{i_s^2}{i_w^2} \cdot \frac{A_w}{A_s} \cdot k_w. \quad . \quad . \quad . \quad . \quad . \quad . \quad (4)$$

Hence the specific susceptibility can be calculated from the relation

$$\chi_s = \frac{k_s}{\rho} = \frac{i_s^2}{i_w^2} \cdot \frac{A_w}{A_s} \cdot \frac{k_w}{\rho}$$

$$= \frac{i_s^2}{i_w^2} \cdot \frac{d_w^2}{d_s^2} \cdot \frac{k_w}{\rho}, \quad . \quad . \quad . \quad . \quad . \quad (5)$$

where d_w and d_s are the diameters of the water and the crystal tubes and ρ is the density of the metal. The required density data for the elements investigated have been taken from the International Critical Tables.

3. Results.

(a) *Lead.*

In the case of this metal no variation in the susceptibility of the metal was observed when the crystal was rotated and placed at different positions. This is just what is to be expected, since lead crystallizes in the cubic system.

Measurements were also made at different field strengths ranging from 11 to 18 kilogauss. The graph in fig. 3 shows that there is very little variation in the susceptibility as H is altered. The specific diamagnetic susceptibility at $H=\infty$ is found to be 0·107 [8]. This value agrees very satisfactorily with 0·120 obtained by Honda and Owen and 0·118 by Kœnigsberger [9].

The crystal was then heated and measurements were made at different temperatures up to 360° C. At some

intermediate temperatures tests were made to find whether there was any susceptibility variation on rotating the crystal, but no such variations were observed. The values of the specific susceptibility at different temperatures are plotted in fig. 3. It will be noted that the diamagnetic susceptibility is constant up to the

Fig. 3.

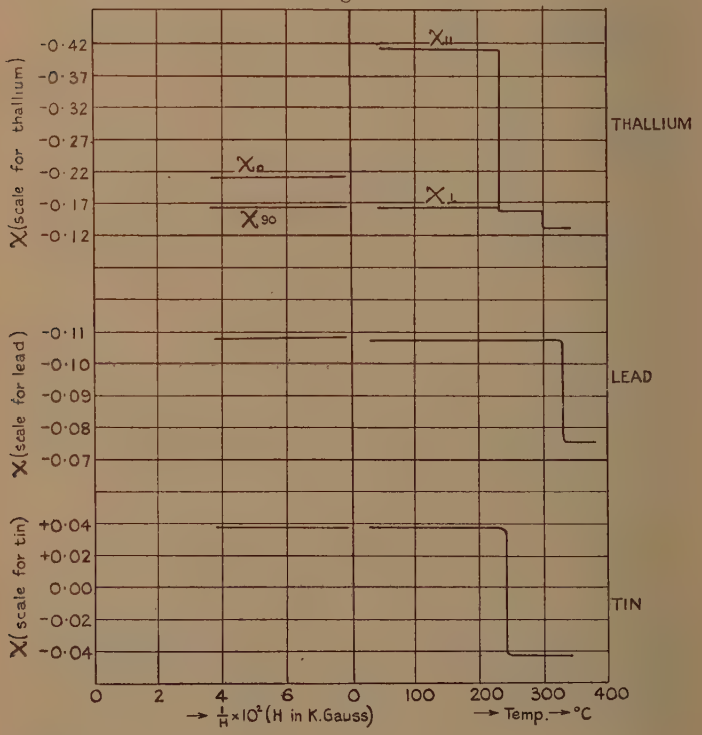

melting-point. At this temperature (330° C.) there is a sudden decrease in the value from 0·107 to 0·075, and up to 360° C. the liquid value remains constant.

These results agree remarkably well with those of Honda. Such an agreement indicates that the apparatus is thoroughly trustworthy. It has the further advantage that the measurements could be made rapidly and accurately.

(b) *Thallium.*

Thallium is of special interest because of its remarkable crystalline properties. This metal has two allotropic modifications, the α-variety at ordinary temperatures and the β-variety at temperatures above 230° C. The α-variety crystallizes in the hexagonal system with a close-packed structure, the a and c values being 3·47 Å. and 5·52 Å. respectively [10]. At 230° C. this structure changes into the face-centred cubic, the side of the unit cell being 4·84 Å.[10]. The metal melts at 300° C. All these changes are also indicated by the magnetic properties of thallium single crystals. Honda obtained a diamagnetic susceptibility value of 0·25 for polycrystalline α-thallium, 0·19 for the β-variety, and 0·17 for the liquid metal. His results show also strikingly that the change in the crystalline structure occurs sharply at 230° C.

Extra pure thallium from Kahlbaum was used in the preparation of the single crystals. These were about 10 cm. long and 5 mm. in diameter. The effect of the magnetic field at the other end of the crystal was neglected, since approximate measurements with water showed that by increasing the length of the water column there was no variation of the Guoy force.

(i.) *Rotation of the Crystal about a Vertical Axis.*

McLennan, Ruedy, and Cohen have shown that if $\chi_{\parallel}$ and $\chi_{\perp}$ be the principal susceptibilities of the crystal parallel and perpendicular to the hexagonal axis, χ_0 and χ_{90} the maximum and minimum susceptibilities as the crystal is rotated about a vertical axis, and ϕ the angle between the axis of the cylinder and the principal axis of the crystal,

$$\chi_{\perp}=\chi_{90} \quad \text{and} \quad \chi_{\parallel}=(\chi_0-\chi_{90}\cos^2\phi)/\sin^2\phi. \quad . \quad (6)$$

The crystal was rotated and the position was read on the circular scale. Measurements were taken every 15° for a definite current of 6 amperes in the electromagnet. The results obtained in the case of one of the thallium crystals are given below. It may be mentioned here that the zero of the circular scale was chosen to coincide with one of the maximum positions.

The results are plotted in fig. 4. It will be noticed that i^2 is maximum at 0°, 180°, and 360°, and minimum at 90° and 270°. There is general agreement between the variations obtained by McLennan and others for

Readings on the circular scale in °.	Balancing current in milliamps. i.	i^2.	Readings on the circular scale in °.	Balancing current in milliamps. i.	i^2.
0	63·6	4046	195	62·0	3844
15	62·5	3906	210	60·2	3624
30	60·8	3697	225	59·1	3493
45	58·8	3456	240	58·1	3376
60	57·4	3295	255	57·7	3330
75	56·8	3225	270	56·9	3238
90	56·9	3238	285	57·7	3330
105	57·8	3340	300	58·4	3410
120	58·9	3469	315	59·6	3551
135	60·4	3648	330	61·6	3795
150	61·6	3709	345	62·8	3945
165	62·7	3931	360	63·8	4070
180	63·7	4058	375	63·6	4046

Fig. 4.

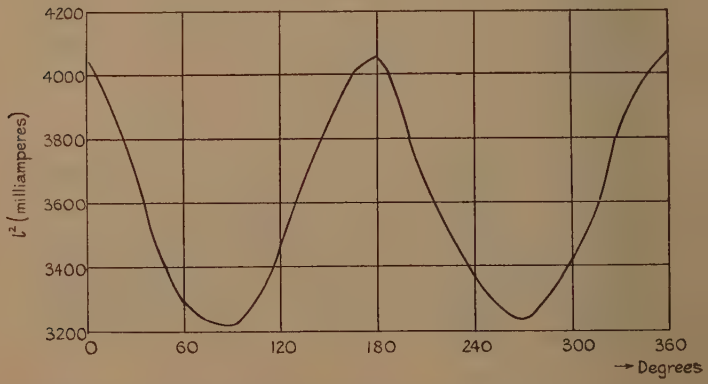

zinc and those of thallium recorded here, the structure being the same in both cases.

(ii.) *Determination of* $\chi_\perp$ *and* $\chi_{||}$.

The crystal was next placed in the position of maximum force and measurements were taken at different field strengths. Similar observations were made also at

the minimum positions. The results are plotted in fig. 3. The specific diamagnetic susceptibilities corresponding to the two positions (χ_0 and χ_{90}) at infinite field strengths are 0·209 and 0·165 respectively.

By etching the end of the cylindrical specimen with dilute sulphuric acid the cleavage plane (*i. e.*, the hexagonal plane) was found to make an angle of 65° with the cylindrical axis of the crystal. This gives a value of 25° for the angle between the axis of the cylinder and the hexagonal axis. It follows then from (6) that

$$\chi_\perp = -0{\cdot}165 \quad \text{and} \quad \chi_{\parallel} = -0{\cdot}412.$$

From these values we could also calculate the mean susceptibility of a polycrystalline aggregate of thallium, since

$$\chi = 1/3[2\chi_\perp + \chi_{\parallel}].$$

This gives for thallium an average susceptibility of −0·247, which agrees remarkably well with Honda's value of −0·25.

The magnetic anisotropy is found to be 2·50. This value is much higher than the values for other metals having a similar structure, as, for example, cadmium (1·31) and zinc (1·63). It is of great interest to consider why thallium should have such a large anisotropy.

(iii.) *Temperature Variation and β-Thallium.*

The single crystal was heated by enclosing it in the furnace already described. Measurements were made of the Guoy force in the positions of maximum and minimum forces at a few intermediate temperatures. The results shown in fig. 3 indicate that $\chi_\perp$ remains constant at different temperatures while $\chi_{\parallel}$ decreases slightly at higher temperatures. The average susceptibility of the metal should also remain nearly constant.

At 235° C. the balancing current suddenly decreases and remains constant for all orientations of the crystal in the magnetic field. The constant susceptibility works to −0·158. The change in the crystal structure is thus clearly indicated by the observations. No directional variations are obtained above 235° C., since the structure becomes face-centred cubic.

At 300° C. there is a further reduction in the susceptibility value, since the metal melts at that temperature. This liquid value (−0·131) remains constant till about 330° C., the maximum temperature reached in this experiment.

It is interesting to note that these results agree with those of Honda obtained for the polycrystalline metal.

(c) *Tin.*

Honda and Owen have investigated the magnetic properties of this element at different temperatures. According to Owen white tin has a paramagnetic susceptibility of 0·02, while Honda obtains 0·027. As the temperature is increased the susceptibility of white tin remains constant up to the melting-point (233° C.). At this temperature the paramagnetic value decreases to a diamagnetic value of 0·037. As the liquid tin is heated this value remains constant. Similar results were obtained by Rao [11], who obtained for white tin a paramagnetic susceptibility of 0·036 and for molten tin a diamagnetic value of 0·0455.

White tin crystallizes in the tetragonal system, the value of a and c being 5·82 Å. and 3·16 Å. respectively. Each atom has four neighbours 3·02 Å. away and two others slightly more distant (3·25 Å.). Under these conditions it is probable that the magnetic anisotropy would be very small, and that is exactly what is observed in the case of single crystals of white tin.

No variation of the Guoy force was noted as the single crystal was rotated about its axis. Measurements made at different fields strengths and plotted in fig. 3 show that there was no appreciable ferromagnetic impurity in the specimen. At 30° C. the specific paramagnetic susceptibility was found to be 0·038. This agrees satisfactorily with the values obtained by other investigators.

The crystal was then heated and measurements were taken at different temperatures right up to 250° C. Rotation of the crystal at a few intermediate temperatures showed that the susceptibility remained constant at all positions. The values of the specific susceptibility at different temperatures are plotted in fig. 3. It will be seen that the susceptibility remains constant up to the melting-point, and at this temperature there is a sharp change from a paramagnetic susceptibility of 0·038 to a

diamagnetic value of 0·043. This agrees with earlier observations by Honda and Rao.

That the susceptibility along the a and c axes in the crystal of white tin has the same value was verified by us by some preliminary experiments on tin crystals with the Curie method. This constancy was also observed by McLennan. It is now well recognized that the paramagnetism of white tin is due to the superficial electrons (of the atoms) considered as free. Under the circumstances the observed variation of the electrical conductivity in different directions by Bridgmann [12] is difficult to explain*.

4. Discussion.

The results for tin and lead are in agreement with the results of earlier observers, and no new facts have been established in this investigation. On the other hand, thallium is perhaps the most interesting of the substances studied here because of its allotropic modifications. At ordinary temperatures the metal crystallizes in the hexagonal system with a close-packed structure, the a and c values being 3·47 Å. and 5·52 Å. respectively. Above 235° C. the structure changes into the face-centred cubic. Our measurements give for α-thallium an atomic susceptibility of $-84{\cdot}2$ parallel to the hexagonal axis $(\chi_{\parallel})_A$ and $-33{\cdot}7$ perpendicular $(\chi_{\perp})_A$ to the same axis. The ionic susceptibility of Tl^{+3} does not seem to have been studied before, but the results of Meyer for thallic chloride enable us to calculate a value of $-32{\cdot}6$ [13] for the trivalent ion. The calculated value of Angus [14] based on the Zener-Slater method works to $-39{\cdot}68$. The ionic diamagnetic susceptibility of Tl^{+3} consequently becomes nearly equal to $(\chi_{\perp})_A$, while $(\chi_{\parallel})_A$ is much larger, being 84·2.

The definite and large anisotropy indicates that in the hexagonal close-packed structure of α-thallium the three valency electrons are divided such that two of them

* *Note added in proof.*—Since the above was written, we have seen the paper of Hoge (Phys. Rev. xlviii. p. 615 (1935)), who gives the value of 1·12 for the magnetic anisotropy of pure white tin. He worked with much larger field strengths and measured the small Guoy forces with a compensated microbalance. His results show that small quantities of impurities profoundly affect the anisotropy value. The paramagnetic susceptibility value of white tin obtained by him (0·0259) is, however, slightly different from our value (0·038).

have their orbits in the hexagonal plane while the third may be considered to be free. The above magnetic properties can be understood if we assume that the binding of the two electrons is homopolar while that of the third is metallic.

We shall consider the cases of zinc and cadmium, which also crystallize in the hexagonal close-packed structure. McLennan, Ruedy, and Cohen obtained for these crystals a magnetic anisotropy of 1·30 and 1·63 respectively. Stoner [15] has drawn attention to the fact that the anisotropy in these cases lies in the diamagnetic part of the susceptibility. There is also the paramagnetic contribution of the valency electrons when considered as free : the less the energy of the band occupied by these electrons the larger the paramagnetic contribution.

The large magnetic anisotropy of thallium now becomes clear.

The single valency electron having a low energy of binding may be considered to give a large paramagnetic contribution. The other two valency electrons give rise to a large diamagnetism due to homopolar binding in the hexagonal plane. Thus in a direction normal to the hexagonal plane we have (1) the diamagnetic susceptibility of the Tl^{+3} ions, (2) the diamagnetic susceptibility of the two valency electrons, (3) the paramagnetic susceptibility component of the single valency electron. Along the hexagonal plane we have (4) the diamagnetic susceptibility of the Tl^{+3} ions, and (5) the paramagnetic susceptibility component of the single valency electron mentioned above. The items (1) and (4) are identical, while (2) has a fairly large value. The paramagnetic components (3) and (5) may be taken as nearly equal ; in any case their difference must be small compared with the quantities we are considering. This will lead to an approximate value of 50·5 for the diamagnetic susceptibility of the two valency electrons having their orbits in the hexagonal plane. Applying the Langevin equation we get for the radius of the orbits of these electrons 3 Å., which is of the right order of magnitude. These results also account for the high anisotropy of α-thallium.

It has been mentioned that β-thallium has a face-centred cubic structure. It is obvious that in this case we have Tl^{+1} ions with the single valency electron in the

atom having a metallic linkage, as in copper. Our investigation gives for the atomic susceptibility of β-thallium a value of $-32{\cdot}3$. The ionic susceptibility of Tl^{+1} according to Kido [16] is $-38{\cdot}5$. These results suggest that the valency electrons contribute a paramagnetic susceptibility of 6·2 per gram atom of the metal. This is of the same order of magnitude as the corresponding values for copper, silver, and gold.

As far as we are aware there have been no measurements made on the electrical conductivity of thallium single crystals. These data are bound to throw more light on the nature of binding of the valency electrons.

5. Summary.

Single crystals of lead, thallium, and tin were prepared by the method of slow cooling, and their magnetic susceptibilities were investigated by the Guoy method, the magnetomotive force being balanced against an electrodynamic one. No change of susceptibility was noted as the crystals of lead or tin were rotated about the cylindrical axis. For α-thallium the diamagnetic susceptibility parallel to the hexagonal axis was 0·412 (in 10^{-6} units), while the value normal to this axis was 0·165. This gives a magnetic anisotropy of 2·5, which is larger than the corresponding values for other similar metals. The average value for polycrystalline thallium works out to 0·247.

On heating, α-thallium passes into the β-variety at 235° C. Since the structure of this form is cubical no variation of the diamagnetic susceptibility was observed as the crystal was rotated, but the mean diamagnetic susceptibility decreased to 0·158. On melting at 300° C. this value became 0·131. These results agree with the observations of other investigators.

These results are explained by assuming that in α-thallium two of the three valency electrons have their orbits in the hexagonal planes and that their binding is homopolar. The third electron is considered as free. In the β-variety there are only Tl^{+1} ions, with the remaining electron in the atom being considered as free. These considerations explain the observed magnetic properties.

We take this opportunity of thanking the authorities of the Annamalai University for the award of a studentship to one of us (K. C. Subramaniam), which has rendered this work possible.

References.

(1) *Ann. der Phys.* xxxii. p. 1027 (1910).
(2) *Ibid.* xxxvii. p. 657 (1912).
(3) *Zeits. f. Phys.* xli. p. 81 (1927); see also Frenkel, *Zeits f. Phys.* xlix. p. 31 (1928).
(4) Stoner, 'Magnetism and Matter,' p. 502.
(5) Proc. Roy. Soc. cxxi. p. 9 (1928); Roy. Soc. Canada Trans. xxiii. p. 159 (1929).
(6) Phys. Rev. xxxvi. p. 319 (1930).
(7) *Ann. der Phys.* xxi. p. 791 (1935).
(8) All χ values in this paper are given in 10^{-6} units.
(9) Quoted by Owen, *Ann. der Phys.* xxxvii. p. 667 (1912).
(10) Wyckoff, 'The Structure of Crystals,' p. 207.
(11) Proc. Ind. Acad. Sci. i. p. 123 (1934).
(12) Given in Int. Crit. Tables, vi. p. 135.
(13) Int. Crit. Tables, vi. p. 357.
(14) Proc. Roy. Soc. cxxxvi. p. 569 (1932).
(15) Stoner, 'Magnetism and Matter,' p. 512.
(16) Sc. Rep. Tohoku Imp. Univ. xxii. p. 835 (1933).

L. *A Method of Numerical Solution of Differential Equations.* *By* V. M. Falkner, *B.Sc., A.M.I.Mech.E., of the Aerodynamics Department, The National Physical Laboratory* *.

§ 1. *Introduction.*

IN attempting the solution of certain non-linear differential equations by the step-by-step method of integration due to Adams [1] it was found that, by employing what is believed to be a new modification of this method, the following advantages were gained :— (*a*) if differences up to a given order were used, a marked increase in accuracy was obtained; (*b*) an indication of the accuracy of the integration could be obtained.

The object of this paper is to give an account of this modification, and its application to the solution of two

* Communicated by E. F. Relf, A.R.C.Sc.

differential equations chosen as examples *. The wider question of the relative merits of this and other methods is outside the scope of the paper, and no claim is made for the present method other than that it can be used for any equation which is integrable by Adams's method, and that a very high degree of accuracy is obtainable.

§ 2. *Basis of the Method.*

The method is based on the use of the difference table of the highest order derivative occurring in the equation to be integrated. If this derivative be denoted by y, the independent variable by x, and the interval by w, the difference table in central-difference notation [2] up to δ^4, the highest order difference to which the analysis is extended here, is as follows :—

Value of x,	Variable.	δ.	δ^2.	δ^3.	δ^4.
		$\delta y_{-7/2}$			
$a-4w$	y_{-4}		$\delta^2 y_{-3}$		
		$\delta y_{-5/2}$		$\delta^3 y_{-5/2}$	
$a-3w$	y_{-3}		$\delta^2 y_{-2}$		$\delta^4 y_{-2}$
		$\delta y_{-3/2}$		$\delta^3 y_{-3/2}$	
$a-2w$	y_{-2}		$\delta^2 y_{-1}$		
		$\delta y_{-1/2}$			
$a-w$	y_{-1}				
a	y_0				
$a+w$	y_1				

Let the successive integrals of y be denoted by Qy, Q^2y, and so on, where

$$Q_1^n y - Q_0^n y = \int_a^{a+w} Q^{n-1} y.$$

The basic formulæ are derived by expressing the values of y_1, Qy_1, Q^2y_1, ..., *i. e.*, the values at the end of the next forward interval, entirely in terms of y_0, Qy_0, Q^2y_0, etc., and the diagonal row of differences through y_0. The first integral Qy was obtained by Adams [1].

* Permission to publish this work has been kindly granted by the Aeronautical Research Committee.

from integration of the Gregory-Newton formula over the interval a to $a+w$, and is, in the present notation,

$$Qy_1 = Qy_0 + uy_0 + \frac{1}{2}w\delta y_{-1/2} + \frac{5}{12}w\delta^2 y_{-1} + \frac{3}{8}w\delta^3 y_{-3/2} + \frac{251}{720}w\delta^4 y_{-2}. \quad . \quad . \quad (1)$$

The next integral $Q_2 y$ is given by the following formula, corresponding to (1) :—

$$Q^2 y_1 = Q^2 y_0 + wQy_0 + \frac{1}{2}w\delta Qy_{-1/2} + \frac{5}{12}w\delta^2 Qy_{-1} + \frac{3}{8}w\delta^3 Qy_{-3/2} + \frac{251}{720}w\delta^4 Qy_{-2} + \frac{95}{288}w\delta^5 Qy_{-5/2}. \quad . \quad . \quad . \quad (2)$$

Integration of the Gregory-Newton formula over the interval $a-w$ to a gives, however, the following relation :—

$$\delta Qy_{-1/2} = wy_0 - \frac{1}{2}w\delta y_{-1/2} - \frac{1}{12}w\delta^2 y_{-1} - \frac{1}{24}w\delta^3 y_{-3/2} - \frac{19}{720}w\delta^4 y_{-2}, \quad . \quad . \quad . \quad . \quad (3)$$

and hence

$$\delta^2 Qy_{-1} = w\delta y_{-1/2} - \frac{1}{2}w\delta^2 y_{-1} - \frac{1}{12}w\delta^3 y_{-3/2} - \frac{1}{24}w\delta^4 y_{-2}, \quad (4)$$

and so on, to

$$\delta^5 Qy_{-5/2} = w\delta^4 y_{-2}. \quad . \quad . \quad . \quad . \quad . \quad . \quad (5)$$

On substitution in (2) of the relations (3) to (5), the following formula for $Q^2 y_1$ results :—

$$Q^2 y_1 = Q^2 y_0 + wQy_0 + \frac{1}{2}w^2 y_0 + \frac{1}{6}w^2\delta y_{-1/2} + \frac{1}{8}w^2\delta^2 y_{-1} + \frac{19}{180}w^2\delta^3 y_{-3/2} + \frac{3}{32}w^2\delta^4 y_{-2}. \quad . \quad (6)$$

This process may be repeated indefinitely. The resulting formulæ, up to the third integral, with differences up to the fourth order, would appear, however, to be adequate for any but exceptional requirements. These

formulæ, which are now given, are the fundamental formulæ of the method.

$$\left.\begin{aligned}
y_1 &= y_0 + \delta y_{-1/2} + \delta^2 y_{-1} + \delta^3 y_{-3/2} + \delta^4 y_{-2}, \\
\mathrm{Q}y_1 &= \mathrm{Q}y_0 + wy_0 + \frac{1}{2} w\delta y_{-1/2} + \frac{5}{12} w\delta^2 y_{-1} + \frac{3}{8} w\delta^3 y_{-3/2} \\
&\quad + \frac{251}{720} w\delta^4 y_{-2}, \\
\mathrm{Q}^2 y_1 &= \mathrm{Q}^2 y_0 + w\mathrm{Q}y_0 + \frac{1}{2} w^2 y_0 + \frac{1}{6} w^2\delta y_{-1/2} + \frac{1}{8} w^2\delta^2 y_{-1} \\
&\quad + \frac{19}{180} w^2\delta^3 y_{-3/2} + \frac{3}{32} w^2\delta^4 y_{-2}, \\
\mathrm{Q}^3 y_1 &= \mathrm{Q}^3 y_0 + w\mathrm{Q}^2 y_0 + \frac{1}{2} w^2\mathrm{Q}y_0 + \frac{1}{6} w^3 y_0 + \frac{1}{24} w^3\delta y_{-1/2} \\
&\quad + \frac{7}{240} w^3\delta^2 y_{-1} + \frac{17}{720} w^3\delta^3 y_{-3/2} + \frac{41}{2016} w^3\delta^4 y_{-2}.
\end{aligned}\right\} \quad (7)$$

§ 3. *Description of the Method.*

In order to start the solution, a succession of values of the variable—y_0, y_{-1}, y_{-2}, etc.,—and initial values of the integrals—$\mathrm{Q}y_0$, $\mathrm{Q}^2 y_0$, etc.,—must be known. The difference table for y can then be constructed. The method of solution is to use the relations (7) in conjunction with the equation relating y and its integrals in order to obtain a series of approximations to the values of y, and its integrals at the end of the next forward interval.

The first approximation is obtained by taking $\delta y_{-\frac{1}{2}}$ as an unknown quantity, denoted by ϵ, and treating all higher differences as zero. The relations (7) then become

$$\left.\begin{aligned}
y_1 &= y_0 + \epsilon, \\
\mathrm{Q}y_1 &= \mathrm{Q}y_0 + wy_0 + \frac{1}{2} w\epsilon, \\
\mathrm{Q}^2 y_1 &= \mathrm{Q}^2 y_0 + w\mathrm{Q}y_0 + \frac{1}{2} w^2 y_0 + \frac{1}{6} w^2\epsilon, \\
\mathrm{Q}^3 y_1 &= \mathrm{Q}^3 y_0 + w\mathrm{Q}^2 y_0 + \frac{1}{2} w^2\mathrm{Q}y_0 + \frac{1}{6} w^3 y_0 + \frac{1}{24} w^3\epsilon.
\end{aligned}\right\} \quad (8)$$

The value of ϵ can now be found by substituting these values in the equation relating y and its integrals, and

the resulting numerical values of y_1, Qy_1, etc. are used as the starting point for a repetition of the process.

An infinite series of approximations is obtained by taking $\delta^2 y_{-1}$, $\delta^3 y_{-3/2}$, etc. in succession as the unknown ϵ. In the case of the fourth approximation, the highest to which the present analysis extends, the relations (7) become

$$\left.\begin{aligned}
y_1 &= y_0 + \delta y_{-1/2} + \delta^2 y_{-1} + \delta^3 y_{-3/2} + \epsilon, \\
Qy_1 &= Qy_0 + wy_0 + \frac{1}{2} w\delta y_{-1/2} + \frac{5}{12} w\delta^2 y_{-1} + \frac{3}{8} w\delta^2 y_{-3/2} \\
&\quad + \frac{251}{720} w\epsilon, \\
Q^2 y_1 &= Q^2 y_0 + wQy_0 + \frac{1}{2} w^2 y_0 + \frac{1}{6} w^2 \delta y_{-1/2} + \frac{1}{8} w^2 \delta^2 y_{-1} \\
&\quad + \frac{19}{180} w^2 \delta^3 y_{-3/2} + \frac{3}{32} w^2 \epsilon, \\
Q^3 y_1 &= Q^3 y_0 + wQ^2 y_0 + \frac{1}{2} w^2 Qy_0 + \frac{1}{6} w^3 y_0 + \frac{1}{24} w^3 \delta y_{-1/2} \\
&\quad + \frac{7}{240} w^3 \delta^2 y_{-1} + \frac{17}{720} w^3 \delta^3 y_{-3/2} + \frac{41}{2016} w^3 \epsilon.
\end{aligned}\right\} \quad (9)$$

It is clear that the process consists in calculating values of y and its integrals which satisfy the equation at regular intervals, and which are further related by the condition that the form of the y curve over any interval is a polynomial of the 1st, 2nd, 3rd and higher degrees for the 1st, 2nd, 3rd and higher approximations respectively. This process is a distinct modification of Adams's method, in which the latter condition is not used. Thus, for an equation containing y and Qy Adams first calculates Qy_1 from the second of the relations (7), and finally calculates y_1 by substitution in the equation of the value for Qy_1 thus obtained. The present modification aims to eliminate as far as possible the errors which thus result in Qy_1 and y_1, by the simultaneous use of the equation and the relations (7).

Two remarks relating to the method may be made at this point. The first is that, in any normal application, ϵ^2 and higher powers are negligible. Thus the substitution of the relations for y_1, Qy_1, etc., in the equation

results in a simple equation for the determination of ϵ. The second is that, assuming that successive approximations are rapidly convergent, an estimation of the order of accuracy of any approximation can be made by occasionally computing also the next higher approximation over any interval.

§ 4. *Example No.* 1.

For the first example an equation is chosen which is of a form suitable for step-by-step integration, and which has a known solution.

The solution of the equation

$$Y''-YY'=0, \quad . \quad . \quad . \quad . \quad . \quad (10)$$

with the given initial conditions $X=0$, $Y=0$, $Y'=2$, is $Y=2\tan x$, $Y'=2\sec^2 x$, $Y''=4\sec^2 x\tan x$.

Noting that the function y of the formulæ (9) is the highest order differential occurring in the equation, the formulæ of the fourth approximation may be written :

$$Y_1''=Y_0''+\delta Y''_{-1/2}+\delta^2 Y''_{-1}+\delta^3 Y''_{-3/2}+\epsilon,$$

$$Y'=Y_0'+wY_0''+\frac{1}{2}w\delta Y''_{-1/2}+\frac{5}{12}w\delta^2 Y''_{-1}+\frac{3}{8}w\delta^3 Y''_{-3/2}+\frac{251}{720}w\epsilon,$$

$$Y_1=Y_0+wY'+\frac{1}{2}w^2Y_0''+\frac{1}{6}w^2\delta Y''_{-1/2}+\frac{1}{8}w^2\delta^2 Y''_{-1}+\frac{19}{180}w^2\delta^3 Y''_{-3/2}+\frac{3}{32}w^2\epsilon.$$

The work may be simplified by substitution of these formulæ in the equation, when, neglecting powers of ϵ other than the first, the following relations are obtained :

If $a=Y_0''+\delta Y''_{-1/2}+\delta^2 Y''_{-1}+\delta^3 Y''_{-3/2}$,

$$b=Y_0'+wY_0''+\frac{1}{2}w\delta Y''_{-1/2}+\frac{5}{12}w\delta^2 Y''_{-1}+\frac{3}{8}w\delta^3 Y''_{-3/2},$$

$$c=Y_0+wY_0'+\frac{1}{2}w^2Y_0+\frac{1}{6}w^2\delta Y''_{-1/2}+\frac{1}{8}w^2\delta^2 Y''_{-1}+\frac{19}{180}w^2\delta^3 Y''_{-3/2},$$

$$d=\frac{251}{720}wc+\frac{3}{32}w^2b-1,$$

then $$\epsilon = \frac{a - bc}{d},$$

and $$Y_1'' = a + \epsilon,$$

$$Y_1' = b + \frac{251}{720} w\epsilon,$$

$$Y_1 = c + \frac{3}{32} w^2 \epsilon.$$

TABLE I.

The Solution of $Y'' - YY' = 0$ to the Fourth Approximation as far as $X = 1{\cdot}0$ for Intervals of 0·05.

Initial Conditions, $X = 0$, $Y = 0$, $Y' = 2$.

X.	Y.	Y′.	Y″.
0	0	2·0	0
0·05	0·1000834	2·005008	0·2006680
0·1	0·2006693	2·020134	0·4053789
0·15*	0·3022704	2·045684	0·6183496
0·2	0·4054200	2·082183	0·8441586
0·25	0·5106838	2·130399	1·087960
0·3	0·6186725	2·191378	1·355745
0·35	0·7300570	2·266493	1·654669
0·4	0·8455865	2·357510	1·993479
0·45	0·9661103	2·466687	2·383092
0·5	1·092605	2·596896	2·837383
0·55	1·226211	2·751801	3·374289
0·6	1·368275	2·936094	4·017382
0·65	1·520410	3·155833	4·798160
0·7	1·684579	3·418916	5·759434
0·75	1·863196	3·735770	6·960471
0·8	2·059282	4·120351	8·484964
0·85	2·276673	4·591667	10·45372
0·9	2·520328	5·176102	13·04547
0·95	2·796783	5·911124	16·53213
1·0	3·114845	6·851346	21·34088

* To start the solution true values were assumed to be known as far as $X = 0{\cdot}15$.

The solution of equation (10) has been computed by these formulæ over the range of X from 0 to 1·0 by intervals of 0·05, the true solution being assumed known as far as $X = 0{\cdot}15$. The results are given to seven figures, but the calculation for each interval was made to

eight figures, the last of which was dropped when setting down the values obtained at the end of the interval. Tables I. and II. give the results obtained by the present process and the true solution respectively. It is seen that Y'' tends to change rapidly as X approaches the value 1, and the accuracy of the computation would be improved considerably by reducing the interval after, say, $X=0{\cdot}5$.

TABLE II.

The True Solution of $Y''-YY'=0$, as far as $X=1{\cdot}0$, for the Initial Conditions $X=0$, $Y=0$, $Y'=2$.

X.	Y.	Y′.	Y″.
0	0	2·0	0
0·05	0·1000834	2·005008	0·2006680
0·1	0·2006693	2.020134	0·4053789
0·15	0·3022704	2·045684	0·6183496
0·2	0·4054201	2·082183	0·8441586
0·25	0·5106838	2·130399	1·087960
0·3	0·6186725	2·191378	1·355745
0·35	0·7300570	2·266492	1·654668
0·4	0·8455864	2·357508	1·993477
0·45	0·9661101	2·466684	2·383089
0·5	1·092605	2·596893	2·837378
0·55	1·226210	2·751796	3·374281
0·6	1·368274	2·936086	4·017369
0·65	1·520409	3·155822	4·798139
0·7	1·684577	3·418900	5·759399
0·75	1·863193	3·735744	6·960412
0·8	2·059277	4·120311	8·484862
0·85	2·276665	4·591603	10·45354
0·9	2·520316	5·175997	13·04515
0·95	2·796765	5·910948	16·53153
1·0	3·114815	6·851038	21·33972

§ 5. *Example No.* 2.

As an example of application to a non-linear equation, of which the true solution is not known, consider the equation

$$Y'''-YY''=0$$

with the conditions

$$X=0, \quad Y=0, \quad Y'=0,$$

$$X\to\infty, \quad Y'=-1.$$

This equation, which is derived from the boundary layer equations of fluid flow past a semi-infinite plane parallel to the stream [3], is typical of the type of equation associated with fluid flow past aerofoils and other bodies at high values of Reynolds's number. Toepfer [4] has shown that the equation may be solved by using an assumed value of Y'' when $X=0$, instead of the condition $Y'=-1$ when $X\to\infty$. It is convenient to assume that $Y''=-1$ when $X^*=0$, or $(Y'')_0=-1$, and, by repeated differentiation of the equation, the values of $(Y''')_0$, $(Y^{IV})_0$, and so on, can then be evaluated. The solution is now started by expanding Y and its derivatives in terms of Y_0, $(Y')_0$, etc. by Taylor's theorem.

The formulæ to be used are obtained in the manner outlined in § 4, and for the fourth approximation are as follows :—

$$\text{If}\quad a=Y_0'''+\delta Y_{-1/2}'''+\delta^2 Y_{-1}'''+\delta^3 Y_{-3/2}''',$$

$$b=Y_0''+wY_0'''+\frac{1}{2}w\delta Y_{-1/2}'''+\frac{5}{12}w\delta^2 Y_{-1}'''+\frac{3}{8}w\delta^3 Y_{-3/2}''',$$

$$c=Y_0'+wY_0''+\frac{1}{2}w^2Y_0'''+\frac{1}{6}w^2\delta Y_{-1/2}'''+\frac{1}{8}w^2\delta^2 Y_{-1}'''+\frac{19}{180}w^2\delta^2 Y_{-3/2}''',$$

$$d=Y_0+wY_0'+\frac{1}{2}w^2Y_0''+\frac{1}{6}w^3Y_0'''+\frac{1}{24}w^3\delta Y_{-1/2}'''+\frac{7}{240}w^3\delta^2 Y_{-1}'''+\frac{17}{720}w^3\delta^3 Y_{-3/2}''',$$

$$e=1-\frac{251}{720}wY_0-\frac{251}{720}w^2Y_0'-\frac{109}{560}w^3Y_0''-\frac{593}{7560}w^4Y_0'''-\frac{2987}{120960}w^4\delta Y_{-1/2}'''-\frac{22549}{1209600}w^4\delta^2 Y_{-1}'''-\frac{251269}{3628800}w^4\delta^3 Y_{-3/2}''',$$

then

$$\epsilon=\frac{bd-a}{e},$$

* This X is a function of distance normal to the plane, and must not be confused with distance along the plane.

and

$$Y_1''' = a + \epsilon,$$

$$Y_1'' = b + \frac{251}{720} w\epsilon,$$

$$Y_1' = c + \frac{2}{32} w^2\epsilon,$$

$$Y_1 = d + \frac{41}{2016} w^3\epsilon.$$

TABLE III.

The Solution of the Equation $Y''' - YY''$ from $X = 0$ to $X = 0{\cdot}5$ calculated by Taylor's theorem.

X.	$-Y.$	$-Y'.$	$-Y''.$	$Y'''.$
0	0	0	1·0	0
0·1	0·0049999	0·0999958	0·9998334	0·0049991
0·2	0·0199973	0·1999333	0·9986677	0·0199707
0·3	0·0449798	0·2996630	0·9955111	0·0447779
0·4	0·0799149	0·3989369	0·9893956	0·0790674
0·5	0·1247407	0·4974128	0·9794034	0·1221714

TABLE IV.

Difference Table for Y''' from $X = 0$ to $X = 0{\cdot}5$.

X.	$Y'''.$	$\delta.$	$\delta^2.$	$\delta^3.$	$\delta^4.$
0	0				
		0·0049991			
0·1	0·0049991		0·0099725		
		0·0149716		−0·0001369	
0·2	0·0199707		0·0098356		−0·0002164
		0·0248072		−0·0003533	
0·3	0·0447779		0·0094823		−0·0003145
		0·0342895		−0·0006678	
0·4	0·0790674		0·0088145		
		0·0431040			
0·5	0·1221714				

The solution obtained by Taylor's theorem for the range of X from 0 to 0·5 by intervals of 0·1 is given in Table III., and Table IV. gives the resulting difference table for Y'''. The values of Y' and Y''' for $X = 0{\cdot}6$

as given by four successive approximations are compared in Table V. with the true values calculated by Taylor's theorem. The values of ϵ and the corresponding true difference from Table IV. are also given for the four approximations. The figures in these Tables are correct to the seventh place of decimals.

It was considered desirable that the calculations should be extended in order to establish the results to be expected from successive approximations. The solution has therefore been calculated by the third approximation over the range of X from 0 to 4·6 by intervals of 0·1, and repeated over the same range by the use of the fourth

TABLE V.

Approximations to Y′ and Y‴ for X = 0·6.

	$-Y'$.	Y'''.	ϵ.	Value of corresponding true difference.
Approxn. 1.....	0·5946575	0.1730152	0·0508438	$\delta = 0{\cdot}0431040$
Approxn. 2.....	0·5946608	0·1730268	0·0077514	$\delta^2 = 0{\cdot}0088145$
Approxn. 3.....	0·5946605	0·1730260	− 0·0010639	$\delta^3 = -0{\cdot}0006678$
Approxn. 4.....	0·5946605	0·1730258	− 0·0003963	$\delta^4 = -0{\cdot}0003145$
True value by Taylor's series.	0·5946605	0·1730257		

approximation. In each case the solution used over the range of X from 0 to 0·5 was that calculated by means of Taylor's theorem. The solutions to the third and fourth approximations are given in Tables VI. and VII. respectively to seven significant figures generally, and to eight figures when the values are greater than unity. One extra figure was used in the computation, and this was dropped when setting down the values at the end of each interval prior to integration over the next interval.

The equation has also been integrated by Toepfer [4] using the Runge-Kutta method of solution, and a comparison of the final values at X = 4·6 as given by Toepfer and the present approximations is made in Table VIII. The results are in agreement, although the solution by the present method is given to much greater accuracy than that of Toepfer. In the same Table the maximum difference between the two approximations

Table VI.

The Solution of $Y'''-YY''=0$ to the Third Approximation for the Initial Condition $Y''=-1$ at the Origin.

X.	$-Y.$	$-Y'.$	$-Y''.$	$Y'''.$
0	0	0	1·0	0
0·1	0·0049999	0·0999958	0·9998334	0·0049991
0·2	0·0199973	0·1999333	0·9986677	0·0199707
0·3	0·0449798	0·2996630	0·9955111	0·0447779
0·4	0·0799149	0·3989369	0·9893956	0·0790674
0·5*	0·1247407	0·4974128	0·9794034	0·1221714
0·6	0·1793566	0·5946605	0·9647037	0·1730260
0·7	0·2436150	0·6901729	0·9445922	0·2301169
0·8	0·3173144	0·7833807	0·9185403	0·2914660
0·9	0·4001940	0·8736723	0·8862390	0·3546675
1·0	0·4919307	0·9604181	0·8476378	0·4169790
1·1	0·5921387	1·0429973	0·8029713	0·4754703
1·2	0·7003718	1·1208275	0·7527685	0·5272178
1·3	0·8161286	1·1933933	0·6978413	0·5695283
1·4	0·9388608	1·2602734	0·6392500	0·6001667
1·5	1·0679834	1·3211628	0·5782468	0·6175578
1·6	1·2028877	1·3758881	0·5162022	0·6209335
1·7	1·3429546	1·4244154	0·4545201	0·6104000
1·8	1·4875683	1·4668494	0·3945502	0·5869203
1·9	1·6361295	1·5034233	0·3375074	0·5522058
2·0	1·7880691	1·5344825	0·2844052	0·5085361
2·1	1·9428566	1·5604615	0·2360099	0·4585333
2·2	2·1000085	1·5818582	0·1928185	0·4049204
2·3	2·2590932	1·5992066	0·1550601	0·3502952
2·4	2·4197331	1·6130510	0·1227182	0·2969454
2·5	2·5816045	1·6239235	0·09556865	0·2467205
2·6	2·7444356	1·6323252	0·07322714	0·2009672
2·7	2·9080025	1·6387129	0·05520037	0·1605228
2·8	3·0721246	1·6434907	0·04093522	0·1257581
2·9	3·2366587	1·6470063	0·02986177	0·09665236
3·0	3·4014936	1·6495510	0·02142797	0·07288712
3·1	3·5665445	1·6513628	0·01512451	0·05394223
3·2	3·7317481	1·6526318	0·01050041	0·03918489
3·3	3·8970578	1·6535060	$0{\cdot}0_2$7170481†	0·02794379
3·4	4·0624400	1·6540984	$0{\cdot}0_2$4816156	0·01956535
3·5	4·2278709	1·6544932	$0{\cdot}0_2$3181684	0·01345174
3·6	4·3933341	1·6547520	$0{\cdot}0_2$2067340	$0{\cdot}0_2$9082510
3·7	4·5588183	1·6549189	$0{\cdot}0_2$1321169	$0{\cdot}0_2$6022969
3·8	4·7243159	1·6550247	$0{\cdot}0_3$8304048	$0{\cdot}0_2$3923095
3·9	4·8898219	1·6550907	$0{\cdot}0_3$5133323	$0{\cdot}0_2$2510104
4·0	5·0553332	1·6551312	$0{\cdot}0_3$3120873	$0{\cdot}0_2$1577706
4·1	5·2208476	1·6551556	$0{\cdot}0_3$1866003	$0{\cdot}0_3$9742110
4·2	5·3863640	1·6551701	$0{\cdot}0_3$1097227	$0{\cdot}0_3$5910062
4·3	5·5518815	1·6551786	$0{\cdot}0_4$6344746	$0{\cdot}0_3$3522527
4·4	5·7173996	1·6551834	$0{\cdot}0_4$3607883	$0{\cdot}0_3$2062770
4·5	5·8829181	1·6551862	$0{\cdot}0_4$2017406	$0{\cdot}0_4$1186823
4·6	6·0484368	1·6551877	$0{\cdot}0_4$1109221	$0{\cdot}0_4$6709052

* The solution up to this value of X was calculated by Taylor's theorem.

† The suffix indicates the number of noughts between the decimal point and the first integer.

Table VII.

The Solution of $Y'''-YY''=0$ to the Fourth Approximation for the Initial Condition $Y''=-1$ at the Origin.

X.	$-Y$.	$-Y'$.	$-Y''$	Y'''.
0	0	0	1·0	0
0·1	0·0049999	0·0999958	0·9998334	0·0049991
0·2	0·0199973	0·1999333	0·9986677	0·0199707
0·3	0·0449798	0·2996630	0·9955111	0·0447779
0·4	0·0799149	0·3989369	0·9893956	0·0790674
0·5*	0·1247407	0·4974128	0·9794034	0·1221714
0·6	0·1793566	0·5946605	0·9647027	0·1730258
0·7	0·2436150	0·6901727	0·9445901	0·2301163
0·8	0·3173144	0·7833802	0·9185371	0·2914650
0·9	0·4001939	0·8736715	0·8862348	0·3546658
1·0	0·4919305	0·9604169	0·8476330	0·4169765
1·1	0·5921384	1·0429957	0·8029663	0·4754672
1·2	0·7003713	1·1208254	0·7527639	0·5272143
1·3	0·8161279	1·1933908	0·6978377	0·5695247
1·4	0·9388598	1·2602706	0·6392479	0·6001642
1·5	1·0679822	1·3211598	0·5782466	0·6175570
1·6	1·2028862	1·3758852	0·5162042	0·6209348
1·7	1·3429525	1·4244128	0·4545241	0·6104043
1·8	1·4875655	1·4668472	0·3945559	0·5869277
1·9	1·6361265	1·5034217	0·3375142	0·5522159
2·0	1·7880659	1·5344816	0·2844124	0·5085481
2·1	1·9428534	1·5604614	0·2360167	0·4585459
2·2	2·1000054	1·5818586	0·1928243	0·4049321
2·3	2·2590902	1·5992075	0·1550645	0·3503047
2·4	2·4197301	1·6130523	0·1227210	0·2969517
2·5	2·5816016	1·6239250	0·09556984	0·2467233
2·6	2·7444328	1·6323267	0·07322691	0·2009664
2·7	2·9079999	1·6387143	0·05519905	0·1605188
2·8	3·0721221	1·6434919	0·04093318	0·1257517
2·9	3·2366563	1·6470073	0·02985941	0·09664466
3·0	3·4014913	1·6495518	0·02142562	0·07287904
3·1	3·5665423	1·6513632	0·01512241	0·05393473
3·2	3·7317459	1·6526320	0·01049871	0·03917853
3·3	3·8970555	1·6535060	$0{\cdot}0_27169254$	0·02793898
3·4	4·0624377	1·6540983	$0{\cdot}0_24815375$	0·01956217
3·5	4·2278687	1·6544930	$0{\cdot}0_23181292$	0·01345008
3·6	4·3933317	1·6547518	$0{\cdot}0_22067252$	$0{\cdot}0_29082126$
3·7	4·5588159	1·6549187	$0{\cdot}0_21321295$	$0{\cdot}0_36023542$
3·8	4·7243134	1·6550246	$0{\cdot}0_38306626$	$0{\cdot}0_33924310$
3·9	4·8898195	1·6550906	$0{\cdot}0_35136527$	$0{\cdot}0_22511668$
4·0	5·0553307	1·6551311	$0{\cdot}0_33124194$	$0{\cdot}0_21579383$
4·1	5·2208452	1·6551556	$0{\cdot}0_31869105$	$0{\cdot}0_39758307$
4·2	5·3863615	1·6551701	$0{\cdot}0_31099923$	$0{\cdot}0_35924580$
4·3	5·5518790	1·6551786	$0{\cdot}0_46366921$	$0{\cdot}0_33534838$
4·4	5·7173971	1·6551835	$0{\cdot}0_43625298$	$0{\cdot}0_32072727$
4·5	5·8829156	1·6551862	$0{\cdot}0_42030553$	$0{\cdot}0_31194558$
4·6	6·0484343	1·6551877	$0{\cdot}0_41118801$	$0{\cdot}0_46766993$

* The solution up to this value of X was calculated by Taylor's theorem.

is also given. The fact that the values of Y and Y′, after diverging slightly, appear to be converging to the same final value must be ascribed to some accidental relation between the equation and the method of solution.

It is desirable to make an estimation of the final asymptotic value of Y′. The known asymptotic solution of the equation is not suited to a rapid evaluation of the limit, and a limiting value for Y′ has been found by a method which is believed to give a value closer to the

TABLE VIII.

Comparison of the Solution of $Y'''-YY''=0$ when $X=4{\cdot}6$, obtained from the Third and Fourth Approximations and by Toepfer; and the Maximum Difference between the two Approximations.

Function.	Value of function when X=4·6			Max. difference between 3rd and 4th approxns.	
	3rd approxn.	4th approxn.	Toepfer.	X.	Max. difference.
$-Y$	6·0484368	6·0484343	$6{\cdot}048429\pm0{\cdot}0_{1}10$	1·8	1 in 530,000
$-Y'$	1·6551877	1·6551877	$1{\cdot}655180\pm0{\cdot}0_{4}10$	1·5	1 in 440,000
$-Y''$	$0{\cdot}0_{4}1109221$	$0{\cdot}0_{4}1118801$	$0{\cdot}0_{4}11\quad\pm0{\cdot}0_{4}10$	4·6	1 in 111
Y'''	$0{\cdot}0_{4}6709052$	$0{\cdot}0_{4}6766993$		4·6	1 in 116

asymptotic value of Y′ than that when X=4·6. This method, which consists in the identifying of the given curve with a curve of the form $Y'_{x}-Y'=Ke^{-P(X)}$, where P(X) is a polynomial in X, and K is a constant, is described in an Appendix to the paper. A series of approximations to the value of Y′ is obtained, the order of any of which is the same as the degree of P(X); thus, the first approximation is given when $P(X)\equiv k_1X$, the second when $P(X)\equiv k_1X+k_2X^2$, and so on, k_1 and k_2 being constants.

The asymptotic value of Y′ has been calculated for approximations one to four using three ranges of X, 3·6 to 4·6 by 0·2, 2·6 to 4·6 by 0·4, and 2·6 to 3·6 by 0·2, and the results of the calculation are given in Table IX.

The fourth approximations obtained from the first two ranges agree very closely, and the mean value $Y' = -1{\cdot}6551893$ is taken to be the final asymptotic value obtained from the present work. Since the value 1·6551880 was obtained from the range 2·6 to 3·6, the further accuracy obtained from the calculations over the range of X from 3·6 to 4·6 is not great.

In order to convert the solution given in Table VII. to the solution of $Y''' - YY'' = 0$ with the condition $Y' = -1$, when $X \to \infty$, it can be shown that the given values of X, Y, Y′, Y″, and Y‴ must be multiplied

TABLE IX.

Estimated Asymptotic Value of $-Y'$ for the Fourth Approximation by the Method described in the Appendix.

Range of X.	Successive approximations to asymptotic value of $-Y'$.			
	First.	Second.	Third.	Fourth.
3·6 to 4·6 by 0·2	1·6551896	1·6551893	1·6551892	1·6551891
2·6 to 4·6 by 0·4	1·6551901	1·6551895	1·6551895	1·6551895
2·6 to 3·6 by 0·2	1·6552772	1·6551903	1·6551886	1·6551880

by the factors $A^{1/2}$, $A^{-1/2}$, A^{-1}, $A^{-3/2}$, and A^{-2} respectively, where A is the asymptotic value 1·6551893. An alternative form of the equation which is sometimes used is $Y''' - \frac{1}{2}YY'' = 0$, and, in order to convert the solution of Table VII. to the solution of this equation, with the condition $Y' = -1$, when $X \to \infty$, the appropriate factors for the given values of X, Y, Y′, Y″, and Y‴ are $(2A)^{1/2}$, $2^{1/2}A^{-1/2}$, A^{-1}, $2^{-1/2}A^{-1/2}$, and $2^{-1}A^{-2}$ respectively. The Blasius formula [3] for the drag of unit width of two sides of a plane parallel to the direction of flow of the fluid becomes

$$\frac{F}{\rho v^2 l} = 2\sqrt{2}A^{-3/2}R^{-1/2} = 1{\cdot}3282306R^{-1/2},$$

where F is the drag, ρ the fluid density, v the fluid velocity, and R the Reynolds's number of the plane, *i. e.*, $\frac{vl}{\nu}$, where

l is the length of the plane parallel to the direction of flow, and ν the kinematic coefficient of viscosity.

§ 6. *Conclusion.*

In conclusion, the writer wishes to express his indebtedness to Professor D. R. Hartree, F.R.S., for valuable criticism of the paper, and to Miss S. W. Skan, who carried out a large part of the calculations.

Appendix.

If the coordinates of a number of points on a curve be given, together with the condition that the curve is approaching an asymptote parallel to the x-axis, an estimate of the position of the asymptote can be made if the given points are at equal intervals of the abscissa x, by identifying the curve with a curve of the form $y_\infty - y = \mathrm{K}e^{-\mathrm{P}(x)}$, where $\mathrm{P}(x)$ is a polynomial in x, and K a constant.

Let A, B, C, ... be the given points, the coordinates referred to the axes of x and y being (x_a, y_a), (x_b, y_b), and so on. The point A is that nearest to the asymptote.

Let $y_a - y_b = \alpha_1$, $y_a - y_c = \alpha_2$, etc. The perpendicular distances of the points from a line parallel to the x-axis and distant p from A are p, $p+\alpha_1$, $p+\alpha_2$, etc. These quantities may be arranged in a *ratio* table, thus :—

$p+\alpha_5$					
	R_4				
$p+\alpha_4$		$\mathrm{R}_3{}^2$			
	R_3		$\mathrm{R}_2{}^3$		
$p+\alpha_3$		$\mathrm{R}_2{}^2$		$\mathrm{R}_1{}^4$	
	R_2		$\mathrm{R}_1{}^3$		$\mathrm{R}_0{}^5$
$p+\alpha_2$		$\mathrm{R}_1{}^2$		$\mathrm{R}_0{}^4$	
	R_1		$\mathrm{R}_0{}^3$		
$p+\alpha_1$		$\mathrm{R}_0{}^2$			
	R_0				
p					

in which

$$\mathrm{R}_0 = \frac{p}{p+\alpha_1}, \quad \mathrm{R}_1 = \frac{p+\alpha_1}{p+\alpha_2} \ldots,$$

$$\mathrm{R}_0{}^2 = \frac{\mathrm{R}_0}{\mathrm{R}_1}, \quad \mathrm{R}_1{}^2 = \frac{\mathrm{R}_1}{\mathrm{R}_2} \ldots,$$

$$R_0^3 = \frac{R_0^2}{R_1^2} \cdot \cdot \cdot \cdot \cdot \cdot \cdot, \text{ and so on.}$$

Hence

$$R_0 = \frac{p}{p+\alpha_1},$$

$$R_0^2 = \frac{p}{p+\alpha_1} \Big/ \frac{p+\alpha_1}{p+\alpha_2} = p(p+\alpha_1)^{-2}(p+\alpha_2),$$

$$R_0^3 = p(p+\alpha_1)^{-3}(p+\alpha_2)^3(p+\alpha_3)^{-1},$$

$$R_0^4 = p(p+\alpha_1)^{-4}(p+\alpha_2)^6(p+\alpha_3)^{-4}(p+\alpha_4),$$

and so on.

Successive approximations to the value of p are found by equating to unity, in turn, the quantities R_0^2, R_0^3, R_0^4, ..., the resulting values of p being called the first, second, third approximations, and so on. The first approximation $R_0^2 = 1$ gives the simple expression

$$p = \frac{\alpha_1^2}{\alpha_2 - 2\alpha_1}.$$

The higher approximations are admirably suited for solution by trial by the use of logarithms.

The approximations are easily shown to be equivalent to the fitting of curves which satisfy $y_\infty - y = Ke^{-P(x)}$, $P(x)$ being of the same degree as the order of the approximation.

Thus, if $y_\infty - y = Ke^{-k_1 x}$,

$$R_0^2 = p(p+\alpha_1)^{-2}(p+\alpha_2) = Ke^{-k_1 x}K^{-2}e^{2k_1(x-1)}Ke^{-k_1(x-2)} = 1,$$

and a similar argument applies to the higher approximations.

The method appears to be suited to curves which approach the asymptote rapidly, but is obviously unsuitable for use if any of the ratios of the ratio-table exceed unity or if the successive approximations do not tend to converge to a definite value.

References.

(1) F. Bashforth and J. C. Adams, ' Theories of Capillary Action,' Cambridge, 1883 ; also Whittaker and Robinson, ' The Calculus of Observations,' p. 363.
(2) Whittaker and Robinson, *loc. cit.* p. 35.
(3) A. Blasius, *Zeits. für Math. und Phys.* lvi. (1908).
(4) H. Toepfer, *Zeits. für Math. und Phys.* lx. p. 397 (1912).

LI. *The Distribution of Temperature in a Cylindrical Conductor electrically heated* in vacuo. *By* H. G. Baerwald. (Communication from the Staff of the Research Laboratories of The General Electric Company, Limited, Wembley, England.*)

Summary.

The temperature distribution in cylindrical conductors electrically heated *in vacuo* is investigated. It is shown that the transversal variations are negligible. A simple method is given for deriving the longitudinal temperature distribution directly from the empirical data of the emissivity, thermal and electrical conductivity functions. If the conductor can be regarded as "infinite," for which a criterion is given, the dependence of the temperature gradient on temperature is given at once in terms of functions which are known for every metal for which measurements exist. This is of importance for the design of cooling devices for thermionic valves. The temperature distribution itself is obtained simply by integration. If the conductor is not "infinite," the determination of a constant is necessary; it is shown, for different end conditions, how it can be obtained conveniently.

List of Symbols.

T = Temperature.
T_∞ = Temperature of an infinitely long conductor.
T_0 = Temperature at the cool end of a semi-infinite conductor.
T_a, T_b = End temperatures of a conductor of finite length.
T_m = A particular temperature arising in the definition of the integration constant.
θ = Transversal temperature variation.
θ = Difference between the equivalent conduction and radiation temperatures.

(degree abs.).

* Communicated by C. C. Paterson, M.I.E.E.

x = Coordinate along the conductor.
y, z = Cross-coordinates across the conductor.
r = Radial coordinate across the conductor.
} (cm.).

ϕ = Angular coordinate across the conductor.
S = Cross-sectional area of the conductor (cm.^{2}).

U = Perimeter of the conductor.
$l = \frac{S}{U}$.
R = Radius of a circular cross-section.
$2b, 2c$ = Sides of a rectangular cross-section.
x_0 = Cool end of the semi-infinite conductor.
x_a, x_b = End points of the finite conductor.
$L = |x_a - x_b|$.
x_m = Coordinate of T_m.
l_0 = Length constant.
l_{Stead} = Stead's definition of the length of the end.
} (cm.).

μ = Reciprocal length (cm.$^{-1}$).
I = Total current (amp.).

i = Current density $\frac{\text{amp.}}{\text{cm.}^2}$, $i_0 = \frac{I}{S}$

$\sigma(T)$ = Emissivity (watt cm.$^{-2}$).
$\rho(T)$ = Electrical resistivity (Ω cm.).
$\gamma(T)$ = Thermal conductivity (watt cm.$^{-1}$ degree^{-1}).
Θ, N = Numerical constants.
n = Numerical constant, or = normal coordinate at a point of the circumference.
Δ_2 = Laplace operator in two dimensions.
$B(T) = i_0^2\rho(T) - k\sigma(T)$ (watt cm.$^{-3}$).

$$Q = \left| \sqrt{2\left[\frac{\rho}{\gamma}\frac{d}{dT}\left(\frac{\sigma}{\rho}\right)\right]_{T=T_\infty}} \right| \text{(cm.}^{-\frac{1}{2}}\text{)}.$$

$$\beta = \left| \sqrt{\frac{k}{2}} \right| Q = \left| \sqrt{\frac{-B'(T_\infty)}{\gamma(T_\infty)}} \right| \text{(cm.}^{-1}\text{)}.$$

$$\xi = \left[\gamma(T)\frac{dT}{dx}\right]^2 \text{(watt}^2 \text{ cm}^{-4}\text{.)}.$$

THE temperature distribution in electrically heated filaments *in vacuo* and related problems have been treated by Worthing * and Stead †. They investigated the reduction of the total brightness, emission, etc., by the cooling effect of the ends, represented by corresponding "equivalent" lengths of filament at constant temperature. As both radiation and electron emission vary rapidly with temperature, the exact temperature distribution $T(x)$ near the cool ends is of little influence on the equivalent lengths, all the more as there is the steepest temperature gradient. Therefore $T(x)$ has never been evaluated accurately, the authors referred to being content with the simple approximation formulas

$$\frac{T}{T_\infty} = 1 - e^{-\frac{Q}{\sqrt{R}}(l_0+x)} \quad . \quad . \quad . \quad . \quad (a)$$

or

$$\frac{T}{T_\infty} = \{1 - e^{-\mu(l_0+x)}\}^n ; \quad . \quad . \quad . \quad . \quad (b)$$

(a) is obtained by neglecting the variations of radiation, thermal, and electrical conductivity with temperature, and is, therefore, confined to the middle part of a long filament, where $T \sim T_\infty$, while (b) is half empirical, and tries to account, roughly, for the variations of these quantities.

While, for the reasons stated, formulas (a) and (b) prove satisfactory for calculating equivalent lengths, they are not applicable when the accurate temperature distribution near a relatively cool end is required. This is the case, *e. g.*, in problems connected with the design of large transmitting valves. For keeping filament ends or supporting conductors through which current passes, at prescribed temperatures, cooling must be so designed as to pass away a certain heat-flow. The flow is the product of the cross-section with the thermal conductivity and the temperature gradient $\frac{dT}{dx}$ at the end x_0. Supposing the far end of the filament being of negligible influence ("infinite" conductor), T_0 is a certain function of $\left[\frac{dT}{dx}\right]_{x=x_0}$ only, and it is seen that its knowledge is essential for the

* A. G. Worthing, Phys. Rev. iv. pp. 524–34 and 535–43 (1914); Journ. Franklin Inst. cxciv. pp. 597–616 (1922) (there further publications mentioned).

† G. Stead, Journ. Inst. Elect. Eng. lviii. pp. 107–17 (1920).

design of the cooling. The application of formula (a) to typical numerical conditions is likely to produce errors of the gradient of about 50 per cent., while at the same time the error of equivalent lengths is of the order of 1 per cent.

In the following a simple method is given by which the exact temperature distribution is obtained directly from the empirical data of $\sigma(T)$, $\rho(T)$, and $\gamma(T)$. The process gives at once $\frac{dT}{dx}$, as function of T, if the conductor is "long," and otherwise merely requires the determination of a constant; the temperature distribution itself follows simply by integration. The method involves only two assumptions, viz., that the area S and the perimeter U of the conductor are constant (for each partial length considered), and that variations of temperature over the cross-section may be neglected; a criterion is given for this, and it shows that this simplification is always justified.

When making the said assumptions, $T=T(x)$ means a suitable mean temperature of the cross-section. The power $Si_0^2\rho(T(x))$ is supplied per unit length of the conductor by the electric current I, while the amount of $U\sigma(T(x))$ is lost by radiation and $-S\frac{d}{dx}\left[\gamma(T(x))\frac{dT}{dx}\right]$ by conduction. That gives the fundamental equation:

$$\frac{d}{dx}\left[\gamma(T(x))\frac{dT}{dx}\right]+\underbrace{i_0^2\rho(T(x))-k\sigma(T(x))}_{B(T(x))}=0. \quad . \quad (1)$$

If the conductor is infinite in the x-direction, $\frac{d}{dx}=0$; *i. e.*, there is equilibrium between supply and radiation at the temperature T_∞, which is determined by

$$B(T_\infty)=i_0^2\rho(T_\infty)-k\sigma(T_\infty)=0. \quad . \quad . \quad . \quad (2)$$

σ, ρ, and γ are plotted in fig. 1 for tungsten and molybdenum *. Over a large temperature range $\sigma(T)$ rises

* The values for tungsten are taken from the book of C. J. Smithells ('Tungsten,' Chapman and Hall, 1926; see there for references to the original papers), those for molybdenum from A. G. Worthing (Phys. Rev. xxviii. p. 190 (1926)). The values of γ must be regarded as doubtful, at least for the lower temperature range, as more recent measurements by W. G. Kannuluik (Proc. Roy. Soc. A, cxxxi. p. 320 (1931), and cxli. p. 159 (1933)) gave values in the range from $-183°$ to 100° C. which are 2 to $2\frac{1}{2}$ times higher.

much more rapidly than $\rho(T)$, and still more rapidly than $\gamma(T)$, $\frac{T}{\sigma}\frac{d\sigma}{dT}$ being $4\frac{1}{2}$ to 5, while $\frac{T}{\rho}\frac{d\rho}{dT} \sim 1{\cdot}2$ to $1{\cdot}25$ and $\frac{T}{\gamma}\frac{d\gamma}{dT} \sim 0{\cdot}34$. Therefore the first term of B(T) prevails

Fig. 1.

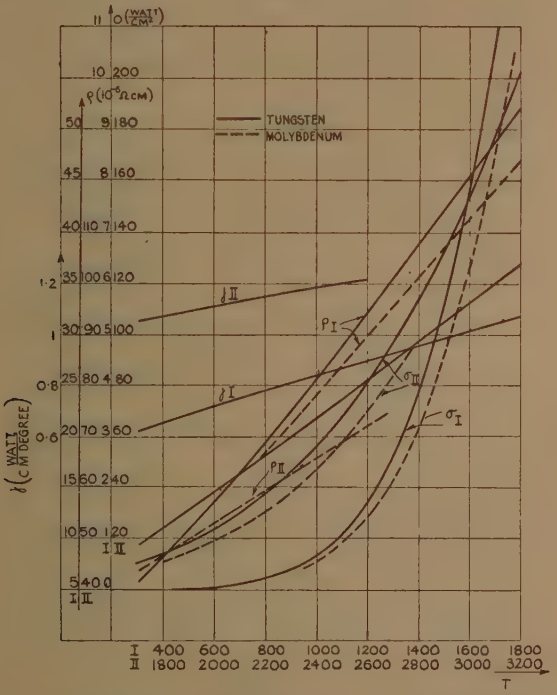

at low temperatures, the second term at high temperatures; B(T) increases first, then reaches a maximum, and decreases, the more rapidly the higher the temperature. This is illustrated by figs. 2 and 3, which refer to two numerical examples, viz. :—

(1) Tungsten wire, $2R = 0{\cdot}1$ cm., $I = 48$ amp.; $T_\infty \approx 2550°$ (filament of transmitting valve).

(2) Molybdenum rod, $2R = 0{\cdot}65$ cm., $I = 210$ amp.; $T_\infty \approx 1290°$ (filament support of transmitting valve).

It is generally

$$B(T_\infty)=0, \quad B'(T_\infty)<0, \quad B''(T_\infty)<0. \quad . \quad (3)$$

To examine how far we are entitled to neglect transversal temperature variations, we write

$$T(x)-\theta(x, y, z) \quad . \quad . \quad . \quad . \quad . \quad . \quad (4\,a)$$

for the temperature and calculate θ approximately, supposing

$$\frac{|\theta|}{T} << 1 \text{ for any } x. \quad . \quad . \quad . \quad (4\,b)$$

Fig. 2.

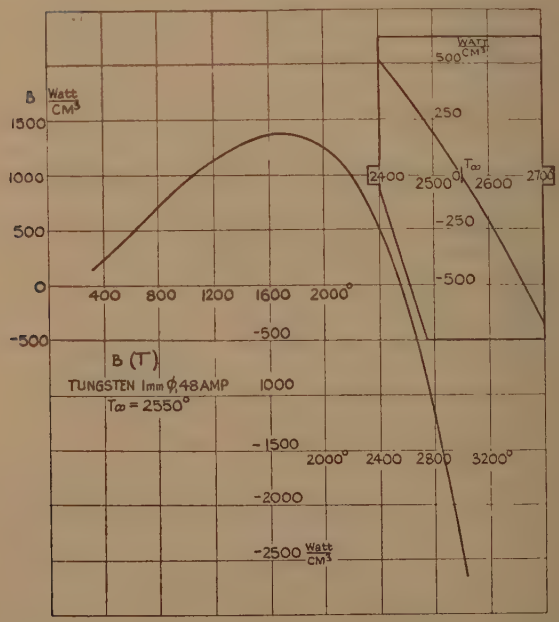

The heat equation for the interior of the conductor,

$$i^2\rho(T)+\text{div}\,(\gamma(T)\,\text{grad}\,T)=0, \quad . \quad . \quad . \quad (5)$$

with the surface condition,

$$\gamma(T_S)\left(\frac{\partial T}{\partial n}\right)_S+\sigma(T_S)=0 \text{ (index S=surface)}, \quad . \quad (6)$$

reduces, for $x = \text{const.}$, in virtue of (4), to the linear equation

$$\gamma \Delta_2 \theta \approx i_0^2 \rho - \frac{d}{dx}\left(\gamma \frac{dT}{dx}\right) = k\sigma \text{ (applying (1))} ; \quad . \quad (5\,a)$$

here σ, ρ, and γ are meant for $T(x)$, as well as in (6), because of $T_S \approx T$ (4 *b*). (5 *a*) and (6) can be solved in an elementary way for the circle and the rectangle, which are the most usual cross-sections. The result for the circle is

$$\theta - \theta_0 = \frac{\sigma}{\gamma} \cdot \frac{r^2}{2R} . \quad . \quad . \quad . \quad . \quad . \quad (7\,a)$$

Fig. 3.

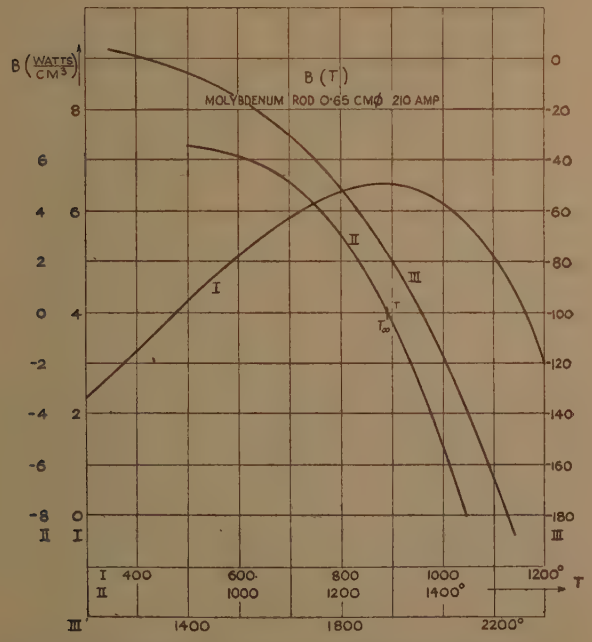

θ_0 being an arbitrary constant; for the rectangle

$$\theta - \theta_0 = \frac{\sigma}{\gamma}\left(\frac{y^2}{2\,b} + \frac{z^2}{2\,c}\right) \quad . \quad . \quad . \quad . \quad (7\,b)$$

Mainly important is the difference $\bar{\theta}$ between the two mean values

$$\bar{\theta}_\sigma = \frac{1}{U}\int_{(U)} \theta\, ds \quad \text{and} \quad \bar{\theta}_{\rho,\gamma} = \frac{1}{S}\iint_{(S)} \theta\, df \quad . \quad (8\,a, b)$$

taken over the circumference U and cross-section S, respectively, as the first step of accounting for the transversal variations is to take in (1) the values of ρ and γ for $(T-\theta_{\rho,\gamma})$, while σ for $(T-\theta_\sigma)$; thus

$$\frac{\bar{\theta}}{T} \ll 1 \quad . \quad . \quad . \quad . \quad . \quad . \quad . \quad (4\,c)$$

is the true criterion for the above assumption. It follows, for the circle

$$\bar{\theta}_\sigma - \theta_0 = \frac{\sigma}{\gamma}\frac{R}{2}, \quad \bar{\theta}_{\rho,\gamma} - \theta_0 = \frac{\sigma}{\gamma}\frac{R}{4}; \quad \bar{\theta} = \frac{\sigma}{\gamma}\frac{R}{4} = \frac{1}{2}\cdot\frac{1}{k}\frac{\sigma}{\gamma}; \quad (9\,a)$$

for the rectangle

$$\left.\begin{aligned} \bar{\theta}_\sigma - \theta_0 &= \frac{\sigma}{\gamma}\frac{bc+\frac{1}{6}(b^2+c^2)}{b+c}, \quad \bar{\theta}_{\rho,\gamma} - \theta_0 = \frac{\sigma}{\gamma}\frac{b+c}{6}; \\ \bar{\theta} &= \frac{2}{3}\frac{\sigma}{\gamma}\frac{bc}{b+c} = \frac{2}{3}\cdot\frac{1}{k}\frac{\sigma}{\gamma}. \end{aligned}\right\} \quad (9\,b)$$

Fig. 1 shows that $\frac{\sigma}{\gamma}$ is of the order 1 cm.$^{-1}$ at 1000°, 10 cm.$^{-1}$ at 1800°, 100 cm.$^{-1}$ at 2700°, and of the order $10^{2\frac{1}{2}}$ cm.$^{-1}$ at 3250°; these figures are fairly representative for any metal. On the other hand, $\frac{1}{k}$ is of the order 10^{-3} cm. for small bulb filaments, 10^{-1} cm. for large transmitting valve filaments. Thus $\bar{\theta}$ will be of the order $10^{-1\frac{1}{2}}$ to $10^{\frac{1}{2}}$ degree under most practical conditions, *i. e.*, the assumption (4 *c*) is certainly fulfilled. In the above numerical examples we find $\bar{\theta} \sim \frac{3}{4}°$ and $\bar{\theta} \sim \frac{1}{5}°$, respectively.

To obtain a unique solution of (1), two end conditions must be prescribed; usually two of the four end quantities T_a, $\left[\frac{dT}{dx}\right]_{x_a}$, T_b, $\left[\frac{dT}{dx}\right]_{x_b}$ are given. If the conductor is semi-infinite, there is the condition $\frac{d}{dx} = 0$ at $x = +\infty$ or $x = -\infty$, according to whether the conductor extends towards positive or negative x; thus only one condition remains to be fixed at the finite end x_0.

The case of the semi-infinite conductor, though being an idealization, is, nevertheless, of particular practical

interest. For if in the middle part the conduction term in (1) is negligible compared with the radiation term, the conductor may be looked upon as being composed of two semi-infinite ones which extend in either direction. Then $T \gtrsim T_\infty$ in the middle part, *i. e.*,

$$\gamma \approx \gamma(T_\infty), \quad B \approx -B'(T_\infty)\,.\,(T_\infty - T). \quad . \quad . \quad (10)$$

(10) leads to linearization of equation (1), which can thus be solved at once :

$$1-\frac{T}{T_\infty} \approx \Theta e^{\pm \beta x} \quad \text{or} \quad \frac{1}{T_\infty - T}\cdot\frac{dT}{dx} \approx \pm\beta,$$

where

$$\beta = \left|\sqrt{\left[\frac{-B'}{\gamma}\right]_{T_\infty}}\right| = \left|\sqrt{k\left[\frac{\rho}{\gamma}\frac{d}{dT}\left(\frac{\sigma}{\rho}\right)\right]_{T_\infty}}\right|, \quad (11)$$

and Θ = integration constant.

This is identical with the approximate solution (*a*) of Worthing and Stead.

Considering the rapid variation of $\sigma(T)$, (10), (11) are only valid for a small temperature range $\left|1-\frac{T}{T_\infty}\right| \ll 1$, which usually will not contain the end temperatures T_a and T_b ; therefore Θ cannot be determined accurately in this way in terms of the end condition. But it is true that, when evaluating Θ, nevertheless by extending the approximation (11) to the ends, the error thus committed will decrease with increasing length. Therefore we obtain a satisfactory criterion for whether the conductor can be considered as "long" (*i. e.*, may be approximated by two semi-infinite conductors), or not, when thus applying (11) to both sides, and prescribing at the jointing point, a certain small value e^{-N} for $\left|1-\frac{T}{T_\infty}\right|$. It results that the conductor is "long" if

$$\beta L \gtrsim 2N - \ln \frac{1}{\left|1-\frac{T_a}{T_\infty}\right|\cdot\left|1-\frac{T_b}{T_\infty}\right|}. \quad . \quad . \quad . \quad (12)$$

When following Stead's definition *, we put $e^N = 1000$,

$$2N \sim 13{\cdot}8. \quad . \quad . \quad . \quad . \quad . \quad (12\,a)$$

* G. Stead, Journ. Inst. Elect. Eng. lviii. pp. 107–17 (1920).

Numerical considerations show that the criterion is reliable when using the values

$$2N \sim 11 \text{ to } 16 \left(\text{corresponding to } \left|1-\frac{T}{T_\infty}\right|_{\min} \sim \frac{1}{250} \text{ to } \frac{1}{3000}\right), \quad (12b)$$

depending on the accuracy required.

Postulating that the conduction term in (1) should be negligible compared with the radiation term, we are led to the corresponding criterion,

$$\beta L \gtrapprox 2N' + 2\ln\left[T\frac{\rho}{\sigma}\frac{d}{dT}\left(\frac{\sigma}{\rho}\right)\right]_{T_\infty} - \ln \frac{1}{\left|1-\frac{T_a}{T_\infty}\right| \cdot \left|1-\frac{T_b}{T_\infty}\right|}. \quad . \quad . \quad . \quad (12c)$$

(when determining Θ in the same way as for (12)). As $T\frac{\rho}{\sigma}\frac{d}{dT}\left(\frac{\sigma}{\rho}\right) \sim 3\frac{1}{2}$ changes very little for most metals and different temperatures, this is practically identical with (12) with

$$N' \sim N - 2\tfrac{1}{2}.$$

The approximation (11) may be improved by continuing (10) as a Taylor expansion, which gives

$$\left.\begin{aligned} 1-\frac{T}{T_\infty} &= \Theta e^{\pm\beta x}\{1 - a_1\Theta e^{\pm\beta x} + a_2\Theta^2 e^{\pm 2\beta x} \ldots\}, \\ a_1 &= \left[T\left(\frac{1}{6}\frac{B''}{B'} - \frac{2}{3}\frac{\gamma'}{\gamma}\right)\right]_{T_\infty}, \quad a_2 = \left[T^2\left(\frac{B'''}{48B'}\right.\right. \\ &\left.\left. - \frac{3\gamma''}{16\gamma'} + \frac{1}{48}\left(\frac{B''}{B'}\right)^2 - \frac{7B''\gamma'}{48B'\gamma} + \frac{1}{4}\left(\frac{\gamma'}{\gamma}\right)^2\right)\right]_{T_\infty}, \ldots \end{aligned}\right\}. \quad (13)$$

Comparing the first two terms with (*b*), we obtain the value $n = 2a_1 + 1$. The application of (13) is very limited, for, quite apart from the fact that the expansion is purely formal, *i. e.*, of doubtful convergence, there are the practical disadvantages that the convergence becomes very slow when $\left|1-\frac{T}{T_\infty}\right|$ increases, owing to the rapid variation of B(T), and that the determination of Θ becomes involved. But the coefficients, e. g., a_1, give a useful

illustration of the physical influences which cause the deviations of $T(x)$ from the exponential shape. The term $\left[\frac{B''}{B'}\right]_{T_\infty} > 0$ (see (3)) shows that the rapid decrease of B′ with temperature tends to flatten the curve $T(x)$, while the slight increase of γ with T has the opposite effect by throttling the heat-flow towards the end. It may be anticipated from the illustration (fig. 1) that usually the first influence will prevail, except at very low temperatures.

We now come to the general solution of (1). It is obtained by making use in a well known way of the fact that the equation (1) does not contain the independent variable explicitly. The substitution

$$\xi = \left(\gamma(T)\frac{dT}{dx}\right)^2 \quad . \quad . \quad . \quad . \quad . \quad (14)$$

leads to the equation

$$\frac{d\xi}{dT} = -2\gamma(T)B(T) \quad . \quad . \quad . \quad . \quad (15)$$

between $\frac{dT}{dx}$ and T, which can be integrated at once.

$$\xi(T) = \xi_m + \int_T^{T_m} 2\gamma B\, dT; \quad \xi_m = \left(\gamma\frac{dT}{dx}\right)^2_{T=T_m}, \quad (16)$$

ξ_m being the integration constant and T_m a constant temperature to be fixed later; or

$$\gamma(T)\frac{dT}{dx} = \sqrt{\left(\gamma\frac{dT}{dx}\right)^2_{T=T_m} + \int_T^{T_m} 2\gamma B\, dT}. \quad (16\,a)$$

Integrating again, it follows that

$$x = x_0 + \int_{T_0}^{T} \frac{\gamma(T)\,dT}{\sqrt{\xi_m + \int_T^{T_m} 2\gamma B\, dT}}, \quad . \quad . \quad (17)$$

which gives the final solution $T(x)$. x_0 is here the (arbitrary) coordinate of the point with the temperature T_0 (conveniently one of the ends, *i. e.*, $T_0 = T_a$ or T_b).

As the functions $\int^T \gamma\rho\, dT$ and $\int^T \gamma\sigma\, dT$ are numerically well known for any material for which measurements

exist, (16 *a*) gives at once the gradient as function of temperature after ξ_m has been determined from the end conditions; then $x(T)$ follows simply by integration (17). Thus it remains only to show how to determine ξ_m.

This is done at once for the "long" conductor by fixing

$$\left.\begin{aligned} &T_m = T_\infty, \text{ which implies } \xi_m = 0, \textit{ i. e.,} \\ &\gamma \frac{dT}{dx} = \sqrt{\int_T^{T_\infty} 2\gamma B\, dT} \\ &\qquad \left[\int_T^{T_\infty} \gamma B\, dT > 0 \text{ for any T, because of (3)}\right]. \end{aligned}\right\} \quad (18)$$

The sign of $\frac{dT}{dx}$ is given by

$$\operatorname{sign} \frac{dT}{dx} = \operatorname{sign} (x - x_0) \,.\, \operatorname{sign} (T_\infty - T_0), \quad . \quad (18a)$$

the sign of the two factors depending on the sense of direction and on whether heat is removed or supplied at the end. The four possible combinations are represented by the curves *a*–*d* in fig. 4 (gradient) and fig. 5 (temperature) *. As by (11),

$$\lim_{T \to T_\infty} \left\{ \frac{1}{T_\alpha - T} \cdot \frac{dT}{dx} \right\} = \left| \sqrt{\left[\frac{-B'}{\gamma}\right]_{T_\infty}} \right| \equiv \beta, \quad (19)$$

the zero tangents of the curves *a*–*d* and *b*, *c* in fig. 4 have the inclination $\pm 45°$ when plotted for the abscissa scale

$$\frac{T}{T_\infty}$$

and ordinate scale

$$T_\infty \left| \sqrt{[-B'\gamma]_{T_\infty}} \right| \cdot \gamma(T) \frac{dT}{dx} \text{ (lines } a'\text{–}d'\text{).}$$

Figs. 6 and 7 show the result of (18) for the two above numerical examples †. Fig. 6 corresponds to the range "*a*" of fig. 4, fig. 7 to both "*a*" and "*b*" (I. and II.). The tangent (19) at T_∞ corresponding to (*a*) or (11) is drawn in each case. The dashed curve of fig. 6 represents

$$\frac{\gamma(T)}{\gamma(T_\infty)} \cdot \frac{dT}{dx}.$$

* Figs. 4, 5, and 9 are merely illustrations and do not represent numerical conditions.

† With the proviso shown in footnote (*) on p. 644.

Fig. 4.

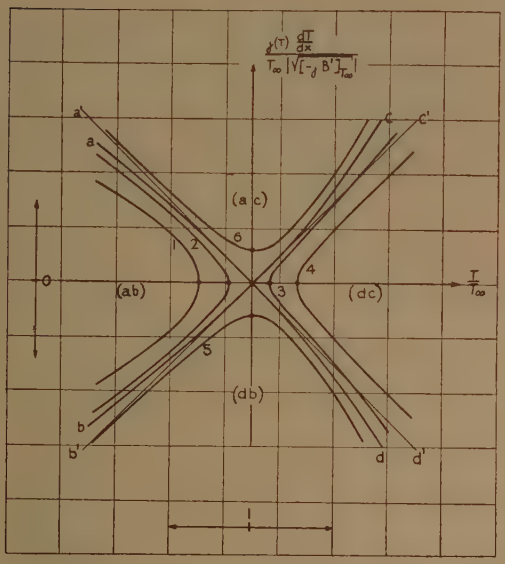
a'
a
c
c'
(a c)
1
2
6
4
0
(ab)
3
(dc)
5
(db)
b
b'
d
d'
l

Fig. 5.

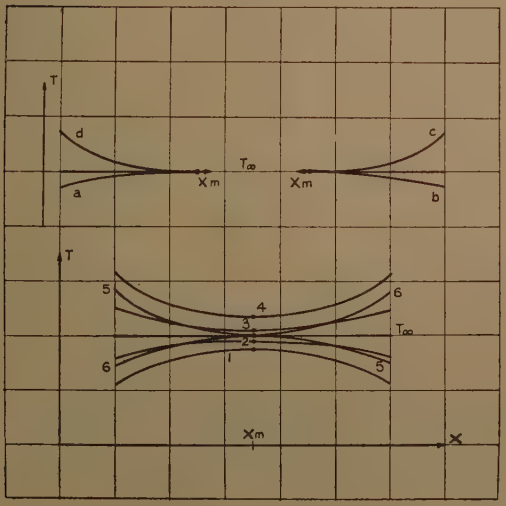
T
d
c
T_∞
a
Xm
Xm
b
T
5
6
4
3
T_∞
2
1
6
5
Xm
X

Comparison shows that in fig. 6 the constrictive effect of $\gamma' > 0$ supersedes the opposite influence of $B'' < 0$ only at very low temperatures, while in fig. 7 the latter one prevails everywhere, owing to the lower T_∞ ; that agrees with the anticipations connected with (13). Fig. 8 shows $T(x)$ for the second example as given by (17), with $x_0 = 0$ at $T_0 = 300°$. The dashed curve is the exponential approximation (11) which fits at $T \to T_\infty$, *i. e.*, with Θ

Fig. 6.

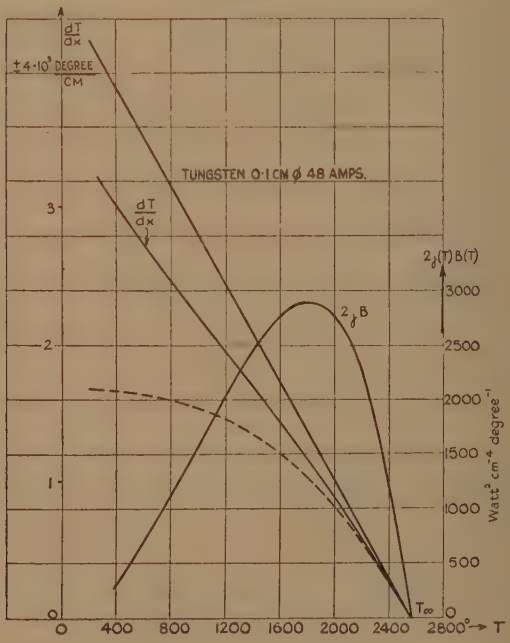

determined in the same way as in (12). The resulting length-error at $T_0 = 300°$ is about 2 cm. As the accurate value of the length $l_{\text{stead}}\left(\frac{T}{T_\infty} = 99{\cdot}9 \text{ per cent.}\right)$ is found to be 34·8 cm., this means an error of only 5·2 per cent., and the error of the equivalent emission length would be < 1 per cent. It is remarkable that the corresponding error of the gradient is about 45 per cent., as shown by fig. 7.

Fig. 7.

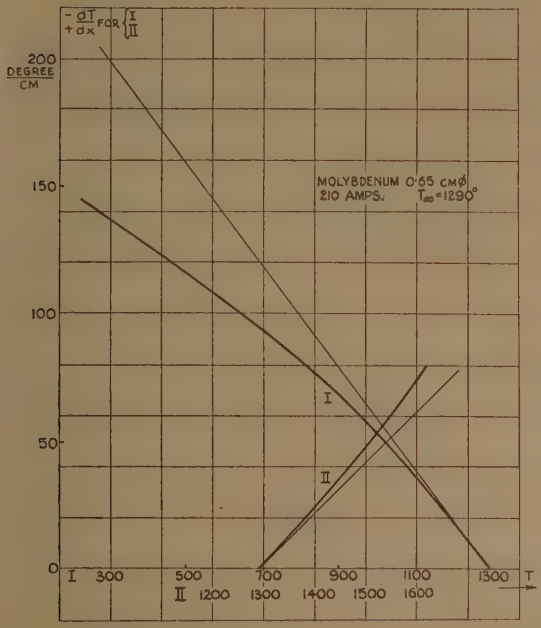
$-\frac{dT}{dx}$ FOR {I II
200
DEGREE CM
150
100
50
0
MOLYBDENUM 0·65 CMØ
210 AMPS. T_∞ = 1290°
I
II
I 300 500 700 900 1100 1300 T
II 1200 1300 1400 1500 1600

Fig. 8.

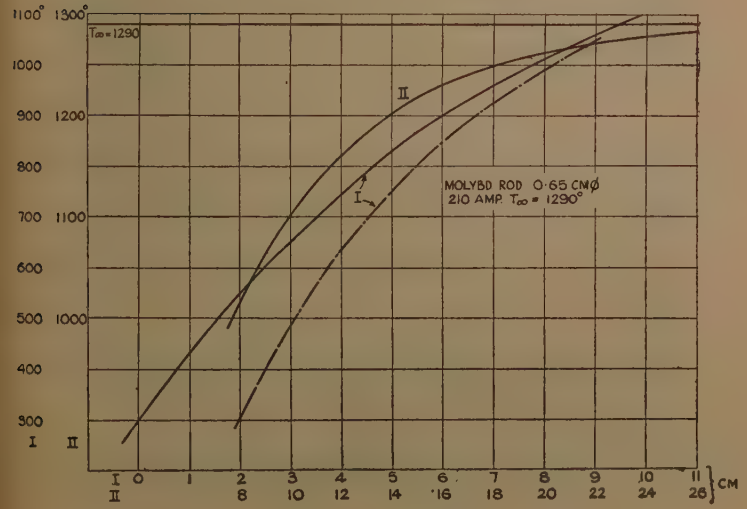
1100° 1300°
T_∞ = 1290
1000
900 1200
800
700 1100
600
500 1000
400
300
I II
II
I
MOLYBD ROD 0·65 CMØ
210 AMP. T_∞ = 1290°
I 0 1 2 3 4 5 6 7 8 9 10 11
II 8 10 12 14 16 18 20 22 24 26 CM

The point

$$T=T_\infty, \quad \gamma\frac{dT}{dx}=T_\infty\sqrt{[-B'\gamma]_{T_\infty}} \quad . \quad . \quad (20\,a)$$

is a singular point of the differential equation (15), as there is

$$\frac{d\xi}{dT}=0\,; \quad . \quad . \quad . \quad . \quad . \quad . \quad (20\,b)$$

it is the only (real) singularity of (15), since B(T) vanishes at $T=T_\infty$ only. From its property as a saddle-point it follows that every solution curve $\gamma\frac{dT}{dx}=f(T)$ of (15) adjacent to the two singular curves (*ad*) and (*bc*), is wholly situated within a domain bordered by two consecutive branches of the singular curves, as shown in fig. 4 (curves 1–6). This may be concluded likewise from the fact that, by (15) and (3),

$$\left[\gamma\frac{dT}{dx}\cdot\frac{d^2}{dT^2}\left(\gamma\frac{dT}{dx}\right)\right]_{T_\infty}=\left[-\gamma B'\right]_{T_\infty}>0, \text{ i. e.,}$$

$$\operatorname{sign}\left[\frac{d^2}{dT^2}\left(\gamma\frac{dT}{dx}\right)\right]_{T_\infty}=\operatorname{sign}\left[\gamma\frac{dT}{dx}\right]_{T_\infty}.$$

The solution curves situated within the four domains of fig. 4 evidently belong to conductors of "finite" length, the categories being separated by the singular infinite conductor. It is seen (and follows from (20 *b*)) that if a physical case belongs to the domain (*ac*) or (*db*), the temperature gradient is of equal sign all over the conductor, and when T_∞ is reached at any point x_m there is a positive minimum or negative maximum, respectively, of the gradient. If, on the other hand, a case belongs to (*ab*) or (*dc*), the temperature is everywhere either below or above T_∞, and if it goes through a maximum or minimum, respectively, the gradient changes the sign at this point. Therefore it lends itself to fix

$$T_m=T_\infty, \qquad \xi_m>0 \text{ for the domains } (ac),\,(db), \quad (21\,a)$$

$$T_m=T_{\left\{\begin{smallmatrix}\text{max.}\\ \text{or}\\ \text{min.}\end{smallmatrix}\right.}, \quad \xi_m=0, \quad \text{,,} \quad \text{,,} \quad (ab),\,(dc). \quad (21\,b)$$

[These definitions become identical for the bordering cases, as it must be; it would be possible to use (21 *a*)

throughout, but then $\xi_m<0$, *i. e.* $\left(\frac{dT}{dx}\right)_{T_m}$ =imaginary for (ab) (dc), which is inconvenient.] Fig. 5 shows the corresponding conditions in the T—x-diagram. T_m, x_m is marked by dot in both figs. 4 and 5.

In order to determine the numerical value of ξ_m in any practical case, the corresponding domain must be found first. Very often this can be concluded directly from the prescribed end conditions. If, *e.g.*, $T_a<T_\infty$, $T_b>T_\infty$, it is obvious that the domain is (ac), when fixing $x_b>x_a$. Or, if $\left(\frac{dT}{dx}\right)_{x_a}>0$, $\left(\frac{dT}{dx}\right)_{x_b}<0$, the case must belong to (ab). Generally, the domain is given at once, if it is obvious that either $(T-T_\infty)$ or $\frac{dT}{dx}$ is of opposite sign at the two ends, as then certainly either of the coordinate axes is passed in fig. 4. Otherwise the classification is settled by comparison with the semi-infinite conductor. To take a concrete case, let us suppose $T_a<T_b<T_\infty$; $x_i<x_b$. Then the solution may be of the type of curves 1, 2 (with or without containing $T=T_m$), or it may be of the type of curve 6 for $T<T_\infty$. We draw the well-known T—x-curve of the semi-infinite conductor corresponding to curve (a) (fig. 5), and thus determine a length L′ between T_a and T_b. If L′<L, the solution belongs to the left part of the domain (ac), as then the gradient must be higher than that of the infinite conductor; likewise L′<L means the domain (ab).

Knowing the class of the solution, the determination of ξ_m is a matter of numerical calculation, and is carried out conveniently by trial and error. If the conductor is not very "short" (*i. e.*, L not very small compared with the right side of (12)), a first approximative value T_m^* or $\left(\frac{dT}{dx}\right)^*_{T_\infty}$ for T_m and $\left(\frac{dT}{dx}\right)_{T_\infty}$, respectively, is obtained graphically by smoothly connecting two infinite conductor branches which fulfil either of the conditions at x_a, x_b, as shown by fig. 9. Drawing the solution curve belonging to T_m^* or $\left(\frac{dT}{dx}\right)^*_{T_\infty}$, respectively, and to one of the end

conditions by means of (16), (17), the other condition will, in general, not be fulfilled; but the sign and amount of the error indicate the necessary correction of T_m^* or $\left(\frac{dT}{dx}\right)_x^*$, respectively; thus the solution is readily obtained with sufficient accuracy.

If the conductor is "very short," a first approximation is obtained by taking in (1), constant mean values of σ, ρ, and γ in the given temperature range, as then the

Fig. 9.

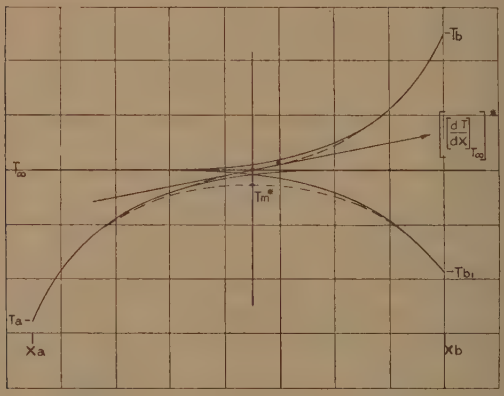

radiation term is small compared with the conduction term, and $\rho(T)$ and $\gamma(T)$ vary comparatively slowly. Then (1) yields the parabolic approximation

$$T \approx \frac{T_a x_b - T_b x}{x_b - x_a} + \frac{(T_b - T_a)x}{x_b - x_a} - \frac{B}{2\gamma}(x_b x_a - (x_b + x_a)x + x^2) \quad . \quad . \quad . \quad . \quad (22)$$

which gives a value T_m^* or $\left(\frac{dT}{dx}\right)_{T_\infty}^*$, respectively, to start with.

LII. *The Glow Discharge through Oxygen.* *By* F. D. Greeves, *M.Sc.*, *and* J. E. McF. Johnston, *M.Sc.*, *Department of Physics, Queen's University, Belfast* *.

[Plate X.]

1. *Introduction.*

SINCE the publication of Langmuir's interpretation of the current voltage characteristic curve of a probe inserted into the plasma of a mercury arc [1] there have been numerous attempts to apply his method to discharges through various gases. These have shown that in many cases Langmuir's analysis is immediately applicable. From the published curves of Bramley [2], Childs [3], Trevelyan [4], and Rusk [5], and from experience in this laboratory it is clear, however, that Langmuir's original treatment is not satisfactory in all cases. Further, there is little published work which gives anything like a complete account of the exact dependence of the collector characteristic on conditions in the discharge. The work that has been done is on the whole of an exploratory nature, the most important exception being Seeliger's study of the positive column [6]. This is not surprising, because the number of factors upon which the discharge depends is large (*e. g.*, the nature of the gas, its pressure, the voltage between the electrodes and their geometry), and the work involved in a comprehensive study of the discharge by this method is laborious. The present investigation was undertaken to provide for a simple molecular gas, oxygen, as complete an account as appears worth while of its electrical properties in the negative end of the discharge, using primarily probe methods, and to test the validity of these as far as possible.

2. *Experimental Arrangements.*

The discharge-tubes used were made of soda-glass 6 cm. in internal diameter, with two disk electrodes made of non-magnetic nichrome perpendicular to the axis. These electrodes were mounted on a glass frame 18 cm. apart, and could be moved along the discharge-tube by tilting, since between the liquid-air trap immediately preceding

* Communicated by Prof. K. G. Emeléus, M.A., Ph.D.

the tube and the pumping-train there was a ground-glass joint perpendicular to the discharge-tube. Two side-arms were fused on to the main tube diametrically opposite each other, so that comparative measurements could be taken with two different probes admitted simultaneously through these under as nearly as possible the same discharge conditions. The type of probe employed is shown in fig. 1, *a*.

Fig. 1.

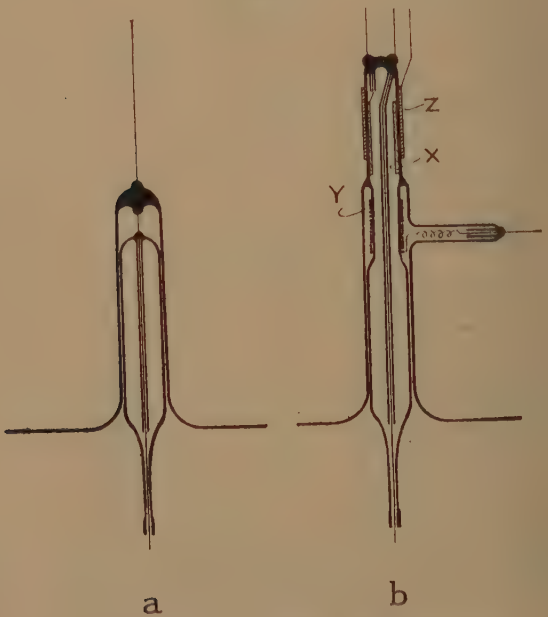

a. Ordinary probe. *b*. Probe with guard-rings.

The oxygen was prepared by heating potassium permanganate, and showed no spectroscopic impurity. The usual procedure for baking and degassing the tube and electrodes and for excluding condensible vapours was employed. Taps and joints were lubricated with the grease Apiezon L.

Discharges were run over a pressure range from 0·02 mm. to 2·00 mm. Hg., the maximum potential difference between the electrodes being 720 volts. The tube was

never warm to the touch with the discharge running. The voltage was varied by altering the filament current of a diode in series with the discharge-tube. A Ferranti electrostatic voltmeter was used to measure the potential difference across the tube. The conventional electrical circuit was used for varying the potential on the probe (fig. 2). The sensitivity of the tube galvanometer was 26·3 mm. per microamp., that of the probe galvanometer 278 mm. per microamp.

With 720 volts across the tube the discharge could not be maintained below 0·02 mm. Hg. The faintest dis-

Fig. 2.

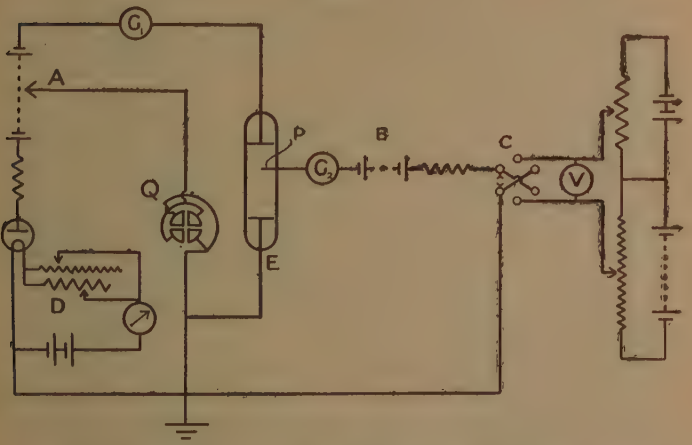

Circuit for obtaining current-voltage characteristic curve for a probe, and for recording small changes in potential between the anode and cathode of a discharge-tube. Galvanometer shunts are not shown. The bank of accumulators A supplies the current to the discharge-tube. Circuit D consists of a diode and auxiliary apparatus for varying the filament current of the diode. The potential of the probe P relative to a main electrode of the tube E is varied by the r.h. potentiometer system and measured by the multirange voltmeter V. C is a commutator. B a biassing p.d. for P. The e.s. voltmeter between anode and cathode of the discharge-tube is not shown.

charge detected was at 0·02 mm. with a current of $6{\cdot}9 \times 10^{-9}$ amp./cm.^{2}, and was barely visible. With increase of pressure and the same applied voltage a very faint green glow appeared filling the greater part of the tube, with the cathode side less luminous than the anode region,

but there was no definite boundary between the two parts ; the current also increased. On further increasing the pressure (and current) the light became more intense, the various regions of the discharge could be distinguished with ease, and a definite negative glow cathode dark space boundary appeared and moved in towards the cathode. At 0·09 mm. with 600 volts between the electrodes the discharge is as shown in Pl. X., I. Next to the cathode there is a pink cushion of light, covering the electrode and parallel to it over the central parts. Then comes the purple cathode dark space, which is separated from the clear green [7], [8] negative glow by a very sharp edge (shown better in Pl. X., II–IV). Under these conditions the green light from the negative glow extends right up to the anode, and no positive column is present. The cathode dark space was 3 cm. wide in this particular case.

Further increase of pressure at 600–700 volts caused the cathode regions to become still more contracted, until at 0·50 mm. the cathode dark space was only 0·7 cm. wide. The negative glow cathode dark space edge then no longer presented quite such a sharp appearance to the eye. The visual negative glow was localized in a small length of the discharge-tube and was a whitish-green colour. At the anode side of the negative glow there was an almost non-luminous Faraday dark space which occupied the tube up to the anode except for a thin non-oscillatory [9] uniform greyish glow covering the latter. The positive column becomes visible at about 1·0 mm. pressure. It has a faint bluish colour and is difficult to detect visually when the gas is free from impurities ; it appears to be non-striated, but it is difficult to be sure of this when the light from it is so feeble. Above 2·0 mm. Hg., with 720 volts applied, the discharge failed to cover the whole of the anode; otherwise its general appearance was unaltered.

Keeping the pressure fixed at 0·09 mm., and starting with 600 volts across the tube, the appearance is as already described. On decreasing the voltage and current the negative glow edge moves towards the anode and some of the green light starts to diffuse through this edge into the cathode dark space (Pl. X., II and III). Under still less energetic discharge conditions the negative glow becomes a hazy cloud of green light, fading off

gradually into both the cathode and anode regions of the discharge with a peculiar sharp edge in the centre of the green region, about 6 cm. from the cathode, corresponding to the original well-developed negative glow edge (Pl. X., IV). Decreasing the current further this sharp visual division in the negative glow disappears (Pl. X., V and VI) and the cathode glow contracts uniformly on to the centre of the electrode. Its faint pink merges into the hazy green region where the cathode dark space originally was, and the negative glow occurs as a green patch of light without any visible sharp edge or internal structure ; a diffuse green ball of light not shown in the plate is emerging from the anode, constituting some form of anode glow.

On now decreasing the current further at the same pressure the discharge changes in type discontinuously. The negative glow jumps in to a position closer to the cathode, and is more sharply defined at the cathode side than towards the anode. The cathode glow covers the whole of the electrode. An anode glow and positive column are visible. Still further decrease of the current results in the negative glow edge moving towards the cathode, coming in from 6 cm. at $1{\cdot}96 \times 10^{-6}$ amp./cm.^{2} to 3 cm. at $0{\cdot}099 \times 10^{-6}$ amp./cm.^{2}, after which the discharge becomes too feeble to permit of visual observations. In these stages the discharge is very easily disturbed, and becomes intermittent if, for example, the voltmeter is connected between the electrodes. Our description of this part agrees well with that given by Taylor for a " corona " discharge in neon-helium mixtures [10].

The manner in which the potential difference between the anode and cathode and between a probe situated 7·4 cm. from the cathode and the cathode vary with the current is shown in fig. 3. On the rising part of the characteristic (AB) the true cathode-space potential differences obtained by Langmuir's method are given. On the " corona " part (DE) only the potential difference between the cathode and floating probe could be measured. Where the potential difference is stationary (BC), just above where the discharge suddenly changes in type (X), may be taken provisionally as the normal cathode fall (V_n) ; at this pressure, as less of the cathode surface becomes covered as the tube current is decreased, the contraction is perfectly regular and steady, in contrast

to the contraction at higher pressures (0·6 mm. and higher) which takes place erratically and appears to be controlled by small irregularities in the build of the discharge-tube.

Fig. 3.

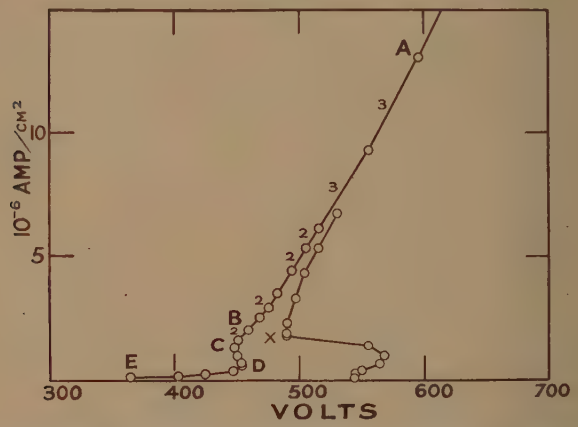

Current-voltage curve for discharge at 0·09 mm. Hg. The curve ABCDE gives the potential difference between a probe in the centre of the negative glow and the cathode. The other curve is for the p.d. between anode and cathode ; it practically joins BA at larger currents. With increase of current beyond that shown the curve BA continues to rise almost linearly. X is where the discharge changes in type discontinuously. The figures against the curve give the number of electron groups found.

TABLE I.

Normal Cathode Fall.

Relation between V_n in volts and p in mm. Hg. for oxygen, cathode of nickel-chrome. Günther-Schulze's results (V_n') with an iron cathode are given for comparison.

p	0·09	0·10	0·12	0·13	0·19	0·26	0·31	0·42	0·61	0·81
V_n	448	—	440	421	386	—	362	357	355	356
V_n'....	—	351	—	—	—	346	—	—	—	351

This difference is also associated, as in Taylor's work [10], with failure of the " corona " regime to develop at the higher pressures. The data for the normal cathode fall

are collected in Table I. It appears to increase considerably at the lower pressures. This may be connected with an effect of the tube walls [11], since it was not noticed by Güntherschulze in his experiments with a large bell-jar as container [12]: some of his data are also given in Table I.

Part of the current (i) *vs* voltage (V) characteristic curve for a probe in the negative glow of a discharge at 0·09 mm. and 565 volts is shown in fig. 9, A. This is of the regular form. The positive ion current is allowed for by extrapolation to obtain the electron current in

Fig. 4.

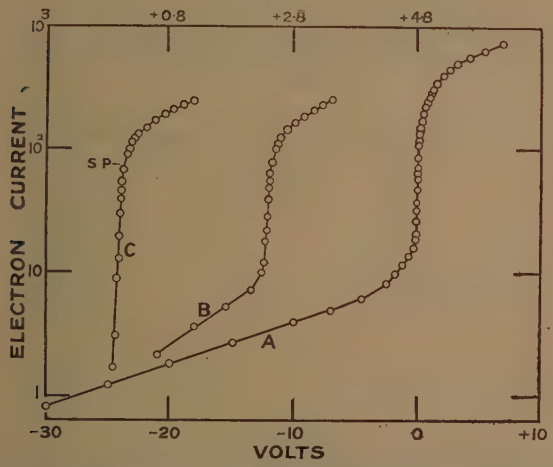

Semilogarithmic electron current plots, corresponding to fig. 9, A. A is the full electron current, B a replot of the rising part of A after allowance for the fast group corresponding to the straight part of A. C is similarly related to B. The bottom voltage scale is for A, the upper for C. The space potential SP is found from C. Current units are arbitrary, but the same for A, B, and C. Full details of the analysis are given in Table II., electron concentrations being from the mean energies and the actual (C) or extrapolated (A, B) currents at SP.

a retarding field, the resulting semi-log plot of which (fig. 4) can be analysed as indicated to show that three groups of electrons, each with an approximately Maxwellian distribution of velocities, are present in the discharge. The data obtained from the curve are given in Table II.

It was found at first extremely difficult to get steady readings of the probe current when the probe was receiving the high concentration, low velocity group of electrons in a retarding field. Similar difficulties have been met with by investigators using discharges in other gases, and in this laboratory oxygen had previously been found a bad offender in this respect [13]. The probe galvanometer spot usually either (*a*) drifted steadily and quite

TABLE II.

Results of Typical Electron Analysis.

Run 107, pressure 0·09 mm. Hg. Tube volts 565, current density $6{\cdot}37 \times 10^{-6}$ amp./cm.^{2}.

Distance cathode-probe 5·1 cm. The probe is in the negative glow, approximately 0·5 cm. from the cathode dark space boundary. Probe, Pt. III.

Group.	Temperature (volts).	Concentration (10^7/cm.^{3}).
Slow	0·07	47·7
Medium	1·84	1·30
Fast	19·0	0·37

rapidly back to about zero deflexion or (*b*) jumped erratically about the scale.

(*a*) When the remainder of the characteristic was re-examined in more detail it was found that this drift also occurred with the probe more negative, but was only noticeable at all on observing for a much longer time, the decrease in current being for example 1 mm. per 200 mm. deflexion in 20 minutes. When electrons were being collected in an accelerating field a very slight decrease in the probe current also took place at about the same slow rate. This occurred with all the probes used (Table IV.), but was not definitely correlated with any change in the main discharge until a circuit with a quadrant electrometer acting as a peak voltmeter for the tube voltage was set up (Q, fig. 2) by means of which we could follow small changes (1 part in 2×10^4) in the tube voltage. It was then found that the drift of the probe

galvanometer was always accompanied by a small change in the tube voltage.

It was subsequently found that the tube voltage could be kept constant and the drift eliminated by simultaneously (i.) arranging the discharge conditions so that the voltage between the electrodes was just above the normal fall, as defined above, (ii.) keeping the liquid air at a high constant level on the trap next the discharge-tube.

TABLE III.

Reproducibility of Data.

Runs 119–120, pressure 0·12 mm. Hg. Tube volts 455, current density $2{\cdot}75 \times 10^{-6}$ amp./cm.^{2}. Probe in the negative glow 4·5 cm. from the cathode. Probe, Pt III.

The series of readings took 80 minutes. A. Changing the probe voltage from negative to positive relative to the anode. B. Probe voltage altered in opposite sense.

	Space potential relative to anode (volts).	Fast.		Medium.		Slow.	
		Temp. (volts).	Conc. (10^7/cm.^{3}).	Temp. (volts).	Conc. (10^7/cm.^{3}).	Temp. (volts).	Conc. (10^7/cm.^{3}).
A ..	−15·0	14·4	0·34	1·63	1·55	0·18	21·7
B ..	−14·7	18·5	0·28	1·75	1·76	0·10	29·9

This indicates that the effects are connected with a slow change of gas content in the tube, as, for example, by formation and freezing out or re-evaporation of ozone and by cathode sputtering [14]. It is not essential to suppose that the probe itself plays an active part, the sensitiveness of the probe current to the change being reasonably referred to the steep slope of its characteristic (i *vs* V) curve when slightly negative to the surrounding ionized gas making it specially sensitive to changes in the potential of the gas.

Taking these precautions it was usual during a period of over an hour to have a change of not more than 0·5 volt in 450 volts across the tube, but as a further precaution in those cases where it was suspected that

drift might just possibly affect the results, the readings were taken at definite time intervals [15]. To illustrate the consistency so obtained fig. 6, A, shows the effect of taking a probe characteristic and then retracing the readings with voltage changes made in the opposite sense ; the numerical results are given in Table III.

(*b*) This also only occurred when the slowest electrons were being received in a retarding field. It was found to be caused by the extraneous action of any low frequency oscillator with a spark-gap, such as a nearby induction coil or electrically driven tuning-fork. The reason that this behaviour is only detected on the one part of the characteristic is probably due to a rectifying and amplifying action of the probe, since its characteristic curve rises steeply and has considerable curvature at this part [16].

3. *Possible Errors in the Interpretation of the Probe Characteristics.*

The original Langmuir theory does not make any attempt to allow for the disturbing effect of the probe itself upon the discharge. This is done in the more comprehensive study of the plasma by Langmuir and Tonks [17], but the nature of the resulting correction is complicated, depending both on conditions in the plasma and its geometry. In the case of the negative glow the problem is particularly intricate owing to the large number of parameters governing the discharge. Hence it was decided to attempt to test experimentally what features of the results obtained might be manufactured by the probe itself.

A. An extensive series of measurements were taken under various discharge conditions with probes of various diameters and materials. The description of the probes is given in Table IV. It was found that the type of characteristic curve obtained was independent of the probe used. This amplifies the results of Emeléus and Brown [18], who used probes of different sizes and materials, generally larger than ours. A few comparative results are given in Table V. for discharges where the Langmuir analysis for groups could be applied. The greatest discrepancies between the electron concentration data

occur from the Wollaston wire and Pt 11. No serious attempt need be made to account for this, since the fact that any measurements at all could be obtained using Wollaston wire as a probe was regarded more as a *tour de force*, owing to the extremely fragile nature of the wire, than an attempt to obtain electron data with any claim to accuracy. The result is quoted simply to show that using an extremely small probe a log i *vs* V curve similar to those for larger wires is obtained, and that, incidentally, the electron temperatures obtained from it agree reasonably well with those found by a wire of fifty-five times the diameter under the same conditions. As to the remainder of the results, it is seen that there is a

TABLE IV.

Details of the Probes.

	Diameter.
Platinum : Wollaston	0·0001 cm.
I.	0·001 cm.
II.	0·0055 cm.
III.	0·04 cm.
Molybdenum I.	0·01 cm.
II.	0·02 cm.
Copper clad iron-nickel	0·06 cm.

fair agreement between the data obtained for the various probes, the greatest discrepancies occurring for the slowest group of electrons in the case of Mo I and Pt I ; in the remainder of the readings the greatest difference in concentration or temperature is of the order 2 : 1.

Considering the great difficulty in obtaining any data for the fastest electrons [18] this is not unsatisfactory so far as they are concerned. We take the same view of the data for the slowest group, which are difficult to obtain with much accuracy, because of the rapid rise in probe current with voltage when they are being received. It is possible, nevertheless, that there is some distortion of the discharge by the probe in relation to the slowest electrons, when the greater constancy obtainable with a single probe is borne in mind (*v.* fig. 10). Finally, the data for the group of medium speed are satisfactorily consistent.

TABLE V.

Comparative Data for probes of various sizes. (The corrections B, C. D. §(3) are negligibly small.)

Run.	Pressure (mm. Hg.).	Current density (10^{-6} amp./cm.^{2}).	Probe.	Distance from cathode (cm.).	Space potential relative to anode (volts).	Fast.		Medium.		Slow.	
						Temperature (volts).	Concentration (10^7/cm.^{3}).	Temperature (volts).	Concentration (10^7/cm.^{3}).	Temperature (volts).	Concentration (10^7 cm.^{3}).
102	0·09	3·77	Pt II	5·0	−0·2	19·9	0.7	1·65	1·26	0·14	22
103	0·09	3·69	Pt Woll.	5·0	+0·1	15·1	34·0	trace	trace	0·09	117
24	0·09	39·3	Mo I	3·8	+1·2	The collector potential was not made sufficiently ve.		2·62	5·60	0·35	56
25	0·09	28·5	Pt I	3·8	+0·8			2·35	6·75	0·20	190
95	0·08	10·4	Pt II	4·7	−0·2	17·7	0·7	1·76	1·66	0·14	64
96	0·08	10·5	Pt I	4·7	−0·2	19·8	1·5	2·17	2·32	0·07	56
104	0·09	8·6	Pt III	6·0	+ 0·0	28·6	0·3	2·78	1·46	0·13	128
105	0·09	8·2	Pt II	6·0	− 0·1	19·9	0·8	2·03	2·41	0·09	162

B. The part of the collector not protruding into the discharge might draw an appreciable current from the plasma, and so modify the results. In two cases where the wire was burnt off after taking a run measurements were taken, using the stump, which was practically level with the glass-sheath. When the current due to the stump and leads was subtracted from the current to the probe before it was burned off the resulting semi-log curve when plotted practically coincided with the original one. Hence it appears that the correction involved due to the current taken by that part of the probe which is partially shielded from the discharge may be neglected. The effect of the length of the probe has been studied in more detail and similar conclusions reached by Emeléus and Sloane [19].

C. A special probe was constructed to obtain an idea of whether the insulation of the probe walls affected the characteristic curve. It was desired to alter the potential of the inner and outer walls of both the sheath and the side-arm holding the probe This was done conveniently by a probe of the construction shown in fig. 1, *b*. X was a cylinder of non-magnetic nichrome pressing tightly against the inner wall of the side-arm. Y consisted of several turns of molybdenum wire wrapped round the constriction below the internal seal. By varying the potential of X or Y the potential of the walls inside the discharge-tube can be effectively altered. Similarly the external metal collar Z controls the potential of the external wall. The potentials of X, Y, and Z were varied separately and together from -120 volts to $+120$ volts with respect to the anode. It was found that this did not produce a detectable change in the probe current under any conditions. Neither could any current to these guard-rings be measured on our galvanometers. An example is given in Table VI. of the results obtained when all three guard-rings and probes had their potential varied together, only the current to the probe being measured ; it is seen that the agreement with the results obtained when the guard-rings were left floating is good. Thus within the above limits the potential of the walls of the glass sheathing has no effect on the probe characteristic. This is also true in those cases where the Langmuir analysis does not apply.

D. As has been pointed out by Wehrli [20] a variation in the tube potential consequent on altering the probe potential may affect considerably the electron data deduced from the log i *vs* V curve. In order to measure accurately any change in potential across the discharge-tube that might occur the circuit shown in fig. 2, to which reference has already been made, was employed [21].

TABLE VI.

Lack of Effect of Guard Rings.

Runs 161–162, pressure 0·13 mm. Hg. Tube volts 450, current density $5{\cdot}45 \times 10^{-6}$ amp./cm.^{2}. Probe in the negative glow 4·0 cm. from the cathode ; a faint anode glow was present. Probe, Pt II.

A. Readings taken with the guard-rings in the circuit.

B. With the guard rings XYZ floating.

	Space potential relative to anode (volts).	Fast group.		Medium group.		Slow group.	
		Temp. (volts).	Conc. (10^7/cm.^{3}).	Temp. (volts).	Conc. (10^7/cm.^{3}).	Temp. (volts).	Conc. (10^7/cm.^{3}).
A ..	−14·6	21·6	1·1	1·94	2·3	0·17	16
B ..	−14·2	24·8	1·1	1·63	2·9	0·16	10

The point A on the bank of accumulators supplying the potential difference for operating the tube was chosen to be as nearly as possible at the same potential as the main tube electrode E ; any variation in potential across the discharge-tube was then given directly by the change in the reading of the quadrant electrometer Q.

As might be expected the maximum effect was found to be produced by a thick probe in a faint discharge, whilst a very fine probe leaves the tube voltage practically unaltered, as shown in fig. 5. Assuming that the whole of this potential change takes place at the point where the probe is situated the true log i *vs* V curve can be obtained by combining the voltage change with the original reading of the probe voltmeter. The greatest change produced in any of the cases studied by us is shown in fig. 5, A, the change in the final results being shown in Table VII. and fig. 6, B. It must be emphasized that the effect was in this case unusually large ;

Fig. 5.

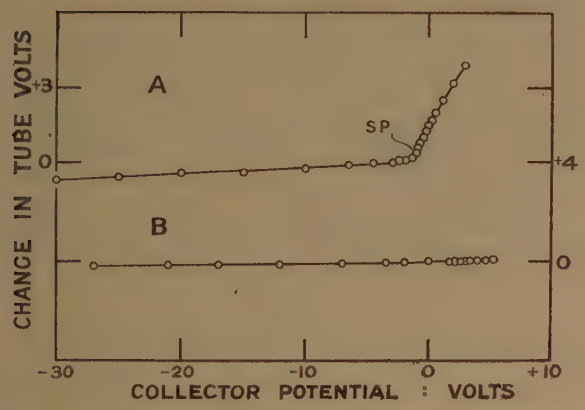

Variation in tube voltage caused by altering probe potential relative to the anode. Only a selection of experimental points are given, and readings retraced decreasing the probe potential are omitted, since they were indistinguishable from points marked. A–Pt III, conditions of Table VII. B–Pt I (runs 157–158). Pressure 0·13 mm. Tube volts 425. Current density $7{\cdot}3\ 10^{-6}$ amp./cm.^{2}. Probe in negative glow 3·3 cm. from cathode. The upper l.h. voltage scale is for A, the lower r.h. scale for B.

Table VII.

The Effect of the Tube Voltage Corrections, the Collector Potential being referred to the Anode.

Runs 121–122, pressure 0·12 mm. Hg. Tube volts 470, current density $2{\cdot}89 \times 10^{-6}$ amp./cm.^{2}. Probe in the negative glow 4·5 cm. from the cathode. Probe, Pt. III.

A. Data for the original runs.

B. The readings corrected for the change in the tube volts.

	Space potential relative to anode (volts).	Fast group.		Medium group.		Slow group.	
		Temp. (volts).	Conc. (10^7/cm.^{3}).	Temp. (volts).	Conc. (10^7/cm.^{3}).	Temp. (volts).	Conc. (10^7/cm.^{3}).
A ..	−12·1	15·5	0·3	2·74	1·1	0·11	9·3
B ..	−12·0	17·8	0·3	1·97	1·4	0·12	4·4

in the other cases investigated it was much less and usually negligible. In all the work with the electrometer in the circuit the measurements were retraced in the reverse order, to make certain that any steady decrease of the tube current or other long period change was not giving rise to spurious results.

It was also found that no essential change was produced when the potential of the probe was varied with respect to the cathode instead of, as usually, with respect to the anode. An example of this with the tube voltage correction applied is given in Table VIII.

Fig. 6.

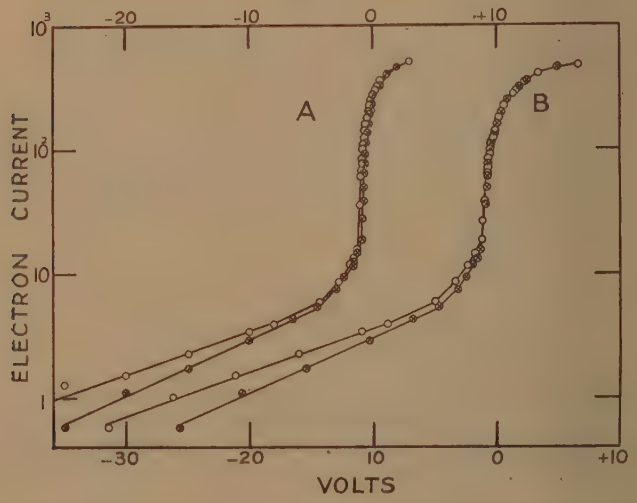

A. Semilogarithmic curve for a probe. B. Same data replotted when the change in tube potential consequent on change in probe potential is taken into account (this corresponds to fig. 5, A). ⊕. Readings obtained varying probe potential from negative to positive relative to the anode. o. Readings obtained for potential changes retraced in opposite sense. Discharge conditions identical with those of Table VIII. The voltage scale along the top is for A, along the bottom for B. In each case there was a biassing potential of −14 volts relative to the anode on the probe. Electron currents in arbitrary units, the same for A and B.

The correction for change in voltage was also studied for a series of runs in helium similar to those described by Emeléus, Brown, and Cowan [15], using probes both

identical with theirs and smaller. Conditions of tables ii. and iii. of their work were reproduced, and measurements similar to the above were taken. Our results agreed extremely well with those given in their paper, thus strengthening our faith in the possibility of at least reproducing the results obtained by probes. It was found that the effect of the electrometer correction on the original results of Emeléus, Brown, and Cowan could

TABLE VIII.

The Effect of Variations in the Tube Voltage, the Collector Potential being referred to the Cathode.

Run 163, pressure 0·13 mm. Hg. Tube volts 460, current density $3{\cdot}15 \times 10^{-6}$ amp./cm.^{2}. Probe in the negative glow 4·5 cm. from the cathode. Probe, Pt II.

A. Data for the original measurements.

B. The data corrected for changes in the tube voltage.

	Space potential relative to cathode (volts).	Fast group.		Medium group.		Slow group.	
		Temp. (volts).	Conc. (10^7/cm.^{3}).	Temp. (volts).	Conc. (10^7/cm.^{3}).	Temp. (volts).	Conc. (10^7/cm.^{3}).
A ..	+434·5	21·7	0·5	1·55	2·6	0·3	8·0
B ..	+434·2	21·4	0·5	1·87	1·3	0·2	10·0

be neglected. In iodine also we found the effect to be completely negligible [22].

E. The directed motion of the electrons in the glow discharge has already been investigated, using disk collectors [18]. The conclusion reached was that it is unimportant for the interpretation of probe characteristics for the plasma regions of the discharge.

Summarizing the foregoing work it appears that the results obtained by the use of probes can with some confidence be regarded as characteristic of the undisturbed discharge. We are fairly certain that the essential conclusions drawn from the measurements taken do not depend on

(*a*) the diameter, length, shape, or material of the probe ;

(*b*) any effect of the probe stump or leaks to the internal leads :

(*c*) the effect of the potential of the walls of the glass sheath ;

(*d*) any change in tube potential caused by altering the collector potential.

It must nevertheless be remembered that with such a complex system as the glow discharge it is difficult to be sure that all sources of uncertainty have been investigated, and it is just possible that some important effect has been overlooked. The data given in Table V. in addition emphasize that if any attempt is to be made to obtain accurate comparative measurements for the discharge under different conditions it is advisable to keep to one particular probe.

4. *Druyvesteyn Analysis.*

Hitherto we have employed the method of analysing the electrons into Maxwellian groups, and it has been seen that under certain conditions three groups of electrons with temperatures of the order 20 volts, 2 volts, and 0·1 volt appear to coexist in the discharge. In many ways Druyvesteyn's alternative method for analysing the data and representing the results is to be preferred, in which the approximation is not made initially of supposing that the distribution is capable of representation in any such simple way. In his method the Langmuir analysis is stopped before the last step, and the electron energy distribution in the plasma calculates from the relation [23]

$$N(V)=\frac{1}{A}\left(\frac{8mV}{e^3}\right)^{1/2}\frac{d^2i}{dV^2}.$$

$V\,dV$ is the concentration of electrons in the plasma with energies between V and $V+dV$ e-volts, V is the potential of the probe negative to the surrounding plasma, i the current to the probe at potential $-V$, and A its area.

We have analysed a large number of characteristic curves in this way. A typical energy distribution curve is given in fig. 7 corresponding to the semi-log plot of fig. 4. The points marked with circles are derived from the actual experimental values, whilst the curve marked

M is a Maxwellian curve that has been fitted to the low-energy part of the curve. It is seen that for the first few tenths of a volt agreement is good. For higher values of V, N(V), shown on two increased scales on the right of the diagram is above the Maxwellian curve M. N(V) can then be represented approximately by two portions of additional Maxwellian curves (not drawn). We find that the number of mean energies and concentrations of the groups revealed by the Druyvesteyn analysis agree quite well with the data obtained from the Langmuir analysis, and in the subsequent discussion we

Fig. 7.

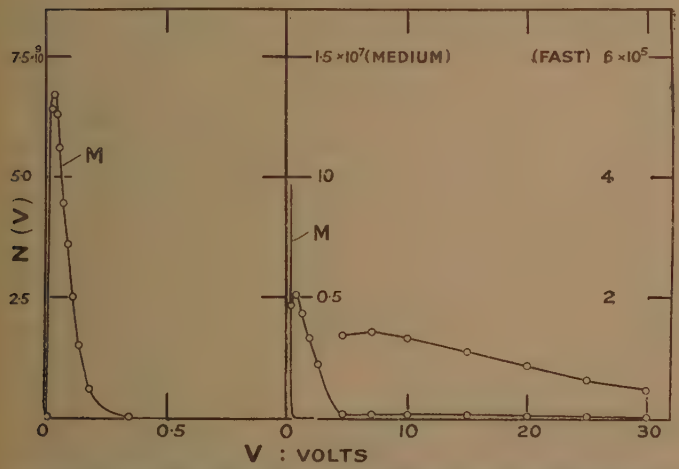

Electron energy distribution N (V) compared with the Maxwellian distribution M. The l.h. part gives N (V) for the slowest electrons; the circles, from experimental data, are close to the theoretical curve M. The r.h. side shows M continued on a smaller voltage scale. The experimental points now lie above it and are equivalent roughly to two groups, a medium fast one (central scale for N (V)) and a still faster one (r.h. scale for N (V)). The discharge conditions are identical with those of fig. 4.

shall use the results obtained by the latter method on account of the ease with which they can be given in collected form. Considered in more detail the N(V) curves obtained by the Druyvesteyn method have interesting features which will be dealt with in a subsequent paper.

5. *Summary of Results for Oxygen.*

The large number of probe characteristic curves which have been analysed were obtained under widely varying discharge conditions, and from them there can be sorted out sets of data corresponding to progressive changes of position, pressure, current, and cathode fall.

It is desirable before giving typical data of this nature to consider a little more fully some of the log i *vs* V curve for electrons which cannot be analysed. In the diffuse discharge at 0·025 mm. pressure with a current density

Fig. 8.

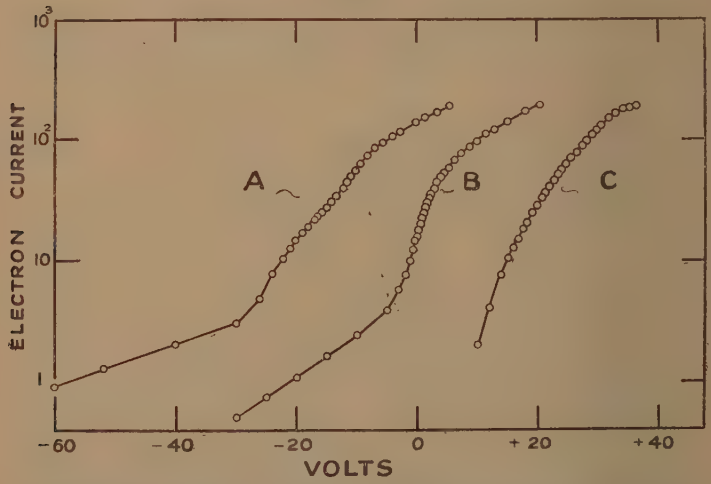

Semilogarithmic curves. Voltages on the same scale for A, B, and C, but zero applicable to B only. A. Transition type (run 51). Pressure 0·09 mm. Current density 1·3 10^{-5} amp./cm.^{2}. Tube volts 490. Probe, Pt I in middle of negative glow "cushion," 7·6 cm. from cathode. B (run 112). A curve showing two groups of electrons. Pressure 0·09 mm. Current density 3·1 10^{-5} amp./cm.^{2}. Tube volts 600. Probe Pt III in Faraday dark space, 13·9 cm. from cathode. C (run 169). High pressure type. Pressure 0·9 mm. Current density 1·6 10^{-4} amp./cm.^{2}. Tube volts 400. Probe Pt II in negative glow 1·4 cm. from the cathode.

of $0{\cdot}6 \times 10^{-6}$ amp./cm.^{2} they are of this class. Fig. 9, B, shows a curve obtained with the probe 12·8 cm. from the cathode. In spite of the position it is similar in type to a curve obtained in the cathode dark space, fig. 9, C, pressure 0·05 mm. Only on increasing the pressure to

about 0·05 mm. does the curve become more nearly normal and give the more regular semi-log plot shown in fig. 8, A. One does not yet feel happy, however, in interpreting this in the usual manner, and although electron data can be deduced from it it seems nevertheless better to regard it as a transitive form between the very low pressure type of curve and the orthodox log i *vs* V curve, fig. 8, B.

Again, at the highest pressures used, above a little less than 1 mm. Hg., the log i *vs* V curves cannot be analysed,

Fig. 9.

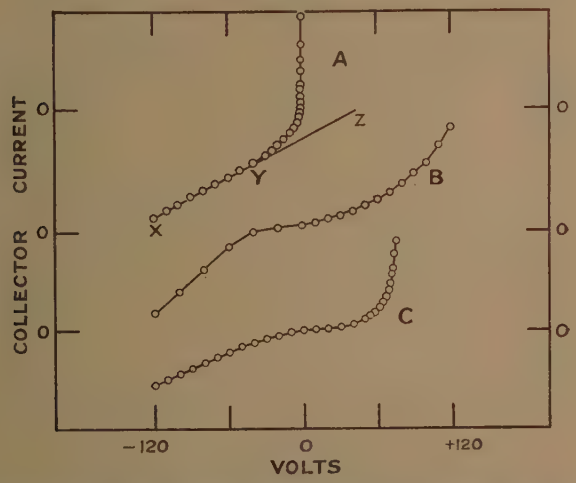

Current voltage probe characteristic curves. A. Normal type corresponding to the discharge conditions of Table II. B. Low pressure type (run 65). Pressure 0·03 mm. Tube volts 600. Current density 6 10^{-7} amp./cm.^{2}. Probe Mo I 12·8 cm. from the cathode in the Faraday dark space as well as could be judged visually. C. Cathode dark space type (run 22). Pressure 0·05 mm. Current density 6·7 . 10^{-6} amp./cm.^{2}. Tube volts 500. Probe Pt I 5·5 cm. from the cathode. The three zeros apply from above downwards to A, B, and C respectively. A current represented by a point above zero represents a net flow of negative electricity from gas to probe. Potentials are relative to the anode.

as they rise uniformly, giving no indication of either electron groups or the space potential (fig. 8, C).

The application of the probe method of analysis is thus limited in this gas and type of discharge to a pressure

range from 0·06 mm. to a little less than 1 mm., with an ill-defined lower limiting current.

(1) *Variation of Discharge Conditions along the Tube.*

With a discharge of the type described in 1 at 0·09 mm. and with 565 volts between the electrodes, starting just to the cathode side of the negative glow edge, the characteristic curve C, fig. 8, is obtained. It is not until the probe is to the anode side of the sharp boundary of the negative glow that the normal type of characteristic curve

Fig. 10.

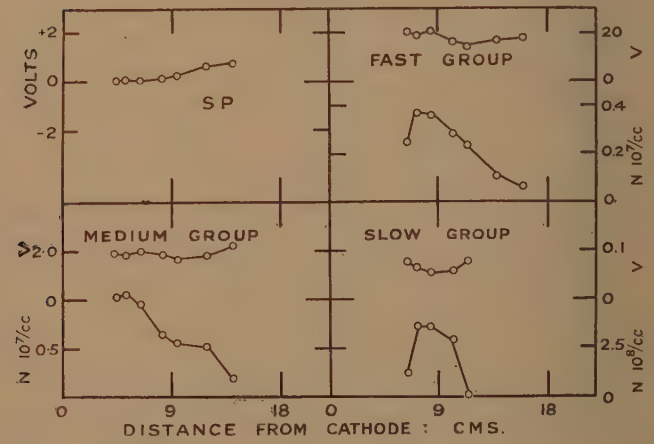

Distribution of space potential relative to the anode (SP), electron concentration (N), and mean electron energy in *e*-volts (V) for various groups along a discharge-tube. Pressure 0·09 mm. Tube volts 565. Probe Pt III. The upper l.h. curve is for SP. In each other rectangle the upper curve is for V, the lower for N for the group there referred to. The scale of distances from the cathode is the same in each case.

appears [24]. Data obtained from the latter type and given in fig. 10 show that the discharge from the negative glow up to the anode is practically an equipotential. The electron temperatures do not vary markedly along the discharge-tube. The electron concentrations have a maximum somewhere in the middle of the green cushion of light forming the negative glow [25], and then fall off rapidly towards the anode, especially the 0·1 volt group,

which cannot be detected when 12·0 cm. from the cathode ; the semi-log curve then obtained is shown in fig. 8, B. For the two points nearest the cathode (fig. 10) the cathode fall in potential in the discharge was 565 volts, for the remainder 600 volts. The tube currents for the points, passing from left to right, were 6·4, 6·1, 6·2, 5·0, 4·3, 3·6, and 3·0 microamperes/cm.^{2}. This alteration in cathode fall—the data for the 600 volt fall were obtained on a different day from those for the 565 volt fall—is without effect on the general features of the results. The change in current has another origin. When the probe was moved back from the neighbourhood of the anode to a point in or near the negative glow the tube current again rose in this and several other instances to within about 1 per cent. of the value it had initially with the probe there. Since change in probe potential with the probe in a definite position produced practically no change in tube current the change in tube current with the position of the probe must be due mainly to disturbance of the discharge by that part of the insulating stem of the probe which projects into the discharge. This is inevitable if the current collecting part of the probe is to be near the axis of the discharge-tube. It is probably due to effective reduction of the conducting cross-section of the tube being greater with the larger sheath which forms on the stem when the random current is small, as it is near the anode, than it is where the random current is larger nearer the cathode. Less alteration in tube current would probably be secured by having a row of probes fixed in the discharge and using each in turn, but the discharge which would then be analysed would not be one in a simple cylindrical tube but in a cylindrical tube with the row of insulating stems projecting into it.

The fact that there is a region in the middle of the negative glow where the electron data do not vary greatly for some 2 cm. enables us, by keeping the probe in this part of the discharge to compare data for the negative glow for different pressures and currents conveniently.

(2) *Variation of the Discharge Conditions with Currents.*

Keeping the probe 1 cm. to the anode side of the negative glow edge at constant pressure, and gradually increasing the tube current, fig. 2 shows how the conditions in the

negative glow vary in a typical case. The change in potential difference between the negative glow and the anode is due to the anode glow disappearing with increase of current.

At first the whole discharge is very diffuse, and an unanalysable curve like fig. 8, A, is obtained. A small increase in the current changes this over to the true Langmuir type showing two groups of electrons (fig. 8, B). On further increase of the current the concentration of the electrons increases, especially that of the 2 volt group, then later the 0·1 volt group appears and the concentra-

Fig. 11.

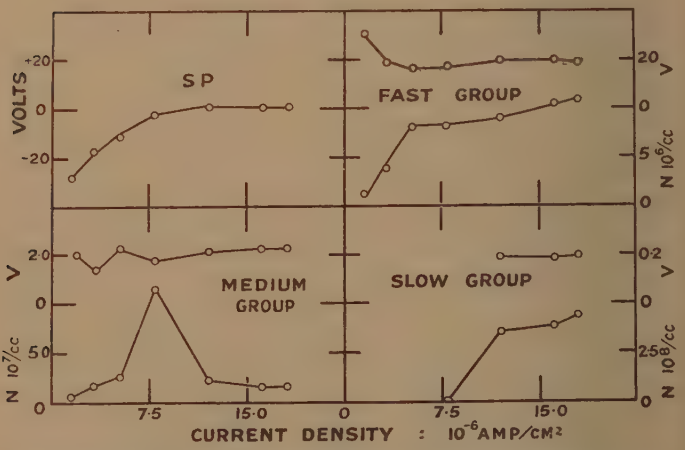

Variation in SP, N, and V (see fig. 10) with change in current density. Pressure 0·09 mm. Probe Mo I, kept in the negative glow about 1 cm. from the cathode dark space. The general features of these results are reproducible, in particular the pronounced maximum in N for the medium speed group just before the slow group appears when the current is being increased.

tion of the 2 volt electrons falls to nearly its former value. Further increase of the tube current beyond that shown in fig. 11 causes the concentration of all three groups to increase. The appearance of the slow group of electrons coincides with the first appearance of the sharp edge at the cathode side of the negative glow. The cathode fall in potential increased with current from about 550 volts to rather over 600 volts, and the probe

was moved in as the current was increased from a distance of 7·6 cm. to 5·3 cm. from the cathode. These measurements were all taken on the rising part of the i *vs* V tube characteristic curve (AB, fig. 3). It was not found possible to keep the discharge lit continuously for long enough to take probe measurements on the corona part of the tube characteristic. The number of groups of electrons obtained with various currents passing is marked in fig. 3.

(3) *Variation of Discharge Conditions with Increase in Pressure.*

As already mentioned (p. 678) in the faint discharge at 0·025 mm. a probe curve of the cathode dark space type is obtained all along the tube. Hence it is likely that the whole region is then similar to the cathode dark space—that is, a region of positive space-charge and not a true plasma. Geddes reached a similar conclusion for a high voltage glow discharge through air under not dissimilar circumstances [26]. On increasing the pressure to 0·06 mm. with the probe 7 cm. from the cathode a log i *vs* V curve of the transition type (fig. 8, A) is obtained, and above 0·06 mm. up to 0·80 mm. good semi-log plots with either two or three groups, according to the current passing.

Fig. 12 shows the results obtained with the probe in the same position relative to the negative glow as in § 5 (2), when the pressure was varied and the cathode fall raised just sufficiently above the normal for three groups of electrons to appear. The increase in p.d. between the anode and negative glow with increase in pressure is due to development of a positive column. The cathode falls in potential for the various points passing from left to right on the graphs were 500–600, 425, 386, 361, 357, 354, and 354 volts respectively, and the corresponding tube current densities, in microamperes/cm.^{2}, 10·4, 5·4, 4·7, 11·6, 26·5, 48·2, and 104. The first cathode fall was not recorded accurately. The distances of the probe from the cathode (pressure increasing) were 4·7, 4·0, 3·3, 3·1, 1·9, 1·4, and 1·4 cm. respectively. It is satisfactory to note the agreement between the above results at 0·60 mm. and those obtained by Carmichael [27].

Finally, above 1·00 mm. a curve of the type of fig. 8, C, is obtained. This type of characteristic was found to be

independent of all the factors already considered, such as the size and material of the probe, guard-rings, and electrometer corrections, potential between anode and cathode, and position of the probe between negative glow and anode.

It is thus seen that in oxygen :

(*a*) Below 0·03 mm. the Langmuir analysis is not applicable.

(*b*) From 0·06–0·80 mm. it is applicable provided the probe is not situated in the C.D.S., and perhaps provided the discharge is not of the corona type.

Fig. 12.

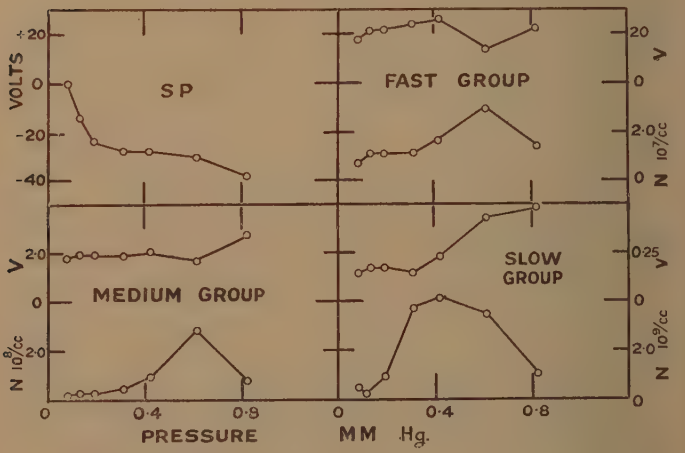

Variation of conditions with pressure. Probe Pt III. Further details in text.

(*c*) From 0·80 mm. upwards it breaks down.

(*d*) From the Langmuir analysis it is found that between 0·05 and 0·80 mm. pressure either two or three groups of electrons are present in the negative glow depending on the excess of the voltage above the normal cathode fall, and to some extent on position in the discharge.

The spectrum of the negative end of the discharge has also been investigated, particular attention being paid to

the variation in intensity at the sharp cathode dark space negative glow edge. The results of this part of the work and the bearing of our data on the plasma theory of the discharge will be discussed later.

Summary.

Results of an extensive series of probe measurements in negative sections of the cold-cathode glow discharge in oxygen are described. Tests have been carried out to investigate the importance of possible sources of error. A range of conditions under which probes can be used has been found. Typical data are given for electron energy distributions and concentrations, and for the potential in the discharge.

Appendix (Description of Plate).

In each case the cathode is on the left, the anode not visible, and the main light that of the negative glow. The white arrow in V shows the position of the sharp edge between the negative glow plasma and the cathode dark space; the edge was barely visible in this case. The relative intensities in the photographs are not those of the actual discharges. The probes and part of their insulating sheaths can be seen. The numbers at the r.h.s. are the current densities in microamperes/cm.^{2}.

References.

(1) Langmuir, Journ. Franklin Inst. cxcvi. p. 751 (1923); extensive studies of the mercury arc have been made later by Langmuir and Mott-Smith and Killian.
(2) Bramley, Phys. Rev. xxvi. p. 794 (1925).
(3) Childs, Phil. Mag. ix. p. 529 (1930).
(4) Trevelyan, Phil. Mag. iv. p. 64 (1927).
(5) Rusk, Phil. Mag. x. p. 244 (1930).
(6) *Cf.* Seeliger, 'Physik d. Gasentladungen,' ii. (Leipzig, 1934).
(7) K. G. Emeléus and F. M. Emeléus, Phil. Mag. viii. p. 383 (1929).
(8) Emeléus, Proc. Nat. Acad. Sci. U.S.A. xx. p. 115 (1934).
(9) Emeléus and Gregg, Phil. Mag. xvi. p. 1079 (1933).
(10) J. Taylor, 'Dissertation,' Utrecht (1927).
(11) Emeléus and Beck, Phil. Mag. xi. p. 54 (1931).
(12) Güntherschulze, *Zeits. f. Phys.* xxxiv. p. 549 (1925).
(13) Scott, Thesis, Belfast (1931).
(14) von Hippel, *Ann. d. Phys.* lxxx. p. 672 (1926).
(15) Emeléus, Brown, and Cowan, Phil. Mag. xvii. p. 146 (1934).
(16) Professor Emeléus informs us that similar effects were noticed in the work of Trevelyan, ref. (4).
(17) Phys. Rev. xxxiv. p. 876 (1929).

(18) Emeléus and Brown, Phil. Mag. vii. p. 17 (1929).
(19) Emeléus and Sloane, Phys. Rev. xliv. p. 333 (1933).
(20) Wehrli, *Helv. Phys. Acta*, iii. p. 180 (1930).
(21) Pike (Dissertation, Princeton, 1934) uses a similar circuit.
(22) Spencer-Smith, Phil. Mag. xix. p. 806 (1935).
(23) A simple transformation of the fromula given by Druyvesteyn, *Zeits f. Phys.* lxiv. p. 781 (1930).
(24) Carmichael obtained the same result; Phil. Mag. viii. p. 909 (1929).
(25) Emeléus and Sloane, Phil. Mag. xiv. p. 355 (1932).
(26) Geddes, Proc. Roy. Soc. Edinburgh, xlvi. p. 136 (1926).
(27) Carmichael, Phil. Mag. viii. p. 362 (1929).

LIII. *Studies on the Oxidation of Metals.*—Part III. *The Kinetics of the Oxidation of Molten Tin.* By L. L. Bircumshaw, *M.A.*, *D.Sc.*, *and* G. D. Preston, *M.A.** (*From the National Physical Laboratory.*)

[Plate XI.]

A CERTAIN amount of work has been recorded on the oxidation of solid metals (chiefly copper), and some very interesting results have been obtained. Pilling and Bedworth [1], from a study of the kinetics of the oxidation, divided metals into two classes according as the oxide occupies a greater or less volume than the metal from which it is formed. In the first case the oxide will protect the underlying unoxidized metal from attack, but in the second case, owing to the porous nature of the oxide, this protective action will not be exerted. It is extremely likely that as soon as a complete layer of oxide is formed the chief factor controlling the rate of oxidation will be the diffusion of oxygen through the oxide. Pilling and Bedworth assumed that the rate of diffusion is inversely proportional to the thickness of the oxide layer, when

$$\frac{dx}{dt} = \frac{k}{x}, \quad . \quad . \quad . \quad . \quad . \quad . \quad . \quad . \quad (1)$$

which on integration gives

$$x^2 = kt, \quad . \quad . \quad . \quad . \quad . \quad . \quad . \quad . \quad (2)$$

where x is the weight of oxide formed in the time t.

* Communicated by C. H. Desch, D.Sc., Ph.D., F.R.S., F.I.C.

This equation was found to describe the rate of oxidation of the first group with fair accuracy.

Later Dunn [2] has found that, although this expression governs the low temperature (200° C.–300° C.) oxidation of commercial copper over short ranges of time, the behaviour of copper, activated by oxidation and reduction, could not be expressed by (2) even over the shortest time.

Feitknetch [3] has studied the high temperature oxidation (830° C., 950° C., and 1020° C.) of copper and found that the constant k decreased to a constant value. He considered that this decrease was due to a sintering which rendered the oxide more impermeable to diffusing oxygen, but Wilkins has shown that Feitknetch's results obey the parabolic law in a more general form

$$x^2 = kt + c. \quad . \quad . \quad . \quad . \quad . \quad . \quad (3)$$

More recently the oxidation of copper has been examined by Wilkins and Rideal [4] and by Wilkins [5], who have suggested that the oxidation of copper is the resultant of three consecutive processes and that its velocity depends upon (*a*) the rate of condensation of oxygen at the oxide-oxygen interface; (*b*) the rate of removal of oxygen from the oxide-oxygen interface into the body of the oxide; and (*c*) the rate of diffusion of oxygen through the oxide. They consider that the initial oxidation at low pressures is governed by (*a*), and the equation describing the rate of oxidation is therefore

$$\log_e \frac{p_0}{p} = kt, \quad . \quad . \quad . \quad . \quad . \quad . \quad (4)$$

where p_0 is the initial pressure of oxygen and p the pressure at time t, but this equation does not hold for the oxidation of active copper at high pressures or inactive copper at low pressures.

With the exception of some observations of Delavault [6] the kinetics of the oxidation of molten metals does not appear to have been studied at all, and the present communication deals with measurements of the rate of oxidation of tin at temperatures from 400° C. to 800° C.

The apparatus used was extremely simple. It consisted of a silica tube (3 cm. wide and 35 cm. long) drawn out at one end to a narrow tube fitted with a tap.

On the open end is a water-cooled brass collar into which fits a glass plate perforated through the centre with a short piece of capillary tubing, which serves as an inlet to the main tube. The capillary connects the latter (through a trap immersed in CO_2 snow) to a capillary manometer and the pumps—a Hyvac oil pump and a butyl phthalate pump were used—and an oxygen reservoir. The main tube fits into an ordinary nichrome wound furnace, contains a silica plug to take up the dead space and at the end of the tube, adjusted to fall in the middle of the furnace, is placed the boat containing the tin. The boats were made of pure alumina, fired at 1940° C., and were 7 cm. long, 1 cm. internal distance between the walls, and 0·9 cm. deep. A thermocouple is placed between the experimental tube and the furnace tube in a position just underneath the boat. The boats were made in a mould and were carefully measured, any not of the correct size being discarded. By placing a constant weight of metal in the boat the same surface of metal was obtained in consecutive experiments. Some trouble was experienced in the preparation of the metal specimens. The first method was to cast the metal in a boat and then scrape the surface free from oxide with a razor blade. It was found, however, that after heating *in vacuo* or argon a few spots of, presumably, oxide were sometimes present on the metal. The procedure ultimately adopted was as follows :—The metal was first melted and cast. In this condition it was covered with a fine film of oxide and showed interference colours. It was then filed down to the correct weight and heated in a current of pure hydrogen for one hour at 700° C. The specimen was then placed in the apparatus, the latter evacuated, and pure argon admitted to a pressure of 20 cm. mercury. The furnace current was then switched on, and on steadying up at the required temperature the argon was rapidly evacuated, oxygen admitted, and the rate of fall of pressure measured. The attainment of the required temperature was effected in argon, as some preliminary experiments showed that tin heated to 650° C. for an hour never failed to give a heavy mirror of metal in the cold part of the tube, and analysis showed this to be largely tin.

The oxygen was prepared by heating dry potassium permanganate in an auxiliary apparatus, which could be

evacuated, attached to the main apparatus. It was found to contain very small traces of CO_2, and was therefore passed over a little soda-asbestos and then through a long tube of phosphorus pentoxide.

The apparatus was tested for leaks and the absorption of traces of oxygen by the boat by filling up to a known pressure with oxygen and noting the fall with time. Two typical experiments are given below :—

At 700° C. :—

Initial pressure of gas at	2.19 P.M.	64·50 cm.
„ „ „	3.19 „	64·50 „

At 600° C. :—

Initial pressure of gas at	3.40 P.M.	40·70 cm.
„ „ „	3.46 „	40·60 „
„ „ „	4.46 „	40·60 „

Observations were commenced at a temperature of 600° C., and a large number of experiments were made. On plotting pressure of oxygen against time for various runs, it was found that although the graphs obtained were quite smooth, very wide differences of rate were exhibited in different experiments. Fig. 1 shows the results obtained for four such similar runs. It is a well-known fact that certain metals, *e. g.*, copper, if oxidized, and then reduced at a fairly low temperature, show a faster rate of absorption of oxygen on a second oxidation and still faster on a third oxidation, the rate ultimately becoming constant. Fig. 2 shows the results obtained on oxidizing tin at 600° C., reducing with carefully purified hydrogen until no trace of water could be detected in the cooled narrow tube beyond the furnace, and re-oxidizing. It will be seen that after each reduction the rate of oxidation is increased. In a similar experiment the film of oxide (SnO_2) weighed 0·945 grammes. This was reduced with purified hydrogen, the water weighed in P_2O_5 tubes, when it was found that only 95 per cent. of the oxide was reduced. To this fact, that oxidation always took place with unreduced oxide present, is attributed the above extraordinary result.

At 400° C. the rate of oxidation was found to be extremely slow, but at 500° C. it was more measurable. Fig. 3

shows the results of three experiments on initial oxidation followed by reduction, then oxidation again, and so on. After a small initial rapid fall the absorption of gas is practically linear with time, *i. e.*, the rate is constant. At this temperature, too, the results could be duplicated with fair accuracy. In one of the reductions both the

Fig. 1.

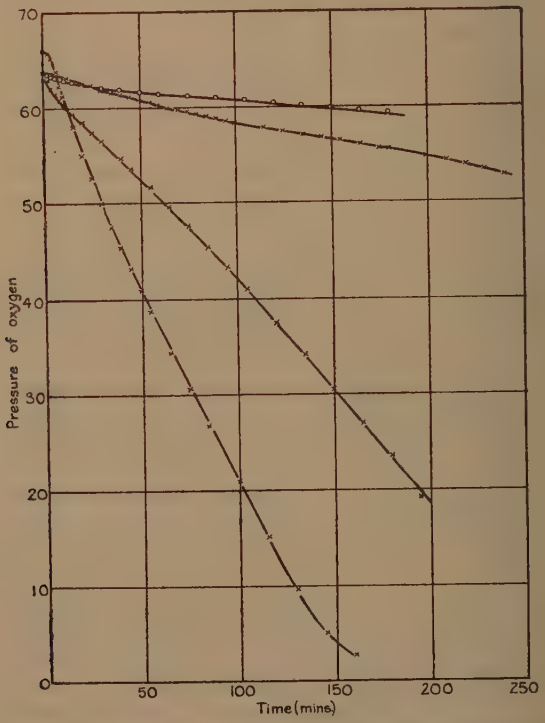

Absorption of oxygen by tin at 600° C. Illustrating the different rates observed under apparently identical conditions.

oxide and the water formed on its reduction were weighed, and it was found that the former was completely reduced. This may be due, however, to the relative thinness of the film, which in this case only weighed 0·0060 grammes. At 700° C. there is a considerable increase in the rate

(fig. 4), and here again very wide differences are observed in the rate.

Fig. 2.

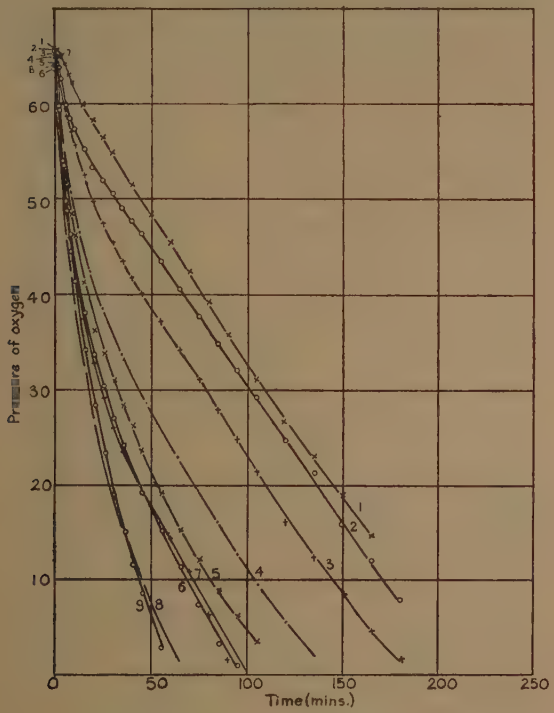

Absorption of oxygen by tin at 600° C.
The oxide film was reduced by hydrogen after each oxidation.

Fig. 3.

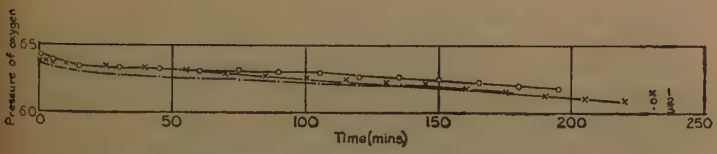

Absorption of oxygen by tin at 500° C.
The oxide film was reduced after each oxidation.

Numerous experiments were made to track down the cause of these large differences. It was thought that slight variations in the dryness of the oxygen might be a factor concerned. The burette from which the apparatus was filled was capable of holding sufficient gas for at least two runs, and considerable differences were found in two consecutive experiments from the

Fig. 4.

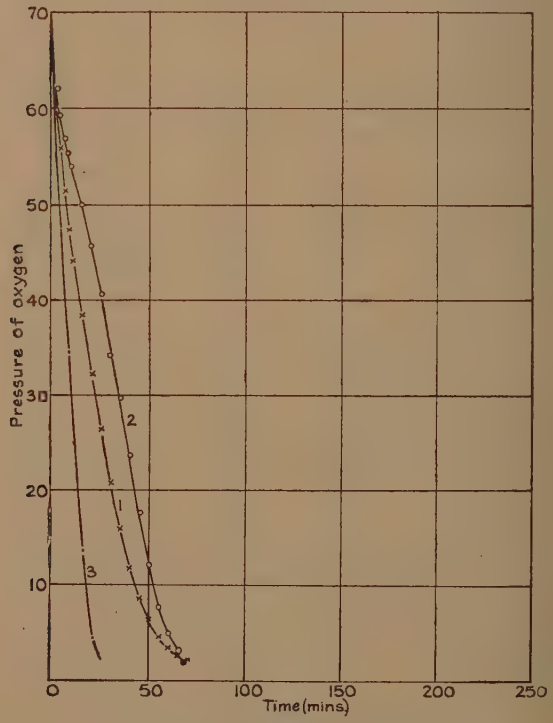

Absorption of oxygen by tin at 700° C.

same burette of gas, from which it was concluded that variations in dryness were not the cause. It was suspected that perhaps the physical state of the very thin initially formed film of oxide might be a determining factor in the observed rate. Some experiments were made in which a thin film of oxide was produced on the metal

by the action of the gas at a relatively low initial pressure, the residual gas was pumped off, oxygen introduced at a pressure of 65 cm., and the rate re-measured. Results of two such experiments are shown graphically in fig. 5.

Fig. 5.

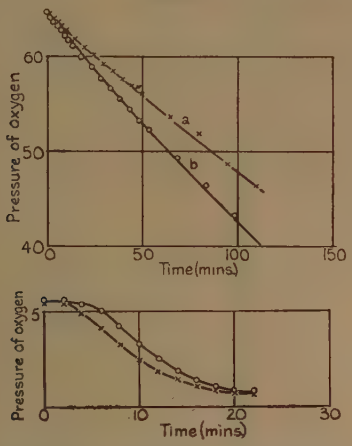

Absorption of oxygen by tin after initial oxidation at a pressure of 5 cm. of mercury.

Fig. 6.

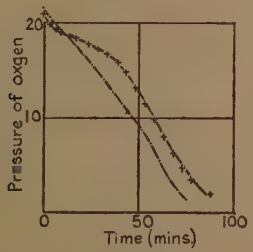

Absorption of oxygen by tin at 600° C.
Time of admission of gas 30 seconds in each case.

There are still considerable differences in the rate. It will also be noticed that the graphs at the low pressure (5 cm.) show a marked period of induction.

The question of the time taken to admit the gas to the apparatus was also investigated. This could be done in ten seconds, but usually it was added more slowly—about thirty seconds. Fig. 6 shows the results of two

experiments with tin at 600° C., the time of entry of the gas being carefully adjusted to thirty seconds. It will be seen, however, that considerable differences are shown in the initial rate.

It was noticed that the oxide produced in various experiments differed considerably in appearance, both

Fig. 7.

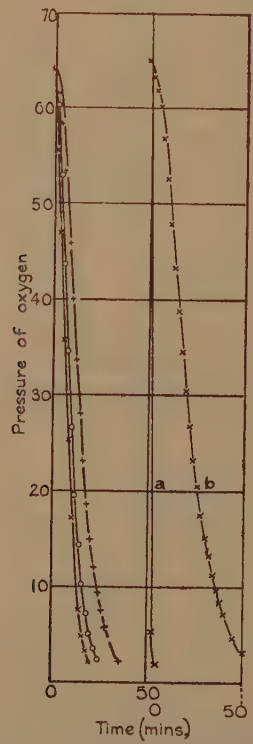

Absorption of oxygen by tin at 800° C.
(*a*) a bulky corrugated film, (*b*) a smooth compact film.

in colour and texture. In colour it varied from almost white through pale yellow to grey. In texture it varied from smooth and compact to heavily corrugated and bulky.

At 800° C. the rate was relatively very fast and again considerable differences were observed. Some of these results are plotted in fig. 7, and the differences were most

marked in *a* and *b*, the absorption of gas in the case *a* being complete in four minutes. A very marked difference was observed in the appearance of the two oxides, *b* which gave the much slower rate being very smooth, hard, and compact. These two oxides were examined by X-ray diffraction, and the photographs are shown in fig. 8, *a* and *b* respectively. *b* shows marked evidence of preferred orientation, the (001) plane of the tetragonal cell of SnO_2 being nearly parallel to the surface of the metal. The other specimen shows only random orientation. This suggests an obvious explanation for the many very variable results obtained. If we make the assumption that the influence on the rate of oxidation of the orientation of the crystals in the oxide film is much greater than the influence of the progressive increase of the thickness of the film as an experiment proceeds, then the many divergent results obtained may be explained by postulating different degrees of preferred orientation of the crystals of the oxide film. That the progressive increase in the thickness of the film during an experiment has very little influence in the present case is shown by the approximate linearity of many of the curves obtained over comparatively large ranges of pressure (fig. 1). Those pressure/time curves, which in part might represent parabolæ, do so only over the middle pressure range. If the square of the oxygen absorbed is plotted against time for the curves, fig. 4 (curve 1) and fig. 7 (curve *b*), a fair straight line is obtained lying between the pressure values 45 and 10 cm. The initial and final stages, however, are a long way removed from a straight line. For solid copper it has been shown by a number of workers that there is a particular pressure below which the parabolic law is not obeyed, so the deviation from the parabolic law in this case (tin) may be due to the same cause at low pressures. However, even at the initial pressures the parabolic law is obviously not obeyed.

In order to see exactly what happens to the surface of the metal when oxygen is admitted at various pressures, a number of experiments were made in a clear silica tube heated at the end by a carefully regulated Meker burner. Although these experiments could, of course, only be regarded as roughly quantitative, it was found that by keeping the temperature of the room constant, temperature conditions along the tube could be reproduced

very well. Again, a large number of experiments were made, but only one or two typical ones will be described.

A clear silica tube (volume 200 c.c.) with a water-cooled end was connected with a graduated gas burette, pumps, etc. The metal was placed in an alumina boat alongside which, in a silica sheath, was a thermocouple. Small quantities of gas were admitted and the appearance of the metal noted. Below is a typical experiment (temperature 650° C.).

Time.	Total gas (c.c.).	
3.14	0·25	Faint tarnish.
	0·6	Surface flattens immediately. Yellow-brown film rapidly turning black.
3.19		Surface almost clear again.
3.20		Whole metal surface quite clear.
3.27	1·05	Uniform silvery grey coating.
3.35		Surface quite clear again.
3.41	1·55	Uniform silvery grey coating.
3.48		Surface quite clear again.
3.48	1·95	Light brown patches.
4.5		Clear again.
4.5	2.90	Uniform silvery grey coating.
4.35		Surface quite clear again.
4.35	3·05	Light brown patches.
4.47		Light brown patches.

The most remarkable observation is the extraordinary manner in which the film formed after the addition of the initial small quantities of oxygen seems to disappear. This may be due to solution in the metal, but an equally likely cause is the dragging of the film to the edge of the metal surface. The latter effect could not be observed, but nevertheless it could presumably have occurred.

Other experiments were made with a manometer attached to the tube. Measurements were made with initial pressures of oxygen of 5, 10, 20, 40, and 60 cm. The same discrepancies between duplicate experiments were again observed. The films nearly always went through the same colour sequence : silvery grey, black, black, pale yellow. It was noticed that, in general, the higher the initial pressure of gas the more rapidly did the final pale yellow stage appear.

One experiment with an unusual result is worth recording. The temperature was 800° C. and the initial pressure of the gas 10 cm. The gas was rapidly added (5 seconds) when the surface of the metal was immediately

covered with a thick jet black film (probably SnO), which in a few seconds became incandescent at one end, the incandescence rapidly travelling to the other end of the boat, leaving an orange coating. In two minutes the colour changed to pale yellow and the whole of the oxygen was absorbed.

Summary.

Measurements have been made of the rate of oxidation of molten tin at various temperatures, and a number of initial pressures of oxygen. The rate rises rapidly in the temperature range 400° C.–800° C. At any particular temperature the rate was found to vary greatly from one (similar) specimen to another. The parabolic law observed by a number of workers for the oxidation of solid metals does not seem to be obeyed for molten tin, especially at low and high pressures of oxygen. It therefore appears that the rate of oxidation is controlled by some factor other than the progressive increase in the film thickness. In the present paper it is suggested that the orientation of the crystals composing the oxide film is a determining condition in the rate of oxidation of the metal.

We should like to thank Dr. C. H. Desch, F.R.S., for his great interest in this work. To Mr. J. Trotter we are indebted for assistance in the experimental portion.

References.

(1) Journ. Inst. Metals, xxix. p. 529 (1923).
(2) Proc. Roy. Soc. cxi. p. 210 (1926).
(3) *Zeit. f. Electrochemie*, xxxv. p. 142 (1929).
(4) Proc. Roy. Soc. cxxviii. p. 394 (1930).
(5) Proc. Roy. Soc. cxxviii. p. 407 (1930).
(6) Bull. Soc. Chim. v. 1, p. 419 (1934).

September, 1935.

LIV. *Derivation of Legendre Function Formulæ from Bessel Function Formulæ.* *By* T. M. MacRobert *.

IN a former paper (Proc. Edin. Math. Soc. xli. 1922, pp. 82–91) it was shown that the asymptotic expansions of the Legendre Functions and of the Hypergeo-

* Communicated by the Author.

metric Function can be derived from the asymptotic expansions of the Bessel Functions and of the Confluent Hypergeometric Function respectively. The method is capable of wide application, as can be seen from the illustrations given in this paper. The process can, in each case, be reversed.

In the first place take Gegenbauer's well-known expansion

$$\lambda^{n+\frac{1}{2}}e^{\lambda\mu}=2^{n-\frac{1}{2}}\Gamma(n+\tfrac{1}{2})\sum_{p=0}^{\infty}(2n+2p+1)\mathrm{C}_p^{n+\frac{1}{2}}(\mu)\mathrm{I}_{n+\frac{1}{2}+p}(\lambda), \quad . \quad . \quad . \quad . \quad (1)$$

where $\mathrm{C}_p^{n+\frac{1}{2}}(\mu)$ is the coefficient of α^p in the expansion in ascending powers of α of $(1-2\mu\alpha+\alpha^2)^{-n-\frac{1}{2}}$. This will be transformed by means of the formula

$$\int_0^{\infty} e^{-\lambda z}\mathrm{I}_{n+\frac{1}{2}}(\lambda)\lambda^{m-\frac{1}{2}}d\lambda=\sqrt{\left(\frac{2}{\pi}\right)}(z^2-1)^{-\frac{1}{4}m}\mathrm{Q}_n^m(z), \quad (2)$$

where $\mathrm{R}(z)>1$ and $\mathrm{R}(m+n)>-1$.

In the integral

$$\int_0^{\infty} e^{-\lambda(z-\mu)}\lambda^{n+m}d\lambda=\frac{\Gamma(n+m+1)}{(z-\mu)^{n+m+1}},$$

where $\mathrm{R}(z-\mu)>0$, $\mathrm{R}(n+m)>-1$, substitute from (1) in the integrand and apply (2). Then (*cf.* Nielsen, 'Fonctions Métasphériques,' p. 143)

$$\frac{\Gamma(n+m+1)}{(z-\mu)^{n+m+1}}=2^n\frac{\Gamma(n+\frac{1}{2})}{\Gamma(\frac{1}{2})}(z^2-1)^{-\frac{1}{4}m} \times\sum_{p=0}^{\infty}(2n+2p+1)\mathrm{C}_p^{n+\frac{1}{2}}(\mu)\mathrm{Q}_{n+p}^m(z), \quad (3)$$

provided that the series is convergent. We now write ζ for μ, and note that, if p is zero or a positive integer,

$$\mathrm{C}_p^{n+\frac{1}{2}}(\zeta)=\frac{\Gamma(\frac{1}{2})\Gamma(2n+p+1)}{2^n\Gamma(n+\frac{1}{2})\Gamma(p+1)}(1-\zeta^2)^{-\frac{1}{4}n}\mathrm{T}_{n+p}^{-n}(\zeta). \quad (4)$$

Then the expansion can be written

$$\frac{\Gamma(n+m+1)}{(z-\zeta)^{n+m+1}}=(1-\zeta^2)^{-\frac{1}{4}n}(z^2-1)^{-\frac{1}{4}m} \times\sum_{p=0}^{\infty}(2n+2p+1)\frac{\Gamma(2n+p+1)}{\Gamma(p+1)}\mathrm{T}_{n+p}^{n}(\zeta)\mathrm{Q}_{n+p}^m(z). \quad . \quad . \quad . \quad . \quad (5)$$

It is valid if ζ is an interior point of that ellipse in the complex plane which has foci at ± 1 and passes through the point z.

Now in (5) replace m by $-m$, and put $n=m$; then it becomes

$$\frac{1}{z-\zeta} = (1-\zeta^2)^{-\frac{1}{2}m}(z^2-1)^{\frac{1}{2}m} \sum_{p=0}^{\infty} (2m+2p+1)\mathrm{T}^{-m}_{m+p}(\zeta)\mathrm{Q}^{m}_{m+p}(z). \quad . \quad . \quad . \quad . \quad (6)$$

If m is a positive integer, so that $(z^2-1)^{\frac{1}{2}m}\mathrm{Q}^{m}_{m+p}(z)$ is holomorphic on the ellipse, and if $f(z)$ is holomorphic within and on the ellipse, it follows, on multiplying by $f(z)$ and integrating round the ellipse, that

$$f(\zeta) = (1-\zeta^2)^{-\frac{1}{2}m} \times \sum_{p=0}^{\infty} (2m+2p+1)\mathrm{T}^{-m}_{m+p}(\zeta) \frac{1}{2\pi i}\int f(z)\,(z^2-1)^{\frac{1}{2}m}\mathrm{Q}^{m}_{m+p}(z)\,dz.$$

By applying the formula

$$-e^{-\frac{1}{2}m\pi i}\mathrm{Q}^{m}_{n}(z)+e^{\frac{1}{2}m\pi i}\mathrm{Q}^{m}_{n}(z,+1-) = i\pi\mathrm{T}^{m}_{n}(z) \quad . \quad (7)$$

this can then be written

$$f(\zeta) = (1-\zeta^2)^{-\frac{1}{2}m} \times \sum_{p=0}^{\infty} (m+p+\tfrac{1}{2})\mathrm{T}^{-m}_{m+p}(\zeta)\int_{-1}^{1} f(x)\,(1-x^2)^{\frac{1}{2}m}\mathrm{T}^{m}_{m+p}(x)\,dx. \quad (8)$$

A proof of this formula, depending on the use of Dirichlet Integrals, and valid for more general values of $f(\zeta)$, was given in the Proc. Edin. Math. Soc. xlii. 1923, pp. 88–92.

Again, take the formula

$$\mathrm{I}_{m+n+1}(\lambda) = \frac{\lambda^{n+1}}{2^n\Gamma(n+1)}\int_0^1 \mathrm{I}_m(\lambda\mu)\mu^{m+1}(1-\mu^2)^n\,d\mu, \quad . \quad (9)$$

where $\mathrm{R}(m)>-1$, $\mathrm{R}(n)>-1$, and insert it, after putting $m+\frac{1}{2}$ for m and $n-1$ for n, in (2), written in the form

$$\mathrm{I} \equiv \int_0^{\infty} e^{-\lambda z}\mathrm{I}_{m+n+\frac{1}{2}}(\lambda)\lambda^{l-\frac{1}{2}}d\lambda = \sqrt{\left(\frac{2}{\pi}\right)}(z^2-1)^{-\frac{1}{2}l}\mathrm{Q}^{l}_{m+n}(z).$$

Then

$$\mathrm{I} = \int_0^{\infty} e^{-\lambda z}\frac{\lambda^{l+n-\frac{1}{2}}}{2^{n-1}\Gamma(n)}d\lambda \int_0^1 \mathrm{I}_{m+\frac{1}{2}}(\lambda\mu)\mu^{m+3/2}(1-\mu^2)^{n-1}d\mu$$

$$= \int_0^1 \frac{\mu^{m+3/2}(1-\mu^2)^{n-1}}{2^{n-1}\Gamma(n)}d\mu \int_0^{\infty} e^{-\lambda z}\mathrm{I}_{m+\frac{1}{2}}(\lambda\mu)\lambda^{l+n-\frac{1}{2}}d\lambda.$$

At this point we take a small positive number ϵ as the lower limit of the outer integral, put $\lambda = \xi/\mu$ in the inner integral, evaluate it by means of (2), and then let $\epsilon \to 0$. Thus

$$I = \int_0^1 \frac{\mu^{m+3/2}(1-\mu^2)^{n-1}}{2^{n-1}\Gamma(n)} \frac{1}{\mu^{l+n+\frac{1}{2}}} \sqrt{\binom{2}{\pi}} \times \left(\frac{z^2}{\mu^2}-1\right)^{-\frac{1}{2}(l+n)} Q_m^{l+n}\left(\frac{z}{\mu}\right) d\mu.$$

Hence

$$(z^2-1)^{-\frac{1}{2}l} Q_{m+n}^l(z) = \frac{1}{2^{n-1}\Gamma(n)} \times \int_0^1 \mu^{m+1}(1-\mu^2)^{n-1}(z^2-\mu^2)^{-\frac{1}{2}(l+n)} Q_m^{l+n}\left(\frac{z}{\mu}\right) d\mu, \quad . \quad (10)$$

where $\quad R(l+2m+n) > -3, \quad R(n) > 0.$

Next, in the formula

$$\int_0^\infty x^{l-1} K_n(x)\, dx = 2^{l-2}\Gamma\left(\frac{l+n}{2}\right)\Gamma\left(\frac{l-n}{2}\right), \quad . \quad (11)$$

where $R(l \pm n) > 0$, put $n+\frac{1}{2}$ for n and $l-m-\frac{1}{2}$ for l, and substitute from

$$K_{n+\frac{1}{2}}(x) = \sqrt{\binom{\pi}{2}} x^{n+\frac{1}{2}} \int_1^\infty e^{-xt}(t^2-1)^{\frac{1}{2}n} P_n^{-m}(t)\, dt, \quad (12)$$

where $R(x) > 0$, $R(m) > -1$. Then, on changing the order of integration and evaluating the inner integral, we get

$$\int_1^\infty (t^2-1)^{\frac{1}{2}m} P_n^{-m}(t)\, t^{-l}\, dt = 2^{l-m-2} \times \frac{\Gamma\left(\frac{l-m+n}{2}\right)\Gamma\left(\frac{l-m-n-1}{2}\right)}{\Gamma(\frac{1}{2})\,\Gamma(l)}, \quad (13)$$

where $R(m) > -1$, $R(l-m+n) > 0$, $R(l-m-n) > 1$.

Formula (12) may be established as follows. From the three formulæ

$$I_n(x) = \frac{x^m}{2\pi i}\sqrt{\binom{2}{\pi}} \int_c e^{x\zeta}(\zeta^2-1)^{\frac{1}{4}(m-\frac{1}{2})} Q_{n-\frac{1}{2}}^{\frac{1}{2}-m}(\zeta)\, d\zeta, \quad (14)$$

where $R(x) > 0$ and the contour of integration starts at

$-\infty$ on the real axis, passes round 1 in the positive direction, and returns to $-\infty$ on the real axis,

$$\mathrm{K}_n(x) = \frac{\pi}{2\sin n\pi}\{\mathrm{I}_{-n}(x) - \mathrm{I}_n(x)\}, \quad \ldots \quad (15)$$

and

$$\mathrm{Q}^{\frac{1}{2}-m}_{-n-\frac{1}{2}}(\zeta) - \mathrm{Q}^{\frac{1}{2}-m}_{n-\frac{1}{2}}(\zeta) = \sin n\pi\,\Gamma(n-m+1)\,\Gamma(1-m-n)\,\mathrm{P}^{m-\frac{1}{2}}_{n-\frac{1}{2}}(\zeta), \quad \ldots \quad (16)$$

it follows that

$$\mathrm{K}_n(x) = \sqrt{\left(\frac{\pi}{2}\right)}\,2i\,\frac{x^m}{\sin(m+n)\pi}\,\frac{\Gamma(n-m+1)}{\Gamma(n+m)} \times \int e^{x\zeta}(\zeta^2-1)^{\frac{1}{2}(m-\frac{1}{2})}\,\mathrm{P}^{m-\frac{1}{2}}_{n-\frac{1}{2}}(\zeta)\,d\zeta. \quad \ldots \quad (17)$$

Now the integrand is uniform at $\zeta=1$ and at the origin, while, near $\zeta=-1$,

$$(\zeta^2-1)^{\frac{1}{2}(m-\frac{1}{2})}\,\mathrm{P}^{m-\frac{1}{2}}_{n-\frac{1}{2}}(\zeta) = \frac{\Gamma(\frac{1}{2}-m)(\zeta+1)^{m-\frac{1}{2}}}{\Gamma(n-m+1)\,\Gamma(1-n-m)} \times \mathrm{F}\left(\tfrac{1}{2}-n,\ \tfrac{1}{2}+n,\ m+\tfrac{1}{2},\ \frac{1+\zeta}{2}\right) + \frac{\Gamma(m-\frac{1}{2})\,2^{m-\frac{1}{2}}}{\Gamma(\frac{1}{2}-n)\,\Gamma(\frac{1}{2}+n)} \times \mathrm{F}\left(n-m+1,\ 1-m-n,\ \tfrac{3}{2}-m,\ \frac{1+\zeta}{2}\right). \quad \ldots \quad (18)$$

Hence

$$\mathrm{K}_n(x) = \sqrt{\left(\frac{\pi}{2}\right)}\,x^m \int_1^\infty e^{-xt}(t^2-1)^{\frac{1}{2}(m-\frac{1}{2})}\,\mathrm{P}^{-m+\frac{1}{2}}_{n-\frac{1}{2}}(t)\,dt, \quad (12a)$$

where $\mathrm{R}(x)>0$, $\mathrm{R}(m)>-\frac{1}{2}$. From this (12) is obtained. Formula (12) was given by H. M Macdonald (Proc. Lond. Math. Soc. xxxv. 1902, p. 437), but the factor $\cos(m+\frac{1}{2})\pi/\sin n\pi$ included there should be omitted.

Again, from the formulæ

$$\mathrm{J}_m(x) = \frac{1}{\pi}\int_0^\pi \cos(m\phi - x\sin\phi)\,d\phi - \frac{\sin m\pi}{\pi}\int_0^\infty e^{-mu-x\sinh u}\,du, \quad (19)$$

where $\mathrm{R}(x)>0$, and

$$\Gamma(m+n+1)\,\mathrm{T}_n^{-m}(x) = \int_0^\infty e^{-\lambda x}\mathrm{J}_m\{\lambda\sqrt{(1-x^2)}\}\,\lambda^n\,d\lambda, \quad (20)$$

where $0<x<1$, $\mathrm{R}(m+n)>-1$, by substitution and change of order of integration we deduce that

$$\Gamma(m+n+1)\,\mathrm{T}_n^{-m}(\cos\theta) = \frac{\Gamma(n+1)}{2\pi}\left\{\int_{-\pi}^{\pi}\frac{e^{im\phi}\,d\phi}{(\cos\theta+i\sin\theta\sin\phi)^{n+1}} - 2\sin m\pi\int_0^{\infty}\frac{e^{-mu}\,du}{(\cos\theta+\sin\theta\sinh u)^{n+1}}\right\}, \quad (21)$$

where $0<\theta<\frac{1}{2}\pi$, $\mathrm{R}(m+n)>-1$.

Similarly from

$$\mathrm{I}_m(x) = \frac{1}{\Gamma(\frac{1}{2})\,\Gamma(m+\frac{1}{2})}\left(\frac{x}{2}\right)^m\int_{-1}^{1}e^{x\xi}(1-\xi^2)^{m-\frac{1}{2}}\,d\xi, \quad (22)$$

where $\mathrm{R}(m)>-\frac{1}{2}$, and

$$\mathrm{P}_n^{-m}(z) = \frac{\Gamma(n-m+1)}{2\pi i}\int_{\mathrm{C}}e^{\lambda z}\,\mathrm{I}_m\{\lambda\sqrt{(z^2-1)}\}\lambda^{-n-1}\,d\lambda, \quad (23)$$

where $\mathrm{R}(z)>0$ and $z\neq1$ (Proc. Edin. Math. Soc. xli. 1923, p. 82), we obtain the formula

$$\mathrm{P}_n^{-m}(z) = \frac{(z^2-1)^{\frac{1}{2}m}}{2^m\Gamma(\frac{1}{2})\,\Gamma(m+\frac{1}{2})}\int_{-1}^{1}\frac{(1-\xi^2)^{m-\frac{1}{2}}\,d\xi}{\{z+\sqrt{(z^2-1)}\,\xi\}^{m-n}},$$

or, since $\mathrm{P}_n^{-m}(z)=\mathrm{P}_{-n-1}^{-m}(z)$,

$$\mathrm{P}_n^{-m}(z) = \frac{(z^2-1)^{\frac{1}{2}m}}{2^m\Gamma(\frac{1}{2})\,\Gamma(m+\frac{1}{2})}\int_0^{\pi}\frac{\sin^{2m}\theta\,d\theta}{\{z+\sqrt{(z^2-1)}\cos\theta\}^{m+n+1}}, \quad \ldots \quad (24)$$

where $\mathrm{R}(m)>-\frac{1}{2}$.

Also, from

$$\mathrm{K}_m(x) = \frac{\sqrt{\pi}}{\Gamma(m+\frac{1}{2})}\left(\frac{x}{2}\right)^m\int_0^{\infty}e^{-x\cosh\phi}\,(\sinh\phi)^{2m}\,d\phi, \quad (25)$$

where $\mathrm{R}(x)>0$, $\mathrm{R}(m)>-\frac{1}{2}$, and

$$\int_0^{\infty}e^{-\lambda z}\mathrm{K}_m\{\lambda\sqrt{(z^2-1)}\}\lambda^n\,d\lambda = \Gamma(n+m+1)\,\mathrm{Q}_n^{-m}(z), \quad (26)$$

where $\mathrm{R}(z)>0$, $\mathrm{R}(n\pm m)>-1$, we find that

$$\mathrm{Q}_n^{-m}(z) = \frac{\sqrt{\pi}}{\Gamma(m+\frac{1}{2})}\,\frac{(z^2-1)^{\frac{1}{2}m}}{2^m}\int_0^{\infty}\frac{(\sinh\phi)^{2m}\,d\phi}{\{z+\sqrt{(z^2-1)}\cosh\phi\}^{n+m+1}}, \quad \ldots \quad (27)$$

where $\mathrm{R}(m)>-\frac{1}{2}$, $\mathrm{R}(n\pm m)>-1$.

Finally, from

$$K_m(x) = \int_0^\infty e^{-x\cosh t}\cosh(mt)\,dt, \quad . \quad . \quad (28)$$

where $R(x)>0$, and (26) we obtain

$$Q_n^m(z) = \frac{\Gamma(n+1)}{\Gamma(n-m+1)}\int_0^\infty \frac{\cosh(mt)\,dt}{\{z+\sqrt{(z^2-1)}\cosh t\}^{n+1}}, \quad (29)$$

where $R(n\pm m)>-1$.

Formulæ (24), (27), and (29) are due to Hobson; they are given on pages 248, 256, and 259 respectively of his 'Spherical and Ellipsoidal Harmonics.'

LV. *The Calculation of Surface Tension from Experiment.* *By* Alfred W. Porter, *D.Sc., F.R.S., Emeritus Professor of Physics in the University of London* *.

Part I.

(See Phil. Mag. (7) xv. p. 163 (1933).)

Part II.

THE rise, h_0, in tubes of circular section of all widths.

Experimentalists are still supplied with a somewhat disconnected and partial series of rules for correcting the rise h_0 in a tube of circular section in an experiment determining the capillary constant.

For very narrow tubes and zero angle of contact there is the Poisson-Rayleigh expansion

$$\frac{\beta^2}{r^2} = \frac{1}{2}\frac{h_0}{r} + \Delta,$$

where

$$\Delta = \frac{1}{6} - \cdot 0322\left(\frac{2r}{h_0}\right) + \cdot 0164\left(\frac{2r}{h_0}\right)^2.$$

This expansion gives an uncertain value when $\frac{1}{2}\frac{h_0}{r}$ is as

* Communicated by the Author.

low as unity, and it leads for smaller values to a divergent series.

Richards and Coombs (J. Am. Ch. S. xxxvii. p. 1667 (1915)) employed the formula

$$\beta^2 = \frac{r}{2}\left(h_0 + \frac{h_m}{3}\right),$$

where h_m is the height of the meniscus, making the plea that both h_0 and h_m vanish when β^2 vanishes so that it is satisfactory at the critical point. It is, however, a poor correction at intermediate temperatures; moreover, they themselves recognized that a better correction was obtained by changing the divisor from 3 to 4 for tubes above 4 or 5 mm. wide. A satisfactory correction can, however, be obtained by making use of Bashforth and Adams's Tables as far as they go, and extending these data by aid of the formula derived by the late Lord Rayleigh for very wide tubes. These last values lead right to the vanishing point of the surface tension (or of β^2) which occurs only at the critical point (see Rayleigh, Proc. Roy. Soc. A, xcii. pp. 184–195 (1915); also Collected Papers, vi. p. 350).

Fig. 1 shows these data collected together in three curves. The numbers plotted are all true numerics, $\frac{1}{2}\frac{h_0}{r}$ and Δ, so that $\frac{\beta^2}{r^2}$ is obtained by addition. The ordinates for all three give the true values of Δ on a single common scale (for all three curves) extending from 0 to ·16. The abscissæ are on different scales, as shown by the numbers *below* each curve. On the top curve these numbers extend from 0·2 to 5, on the second curve from about ·0025 to ·25, and on the bottom scale from 0 to ·0025. In this way all values of $\frac{1}{2}\frac{h_0}{r}$ from 0 to 5 can be shown connected by the curve with the appropriate value of Δ. The small circles on the two first curves give the values of Δ calculated from the Bashforth and Adams's Tables.

It will be observed how sudden is the final drop of Δ; it falls from about ·016 to zero, while $\frac{1}{2}\frac{h_0}{r}$ drops from ·0001 to zero. In this region the surface is nearly flat

and of nearly zero elevation except near the boundary, and the weight of liquid in the meniscus is nearly pro-

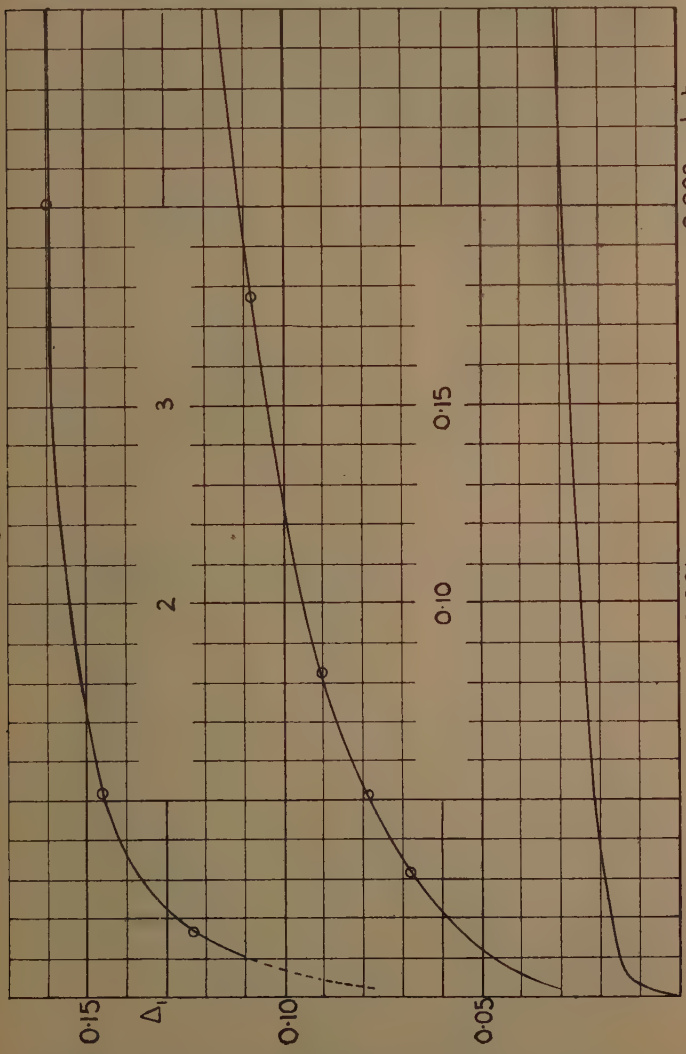

Fig. 1.

portional to the radius instead of to its second power. It is this weight which is sustained by capillarity.

Since β^2 diminishes in general as the temperature rises to the critical point (where it vanishes) the capillary height h_0 must also diminish, but it does so ultimately at a much faster rate and must in the later stages become comparable with molecular dimensions. Since in the derivation of these numbers no account has been taken of the molecular constitution of matter the formulæ must then become inapplicable.

Numerical examples :—

When $\frac{1}{2}\frac{h_0}{r} = 2{\cdot}2$ then $\frac{\beta^2}{r^2} = 2{\cdot}2 + {\cdot}154 = 2{\cdot}354$

" $\frac{1}{2}\frac{h_0}{r} = {\cdot}06$ " $\frac{\beta^2}{r^2} = {\cdot}06 + {\cdot}082 = 0{\cdot}142$

" $\frac{1}{2}\frac{h_0}{r} = {\cdot}001$ " $\frac{\beta^2}{r^2} = {\cdot}001 + {\cdot}024 = 0{\cdot}025$

" $\frac{1}{2}\frac{h_0}{r} = {\cdot}0001$ " $\frac{\beta^2}{r^2} = {\cdot}0001 + {\cdot}016 = 0{\cdot}0161$

Part III.

The height, h, of the meniscus in wide or narrow tubes when the angle of contact is zero; or alternatively, the determination of the capillary constant for sessile drops of all sizes.

This problem has been dealt with by me as far as $\frac{h^2}{r^2} = {\cdot}25$ with special reference to sessile drops in Part I. (Phil. Mag. (7) xv. p. 163 (1933)). When small drops are concerned the quantity Δ in that paper becomes negative and, in the limit, infinite. The solution for β^2/r^2 can, however, be extended, by the aid of Bashforth and Adams's Tables, so as to include the limiting case of very narrow capillaries or exceedingly small sessile drops. To avoid infinite values a convenient formula for graphical representation can be obtained by writing

$$\frac{\beta^2}{r^2} = \frac{\frac{1}{2}\frac{h^2}{r^2}}{\left(1 - \frac{h^2}{r^2}\right) + \Delta_2}.$$

The values of Δ_2 required to fit the tabular data are then plotted against h/r. These are shown in fig. 2. The values up to $\frac{h}{r} = 0{\cdot}5$ correspond to those already published

Fig. 2.

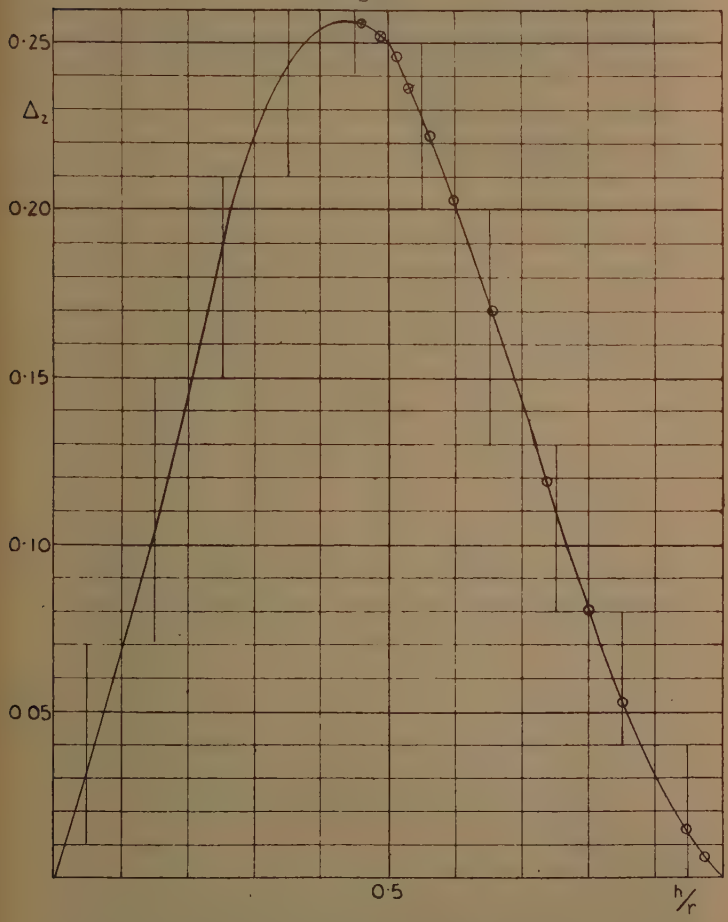

(*loc. cit.* p. 169, fig. 2); those corresponding to the Tables are indicated by small circles. The diagram of Δ_2 obtained in this way is fairly symmetrical. Bashforth and Adams found that the uppermost value was about

the limit at which their method of representation by series ceased to be reliable. This agrees with the indication of fig. 2, where a very rapid change near the summit occurs in the form of the curve. The lowest points on the curve where h/r is nearly unity lead, as they should, to large values of β^2/r^2, but the equation is not well suited in that region for accurate determination of this quantity.

Example 1.—A sessile drop of $r=2$ cm. and $h=0{\cdot}4$ cm. Here $\frac{h}{r}={\cdot}2$ and therefore $\frac{\beta^2}{r^2}=\frac{\frac{1}{2}\times{\cdot}04}{{\cdot}96+{\cdot}145}={\cdot}0181$, and thence $\beta^2={\cdot}0724$ cm.^{2} which is about the value for water.

Example 2.—The cases for which $\frac{h}{r}={\cdot}7$. This leads to several individual values for h and r which can be tabulated For each case $\Delta_2={\cdot}142$.

$r_{\text{cm.}}$	$h_{\text{cm.}}$	β^2.
1·0	·7	·376
·5	·35	·094
·4	·28	·060
·3	·21	·0338

Hence the drop, if of water, would have a little over 4 mm. radius ; and, if of mercury, about 3 mm. radius. In each case the radius would depend on the temperature.

LVI. *Gauss's Theorem in General Relativity—a Correction.*

To the Editors of the Philosophical Magazine.

Gentlemen,—

In a paper on the above subject appearing in the Supplement to the Philosophical Magazine of November last (xx. p. 971) I referred to the solution of Einstein's equations for the field of an electron and gave a reference to papers published in 1918 and 1921. Professor H. Reissner, of Berlin, has courteously drawn my attention to his earlier solution in *Ann. der Phys.* l. p. 106 (1916)

and to an acknowledgment of this by B. Hoffmann, Quart. Journ. Math. iv. p. 183 (1933).

The latter footnote had escaped my notice, and I regret that I was misled in regard to the earlier paper (in good company, as students of English relativity literature will know) by the commonly accepted designation of this solution as the Nordström-Jeffery solution—a designation which no doubt arose from the scarcity of German periodicals in this country in 1916.

I am, Gentlemen,
Yours faithfully,
J. T. Combridge.

LVII. *Notices respecting New Books.*

Annals of Science: a *Quarterly Review of the History of Science since the Renaissance*. Edited by D. McKie, Harcourt Brown, and H. W. Robinson. Vol. I. No. 1. January 15, 1936. Published by Taylor and Francis, Red Lion Court, Fleet Street, London, E.C. 4. (Price 6*s*. per number or 6*s*. 3*d*. post free; or 20*s*. per year post free in advance.)

WE welcome the advent of this new Journal. Bearing in mind the great interest which has in recent years been taken in the history of science it is perhaps a surprise that such a journal has not been originated earlier. But there is naturally some hesitation in multiplying publications. Are there not existing journals in which matter pertaining to the history of science may naturally find a place?

That may be true as regards occasional articles; the Editors, however, express their belief that "there is ample scope for, and much desirability of, a wider study, a more precise knowledge, and a better understanding of the origins, the pioneer stages, and the first exploring steps that led to the great advances and achievements of Science in modern times." As to how far this aim can be achieved is illustrated by this first number.

The first article, by Prof. E. N. da C. Andrade, deals with the "real character of Bishop Wilkins." This is not a study of psycho-analysis, but an account of a proposed Universal language invented by "the late Reverend Prelate my Honoured Friend, Dr. John Wilkins, deceased," and used by Robert Hooke as a secret writing. Much learning was brought to bear on this language, both by the originator and the commentator, although there seems no hope of the proposed

language and the characters in which it is written turning out to be a practicable solution of the problem.

"Early Nautical Charts" (M. B. Donald) and "History of the Chile Nitrate Industry" (N. H. de V. Heathcote) both take one far afield in space and time. Leonora D. Cohen discusses the correspondence between Descartes and Henry More on whether beasts possess souls or are merely machines. Professor T. S. Patterson researches intelligently on a somewhat mysterious Richard Boyle who is mentioned by Birch in his 'History of the Royal Society' as having been admitted as an original member.

W. C. Walker (Minchenden School, London) discusses the development of the detection and estimation of electric charges in the eighteenth century; while Douglas McKie (University College, London) describes notes evidently made of Joseph Black's lectures on the Elements of Chemistry by one of the students attending his lectures (in 1767–8). "The early date of these notes makes them of some historical interest."

There is evidently much here which should be made accessible to those interested in the development of science even when examined chiefly from the historical point of view. We wish the new Journal success.

The Theory of Atomic Spectra. By E. V. Condon and G. H. Shortley. [Pp. xiv+441.] (Cambridge: University Press, 1935. Price 42*s*.)

Although there have been many books dealing with atomic spectra, there is none which presents the theoretical side of the subject with anything approaching the completeness with which it is done in this treatise of Condon and Shortley. After a brief historical introduction the quantum mechanical method, as formulated by Dirac, is developed with ample detail for the purpose in view. The angular momentum relations are derived, and there are comprehensive tables of formulæ. The theory of radiation is then discussed with such completeness as is at present possible. About a quarter of the book is occupied with this development of the fundamental theory, which is then utilized in the discussion of atomic spectra. One electron spectra and the central field approximation are first considered. The Russell-Sanders case is then discussed in detail—energy levels, eigen functions and line strengths; this is followed by a consideration of *jj* and intermediate coupling and a general treatment of transformations in the theory of complex spectra. X-rays are discussed in connection with configurations containing nearly closed shells. Central fields are taken up again, and the numerical methods of solving the equations are described. In the account of the periodic tables there is an admirable

series of diagrams showing the main features of the energy level diagrams of all the atoms whose spectra have been analysed. The last four chapters are concerned with configuration interaction, which accounts for the main anomalies in spectral series, the Zeeman and Stark effects, and nuclear effects.

As the authors remark in their preface, a great part of the theory of atomic spectra may be considered " to be in a fairly closed and highly satisfactory state." It is this part with which they deal, and their book gives a convincing demonstration of the almost uncanny completeness with which the experimental facts may be correlated by the symbolical quantum mechanical scheme. The impression given of the solidity of the theoretical structure is largely due to the fact that the authors have not merely stated vaguely that certain results may be derived, but have given detailed derivations illustrative of all the more important types of calculation. There is, perhaps, a certain lack of excitement in reading of a field of investigation in which the main gaps are those which seem likely to be filled largely by more accurate numerical computations ; but for most readers the book will be a revelation of the amazing scope of the present theory. There is, of course, much further experimental work to be done ; and for the theorist, the very completeness of the partial scheme will focus attention on outstanding questions of relativistic formulations, and of the interpretation of the scheme itself.

Needless to say, the book will not be easy reading, even for the specialist ; but given a good background knowledge of more elementary spectroscopic theory, and of quantum mechanical methods, the exposition will be found clear and straightforward. The production and printing of the book, as shown especially in the setting out of the often elaborate equations, are admirable. The book is one which fitly marks a triumphant phase of recent physical theory.

The Principles of Quantum Mechanics. By P. A. M. Dirac. Second edition. [Pp. xii+300.] (Oxford: Clarendon Press, 1935. Price 17*s.* 6*d.*)

For the second edition much of this book has been rewritten, and a new chapter on field theory has been added. A change from the first edition which has contributed to a clarification of the exposition is that the word " state " has been used in the non-relativistic sense to refer to the condition of a system at one instant of time.

An introductory chapter deals with the need for a quantum theory and with the fundamental " principle of superposition," according to which a state may be regarded as the result of

a superposition of two or more states. The symbolic scheme is then built up, in which states are represented by the directions of vectors in a generalized vector space and observables by linear operators. The rules of manipulation of the symbols are laid down and supplemented by rules connecting the physical facts with the mathematical formalism. The quantum conditions are then introduced and the equations of motion developed, some of the simpler applications being given. The later chapters deal with motion under central forces, perturbation theory, collision problems, systems of similar particles, radiation, the relativistic theory of the electron, and, finally, with field theory.

Dirac's book undoubtedly stands alone as an enduring masterpiece of individual achievement. The symbolical scheme is developed so comprehensively that it embraces the more particularized formulations of quantum mechanics, and particular results of outstanding physical interest seem to emerge as minor incidents. It is almost inevitable that a book which achieves so much should be difficult.

There are few physicists who have some working knowledge of quantum mechanics who could fail to admire this work. It is, however, difficult to avoid the feeling that, although Dirac may see things by the full light of day, he succeeds only in enabling the average physicist to see things through a glass, darkly. This is possibly due not so much to the mathematical difficulties as to the fact that Dirac is primarily concerned with the deductive scheme of quantum mechanics, and deals only incidentally with the manner in which the premises of that scheme were arrived at. After the extremely lucid first chapter the axiomatic basis for the treatment appears, as it were, from thin air. It does, of course, receive posterior justification; but the reader has first to follow the development of a physically empty symbolic algebra in which rules of manipulation seem to be quite arbitrarily introduced, and when the linkage with physical facts is made he is still baffled as to how the physical facts ever suggested the particular symbolic scheme. In particular he is left in doubt as to whether the symbolic scheme gives, in fact, the most appropriate formulation of the physical laws from the point of view of necessity or simplicity.

All physicists who have done some climbing should attempt to follow Dirac as a guide to the heights of quantum mechanics. They will not regret having started even if they drop out on the way. There are easier tracks which go part of the way up, but there is probably no track at present which approaches the summit so nearly as that made by Dirac.

[*The Editors do not hold themselves responsible for the views expressed by their correspondents.*]

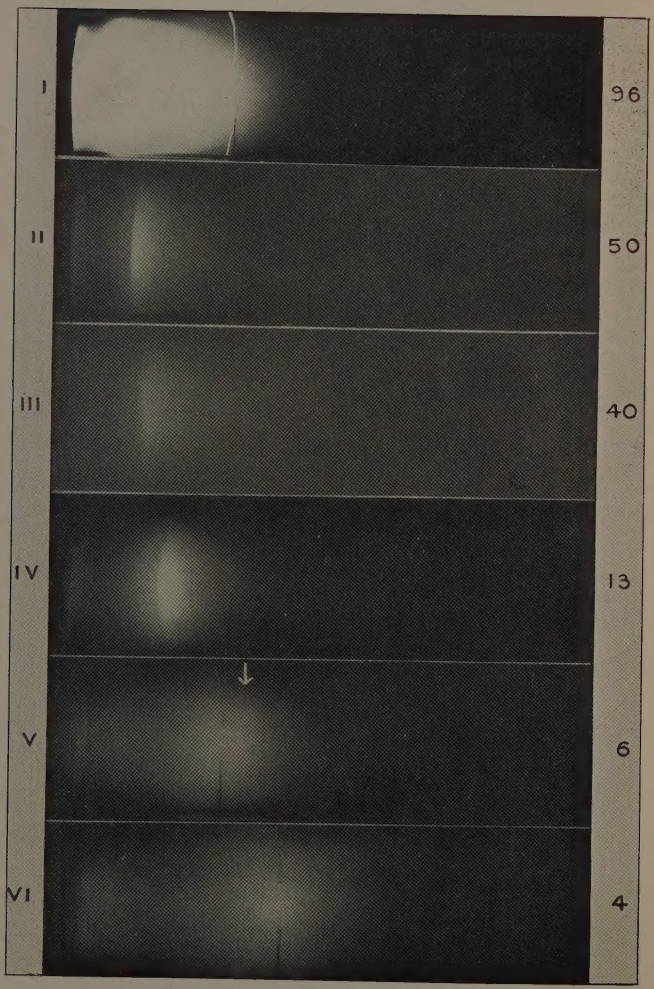
I
II
III
IV
V
VI
96
50
40
13
6
4

Fig. 8.

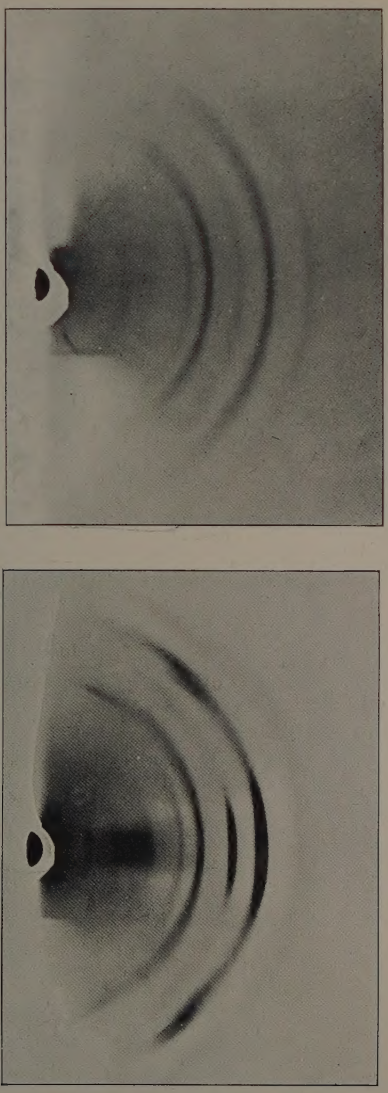

(*a*)

(*b*)

X-ray diffraction photographs of SnO_2 on the surface of two specimens of tin oxidized at 800° C. (*a*) random orientation of SnO_2 crystals and rapid absorption of oxygen; (*b*) oriented film (001) parallel to the surface, slow absorption of oxygen.